NATIONAL RESEARCH COUNCIL OF CANADA

AERONAUTICAL REPORT

LR-349

1/12-SCALE MODEL TESTS OF AN OPEN CIRCUIT VTOL PROPULSION TUNNEL

PART I: SELECTION OF AND BASIC TESTING OF A SUITABLE CONFIGURATION USING AN EXTERNAL AIR SUPPLY.

PART II: TESTS WITH THE ADDITION OF A BELLMOUTH INTAKE AND DRIVING FAN

BY

D. BROWN

DIVISION OF MECHANICAL ENGINEERING

OTTAWA

APRIL 1962

N.R.C. NO. 6964

NATIONAL RESEARCH LABORATORIES

Ottawa, Canada

REPORT

Division of Mechanical Engineering

Gas Dynamics Section

Pages - Preface - 14
Text - 39
Figures - 113

Report: LR-349
Date: April 1962
Lab. Order: 13528A
File: CM2-17-13T-6

For: Internal

Subject: 1/12-SCALE MODEL TESTS OF AN OPEN CIRCUIT VTOL PROPULSION TUNNEL.

PART I: SELECTION OF AND BASIC TESTING OF A SUITABLE CONFIGURATION USING AN EXTERNAL AIR SUPPLY.

PART II: TESTS WITH THE ADDITION OF A BELLMOUTH INTAKE AND DRIVING FAN.

Prepared by: D. Brown

Submitted by: A. J. Bachmeier
Section Head

Approved by: D. C. MacPhail
Director

SUMMARY

PART I

The general performance of the important components of a wind tunnel or test bed designed for testing aircraft propulsion systems and especially those suitable for VTOL and STOL aircraft application has been examined. Tests have been directed at single components (e.g. the inlet diffuser to decide on suitable internal screening arrangements) and the tunnel as a whole with the exception of the driving fan and bellmouth inlet.

From these tests it is concluded that the unconventional layout proposed for the tunnel is acceptable.

PART II

The arrangement of components, which was adopted following the testing of Part I, was initially accepted for the tests subsequently made. Additional components were the fan rotor and stator system and the inlet bellmouth. The performance of the whole tunnel was examined for working section velocity profiles, steadiness of flow, boundary layer growth in the working section, turbulence, and exit diffuser efficiency. Ancillary tests to determine increases in velocity through diminishing working section area were also undertaken.

Two changes in basic layout were made, following examination of the model tunnel as a whole. The first was concerned with cost reduction through elimination of the conventional long exit diffuser. This diffuser was replaced by a much shorter, wide angle diffuser having the same flow area increase. The efficient running of the short diffuser called for the installation of vortex generators at its inlet.

The successful operation of the tunnel with the short exit diffuser led to tests in which the screens mounted in the inlet diffuser were eliminated and improved aerodynamic performance was obtained through the use of a set of vortex generators in the stator spaces.

Apart from the discovery of some flow angularity in the working section, which will be left to full scale development for remedy, the layout of the tunnel as determined by model test is considered to lead to acceptable aerodynamic performance.

TABLE OF CONTENTS

TABLE OF CONTENTS (Cont'd)

LIST OF ILLUSTRATIONS

LIST OF ILLUSTRATIONS (Cont'd)

LIST OF ILLUSTRATIONS (Cont'd)

LIST OF ILLUSTRATIONS (Cont'd)

LIST OF SYMBOLS

Symbol	Definition
P	Total pressure (in. H_2O, lb./in.^{2} or lb./ft.^{2})
p	Static pressure (in. H_2O, lb./in.^{2} or lb./ft.^{2})
U	Velocity (ft./sec.)
N	Fan rotational speed (r.p.m.)
Θ	Non-dimensional ambient temperature $(\frac{\text{ambient temperature } °K}{288})$
q	Dynamic head (in. H_2O, lb./in.^{2}, lb./ft.^{2})
δ	Non-dimensional ambient pressure $(\frac{\text{ambient pressure}}{\text{standard atmospheric pressure}})$
W	Tunnel mass flow (lb./sec.)
u	Perturbation velocity in axial direction (ft./sec.)
I	Heating current applied to hot wire (amps)
I_o	Heating current with no airflow over hot wire (amps)
R	Wire resistance (ohms)
e	RMS voltage applied to hot wire to hold the heating current constant (volts)
u'	Intensity of turbulence in axial direction $(\frac{\sqrt{\overline{u^2}}}{U_\infty})$
η	Diffuser static pressure rise efficiency
E. R.	Tunnel energy ratio $(\frac{\text{kinetic energy rate of working section flow}}{\text{input power to fan}})$
ϕ	Working section airflow pitch angle (positive when flow towards ceiling)
ψ	Airflow yaw angle (positive to right looking downwards)
α	Angle of incidence (degrees)

LIST OF SYMBOLS (Cont'd)

Symbol	Definition
Subscripts	
∞	Free stream
o	Zero airflow
in	Inlet
ATM	Atmospheric
VG	Vortex generator
B	Butterfly valve

1/12-SCALE MODEL TESTS OF VTOL TUNNEL

GENERAL INTRODUCTION

The increasing interest in VTOL aircraft during the last five or six years has created a need for test arrangements, in addition to those already existing, which would in particular be more appropriate for examining VTOL engine configurations and associated components.

Early tests on models indicated clearly the need for careful flight simulation, especially during transition from vertical to horizontal flight, and for the establishment of control procedures during take-off and landing.

Design Considerations

Considerable emphasis was attached to the concept of lifting engines using large bypass ratios and to fan-in-wing schemes.

To facilitate this type of work the following features were considered necessary:

(1) Open circuit operation to permit combustion in the working models without the initial complication of exhaust gas extraction or heat removal.

(2) Large working section to permit tests at realistic Reynolds numbers.

(3) Initial air speed range from zero to 120 ft./sec. with good control.

(4) Compressed air supply with combustion facilities, if required, to permit examination of the interaction of jets and installation of air driven turbines in the models.

(5) Suction supply to permit examination of air inlets and boundary layer suction, and to permit evacuation of the tunnel under specific circumstances.

(6) Provision for icing studies.

(7) Force measurements (lift, drag, roll and pitching moment).

(8) Simulation of ground effect or its absence.

(9) Structural design and arrangement to permit

(a) completion of the circuit to form a closed tunnel at some future date,

(b) installation of additional fan power to increase tunnel velocity by a factor of approximately 2,

(c) operation at reduced pressure if the circuit was completed,

(d) rotation of the working section through 90 deg.

(10) Turbulence levels lower than 0.1 percent.

(11) Minimum cost.

After due consideration of these requirements and existing facilities, the following scheme was decided upon:

(1) Working Section: 10 ft. wide by 20 ft. high by 40 ft. long, with provision for rotating 90 deg.,

(2) Power Plant: Initially 1000-h.p. Ward Leonard drive to give air speed to 120 ft./sec., with provision to take an 8000-h.p. free turbine (to give air speed approximately 250 ft./sec.),

(3) Contraction Ratio: 6 to 1,

(4) $\frac{\text{Effective Fan Area}}{\text{Working Section Area}} = \frac{2}{1}$

(5) Fan: Hub/tip ratio 0.5; a high solidity fan was selected to decrease sensitivity to inlet turbulence and cross wind. The design will permit operation at all power levels up to 9000 h.p. by changing the speed. The fan has 16 wooden blades with a tip diameter of 26 ft.

(6) Structure: Steel to withstand a vacuum of 28 in. Hg.

As soon as the preliminary design was completed, a 1/12-scale model complete with fan was constructed, and this report deals in detail with the tests made on this model.

Part I of the report deals with investigations of several diffuser-screen combinations and with visual flow examination in the working section with a simulated "fan-in-wing" model in place. Since air was supplied for these tests from the general laboratory supply, the inlet bellmouth, fan and stator system were missing. The exit diffuser was also omitted in some of the tests.

Part II is devoted to tests of the entire layout incorporating the selected arrangement of screened wide angle diffuser plus a bellmouth with flow provided at first by connection of the exit diffuser with an exhauster set and later through the installation of the geometrically scaled down fan, located upstream of the working section.

In the latter case the exit diffuser was open to atmosphere. The tests of this part consisted mainly of measurements of working section turbulence using hot wire equipment, boundary layer measurements at working section inlet for two slightly different contraction sections, working section total head and velocity profiles, and working section longitudinal static pressure measurement. These tests are more closely specified in Part II.

PART I

SELECTION OF AND BASIC TESTING OF A SUITABLE CONFIGURATION USING AN EXTERNAL AIR SUPPLY

1.1 Introduction

In this part tests of several arrangements of the model tunnel are reported. The cylindrical fan section, constant area stilling section, contraction section and a diffuser connecting the fan section to the blown air supply are common to all arrangements. These are subsequently referred to as fixed sections.

Tests were conducted on the following arrangements:

(a) Fixed sections plus three combinations of small angle and screened 28-deg. * diffusers between fan section and stilling section, with working section and exit diffuser removed (Fig. 1.2, 1.4 and 1.6).

(b) Fixed section plus screened 28-deg. diffuser plus working section with two sets of corner fillets (Fig. 1.10).

(c) Fixed sections plus screened 28-deg. diffuser with working section and exit diffuser (Fig. 1.19).

Most of the tests were run at a working section velocity of about 150 ft./sec. at the exit from the contraction, and a Reynolds number of about 6×10^5 per foot.

1.2 Tunnel Description

Relevant dimensions are shown in the figures referred to above.

The fan section, inlet and exit diffusers and stilling section were made of sheet metal. The central streamlined body, or bullet, used to simulate the fan hub, was also made of sheet metal with a hardwood nose and was held in place through fixing to wire mesh screens in the fan section. The inlet diffuser was built in short flanged sections to facilitate mounting further wire mesh screens necessary for its successful operation.

The contraction section, which is the only section of the tunnel to employ a double curvature surface, was made of moulded fibreglass and resin.

---

* Total included angle.

The working section vertical sides were cut from 1-in. thick plywood, whilst the top and bottom were of $\frac{1}{2}$-inch thick plexiglass. Steel angle was used as framing for the working section. Corner fillets of hardwood were fixed to the plywood sides by wood screws.

1.3 Instrumentation

Dependent on configuration, static pressures were measured at from 27 to 38 points on a meridian of the duct between the fan inlet section and the stilling section inlet. The spacing of these points varied from 30 in. (between two points in the fan section) to 2 in. (in the neighbourhood of the screens) in the wide angle diffuser.

A further 18 static taps were distributed in the contraction section.

The static taps were effected in the steel work by drilling 1/16-in. dia. holes and soldering short lengths of copper tubing (1/8-in. dia.) on the exterior to cover the hole. In the sections constructed of fibreglass or plywood the tap was made by sinking a short length of copper tubing into the wall so as to be flush with the internal surface. Connection with a Meriam fluid manometer bank was made through plastic tubing.

Some total pressure distributions in the working section were obtained using a probe in the form of a steel tube 1/4 in. in dia. having a .025-in. dia. hole drilled normal to its surface.

Boundary layer surveys were effected with a small conventional total pressure probe having a diameter of 1/32 in. The probe position from datum was set by a micrometer head built into the supporting rig.

Further total head surveys were made, notably in the vertical plane behind a standard aerofoil in the working section, using a rake having 1/16-in. dia. tubing at 1-in. pitch as probes.

Fluid level in the manometer tubes was estimated by eye using magnifying lenses. Except in certain cases (at some points behind the aerofoil section) lowest total pressures were of the order of 1 in. of water gauge so that errors in reading were never more than 3 percent and for most points were about 1 percent.

Tunnel flow was measured with a standard 7-in. dia. orifice plate inserted in a 10-in. pipe upstream of the fan section inlet.

Jet flow rate (for the simulation of a fan-in-wing model) was measured using a standard 1.7-in. dia. orifice plate in a 2-in. pipe. The pressures associated with these flows were high enough to permit accurate measurement with mercury in glass manometers.

given in Figure 1.8 shows a pronounced over-all decrease through the wide angle diffuser owing to the large total head losses of the large number of high solidity screens.

Approximate calculations indicate that tests 1, 2, 3, 4 and 5 produced total head losses (from station 27.5 to the exit from the contraction section) of 3, 9, 3, 9 and 5 lb./ft.^{2} respectively.

Because of its relatively good aerodynamic performance and short length (2.5-deg. diffusers eliminated) and because it also employed robust screening, the layout of Configuration 3 with screens, as given in Figure 1.9, was decided on and all further tests involved this inlet diffuser system.

The results of the boundary layer traverses are shown in Figures 1.12 and 1.13 plotted as the ratio of dynamic head in the boundary layer to that in the free stream against perpendicular distance from the wall. A comparison of the profiles for station 116 with those of station 156 shows the boundary layer growth that takes place along the length of the working section. Pressure measurements showed considerable variation in dynamic head to exist locally. This latter feature may in part be due to the poor junction, with a discontinuity in wall slope, where the contraction section meets the working section (an approximate calculation using the flat plate formula $\delta/x = 0.154/R_E^{1/7}$ indicates that a turbulent boundary layer 0.2 in. thick at station 116 (entrance to the working section) would increase to 0.9 in. at station 156).

Figures 1.14 and 1.15 show the static pressure distribution over a length of ducting, including some of the contraction section and the whole of the working section, exhausting directly to atmosphere. The results given in Figure 1.14 were obtained with a constant geometric flow area along the working section obtained using constant cross-section corner fillets. The use of tapering corner fillets giving an increasing geometric flow area gave the results shown in Figure 1.15. These exhibit a more nearly constant static pressure along the working section length than do those of Figure 1.14. Subsequent tests involving the use of the working section were made with the tapered fillets in place. Figure 1.16 shows the total head profiles (with tapering corner fillets) in the vertical plane in the working section for two settings of working section velocity. The traverses were made off the centre line and 7 in. downstream of the inlet to the working section. Figures 1.17 and 1.18 illustrate total head profiles taken along the vertical centre lines of the working section at inlet and outlet for Configuration 4, i.e. without the exit diffuser. In these tests an aerofoil (10-in. chord) spanned the section horizontally and measurements were made for aerofoil incidences of 17 deg. ($C_{L_{max.}}$) and 30 deg.

Figures 1.20 and 1.21 give longitudinal static pressure distribution for the working section with the exit diffuser attached as indicated in Figure 1.19. Static taps were placed so as to give the pressures along three meridians. The results of Figure 1.20 are for an empty tunnel, whilst Figure 1.21 shows distribution with the aerofoil at 30 deg. It is apparent that at stations near the aerofoil

considerable pressure gradients exist across the working section which may be expected from a relatively large model at high incidence. Figure 1.22 indicates a fairly uniform velocity profile for an empty tunnel at the working section exit when viewed with the results of Figure 1.20. Likewise it may be concluded from Figure 1.23 that, apart from a quite thick boundary layer and some asymmetry, the total head profile at station 194, about half-way between the end of the working section and the tunnel exit, is also fairly uniform. Figures 1.24 and 1.25 indicate the same sort of flow at tunnel exit as at station 194. The greater thickness of the boundary layer in the horizontal plane is probably a result of the greater diffusion in this plane. The pressure levels of test 10 were observed to be steady.

The addition of the exit diffuser has apparently exercised some influence for the better on total head profiles in the working section. A comparison, of the total head profiles at station 117 (inlet to working section) for the aerofoil set at 30 deg. incidence, between the results of test 9 (Fig. 1.18) and test 11 (Fig. 1.26) shows a more uniform distribution of total head when the tunnel was run with the exit diffuser. It is also clear that, without the diffuser, the aerofoil at 17 deg. and 30 deg. incidence affects the flow in the working section more than when the diffuser is fitted. There is a considerable loss of total head across the entire working section in the absence of the diffuser from the measurements made at station 156 (Fig. 1.17 and 1.18).

Some total head readings were taken in the vicinity of the entrance and are shown in Figure 1.27. Curve A, taken upstream of where the fan would normally be, is obtained from a horizontal traverse at station 5 and exhibits about 0.3 in. of water difference between the lowest and highest values. It is expected that with a bellmouth entry to a fan there will be no such asymmetry. With a flatter profile at station 5 it is to be expected that the curve marked B in Figure 1.27 would not fall off quite so rapidly at the wall. However, under proper operating conditions, the total head at station 32 (curve B in Fig. 1.27) will depend on fan performance as well as fan inlet profile. The variation in total pressure along the length of the tunnel is shown in Figure 1.28, in a non-dimensional form, for three tunnel configurations, i.e. complete tunnel, less exit diffuser and less exit diffuser and working section.

With the usual nomenclature for total head loss between any two sections of a duct we have the pressure loss factor K for the tunnel between stations 32 and 232 given by $K = 1.07 - 0.28 = 0.79$, based on the dynamic head in the working section.

Working section total pressure profiles in the vertical plane at a station behind a simulated fan-in-wing model are shown in Figures 1.29 and 1.30 for jet velocities of about 585 ft./sec. and zero, and working section air velocities of 168 ft./sec. and 68 ft./sec. These profiles are of no great practical significance since a large part of the total head loss in the main flow is due to the circular section pipe leading the jet air to the model. Figure 1.31 is more informative since from floor pressure plotting under the aerofoil some idea of the location of impingement of the jet on the floor is obtained. The sensitivity of the maximum pressure

point to the ratio of jet velocity and tunnel velocity is marked. Reduction of working section velocity to 140 ft./sec. resulted in the jet momentarily reaching the floor. Steady pressure measurements could not be taken with the manometers and this result was obtained by observing the movement of the manometer fluid and with tufts.

Tests 17, 18, 19 and 20 consisted of an examination of the flow produced in the working section with a fan-in-wing model simulated by a high velocity jet blowing through a hole in the model wing. Tests 17 and 18 were performed in a closed working section with the floor area under the jet slotted and ducted back into the working section downstream of the model. Tests 19 and 20 were made with the floor and ceiling of the working section removed for comparison purposes. Flow observation through the use of tufts fastened to the walls was made and Figures 1.32 and 1.35 inclusive demonstrate the results. Comparison of Figures 1.32 and 1.35 indicates that the simple ventilated floor is quite effective in producing a flow very similar to that existing with top and bottom of the tunnel removed. It is emphasized that these particular tests were tentative. Further work will be required to determine what corrections will be necessary to obtain real aerodynamic characteristics of VTOL aircraft in the transition mode from force and moment measurement and pressure plotting in this kind of facility.

In tests 17 and 18 the vent entrance was positioned to straddle the stagnation streamline of the jet as far as the floor pressures obtained in tests with the unvented floor would allow.

1.6 Conclusions

(1) The layout of a VTOL engine tunnel has been determined combining reasonably good aerodynamic characteristics with relatively short length and hence fairly low structural weight.

(2) The use of a wide angle diffuser between the fan and the contraction section necessitates the use of seven wire screens which incidentally will aid in dispersing large scale turbulence.

(3) The total pressure loss factor will be about 0.8. A value of 1.0 was taken for performance calculation. The difference in pressure loss factor will only allow about 6 percent increase of working section velocity over the design value, for an empty tunnel. However the drag coefficient of a model can be 20 percent larger than that allowed for in the design calculation for the same flow and power input.

The energy ratio is expected to be rather less than that of a conventional non-return wind tunnel owing to the diffusion introduced between the fan and the working section.

(4) The means for providing flow in these tests was far from ideal. It is known that asymmetry of flow existed at what was termed the inlet to the tunnel. Operation with a scaled fan inside a smooth bellmouth inlet should improve the flow in the working section.

(5) Further work will be required to determine the best form of vented floor for the testing of models which use vertical air jets.

1.7 References

1. Jacobs, E. N.
Abbot, I. N.
Airfoil Section Data Obtained in the NACA Variable-Density Tunnel as Affected by Support Interference and Other Corrections.
NACA Rept. 669, 1939.

2. Squire, H. B.
Hogg, H.
Diffuser-Resistance Combination in Relation to Wind Tunnel Design.
RAE Report Aero 1933, April 1944.

3. Schubauer, G. B.
Spangenberg, W. G.
Effect of Screens in Wide-Angle Diffusers.
NACA TN 1610, July 1948.

PART I

APPENDIX A

THEORETICAL CALCULATION OF SCREEN LOSS COMPATIBLE WITH OVER-ALL AREA RATIO REQUIRED AND AVAILABLE POSITIONS FOR SCREEN POSITIONING

As inferred in Reference 2 the screened wide angle diffuser is able to provide unseparated flow at exit because the effect of the screens is to energize the otherwise thick boundary that would form and ultimately lead to flow break-away. The necessary energy comes from the main part of the stream that would otherwise flow through the centre region of the diffuser. The turbulence introduced by screening provides the necessary vehicle for transferring some of the energy of the normally unaffected part of the stream into the boundary layer.

The net effect is a tendency to hold the stream static pressure constant in spite of the geometric area increase along the diffuser.

With the postulation that the static pressure along a diffuser does remain constant except in the immediate vicinity of the screens the problem degenerates to the simple Rankine-Froude theory applied to a windmill.

The following derivation is essentially that given in Reference 2 and is included for convenience.

In the sketch let an isolated screen be at position '1' and consider two planes '0' and '2' on either side. Static pressures and velocities are as indicated in the sketch and the flow is incompressible.

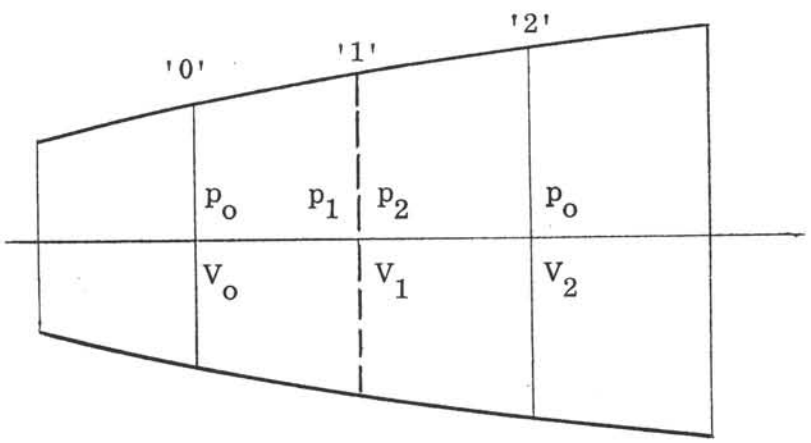

$$p_o + \frac{1}{2}\rho V_o^2 = p_1 + \frac{1}{2}\rho V_1^2 \qquad \text{(Energy)} \qquad (1)$$

$$p_o + \frac{1}{2}\rho V_2^2 = p_2 + \frac{1}{2}\rho V_1^2 \qquad (2)$$

$$V_o A_o = V_1 A_1 = V_2 A_2 \qquad \text{(Continuity)} \qquad (3)$$

$$(p_1 - p_2)A_1 = \rho V_1 A_1 (V_o - V_2) \qquad \text{(Momentum)} \qquad (4)$$

$$P_1 - P_2 = K \cdot \frac{1}{2}\rho V_1^2 \qquad \text{(Screen Loss)} \qquad (5)$$

where P = total pressure.

(1) and (2) give $p_1 - p_2 = \frac{1}{2}\rho(V_o + V_2)(V_o - V_2)$ (6)

and (5) reduces to

$$(V_o^2 - V_2^2) = KV_1^2 \qquad (7)$$

From (4) and (6)

$$\rho V_1(V_o - V_2) = \frac{1}{2}\rho(V_o + V_2)(V_o - V_2)$$

i.e. $$V_1 = \frac{V_o + V_2}{2} \qquad (8)$$

Then in (7)

$$(V_o - V_2)(V_o + V_2) = \frac{K}{4}(V_o + V_2)^2$$

i.e. $$K = \frac{4(V_o - V_2)}{(V_o + V_2)} \qquad (9)$$

Using (3) and (8) with (9)

$$\frac{A_2}{A_o} = \frac{4 + K}{4 - K} \tag{10}$$

$$\frac{A_1}{A_o} = \frac{4 + K}{4} \tag{11}$$

Inspection of (10) shows that this analysis sets an upper limit to K of 4 above which the expression for A_2/A_o becomes meaningless.

$$\text{Setting } K_{max.} = 4 \text{ gives } \frac{A_1}{A_o} = 2.$$

For any given diffuser to be screened the location of the screens should be established and the ratios of the mean cross-sectioned areas between any two sections found.

In the sketch below if A, B, C, etc. are the locations of the screens and if K_A, K_B, K_C, etc. are the respective screen loss coefficients then the mean areas $\overline{A}_{AB}$, etc. are found.

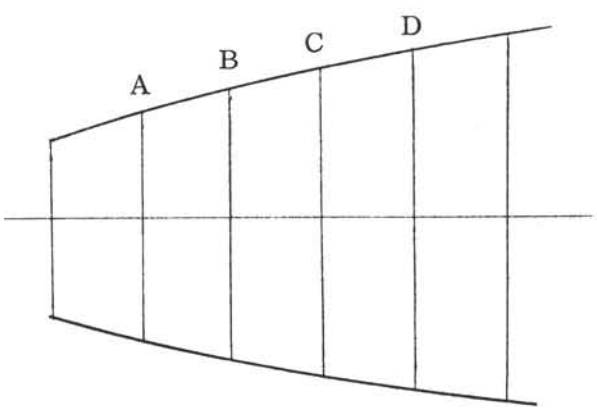

$$\overline{A}_{AB} = \frac{A_A + A_B}{2}$$

Referring now to Figure 1.6, the cross-sectional areas at stations 29, 31, 35, $39\frac{1}{2}$, $44\frac{1}{2}$, $49\frac{1}{2}$ and $54\frac{1}{2}$ were found.

Transposing of equation (10) gives

$$K = \frac{4(A_2 - A_o)}{A_2 + A_o}$$

Then

$$K_A = \frac{4(A_{31} - A_{29})}{(A_{31} + A_{29})}$$

where the subscripts refer to the station.

$$K_B = \frac{4(A_{35} - A_{31})}{(A_{35} + A_{31})}, \text{ etc.}$$

The following table gives the theoretical values of K for each screen.

TABLE I

THEORETICAL LOSS COEFFICIENTS

Screen	Station	$\overline{A}(ft.^2)$	K
	29	2.75	
A	29		0.33
	31	3.25	
B	33		0.486
	35	4.15	
C	37		0.42
	39½	5.125	
D	42		0.364
	44½	6.15	
E	47		0.307
	49½	7.175	
F	52		0.267
	54½	8.2	
G	57	8.7	0.12

The actual value of K is a function of screen solidity and wire Reynolds number.

Availability of mesh led to the use of screens as tabled in Figure 1.9 and the actual values of K are tabled below. The screen Reynolds number is based on the ideal velocity at the screen for a working section velocity of 166 ft./sec.

TABLE II

ACTUAL LOSS COEFFICIENTS

Screen	R_e	Solidity %	K
A	840	22	0.25
B	700	30	0.42
C	560	30	0.42
D	500	26	0.32
E	425	26	0.32
F	370	26	0.32
G	290	30	0.5

With the exception of screen G the actual values are not too far removed from those obtained by calculation.

Reference to Figure 1.9 demonstrates that the screens actually used do effectively hold the static pressure constant in the wide angle diffuser and it was decided that no great advantage would be obtained by following more closely the values of K given in Table I.

PART II

TESTS WITH THE ADDITION OF A BELLMOUTH INTAKE AND DRIVING FAN

2.1 INTRODUCTION

The work reported in Part I is devoted to evolving a satisfactory configuration in the absence of the usual bellmouth intake, owing to the means then at hand of driving the tunnel. Subsequently it became possible to connect with an exhauster set capable of inducing a flow of about 130 cu. ft./sec. of free air through the working section, giving a working section velocity of 100 ft./sec.

With the tunnel being run in this manner tests to determine the suitability of the bellmouth entrance could be made. The desire for simplicity and low cost fabrication led to starting with a very simple inlet which was somewhat sharp lipped but potentially easy to make at full scale. Subsequent smoke tests demonstrated that a more complicated profile was necessary to reduce edge losses due to turbulence caused by a sharp lip at the inlet.

The introduction of a driving fan brings in a new factor which in general will have a powerful effect on the performance of the tunnel compared with that obtained by driving through a supply of compressed air as in Part I or by connection with the exhauster. The fan performance characteristic is of importance since knowledge of its shape will permit one to predict the effect of model size on the tunnel performance.

The fan motor power in the model is 25 b.hp. which is equivalent to approximately 3600 b.hp. at full scale. Use of this power should entail a 50 percent increase in velocity over that obtained with 1000 b.hp. input.

2.2 Tunnel Description

2.2.1 Flow Induced by Exhauster Set

Figure 2.1 shows the tunnel diagrammatically with the connection to the exhausters.

It is seen that the bellmouth has been added immediately upstream of the station 0 referred to in Part I. Figure 2.2 shows the relevant dimensions of the inlet before and after modification. Apart from the addition of the bellmouth the tunnel configuration is identical with Configuration 5 of Part I. A conical duct was used to connect the exit of the diffuser to the inlet of the exhauster set which was a laboratory fixture. In the tests on this set-up Station '0', which is at the junction of the bellmouth and the fan section, is in the same position, relative to the other sections, as in Part I.

2.2.2 Tunnel Equipped with a Scaled Fan

Figure 2.3 shows a schematic of the general final form of the model tunnel.

Figures 2.75 and 2.76 show a three-quarter view and a close-up of the fan, respectively.

Two changes have been made for this arrangement. The fan section is 3 in. shorter than that used in the tests with the exhauster set and those tests described in Part I. Secondly, the contraction section is the one found to be the more suitable following the exhauster set tests.

Station '0' referred to in these tests is at the junction of the bellmouth and the cylindrical fan section and, because this section has been shortened, station numbers of other components are reduced by comparison with those in Part I and the exhauster set tests (e.g. working section entrance, formerly station 116 will now be referred to as station 113).

Figure 2.4 gives some of the fan details. Rotor and stator blade sections are basic C4 profiles on a circular arc camber line. For the rotor the camber at the mean diameter is 13.6 deg., whilst the stator camber is 50.5 deg. along the length. Stagger angles are 67.1 deg. at mean diameter for the rotor and 15.2 deg. along the length of the stator.

Rotor thickness/chord ratio varies from 15 percent at the root to 10 percent at the tip, while the stator value is constant at 15 percent.

At the mean diameter the design angle of attack is -2 deg.

There are 16 rotor blades and 15 stators.

2.3 Instrumentation

A smoke generator set was used to make visual observation of the flow around the intake lips and in the contraction section. Quantitative measurements of turbulence in the working section and in the entrance to the fan section were made using the Shapiro-Edwards hot wire anemometer. The control gear makes it possible to hold the anemometer wire current essentially constant through a stable, high gain, feedback control system.

The hot wire probe was constructed by welding a length of fine tungsten wire (.0002-in. nominal dia.) across the ends of two steel needles held parallel to each other in the probe body[1]. The wire length was about 0.1 in. giving a length/diameter ratio of 500/1. The instrument sensitivity to rapid heating or cooling is enhanced by using large ratios. Figure 2.5 shows the construction of the probe and Figure 2.6 outlines the arrangement of the components of the electronic equipment.

Pressure measurements were made using Kiel total head tubes, a simple round nosed total head tube, wall static taps where applicable, and a sphere type static pressure proble.

Static and dynamic pressure profiles in the working section behind a wing set at 30 deg. incidence were made using a 20-tube total head rake placed in the vertical plane followed by traversing with the sphere type static probe along the line of the rake tube heads (after removal of the rake).

Flow angularity was observed using a wedge type yawmeter with vernier reading on the angular scale. Angular changes of 0.1 deg. could be measured.

2.4 Outline of Tests (Exhauster Driven Tunnel)

2.4.1 Smoke Tests

The smoke generator was positioned ahead of the tunnel and set to give a filament of smoke flowing over the inlet. The visual flow was photographed (Fig. 2.77).

Smoke was also admitted into the stilling section so that the flow near the wall of the contraction section could be noted. A plug wall fitting was manufactured which gave an entrance angle of 30 deg. to the stilling section wall. Viewing was made by eye through holes drilled in the contraction section diametrically opposite the point of admission and also by looking upstream through the transparent ceiling of the working section.

2.4.2 Boundary Layer Tests

The probe used was as described in Part I. Profiles at station 116 (working section entrance) were obtained at intervals of 1/8 in. around one of the corners. Figure 2.7 shows the location and direction in which the traverses were made. To allow entry of the probe a slot was cut in the ceiling of the working section but care was taken to seal the aperture during measurement. Measurements were made with the original contraction section, as used in Part I, and with an improved section which was designed to make a better junction with the working section than the original. All measurements were made with a working section velocity of 80 ft./sec.

2.4.3 Turbulence Measurements - Hot Wire Anemometer Tests

These tests were made only with the modified bellmouth since the simple smoke tests made it obvious that the sharp-lipped entrance was giving a poor flow. The modifications consisted of rounding out the lip with a 1 1/8-in. radius curve blended into the 12-in. radius section. Surveys were principally made in the working section 17 3/4 in. downstream of the working section inlet. They took the form of horizontal traverses at heights of 10 1/4 and 1 3/4 in. above the floor. A further traverse was made along a horizontal radial line at station 15 1/4 (probe in the annulus formed by the bullet and the fan section wall).

In these tests working section velocity was held at 60 ft./sec., wire current varied from 40 to 60 ma. and wire resistance measured at each value of the current.

2.5 Outline of Tests (Fan Driven Tunnel)

2.5.1 Working Section Flow Properties

Total head traverses in a horizontal direction were made using a Kiel probe at three heights above the working section floor at station 129. Fan speeds of 1670, 2510 and 3340 r.p.m. were employed (corresponding to driving motor speeds of 600, 900 and 1200 r.p.m.). Static pressures along a sidewall centre line were also recorded. These measurements were made for an empty working section with and without the exit diffuser attached and with a range of wooden inserts placed in the working section, with and without the exit diffuser. The range of inserts used allowed the minimum area in the working section to be reduced to 30 percent of the full flow area. A typical insert is shown in Figure 2.8.

An undesirable feature of the thicker inserts was that flow breakaway occurred just downstream of the minimum section owing to the large divergence angles necessitated by the fixed working section length.

The purpose of employing the inserts was to obtain some idea of the increases in minimum section velocity that might be obtained through a procedure of this kind and as an incidental it has also given results from which an approximation to the fan characteristic could be made, using these results with the total head losses given in Figure 1.28. Traverses to obtain velocity distribution across the working section were made using a Kiel probe and a ball type static probe.

Pitch and yaw of the airstream with respect to the centre line were measured with a wedge type yawmeter. These latter tests for velocity profile and flow angularity were conducted with the tunnel in Configuration 12, i.e. with the inlet diffuser screens removed and vortex generators substituted to provide the mixing necessary to proper diffuser operation.

2.5.2 Boundary Layer Tests

Measurements were made as outlined in the section on the exhauster driven flow (see Fig. 2.7 for the traverse lines). In addition, profiles were obtained along a sidewall centre line at stations 115 1/4, 133 and 150 5/8 with working section velocities of 60, 95 and 120 ft./sec. (Note that the junction of contraction section and working section is now referred to as station 113.)

2.5.3 Turbulence Measurements - Hot Wire Anemometer Tests

Measurements were mainly restricted to the inlet and the working section, but a few tests were made ahead of the intake and the stilling section. Traverses were made as outlined in Section 2.4.2 for two heights above the floor, 17 3/4 in.

downstream of the entrance to the working section. A working section stream velocity of 60 ft./sec. was used to provide a direct comparison with the results obtained from tests with the exhauster set. In this way the quantitative effect of the fan can be assessed.

Additionally the effect of airspeed has been determined through testing up to airspeeds of 160 ft./sec. The decay of turbulence along the working section has also been investigated by traverses made near the entrance and exit respectively.

2.5.4 Wide Angle Exit Diffuser

To reduce the cost of construction it was decided to test a wide angle exit diffuser equipped with vortex generators. The form of this diffuser is shown in Figure 2.9. The area ratio between its exit and entrance is 2 and mixing is initiated through 24 vortex generators of cambered sheet metal form. These were placed with their 1/4 chord points at station 151 3/8. Sets of four were placed each on the roof and floor respectively and the remainder attached to the vertical walls.

The arrangement was that alternate generators had equal incidence and such that the corner flow passed between two generators having opposite stagger, i.e. a converging passage was formed at the corner.

Tests were made for a range of vortex generator angles with the working section empty. Further tests were made with vortex generators at 16 and 10 deg. incidence and employing a "two-dimensional" wing in the working section at 15 and 30 deg. incidence.

The effect of a large obstruction in the working section on the operation of the wide angle exit diffuser was checked by measuring the static and dynamic pressure profiles behind a wing (described in Section 1.2) fixed horizontally at mid-height for 30 deg. incidence with the 1/4 chord axis at station 132.

Pressures were measured in three vertical planes (5 in., 3 in. and 1 in. from the sidewall) using the 20-tube total head rake which spanned the working section vertically and the sphere type static probe referred to in Section 2.3.

2.5.5 Inlet Diffuser Tests with Screens Removed

Whilst there was no doubt as to the effectiveness of multiple screens in promoting full flow in the wide angle inlet diffuser, it was realized that this filling is only obtained at the expense of diffuser pressure recovery.

It was decided worth while to attempt to run the tunnel with these screens removed and vortex generators placed upstream of the diffuser entrance, their object being to energize the boundary layer and prevent general separation.

A total of 90 vortex generators was placed in the fan stator spaces, 60 being fixed to the outer wall and the remainder to the surface of the bullet. The test was of a cut and try nature since nothing was known of the boundary layer thickness in the stator spaces and the flow direction was only approximately known. Vortex generators of 0.5-in. chord and 0.35-in. span were employed. They were formed from 0.032-in. thick brass plate with 8 percent camber. Their angular setting with respect to the axial direction was found by trial. The usefulness of the vortex generator in preventing or delaying separation in a diffuser depends to some extent on the ratio of span to boundary layer thickness at the plane of the vortex generators. However, in this case, the boundary layer thickness may be expected to be strongly influenced by the presence of the vortex generators, so that it was necessary to guess the thickness and oversize the vortex generator span to allow for later shortening if that should prove necessary.

2.5.6 Fan Characteristic

An approximation to the fan characteristic could be obtained through measurements of total head and static pressures in the working section, using the inserts for applying resistance to flow, and employing the pressure losses between fan outlet station and working section which were reported in Part I (Fig. 1.28).

However, this experimental procedure was cumbersome since installation of the blocks entailed dismantling the exit diffuser and, in any case, it was felt that the more direct approach of measuring total head behind the fan stators would be preferable. Flow restriction was obtained through the use of a rectangular butterfly valve installed at the rear of the working section. Movement of the valve was made through worm gearing. The air weight flow was obtained through measurement of velocity at working section entrance. Fan outlet total pressures were measured using two 8-tube total head rakes placed in two differing angular positions in the stator spaces behind the fan rotor. The pressures were recorded on a multitube manometer.

Pressures were recorded for constant non-dimensional fan speed lines at intervals of 300 r.p.m., starting with $\frac{N}{\sqrt{\Theta}}$ = 1200 r.p.m. and rising to 3300 r.p.m. The weight flow range was obtained using butterfly angles from 0 to 24 deg. in steps of 3 deg. with the working section exhausting directly to atmosphere and from 0 to 12 deg. in steps of 6 deg. with the long exit diffuser attached.

2.5.7 Thick Strut at Intake

The addition of an 8000 b.hp. free turbine drive for the fan calls for a means of supplying approximately 90 lb. of hot gas per second to the fan driving turbine (situated in the bullet) and for piping the exhaust gases away. It was decided that two pipes should run vertically across the intake mouth into the bullet and that both could be enclosed in a symmetrical strut section of 11-ft. chord and a fineness ratio of 3.

A wooden model of the proposed strut was mounted, as indicated in Figure 2.4, interposed to bisect the angle between the lower two bullet support struts.

Wake traverses were made at station 15 (2.5 in. upstream of fan LE at various blade heights) to check on the strength of the wake that the fan would encounter from the proposed strut. It was feared that a strong wake would give rise to unpleasant or dangerous fan vibration.

A further traverse was made in the working section to check on the presence of the wake there.

2.5.8 Crosswind Tests

With the reservation that the proper simulation of the effects of external winds on the working of the fan and on the flow in the working section was impossible, owing to the lack of means of providing (a) an external wind of sufficiently large an extent and (b) correctly scaled surroundings, it was decided to investigate the working section flow with a limited crosswind at right angles to the intake. A duct was constructed and erected so that a quite uniform airstream extending from floor level to a height of 6 ft. with a width of 1 ft. was directed across the bellmouth entrance. Three large cooling fans were installed in the duct and were able to provide a stream of 19 ft./sec. at the duct exit. With the crosswind blowing, total head and static pressure profiles were measured in the working section and used to deduce the velocity profile.

2.5.9 Flow in Working Section with a Perforated Floor

For the testing of large fan-in-wing models it was decided necessary to obtain an effective increase in working section height. This would cause fan flow to discharge more readily downstream. For this purpose a well 5 ft. deep running the length and breadth of the working section was suggested with a light metal grid forming the support for the normal solid floor which would be installed for aerodynamic testing of models sized to the working section.

A plywood box with open top was fitted in place of the normal working section floor. Simulation of the grid was attempted by using a screen of wire mesh (4x4 to the inch with wire diameter of .032 in.).

Measurements of velocity and flow angularity were made with the floor completely open to the well and also for the following partial blockage:

Stations 113 to 123 - blocked

Stations 123 to 133 - open

Stations 133 to 140$\frac{1}{2}$ - blocked

Stations 140$\frac{1}{2}$ - 143 - open

Stations 143 to 153 - blocked

2.6 Results (Exhauster Driven Tunnel)

2.6.1 Smoke Tests

Qualitatively, the tests involving smoke flowing over the inlet suggested that there was nothing unreasonable about the contour of the modified bellmouth (Fig. 2.77), while that of the basic sharp-lipped entry was seen to be obviously unsuitable. The form of this part of the intake was obtained without reference to aerodynamic design, it having been decided that the effort involved in arriving at a contour by approved methods would, in this case, only marginally improve the flow. For these tests the exhauster flow was adjusted to give a velocity of up to 100 ft./sec. in the working section.

Admittance of smoke into the stilling section showed up a certain unsteadiness in flow in the contraction section. Smoke admitted approximately tangential to the wall at the point from which it flowed close to the generator of the contraction section, which meets the working section floor centre line, was seen to be unsteady. At a very low velocity in the stilling section, corresponding to 30 ft./sec. in the working section, the smoke filament was seen to oscillate with a constant amplitude judged to be about 0.5 in. Increasing the flow to give a velocity of 65 ft./sec. in the working section produced a definite change in the smoke pattern. The amplitude of the smoke oscillation changed with time, rising from a minimum of about 0.5 in. to about 2 in., then decreasing, in a periodic manner. The appearance of the smoke train suggests that the airflow was being disturbed by two sources of unsteadiness having a slightly different frequency from each other, hence the 'beating' appearing in the smoke train. With flow increased to give 100 ft./sec. in the working section there was some change in appearance of the smoke. The minimum amplitude remained at 0.5 in. and the maximum amplitude appeared reduced compared with that seen at 65 ft./sec. The frequency of side-to-side fluctuation in the smoke increased while the frequency of 'beating' remained as for 65 ft./sec.

Admittance of the smoke so that it passed over one of the corners at the junction of the contraction and working sections showed the airflow here to be oscillatory with a constant amplitude. With a velocity of 35 ft./sec. in the working section the amplitude was estimated to be 0.5 in. rising to 1.5 in. for 60 ft./sec. then falling to 1 in. for 100 ft./sec. and 0.5 in. at 110 ft./sec. in the working section.

2.6.2 Boundary Layer Measurements

As has been stated in Section 2.3.2 it was found inconvenient to traverse the boundary layer at right angles to the wall. All traverses were made in the vertical direction over the right hand upper corner of the working section (viewed downstream). Typical profiles obtained are shown in Figures 2.25 and 2.27 - but it is emphasized that these are not true boundary layer profiles. The results are best presented in Figures 2.26 and 2.28 which show contours of constant velocity head obtained from the measured 'profiles'. It is apparent that the modified contraction section has

caused the boundary layer at the junction of contraction section and working section to be considerably thinner than that with the original section. Presumably this is due in part to the contraction section having a constant geometrical area over a length of 1 in. upstream from the junction. The appearance of the 'profiles' suggests that in the test on the unmodified contraction section transition has occurred upstream of the junction, whilst for the modified section laminar flow may still exist, as it should, in view of the strong favourable pressure gradient. It should, however, be stated that at the time of these tests the original section had seen much more service than the modified section and had been ducting hot air (see Part I) contaminated with pipe scale which had seriously roughened the surface.

2.6.3 Turbulence Measurement

An estimate of turbulence intensity has been made at two longitudinal positions in the tunnel. The first position was at station 15 3/4 and a radial traverse was made here from a point 1/4 in. from the duct wall to 5 in. from this wall. A traverse across to the inlet bullet was not possible owing to the probe body being too short. In this longitudinal position the probe was 3/4 in. ahead of the first screen. The results shown in Figure 2.34 give the usual form of turbulence intensity in a duct, that is a more or less constant level away from walls with a sharp rise in the vicinity of the wall.

In these tests the probe body was held so that the sensing wire was vertical. In this position it would sense the longitudinal component of the turbulence so that the RMS value of the voltage across the wire will be proportional to the RMS value of u:

$$e_{wire} \propto \sqrt{\overline{u^2}}$$

The second longitudinal position was in the working section 17 3/4 in. downstream of the junction with the contraction section (station 133 3/4). At this position horizontal traverses for heights above the floor of 10 1/4 in. and 1 3/4 in. were made (Fig. 2.35). The traverses ranged from 1/4 in. to 5 in. from the wall. The probe was mounted as above so that again $e_{wire} \propto \sqrt{\overline{u^2}}$.

The results indicate that the free stream turbulence is high both in the inlet and working section, but not too much reliance should be placed on the actual values shown. The estimate was made by observing the output from the amplifier on an RMS voltmeter and roughly estimating the pointer mean position while it was responding to the rapidly varying level of turbulence encountered. However it may be said, as Figures 2.34 and 2.35 indicate, that the intensity of turbulence does increase appreciably between inlet and working section mid-height.

The sharp increase in intensity as the wall is approached is typical. Owing to the nature of the probe positioning device, it was not possible to show the subsequent drop in turbulence which is encountered as the wall distance tends to zero.

The method used was that of 'Constant Current Calibration' developed by Dätwyler[2]. In this paper it is shown that the intensity of turbulence u' is given by

$$u' = \frac{e}{\left(\frac{I}{2}\right)^2 \frac{dR}{dI} \left[1 - \left(\frac{I_o}{I}\right)^2\right]}$$

and

$$u' = \frac{\sqrt{\overline{u^2}}}{U} .$$

Reference should be made to the section on nomenclature for definition of the quantities in the above expression.

The high value of turbulence in the inlet may possibly be ascribed to the unfortunate positioning of the tunnel. The only location available owing to the means of running the tunnel was in a general machinery room. The intake was unavoidably placed close to large fixed objects and the room suffered from considerable thermal gradients.

2.7 Results (Fan Driven Tunnel)

2.7.1 Working Section Flow (Screened Inlet Diffuser)

With the diffuser attached the results given in Figures 2.10, 2.11 and 2.12 show that the stream total head was constant within 4 percent of the maximum over 60 percent of the working section width for the three fan speeds quoted and within 10 percent over 80 percent of the width. However some asymmetry in the flow is evident, particularly at the two lower fan speeds. Variation in total head in the vertical direction at points equidistant from the wall is seen to be about 4 percent or less from that at mid-height so it may be inferred that about 40 percent of the cross-sectional area of the working section is running at essentially constant total head.

The introduction of higher back pressures by removal of the diffuser and subsequent insertion of blocks seems to 'flatten out' the profile (Fig. 2.13 to 2.21 inclusive).

At no time was there any indication of a severe fan stall. A reduction of working section geometrical area to 30 percent of the unrestricted area was obtained by insertion of 7-in. blocks. Figure 2.23 is a form of fan characteristic obtained by restricting flow with blocks in the working section. The total head is that measured in the working section by traversing horizontally. At the lowest mass flows corresponding to each speed it appears that the constant speed line is beginning to assume a positive slope.

Wall static pressure distributions for three fan speeds are shown in Figure 2.22 and are compared for the original contraction section and the modified section. At the lowest fan speed it is seen that the kink in static pressure near the entrance to the working section has been removed by use of the modified section and that at the higher speeds the variation is much reduced.

Figure 2.24 is representative of the changes in minimum section velocity obtained by restricting the working section area.

2.7.2 Boundary Layer (Screened Inlet Diffuser)

Similar traverses to those reported in Section 2.6.2 were made with the fan running and its speed set to give about the same working section velocity as in the exhauster driven case. The 'profiles' (Fig. 2.29) obtained by traversing vertically as outlined in Section 2.6.2 show some resemblance to those obtained with exhauster flow, and the constant velocity head contours (Fig. 2.30) indicate that the boundary layer thickness at the junction of contraction section and working section has been changed little by changing from exhauster to fan drive (it is to be noted that with the fan drive the modified contraction section only was used).

Further traverses were made to note the growth of boundary along the centre line of one working section sidewall. Three points were selected along the centre line, viz. stations 115 1/4, 133 and 151 5/8. At each of these positions, traverses were made normal to the wall for airspeeds of 60, 95 and 120 ft./sec. The experimental points are shown in Figures 2.31 and 2.32. At station 115 1/4 it is apparent that Howarth's solution to the laminar boundary layer equations for a flat plate is a reasonable fit at all three speeds. At stations 133 and 150 5/8 a 1/7th power law velocity distribution seems to be a reasonable fit on the experimental points. Transition is seen to occur at some point between stations 115 1/4 and 133. Figure 2.33 shows the boundary layer growth along the working section sidewall centre line. A slight thinning down of the layer at station 150 5/8 with increasing speed is apparent.

2.7.3 Turbulence Measurement (Screened Inlet Diffuser)

Measurements of the intensity of longitudinal turbulence u' were made mainly in the working section and in the inlet ahead of the fan. A few tests were also made - ahead of the intake and in the stilling section.

The effect of a vertically running, circular section pipe, 32-in. dia. at full scale with its centre line 67 in. ahead of the bellmouth intake plane, was roughly simulated by placing a wooden cylinder (2.7-in. dia.) 5.6 in. ahead of the intake.

Figure 2.36 shows a profile of u' in the working section for heights of 10 1/4 in. and 1 3/4 in. above the floor at station 130 3/4. The trend exhibited with the exhauster driven tunnel has been reversed, the higher level now being 10 1/4 in. above the floor, and at this height there has been some increase compared with the former results with the exhauster drive. For the tests giving these results the screening layout was identical with that for the exhauster driven tests, i.e. Configuration 3, Figure 1.9.

Some changes in screening were now made. Figure 2.37 shows the results with an 18 x 18 mesh screen fixed over the intake. It appears that little change has been effected at the important working section positions, i.e. 10 1/4 in. above the floor.

The 18 x 18 screen was removed from the intake and placed at the downstream end of the stilling section (station 66). The results for measurements made at station 130 3/4, 10 1/4 in. above the floor (Fig. 2.38) show little change from those with the screen over the intake. The application of a 20 x 20 x .016 screen over the intake in addition to the screen at station 66 changed the shape of the curve but did not appreciably alter turbulence values near the centre (Fig. 2.39).

At this juncture the probe was moved to the inlet (station 6 3/4). The typical results of a traverse are shown in Figure 2.43 and it is seen that the turbulence levels are very high (an order greater than in the working section). In contrast two points are shown, for the same probe station, which were obtained at a different time of day and these show the intake level to be of the same order as that in the working section. It should be said that these tests were carried out in the winter time and that the heating system in the room is known to introduce marked thermal gradients. In contrast, the measurements in the inlet with the tunnel driven by the exhauster set were considerably lower - these tests were made during the summer when the shop heating system was not engaged.

The most striking point, however, is that the air in passage from station 6 3/4 through the fan and screens of the wide angle diffuser and stilling section and the contraction section attains a turbulence level which is largely independent of conditions in the intake since the measured values with the above screens invariably attained a value of about 0.6 percent at the centre. The first appreciable decrease in turbulence was obtained by moving the 18 x 18 x .011 screen to station 54 and placing the 20 x 20 x .016 screen at station 66. The turbulence profile for the arrangement of screens is shown in Figure 2.40.

The intensity was progressively decreased through the introduction of fine screens. Figure 2.41 depicts the results obtained with an 18 x 18 x .011 screen at station 54 followed by a 50 x 36 x .010 screen at station 66. Compared with the

results given in Figure 2.40 this arrangement has resulted in approximately 41 percent decrease for the centre of the working section. The replacement of the 18 x 18 x .011 screen by a second 50 x 36 x .010 gave further considerable improvement. With this arrangement the intensity in the centre of the working section was measured at 0.15 percent (Fig. 2.42), i.e. a drop of 35 percent compared with the results obtained using one fine screen.

A few 'ad hoc' tests were made with the 18 x 18 x .011 screen at station 54 and the 20 x 20 x .016 screen at station 66. The first of these consisted of placing a cylindrical object vertically in front of the intake to simulate an unfaired gas feed pipe to a fan driven turbine which is expected as a future development of the tunnel. In the model a wooden cylinder 2.7-in. dia. was used, mounted vertically at the intake.

Intensity measurements were made at station 130 3/4, 5 in. from the wall and 10 1/4 in. above the floor. At a velocity of 60 ft./sec. the 'pipe' effect was very marked - its presence contributed an increase of 90 percent. At 100 ft./sec. it was responsible for a 40 percent increase in turbulence. These figures indicate the need for a faired piping across the intake.

The second test was a measurement of turbulence in the stilling section. Values were obtained at station 60 with the probe at two points, viz. 1 in. and 2 in. from the wall, and a working section velocity of 60 ft./sec. The intensities measured were 2.15 and 2.22 percent respectively or roughly five times the largest measured value in the working section with these screens. With the assumption that the absolute value of the longitudinal turbulent velocities does not change along a contraction section, then, since the contraction area ratio is six, the percentage longitudinal turbulence in the working section would have been one-sixth of those in the stilling section.

2.7.4 Wide Angle Diffuser Tests (Screened Inlet Diffuser)

The results for the efficiency of conversion of working section dynamic pressure to static pressure in the exit diffuser are shown in Figure 2.44.

It is apparent that in terms of static pressure recovery there is little to choose between the short diffuser with vortex generators and the conventional low diffusion rate long diffuser. It is also apparent that for the three settings of the vortex generator angle of attack there is little change in performance.

Figure 2.45 shows the efficiency for α_{VG} = 6 deg. and it is evident that this angle is in the range where angle of attack is critical. The similarity in shape between the curves for α_{VG} = 10 and 6 deg. is thought to be noteworthy. Because of this similarity it seems reasonable to suppose that below 10 deg. the diffuser will be fairly sensitive to vortex generator angle of attack. A further point to be noted is that the efficiency becomes more dependent on the velocity at entrance to the diffuser as α_{VG} is reduced. The test results with a large obstruction in the shape of a wing spanning the section (as in Part I) mounted with its axis

10 in. above floor level and at 30 deg. incidence are shown in Figure 2.46. It appears that the severely distorted velocity profile behind the wing benefits the diffuser efficiency. A possible explanation is that the vorticity shed by the wing aids the vortex generators in obtaining a more continuous mixing of the flow in the diffuser.

2.7.5 Inlet Diffuser Tests with Screens Removed

The pressure recovery of the inlet diffuser with screens removed and vortex generators placed in the stator spaces is shown in Figure 2.47. The results are considered very encouraging, in view of the rough approach to obtaining the vortex generator size and spacing, especially when the performance depicted in this figure is compared with that of Figure 1.9. The 'ideal' curves drawn on Figure 2.47 have been obtained by plotting the ideal pressure rise from the geometry of the duct, i.e. $p_{outlet} - p_{inlet} = q_{inlet} \left(1 - \frac{A^2_{inlet}}{A^2_{outlet}}\right)$ to pass through the experimental point nearest the inlet of the diffuser. On this basis the static pressure rise efficiency of the inlet diffuser is in the neighbourhood of 84 percent of the 'ideal'.

During the tests it was observed that the inlet diffuser wall static pressures were quite steady, but of course this is an observation affected by the manometer response time which is quite large. Wool tufts placed on the rear cone of the central bullet and along the length of the diffuser wall showed that some separation was occurring near the cone tip and at the corresponding station on the outer wall. To investigate further the flow state in the diffuser a radial traverse of total head was made at station 53, i.e. 1 in. upstream of the junction of inlet diffuser and stilling section. The results of this test are shown in Figure 2.48 and indicate a satisfactory distribution of total head at diffuser exit.

Further development could include modifying the planform of the vortex generators to approach constant circulation along the span and hence a single strong vortex, and progressive lengthening or shortening of the span to improve the suitability of the vortex generators if the thickness of boundary layer present could be determined. Conditions were not good for boundary layer measurement at the plane of the vortex generators owing to aerodynamic unsteadiness contributed by the fan shed vorticity. A total head traverse radially inwards to a depth of 1 in. was made (Fig. 2.49). The profiles of this figure suggest a boundary layer thickness of about 0.7 in. for fan speeds from $\frac{N}{\sqrt{\Theta}} = 1665$ to 3170. However in view of the normal blade tip clearance of .04 in. and the short distance from the fan trailing edge to the measuring station (5.1 in.) this thickness appears excessive. These profiles are probably the distribution of total head behind the fan tip and it is possible that only a very thin true boundary layer exists. Reliable measurements of the thickness of this layer would probably present great difficulty.

However, it is felt that the effectiveness of the vortex generator in this application has been demonstrated and that optimization of the form, number and location of vortex generators would be best left to full scale development.

2.7.6 Working Section Flow (Inlet Diffuser Screens Removed)

Following the removal of the screens in the inlet diffuser, total head and static pressure measurements were once more taken in the working section to determine the quality of the flow following the change. Results of the total head surveys are given in Figures 2.50 to 2.54 for fan speeds from $\frac{N}{\sqrt{\theta}} = 1112$ to 3060. It is seen that the profile uniformity is close to that displayed in Figures 2.10 to 2.21 inclusive.

Static pressure surveys made in the same plane as the total head measurements using the ball type static probe showed that the static pressures measured away from the walls were very close to those indicated by the wall tappings so that the variation in velocity profile is even less than that in the total head.

Figure 2.55 exhibits the gain in working section velocity obtained by using vortex generators in place of screens in the inlet diffuser. Electrical measurements taken during the tests showed that, with reasonable assumptions for driving motor efficiency and gearing losses, the energy ratio, E.R., for the tunnel with screened inlet diffuser is 1.07 and 1.33 with vortex generators installed at the entrance to the inlet diffusers.

The experimental results following tests for flow angularity in the working section are seen in Figures 2.56 to 2.59. In pitch they indicate a somewhat more unsatisfactory state of affairs than in yaw, owing to the greater sensitivity of wings to angle of attack changes than to yawing angle changes. Unfortunately the pitch angle picture changes with fan rotational speed especially on the left hand side of the working section (looking downstream) so that trimming of the fan stators by tabs is not expected to be effective over the entire speed range of the tunnel.

During the course of the yaw measurements it became necessary to break the tunnel at the stilling section joints to clean the fine screens which had become coated with oil and dust. Figures 2.57 and 2.59 show the measured yaw angles in the working section before and after this operation respectively. Figures 2.65 and 2.67 show the working section velocities before and after the cleaning.

These figures indicate that there is some doubt as to the applicability of the yaw and pitch measurements on the model tunnel for predicting the flow direction in the full scale working section. The differing values of yaw measured before and after cleaning could be due to a different screen blockage, screen tautness or a change in alignment of the tunnel after rebuilding. Reference to Figure 2.59 indicates that the whirl in the working section is approximated by 'solid' rotation over the range 4 in. from the ceiling to the horizontal centre line and free vortex flow from the ceiling to the 4-in. point.

2.7.7 Turbulence Measurement (Inlet Diffuser Screens Removed)

A penalty in the form of a considerable increase in turbulence as a result

of employing vortex generators at the entrance to the inlet diffuser is seen by comparing the turbulence profile for this condition (Fig. 2.60) with those obtained with the screened diffuser (Fig. 2.42).

An interesting observation is that the profile obtained with the vortex generators is much flatter than that with the screens, presumably as a result of the more thorough mixing obtained.

Figure 2.61 shows the decay of turbulence along the centre line of the working section.

2.7.8 Fan Characteristic (Inlet Diffuser Screens Replaced by Vortex Generators)

Figure 2.62 shows a detailed fan characteristic obtained from total head measurement in the annulus behind the fan rotor. It is clear that, with a virtually empty working section ($\alpha_B = 0$) and an exit diffuser attached, the working line is well to the right of the stall region.

No adverse flow effects were noticed on reducing the mass flow below that for general stall of the rotor - manometer readings continued to be steady for the maximum restriction used.

As previously stated the weight flow through the fan was computed from the measured working section velocity. Preliminary traverses for total head and static pressure near the working section entrance showed that even for the highest restrictions the velocity over the whole cross section near the entrance was very uniform, so that in the actual tests for the fan characteristic the positions of the total head and static pressure probes were left fixed. Figure 2.63 is presented to show the progression of the stall from root to tip.

2.7.9 Thick Strut at Intake (Inlet Diffuser Screens Removed)

Total head traverses, in a circumferential sense, were made for several radii at station 15. Pressure measurements in the wake of the strut made in this manner revealed only a minor deficiency in total head at the measuring station and that the wake itself had widened to a maximum of about two strut thicknesses. (See Figure 2.64 for some representative profiles.)

A total head traverse in the working section did not reveal any total head deficiency which might have persisted from the strut wake. Wool tufts on the strut indicated attached flow for 90 percent of the chord following the fixing of boundary layer trip wires at separation at the one-quarter chord station. Prior to the use of the wires tufts revealed separation at approximately the three-quarter chord point.

2.7.10 Crosswind Tests

Results of the crosswind test (Fig. 2.66) show that no distortion of velocity profile in the working section occurs as a result of a crosswind having a

limited extent and a velocity of 19 ft./sec. The only noticeable effect was that the working section velocity decreased on application of the wind. This can be seen by comparison of Figure 2.66 with Figure 2.65.

The insensitivity of the working section velocity distribution to cross-wind was expected since the fan has a high solidity.

It will be seen that the velocities of Figure 2.65 are considerably lower than those of Figure 2.55 for the same fan speeds. This was found to be due to dirty screens (considerable amount of testing took place between the tests of Figure 2.55 and those of Figure 2.65). Cleaning of the screens resulted in the higher velocities being restored as seen from Figure 2.67 which are the results of tests after cleaning. The results shown in Figures 2.65 and 2.66 can be compared since they are the results of consecutive tests.

2.7.11 Flow in Working Section with Perforated Floor

The velocity traverses shown in Figures 2.67, 2.68 and 2.69 compare the flow quality in the working section for three floor states, i.e. solid floor, partially open to the well and fully open to the well. It is apparent that partial or full opening of the floor did not affect the uniformity of velocity very much, nor the average value of the velocities.

At the highest fan speed possibly the open floor version shows the highest distortion (2 percent of the maximum).

Flow angularity for the partially open and fully open floor states is of a similar nature to that with the floor closed (Fig. 2.70 to 2.73 inclusive for comparison with Fig. 2.56, 2.67 and 2.58).

2.8 Conclusions

The operation of the VTOL tunnel in model form has been explored in some detail and the following conclusions are drawn:

(1) Working section flow is satisfactory with regard to uniformity of velocity but possibly poor with regard to flow angularity, especially pitch. Further work is required to determine the real nature of the whirl and to reduce it to an acceptable amount.

(2) It has been demonstrated that the 28-deg. inlet diffuser can operate satisfactorily in the absence of screens, provided that a sufficient number of suitable vortex generators are placed upstream of the inlet to the diffuser. The power requirement for a given working section velocity is reduced, using vortex generators, by comparison with that necessary when the screening arrangement in Part I of the report is used.

(3) The longitudinal turbulence level in the working section is moderate with screens used in the inlet diffuser. A doubling of this level was obtained when vortex generators were used to replace the screens.

(4) In the absence of an exit diffuser there is a limit to the increased velocities that can be obtained by restricting the working section area. There will be some latitude on the limit for a given fan speed which depends on the form of the restriction, i.e. on whether the working section is lengthened to accommodate nozzle blocks having smaller divergence angles than those used in the test.

(5) An exit diffuser of 2:1 area ratio which is much shorter than the conventional low angle diffuser will operate quite as well if a sufficient number of suitable vortex generators are placed upstream of its inlet. Its efficiency appears to be enhanced by a large blockage upstream.

(6) Fan operation is very tolerant of working section blockage. The weight flow for an empty working section may be at least halved with no apparent ill effects, i.e. fan vibration, unsteady flow.

(7) The presence of a strut fairing thick enough to shroud the piping necessary for a turbine drive does not give a strong enough wake to impede fan operation and the wake is unnoticeable in the working section.

(8) The fan solidity and form of the tunnel seem to be adequate in ensuring undistorted working section velocity profiles for a limited extent crosswind up to 19 ft./sec.

(9) A perforated working section flow with a well beneath has little or no effect on the magnitude of the velocity nor on its uniformity.

(10) The bellmouth intake used in modified form appears to be satisfactory.

(11) The tunnel energy ratio (1.07 with screened inlet diffuser and 1.33 with vortex generators at the inlet to the diffuser) is compatible with other low subsonic non-return wind tunnels.

With the installation of 1000 b.hp. at full scale the design requirement of 120 ft./sec. through the working section should be exceeded by 17 ft./sec. with a screened inlet diffuser and by 27 ft./sec. if vortex generators are used.

2.8.1 Recommendations for Full Scale Tunnel

As a result of the model tests it is suggested that the full scale VTOL tunnel incorporate the following features:

(1) Unscreened inlet diffuser fitted with vortex generators in the stator spaces. The final number, form and setting of these vortex generators should be obtained by full scale development tests. A starting point in the development can be made with a geometrically scaled up model vortex generator using the same number, axial location and setting.

(2) Fine screens to be erected in the stilling section to obtain as low a turbulence level as possible provided that the tunnel velocity is not seriously affected.

(3) The working section should contain a well of about 5-ft. depth running the length and breadth of the working section. (Openings in the floor between working section and well should be available, scaled from areas and locations indicated in Section 2.5.9.)

(4) The piping to and from the power turbine situated in the bullet should be sized to fit a scaled up version of the model strut. The full scale strut sealed up from the model will be able to accommodate pipes of 39 in. I.D. and 31 in. I.D. with sufficient clearance to allow pipe wall thickness commensurate with the internal pressures.

(5) A scaled up fan and stator system will be suitable.

(6) A scaled up bellmouth intake will be adequate.

(7) The exit diffuser should be scaled up from the internal dimensions given for the model short exit diffuser. Provision for attachment of vortex generators upstream of the inlet of this diffuser (in a scaled position indicated from the model arrangement) should be made. The final form, number, location and setting of these vortex generators will be a matter for full scale development.

(8) Provision should be made if necessary for removing or reducing working section flow angularity. The means of doing this will depend on the results of further model tests.

2.9 References

1. Hinze, J. — Turbulence. McGraw-Hill, New York, 1959.

2. Dätwyler, G. — Zwei Beiträge Zur Hitzdraht-Messmethode. (Two Contributions to Hot-Wire Anemometry.) Helvetia Physica Acta, Vol. 15, 1942, pp. 266-272.

3. Taylor, H.D. — Application of Vortex Generator Mixing Principle to Diffusers. United Aircraft Corporation R-15064-5, Dec. 1948.

4. Hall, A.A. — Measurements of the Intensity and Scale of Turbulence. ARC R&M 1842, Aug. 1938.

/LES

PART II

APPENDIX B

CALIBRATION OF TURBULENCE MEASURING EQUIPMENT

The method employed was to measure the turbulence in a duct similar to the 'standard' duct described below.

Some results are given in Reference 4 for the distribution of longitudinal turbulence in a long smooth pipe which had an internal diameter of 1.5 in. The flow through the pipe was obtained from a large reservoir which was maintained to give a centre line velocity (fully developed pipe flow, at a station 80 diameters downstream) such that the Reynolds number based on this velocity, pipe diameter and pertinent kinematic viscosity was 14,800.

The smoothing of any unsteady flow originating from the reservoir was effected by fitting the pipe with a honeycomb at its entrance.

A similar test was made using a 13-ft. length of hard drawn copper tubing of $1\frac{1}{2}$ in. I.D. It was fitted with a bellmouth entrance, and an airflow was obtained by connection to an industrial type vacuum cleaner fitted with a fine speed control. With this arrangement a very steady velocity could be obtained as measured by a centre line pitot tube and a wall static tapping placed 84 diameters downstream of the end of the pipe. The hot wire probe with micrometer adjustment was placed 80 diameters downstream of the inlet and arranged for radial traversing. The airflow was adjusted to give a Reynolds number on the centre line of 14,800.

The turbulence profile is shown in Figure 2.74. From these results it was concluded that the hot wire anemometer and the associated electronic equipment was making a reasonably accurate measure of the turbulence in the tunnel working section.

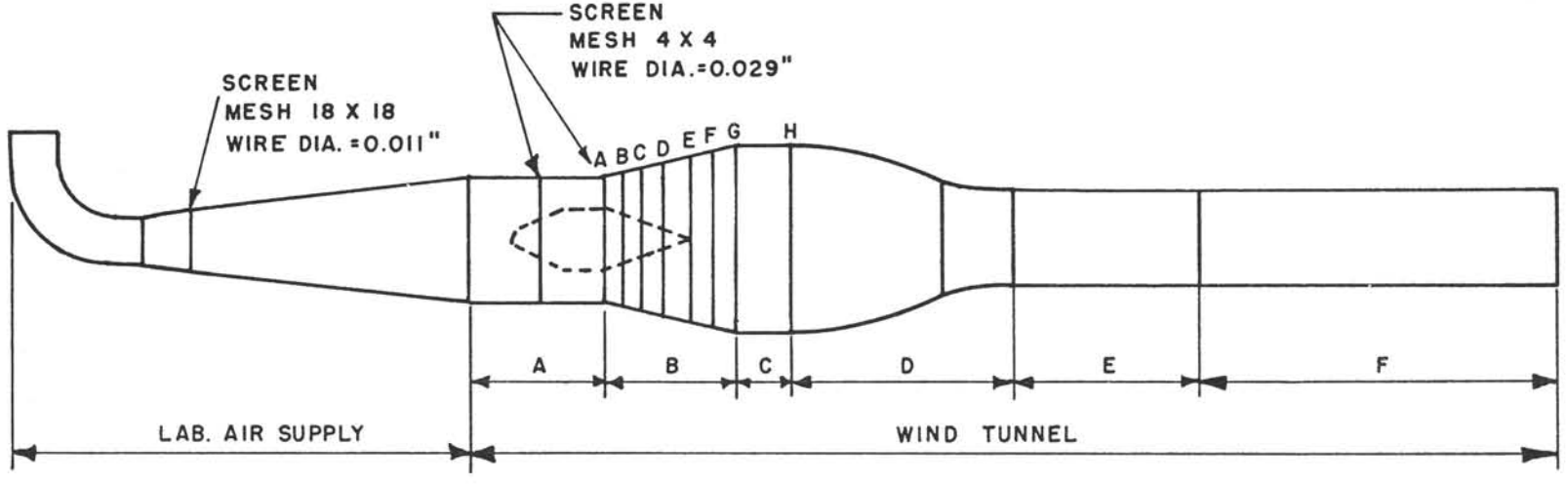

A - FAN SECTION
B - DIFFUSER
C - STILLING SECTION } VARIOUS SCREENS INSTALLED, FLANGE "B" TO FLANGE "H"
D - CONTRACTION SECTION
E - WORKING SECTION
F - EXIT DIFFUSER

GENERAL LAYOUT

1/12 SCALE VTOL WIND TUNNEL

FIG. 1.1
LR-349

FIG. 1.2
LR - 349

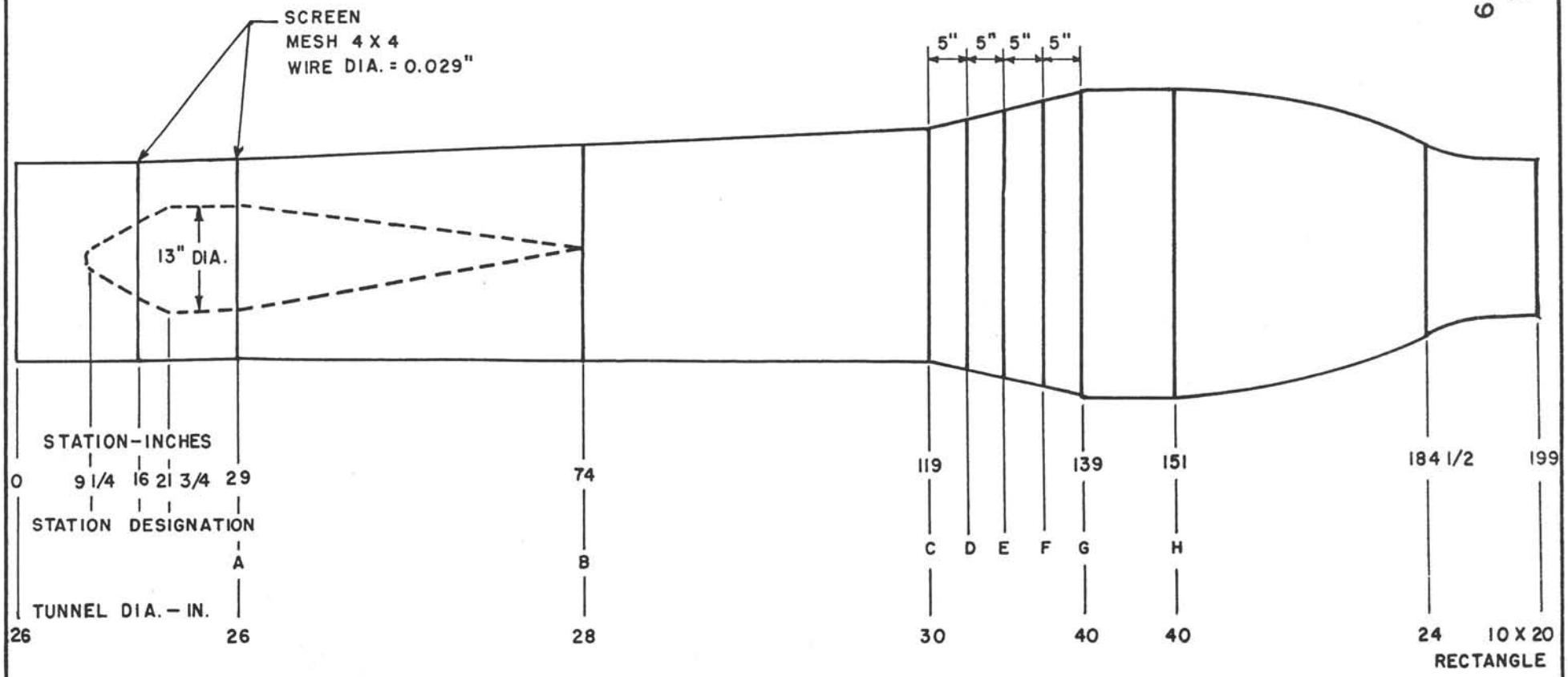

CONFIGURATION I

1/12 SCALE VTOL WIND TUNNEL

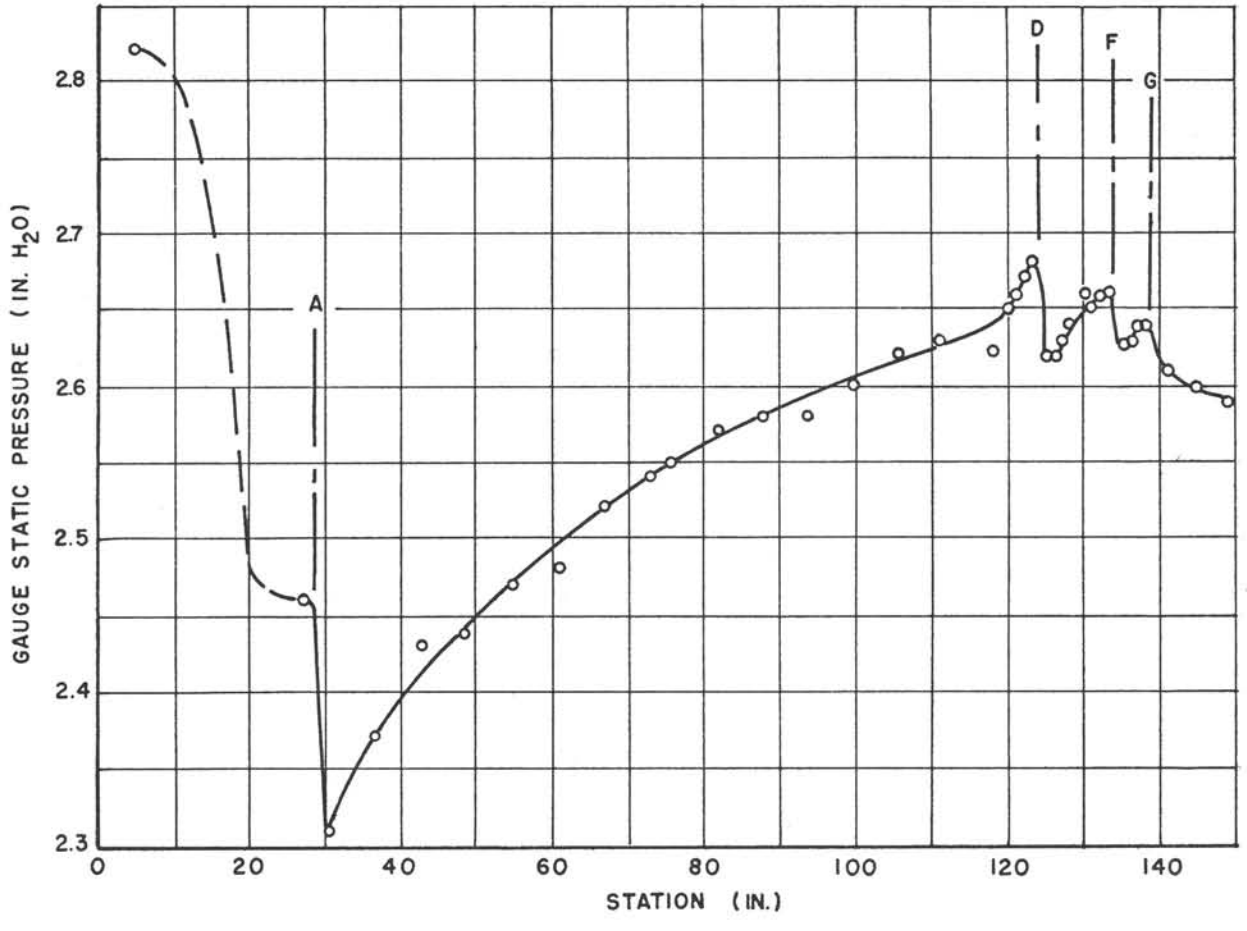

SCREEN AT STATION	MESH	WIRE DIAM. (IN.)
A	4 x 4	.029
D	18x18	.011
F	18 x 18	.011
G	18 x 18	.011

1/12 SCALE VTOL TUNNEL

CONFIGURATION I

LONGITUDINAL STATIC PRESSURE DISTRIBUTION, TEST I

INLET TOTAL HEAD (STATION '0') ≡ 3.13 IN. H_2O GAUGE

OUTLET TOTAL HEAD (STATION 207) ≡ 2.4 IN. H_2O GAUGE

AMBIENT PRESSURE ≡ 29.6 IN. Hg

VELOCITY AT STATION 207 = 117 FT./SEC.

FIG. 1.3
LR-349

FIG. 1.4
LR-349

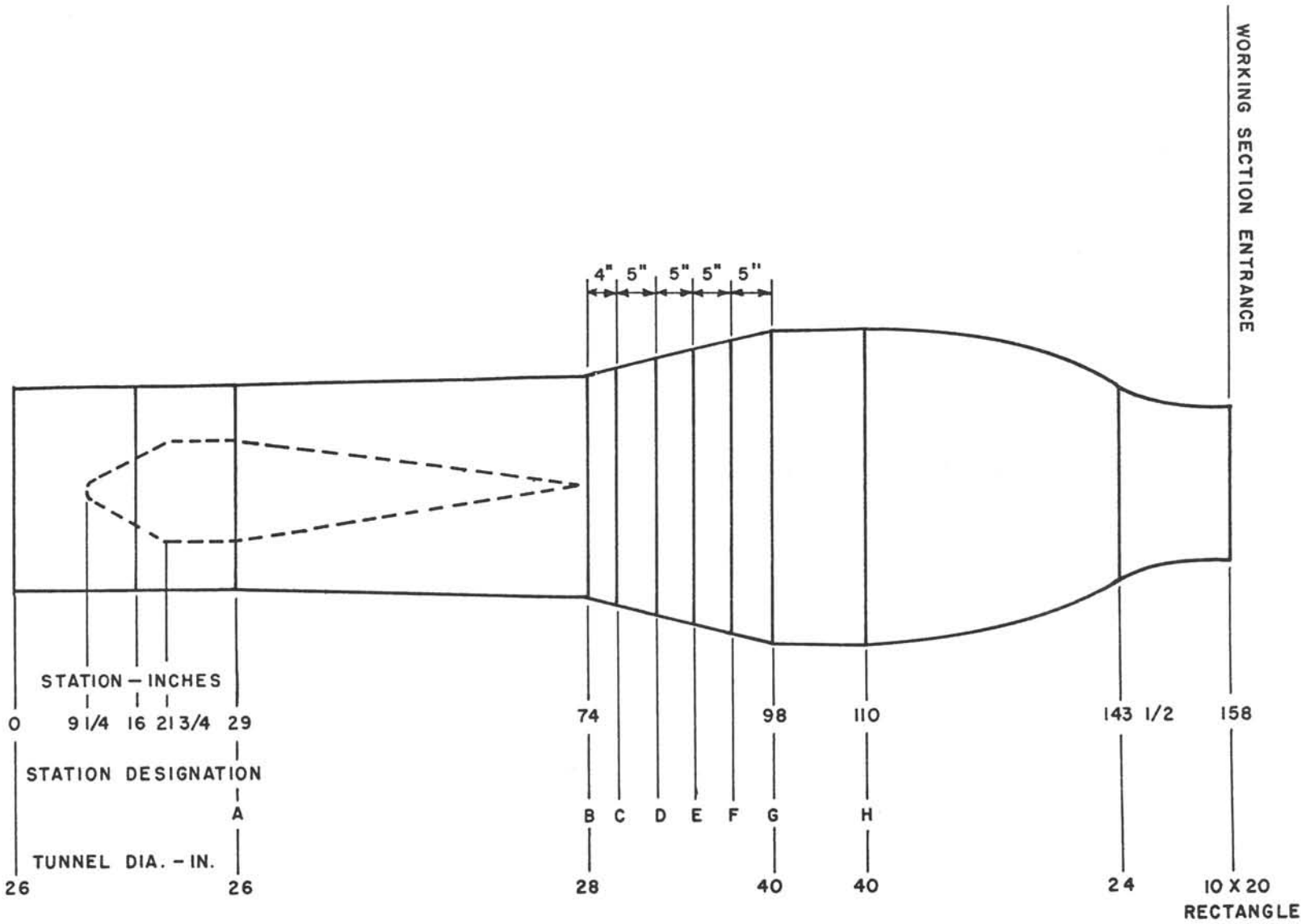

CONFIGURATION 2

1/12 SCALE VTOL WIND TUNNEL

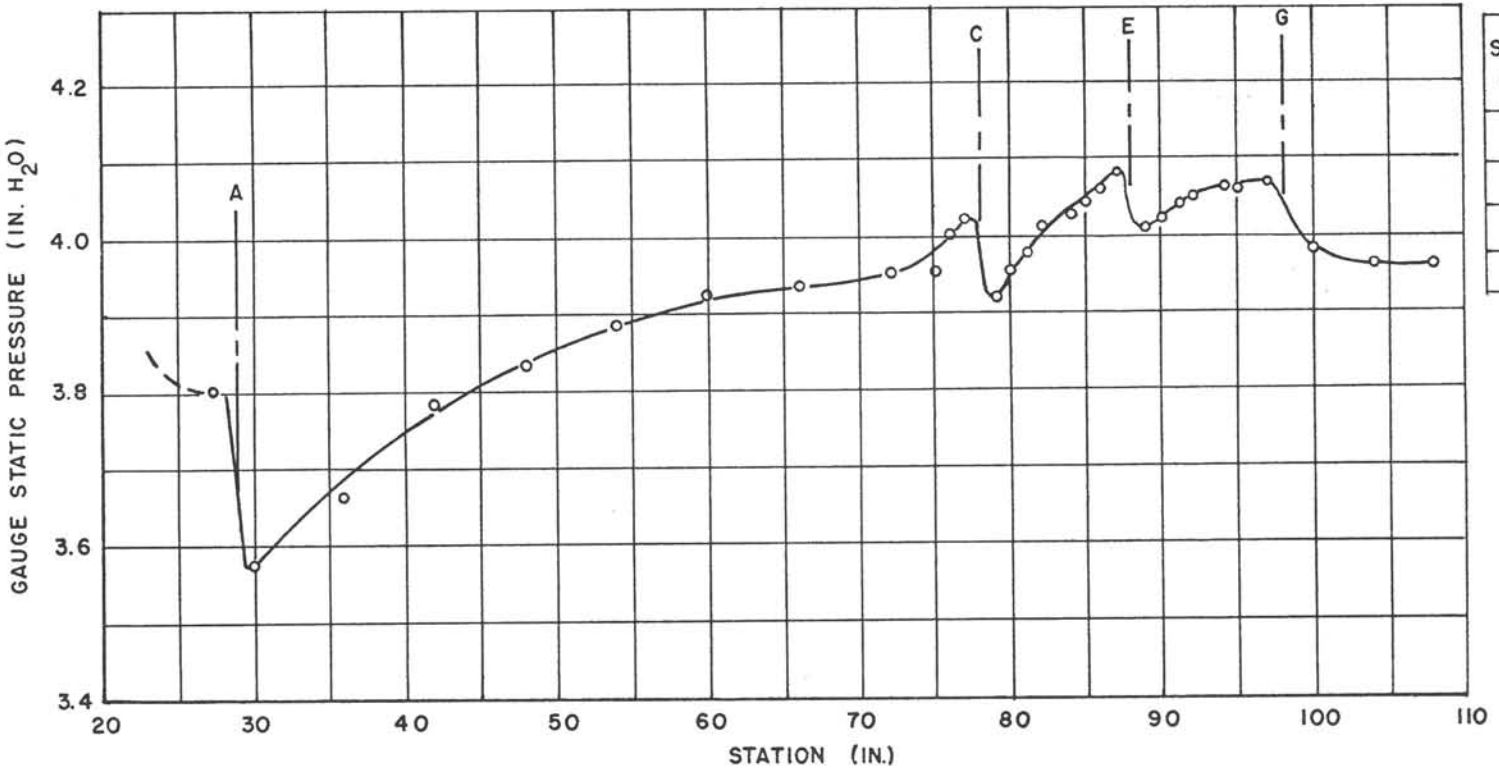

SCREEN AT STATION	MESH	WIRE DIAM. (IN.)
A	4 x 4	.029
C	18 x 18	.011
E	18 x 18	.011
G	18 x 18	.011

1/12 SCALE VTOL TUNNEL

CONFIGURATION 2

LONGITUDINAL WALL STATIC PRESSURE DISTRIBUTION

INLET TOTAL HEAD (STATION 0) ≡ 4.74 IN. H_2O GAUGE
OUTLET TOTAL HEAD (STATION 161) ≡ 3.38 IN. H_2O GAUGE
AMBIENT PRESSURE ≡ 29.6 IN. Hg
VELOCITY AT STATION 161 = 139 FT./SEC.

FIG. 1.5
LR-349

FIG. 1.6
LR-349

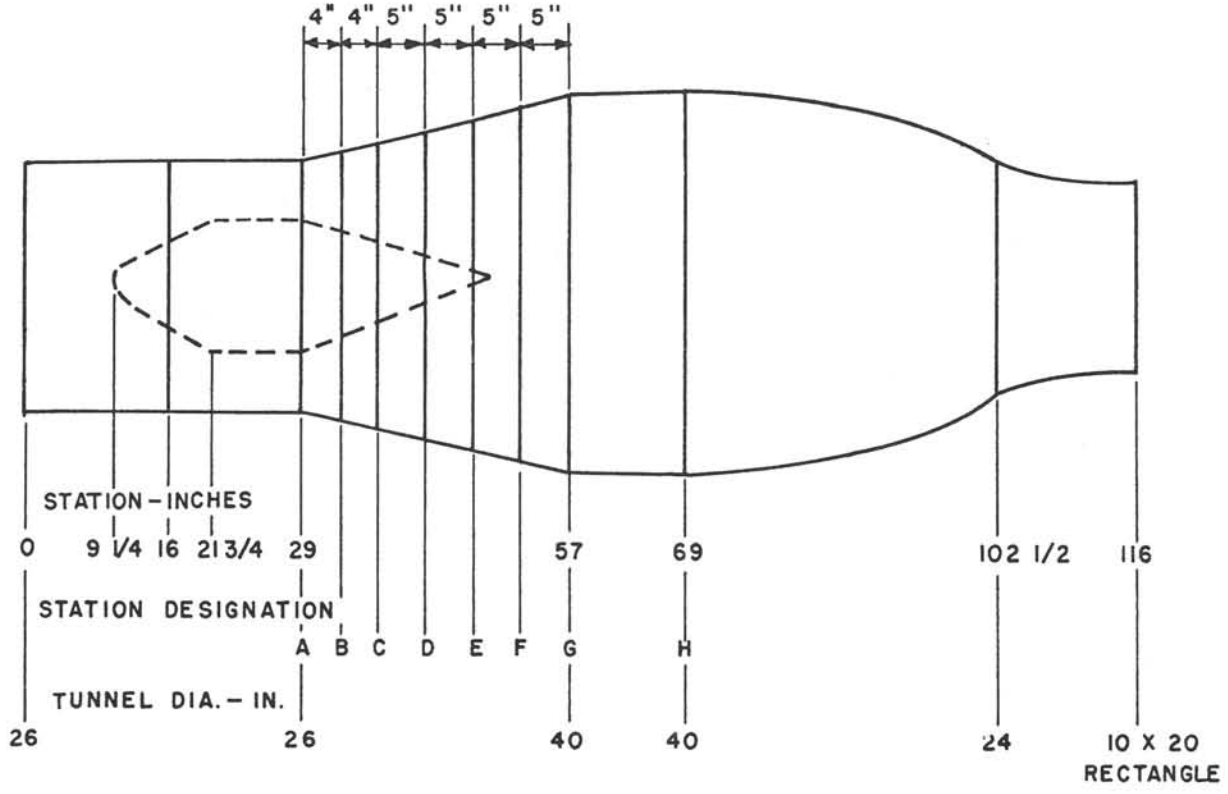

CONFIGURATION 3

1/12 SCALE VTOL WIND TUNNEL

1/12 SCALE MODEL

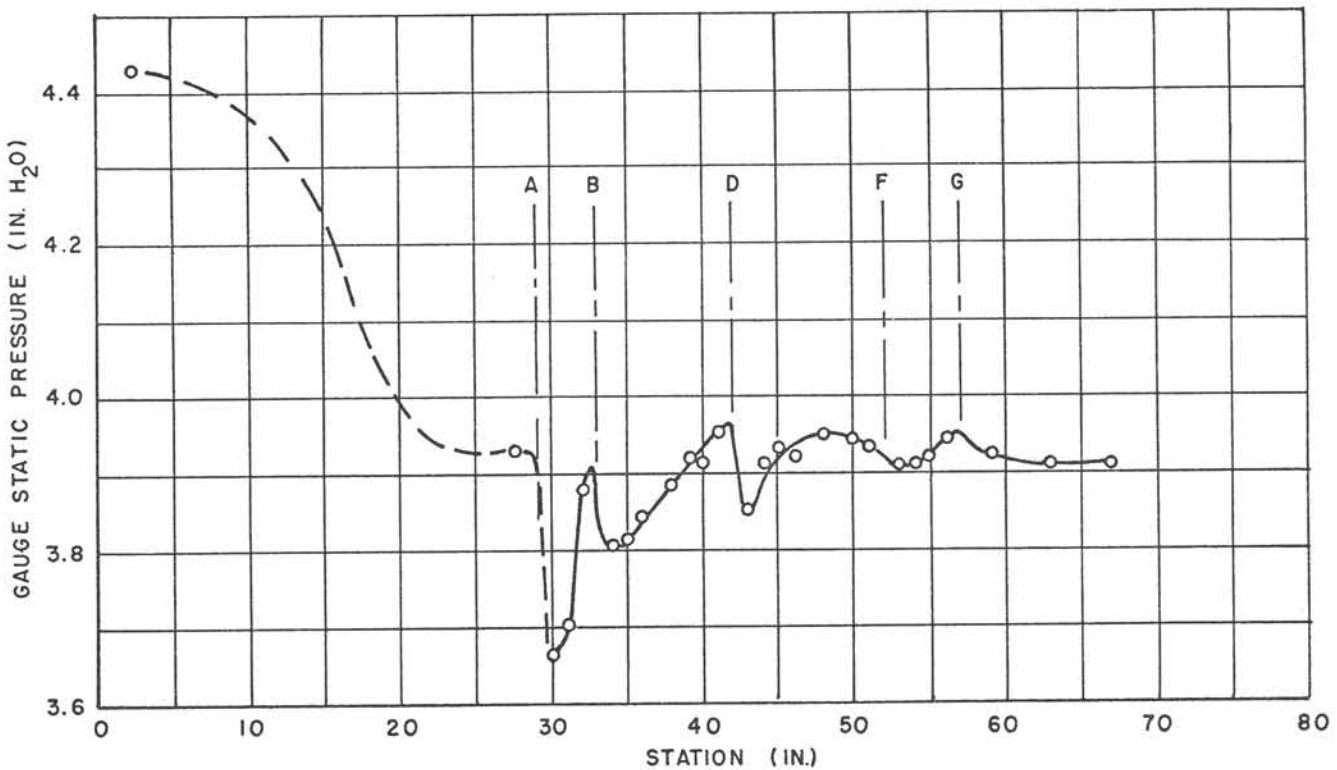

SCREEN AT STATION	MESH	WIRE DIAM. (IN.)
A	18 x 18	.011
B	18 x 18	.011
D	18 x 18	.011
F	18 x 18	.011
G	18 x 18	.011

1/12 SCALE VTOL TUNNEL

CONFIGURATION 3

LONGITUDINAL WALL STATIC PRESSURE DISTRIBUTION, TEST 3

INLET TOTAL HEAD (STATION 0) ≡ 4.98 IN. H_2O GAUGE

OUTLET TOTAL HEAD (STATION 116) ≡ 4.25 IN H_2O GAUGE

AMBIENT PRESSURE ≡ 29.4 IN. Hg

VELOCITY AT STATION 116 = 158 FT./SEC.

FIG. 1.7
LR-349

FIG. 1.8
LR-349

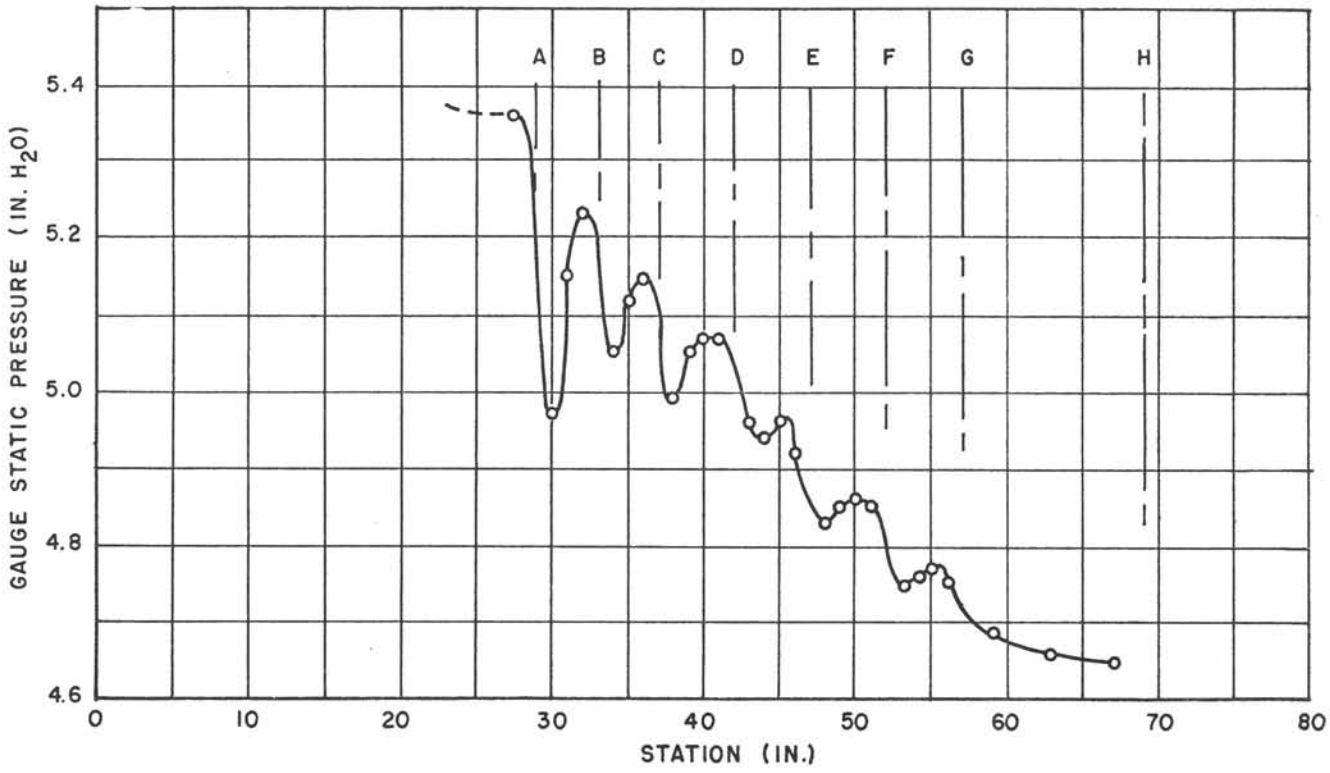

SCREEN AT STATION	MESH	WIRE DIAM. (IN.)
A	4 x 4	.029
B	10 x 10	.020
C	10 x 10	.020
D	10 x 10	.020
E	10 x 10	.025
F	10 x 10	.025
G	10 x 10	.025
H	10 x 10	.025

1/12 SCALE VTOL TUNNEL
CONFIGURATION 3
LONGITUDINAL WALL STATIC PRESSURE DISTRIBUTION, TEST 4
INLET TOTAL HEAD (STATION 0) = 5.95 IN. H_2O GAUGE
OUTLET TOTAL HEAD (STATION 116) = 4.54 IN. H_2O GAUGE
AMBIENT PRESSURE = 29.4 IN. Hg.
VELOCITY AT STATION 116 = 163 FT./SEC.

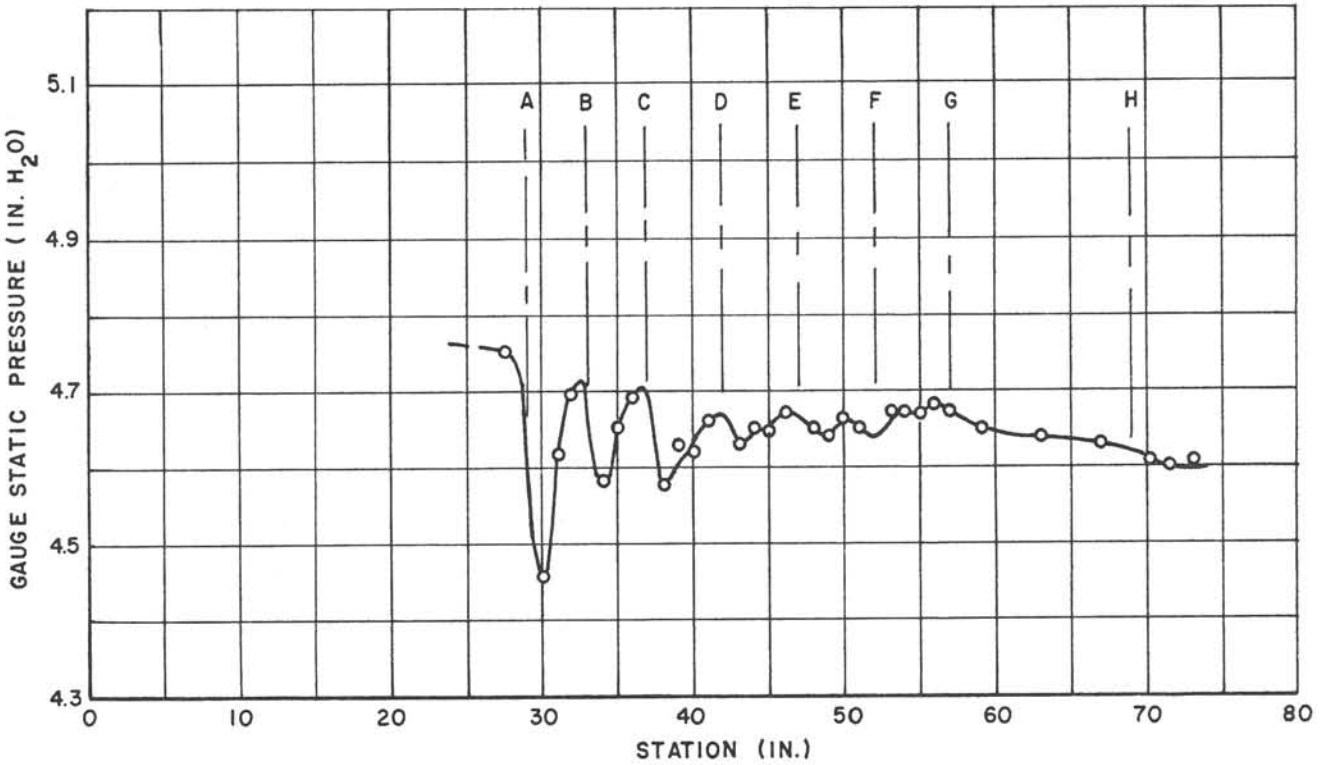

SCREEN AT STATION	MESH	WIRE DIAM. (IN.)
A	4 x 4	.029
B	5 x 5	.032
C	5 x 5	.032
D	4 x 4	.035
E	4 x 4	.035
F	4 x 4	.035
G	5 x 5	.032
H	5 x 5	.032

1/12 SCALE VTOL TUNNEL

CONFIGURATION 3

LONGITUDINAL WALL STATIC PRESSURE DISTRIBUTION, TEST 5

INLET TOTAL HEAD (STATION 0) ≡ 5.89 IN. H_2O GAUGE

OUTLET TOTAL HEAD (STATION 116) ≡ 4.52 IN. H_2O GAUGE

AMBIENT PRESSURE ≡ 29.26 IN. Hg.

VELOCITY AT STATION 116 = 166 FT./SEC.

FIG. 1.9
LR-349

FIG. 1.10
LR-349

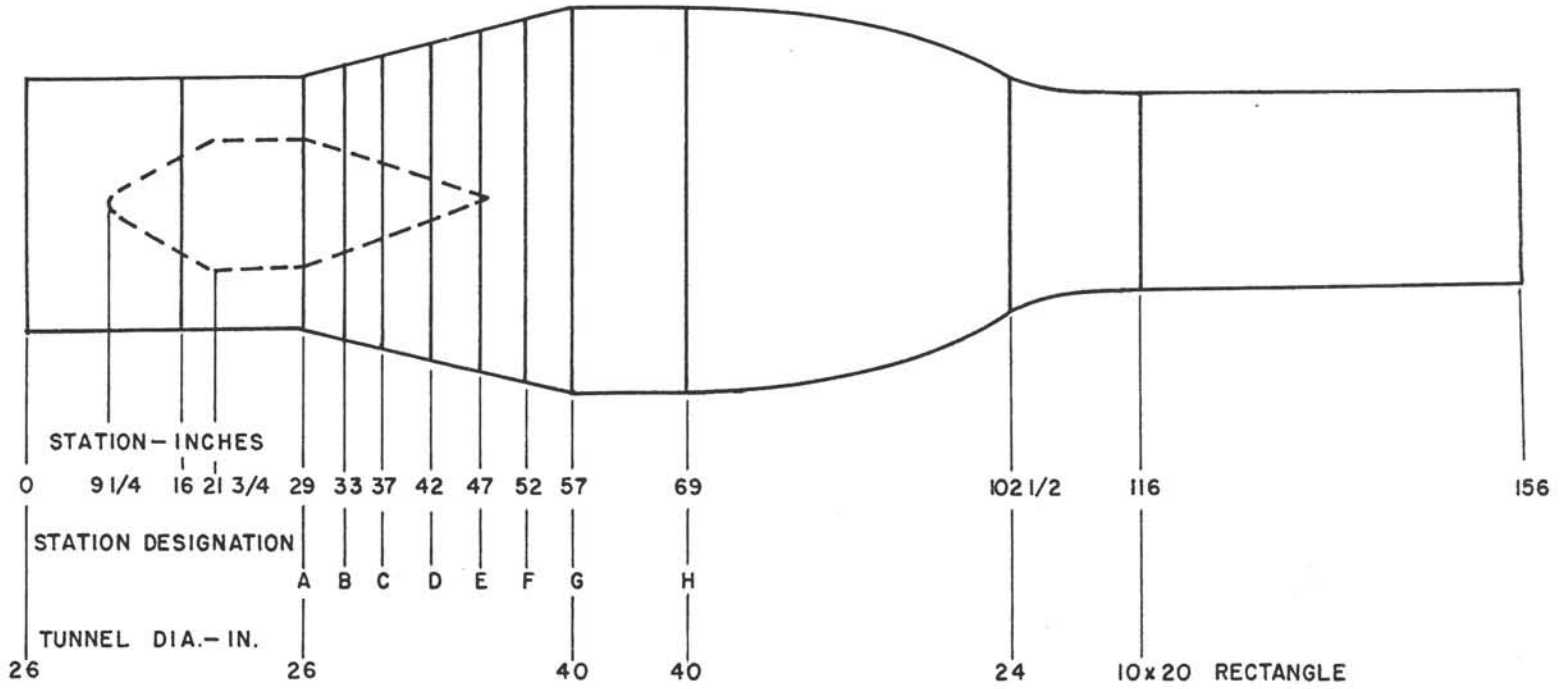

CONFIGURATION 4

1/12 SCALE VTOL WIND TUNNEL

FIG. I.II
LR-349

1/12 SCALE VTOL TUNNEL
CONFIGURATION 3
CONFIGURATION 4 (UNTAPERED FILLETS)

LOCATION OF TRAVERSES FOR BOUNDARY LAYER MEASUREMENTS OF TESTS 5 AND 6

TEST 5 AT STATION 116
TEST 6 AT STATION 156

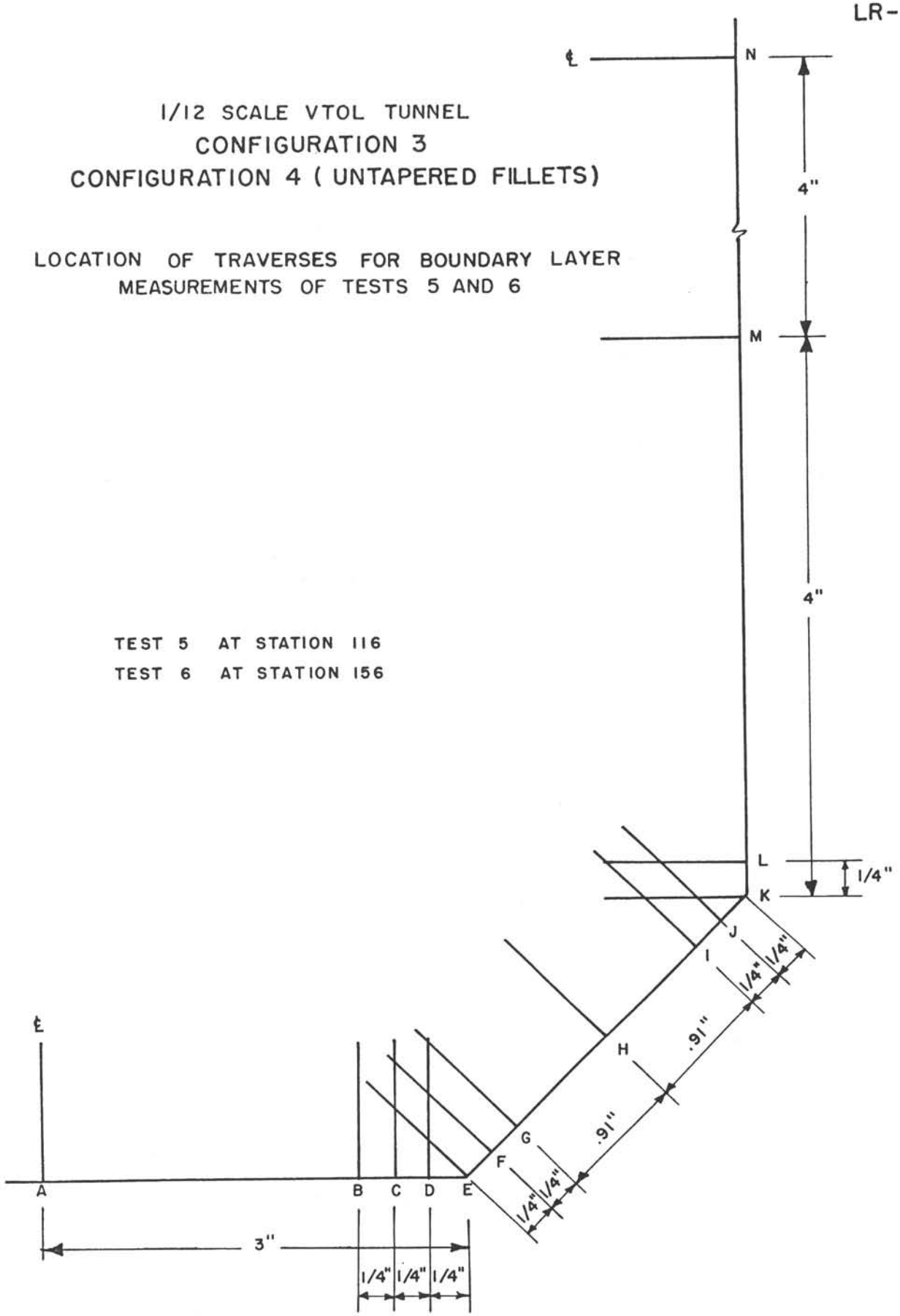

FIG. 1.12
LR-349

STATION 116 — CONFIGURATION 3 — TEST 5 — MEAN VELOCITY = 161 FT./SEC.

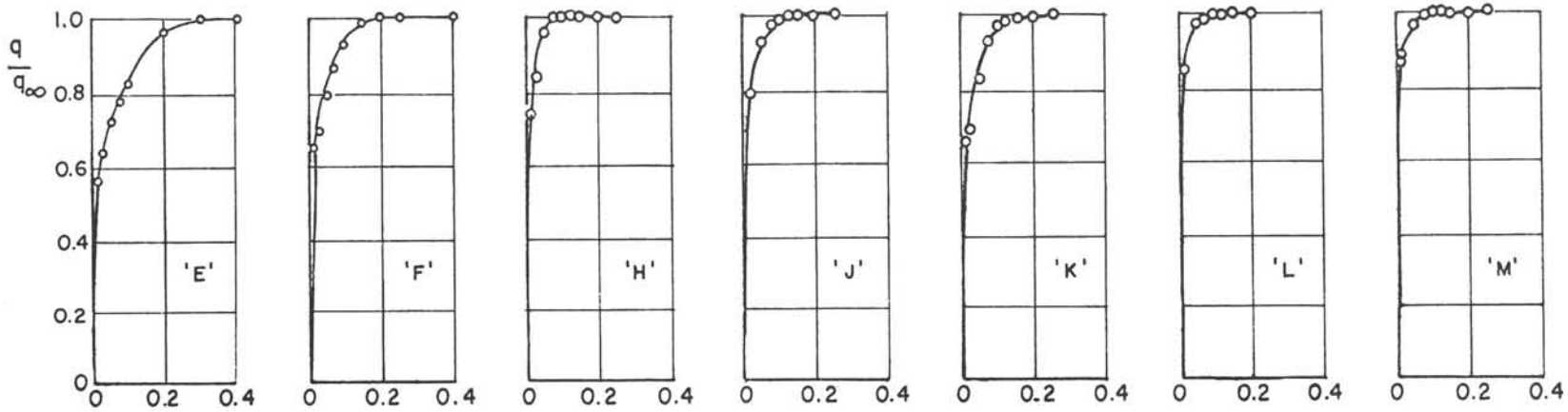

STATION 156 — CONFIGURATION 4 — TEST 6 — MEAN VELOCITY = 162 FT./SEC.

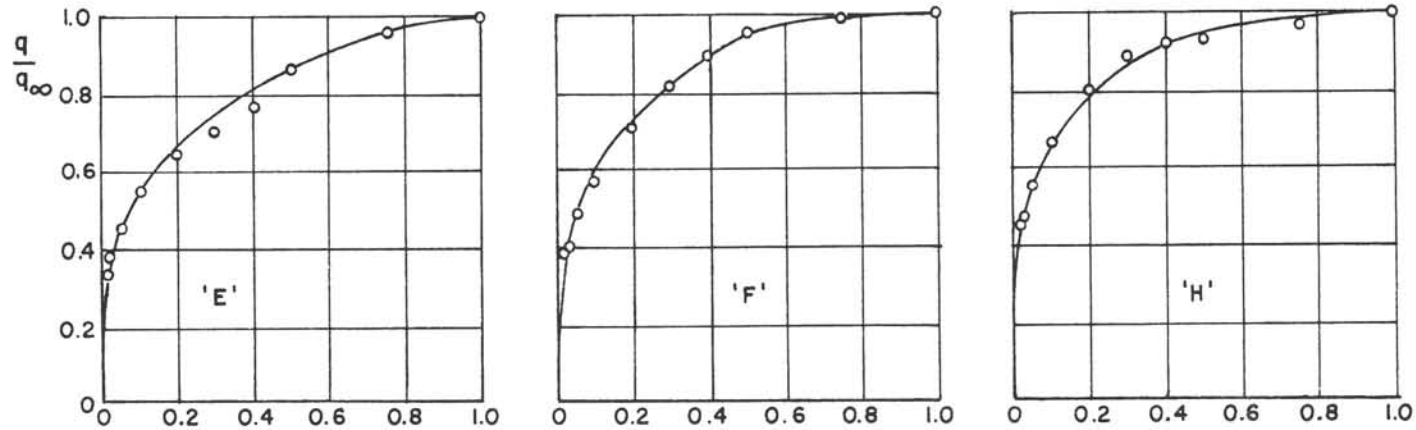

1/12 SCALE VTOL TUNNEL

BOUNDARY LAYER VELOCITY HEAD PROFILES

q_0 = LOCAL MAXIMUM DYNAMIC HEAD

q = DYNAMIC HEAD IN BOUNDARY LAYER

STATION 156 — CONFIGURATION 4 — TEST 6 — MEAN VELOCITY = 162 FT./SEC.

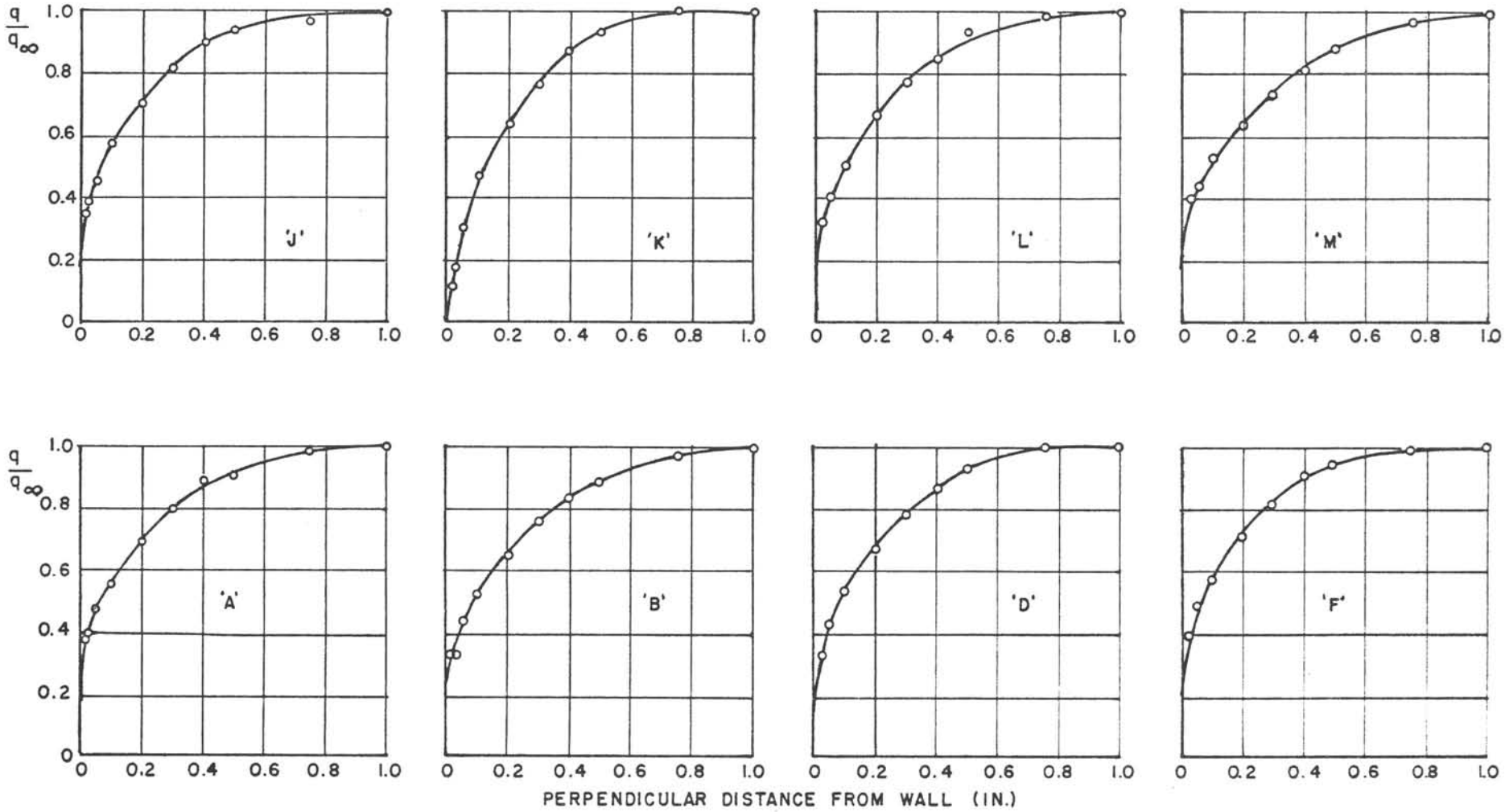

1/12 SCALE VTOL TUNNEL

BOUNDARY LAYER VELOCITY HEAD PROFILES

q_0 = LOCAL MAXIMUM DYNAMIC HEAD

q = DYNAMIC HEAD IN BOUNDARY LAYER

FIG. 1.13
LR-349

FIG. 1.14
LR-349

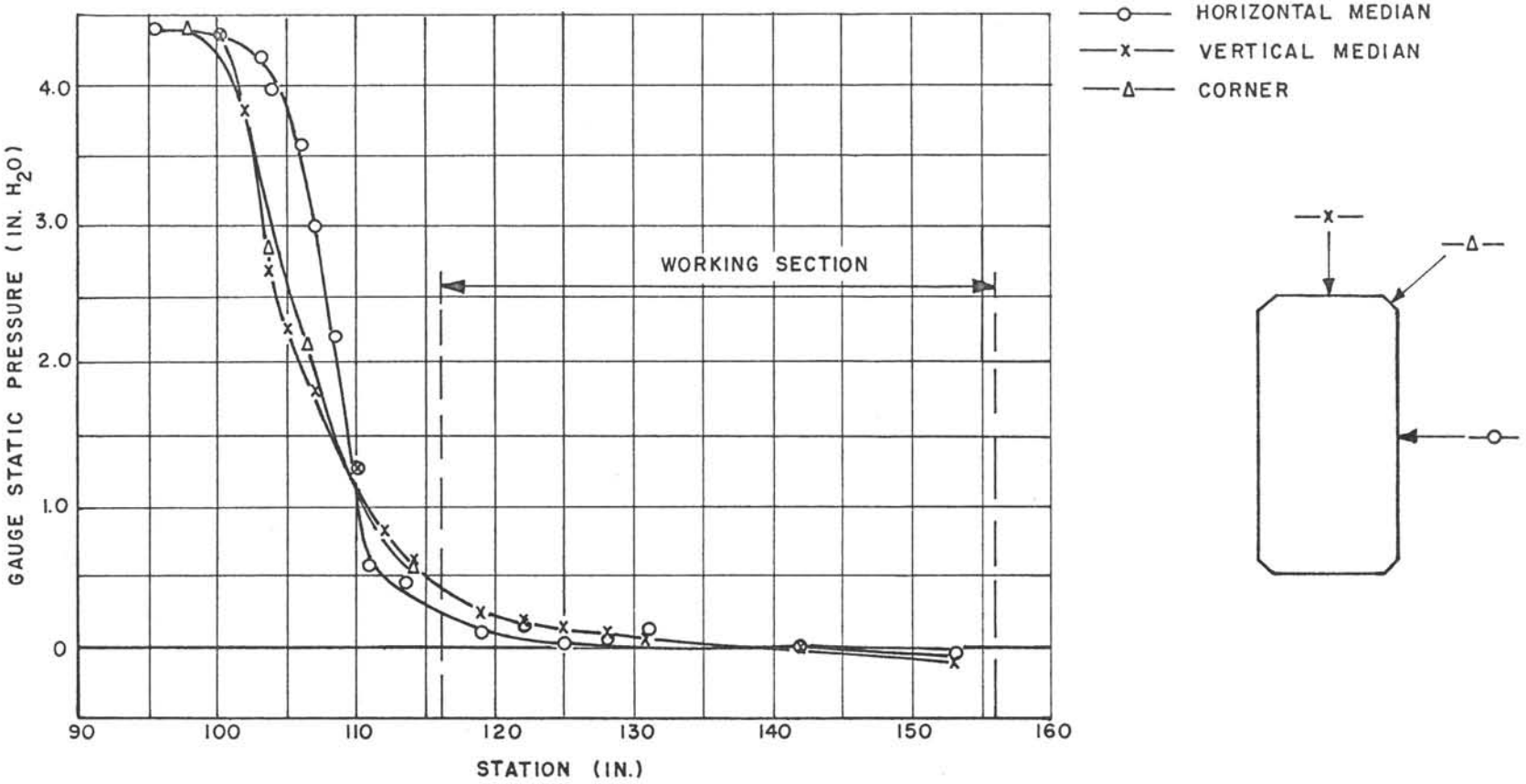

1/12 SCALE VTOL TUNNEL

CONFIGURATION 4

LONGITUDINAL WALL STATIC PRESSURE DISTRIBUTION, TEST 6
(CONTRACTION AND WORKING SECTIONS)

CONSTANT AREA FILLETS IN WORKING SECTION
OUTLET (STATION 156) TOTAL HEAD ≡ 4.77 IN. H_2O GAUGE
AMBIENT PRESSURE ≡ 29.66 IN. Hg
VELOCITY AT STATION 156 = 167 FT./SEC.

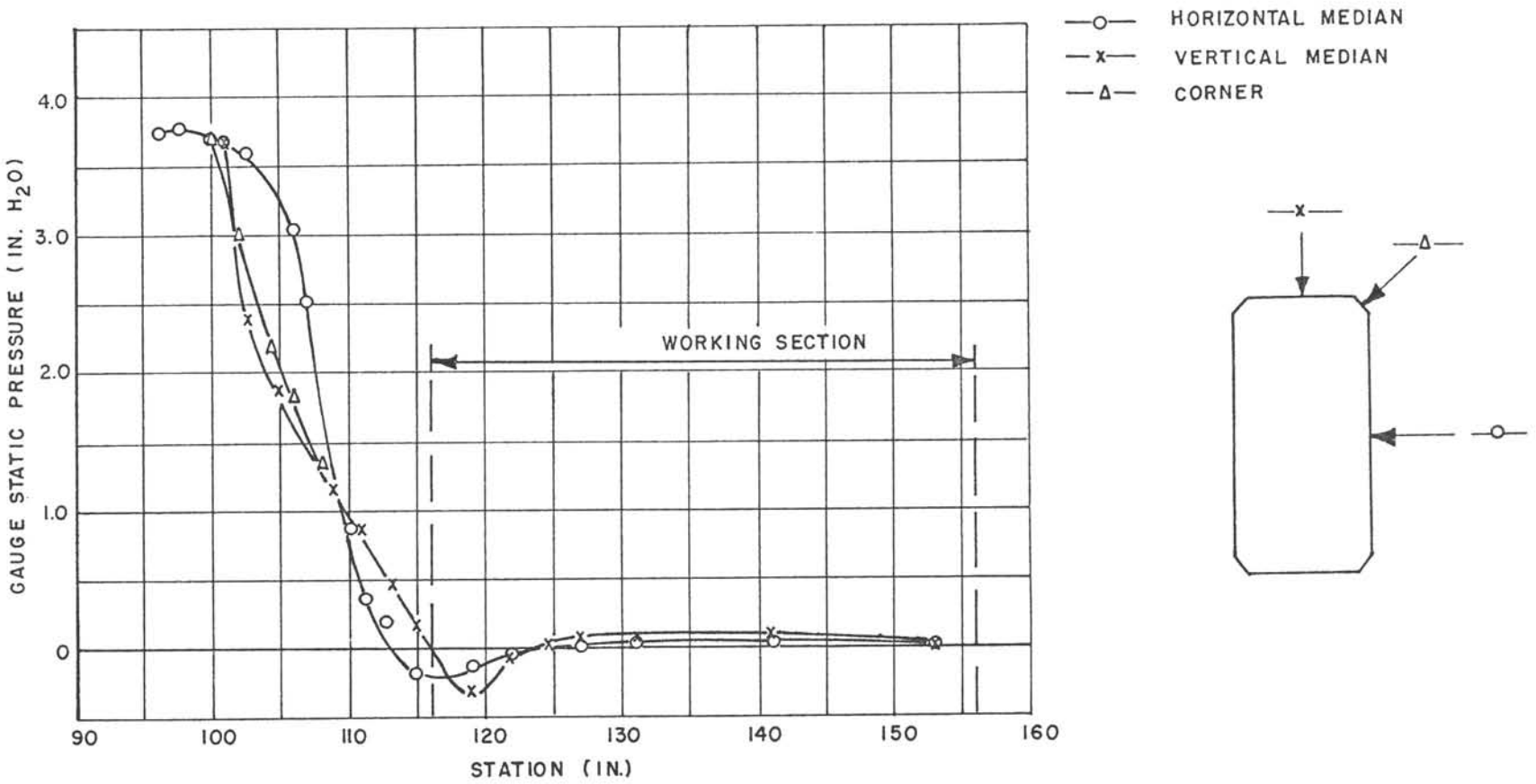

1/12 SCALE VTOL TUNNEL

CONFIGURATION 4

LONGITUDINAL WALL STATIC PRESSURE DISTRIBUTION, TEST 7
(CONTRACTION AND WORKING SECTIONS)

TAPERED FILLETS IN WORKING SECTION
OUTLET (STATION 156) TOTAL HEAD ≡ 4.33 IN. H_2O GAUGE
AMBIENT PRESSURE ≡ 29.66 IN. Hg
VELOCITY AT STATION 156 = 161 FT./SEC.

FIG. 1.15
LR-349

FIG. 1.16
LR-349

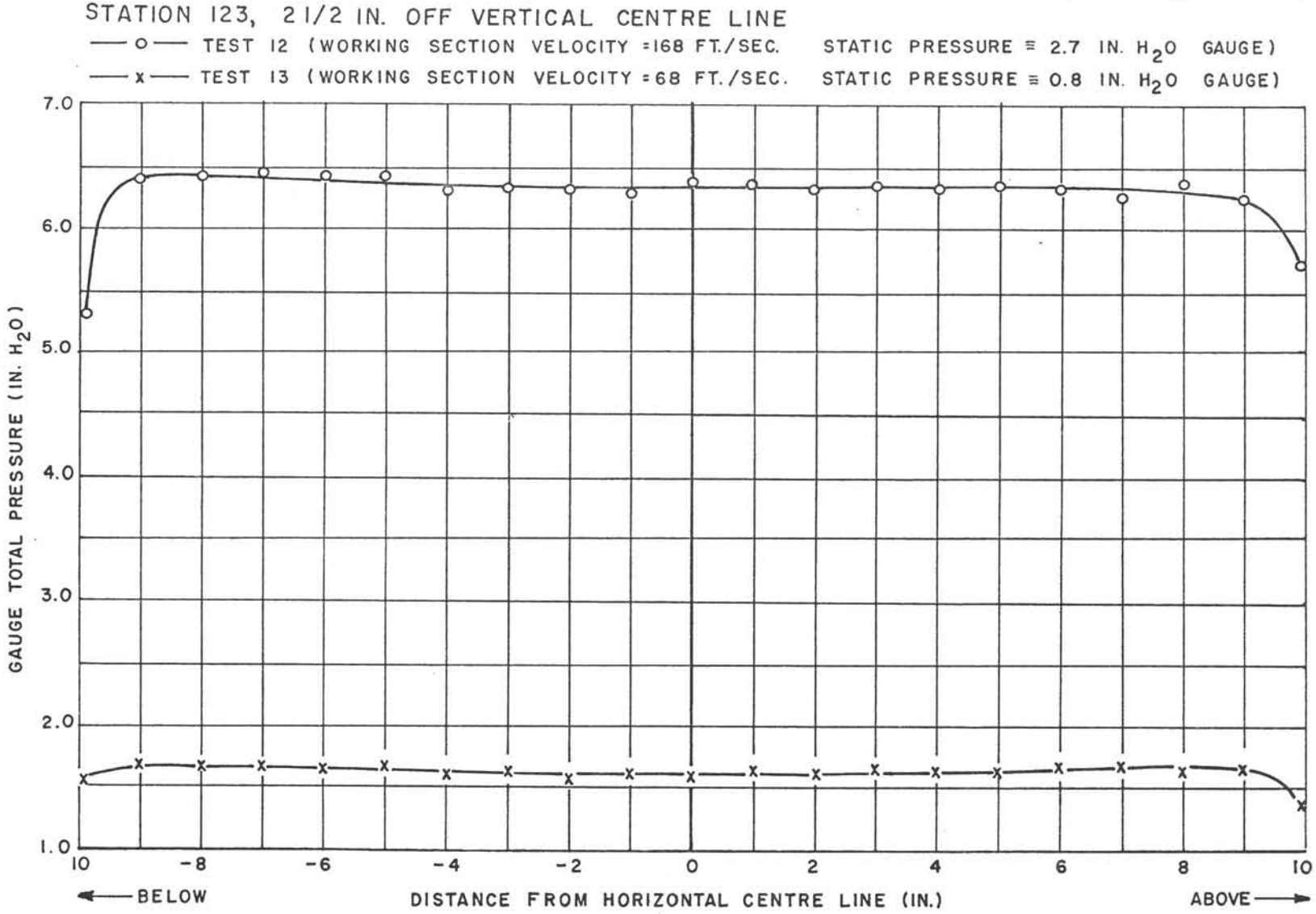

1/12 SCALE VTOL TUNNEL

CONFIGURATION 4

VERTICAL TOTAL HEAD PROFILES IN WORKING SECTION

WORKING SECTION EMPTY

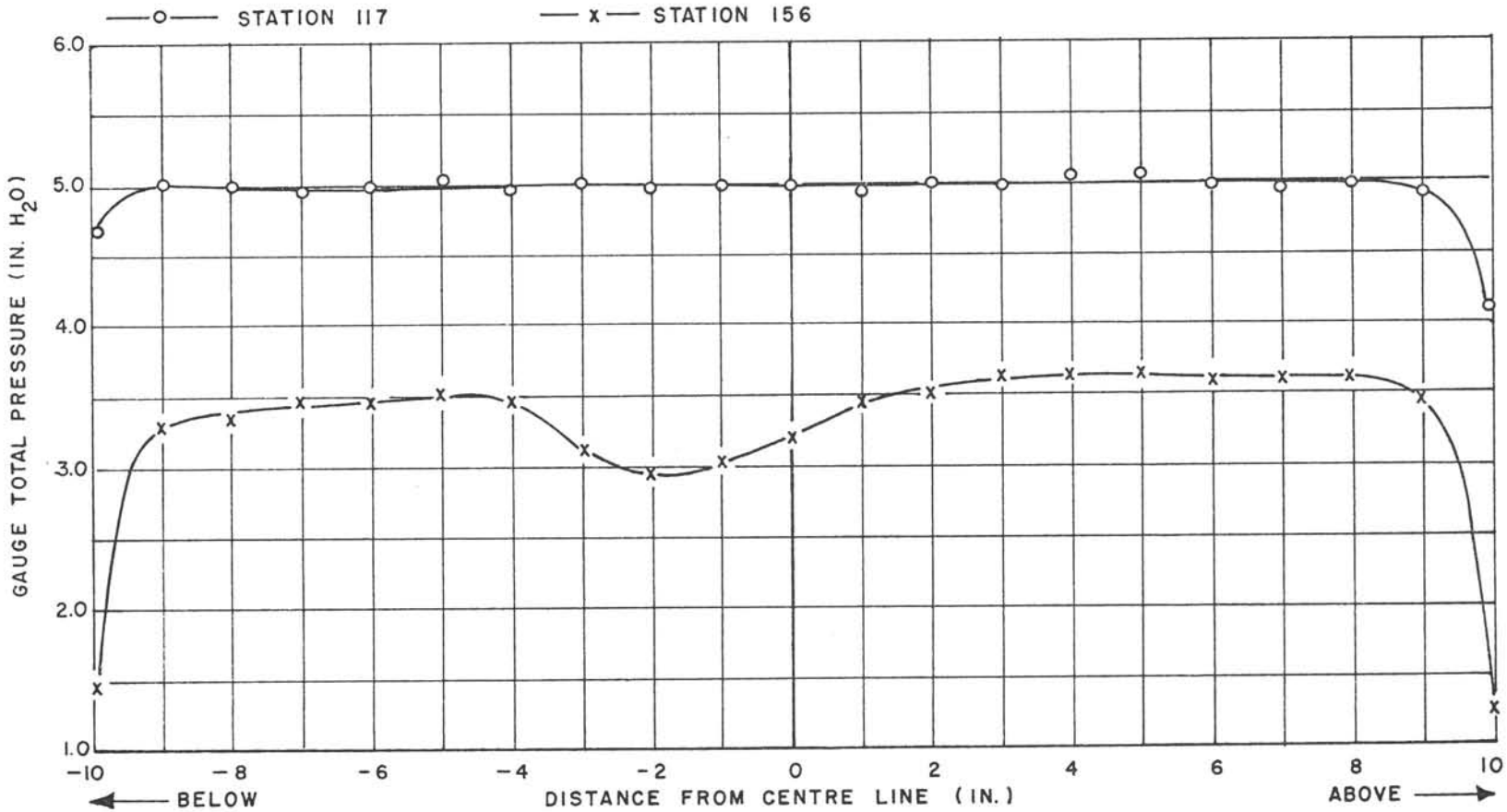

1/12 SCALE VTOL TUNNEL

CONFIGURATION 4

WORKING SECTION TOTAL HEAD PROFILES — AEROFOIL MOUNTED, TEST 8

$\alpha = 17°$

AMBIENT PRESSURE = 29.87 IN. Hg

WORKING SECTION { VELOCITY = 172 FT./SEC.
VELOCITY HEAD = 4.92 IN. H_2O

FIG. 1.17
LR-349

FIG. 1.18
LR-349

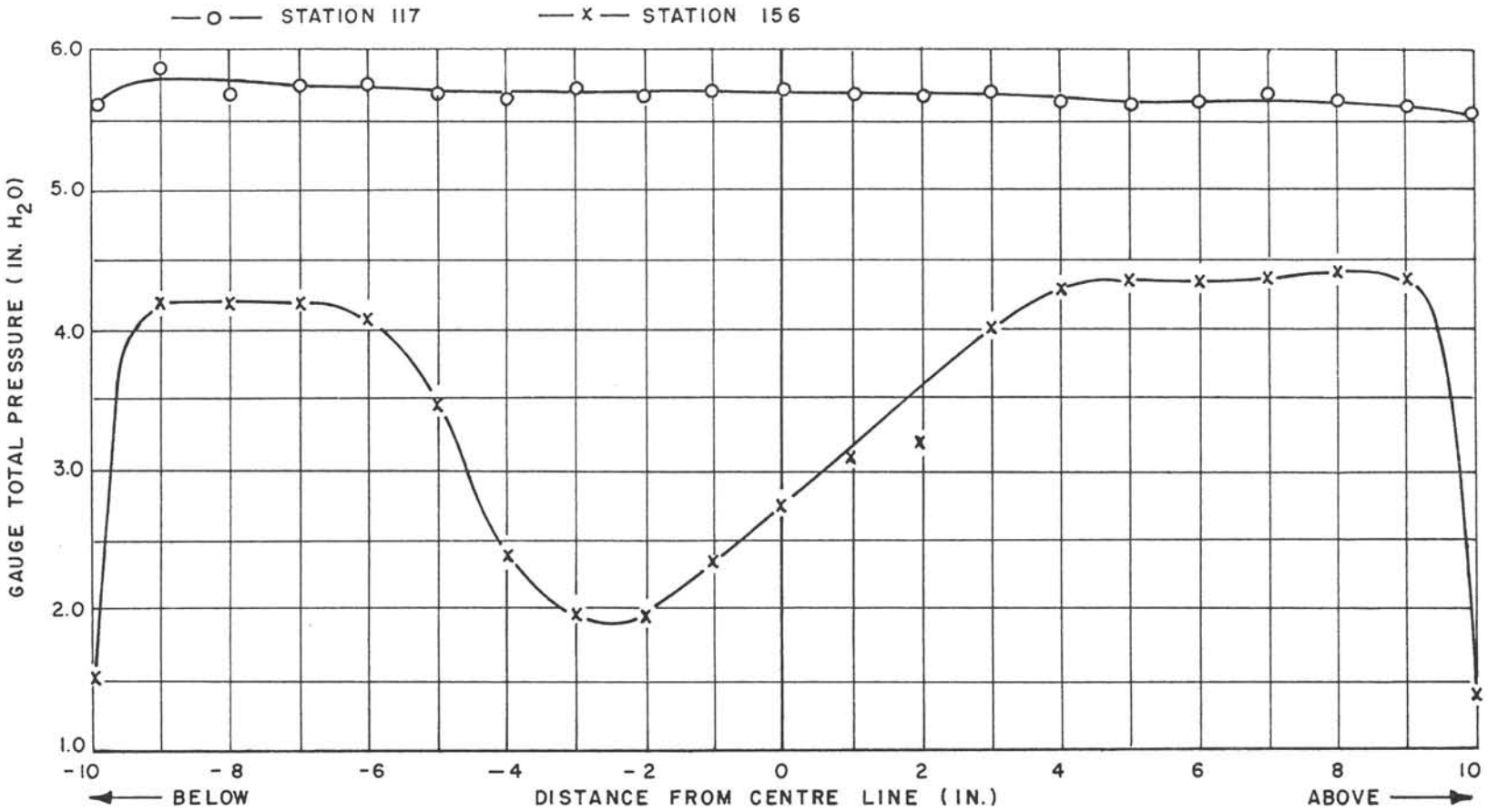

1/12 SCALE VTOL TUNNEL

CONFIGURATION 4

WORKING SECTION TOTAL HEAD PROFILES — AEROFOIL MOUNTED, TEST 9

$\alpha = 30°$

AMBIENT PRESSURE = 29.87 IN. Hg

WORKING SECTION { VELOCITY = 172 FT./SEC.
VELOCITY HEAD = 4.92 IN. H_2O

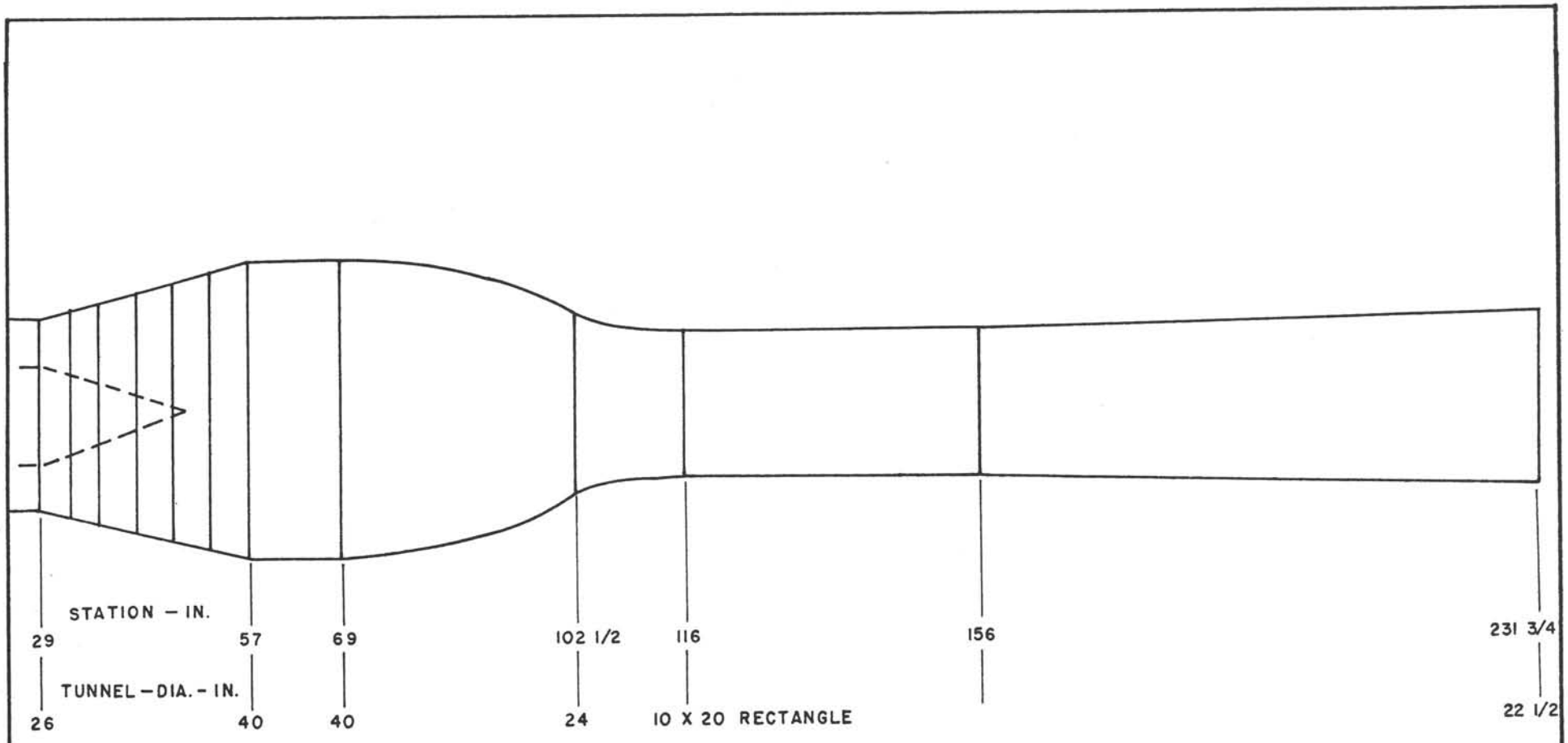

CONFIGURATION 5

1/12 SCALE VTOL WIND TUNNEL

FIG. 1.19
LR-349

FIG. 1.20
LR-349

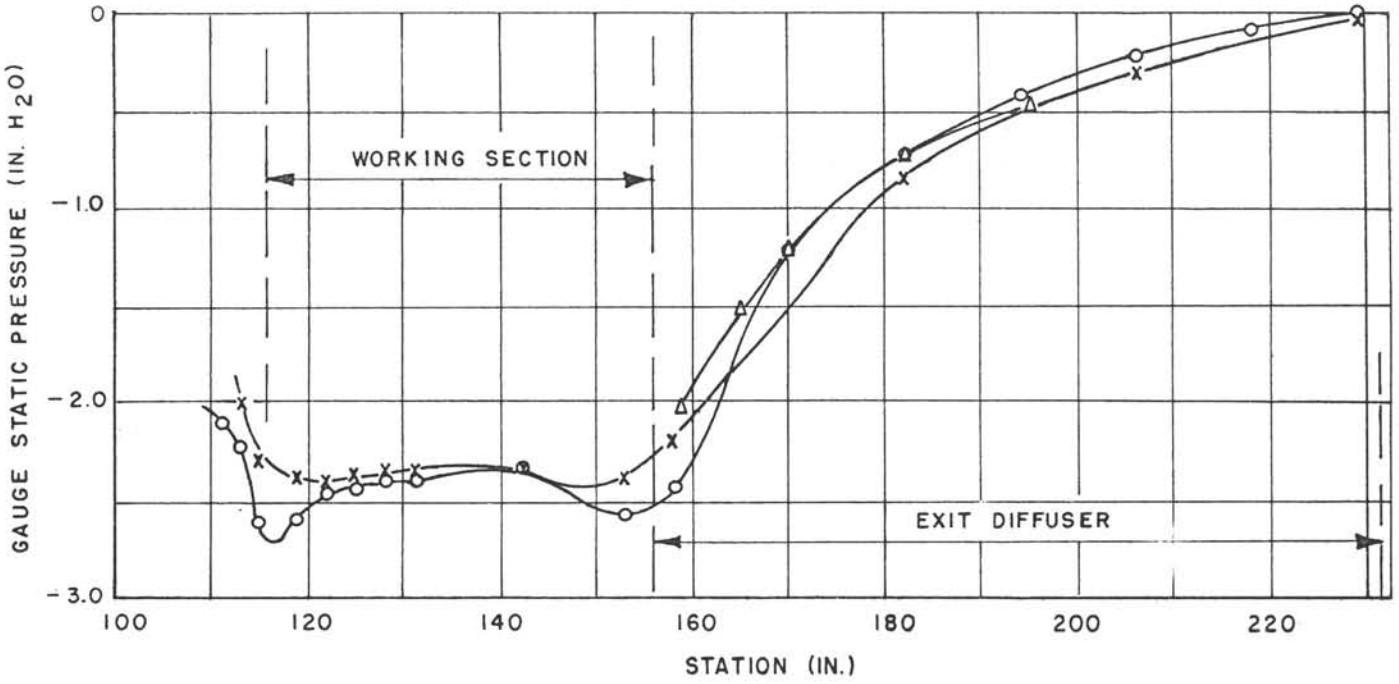

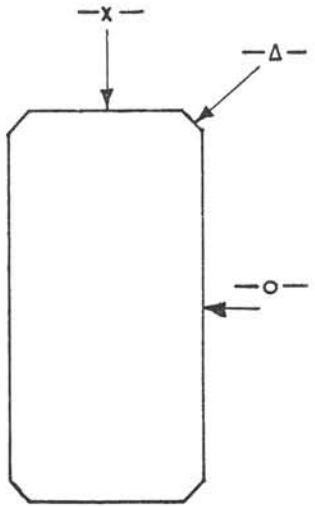

1/12 SCALE VTOL TUNNEL

CONFIGURATION 5

LONGITUDINAL WALL STATIC PRESSURE DISTRIBUTION, TEST 10

(WORKING SECTION EMPTY)

AMBIENT PRESSURE = 30 IN. Hg

TOTAL HEAD AT WORKING SECTION (STATION 116) = 1.65 IN. H_2O GAUGE

VELOCITY AT WORKING SECTION = 156 FT./SEC.

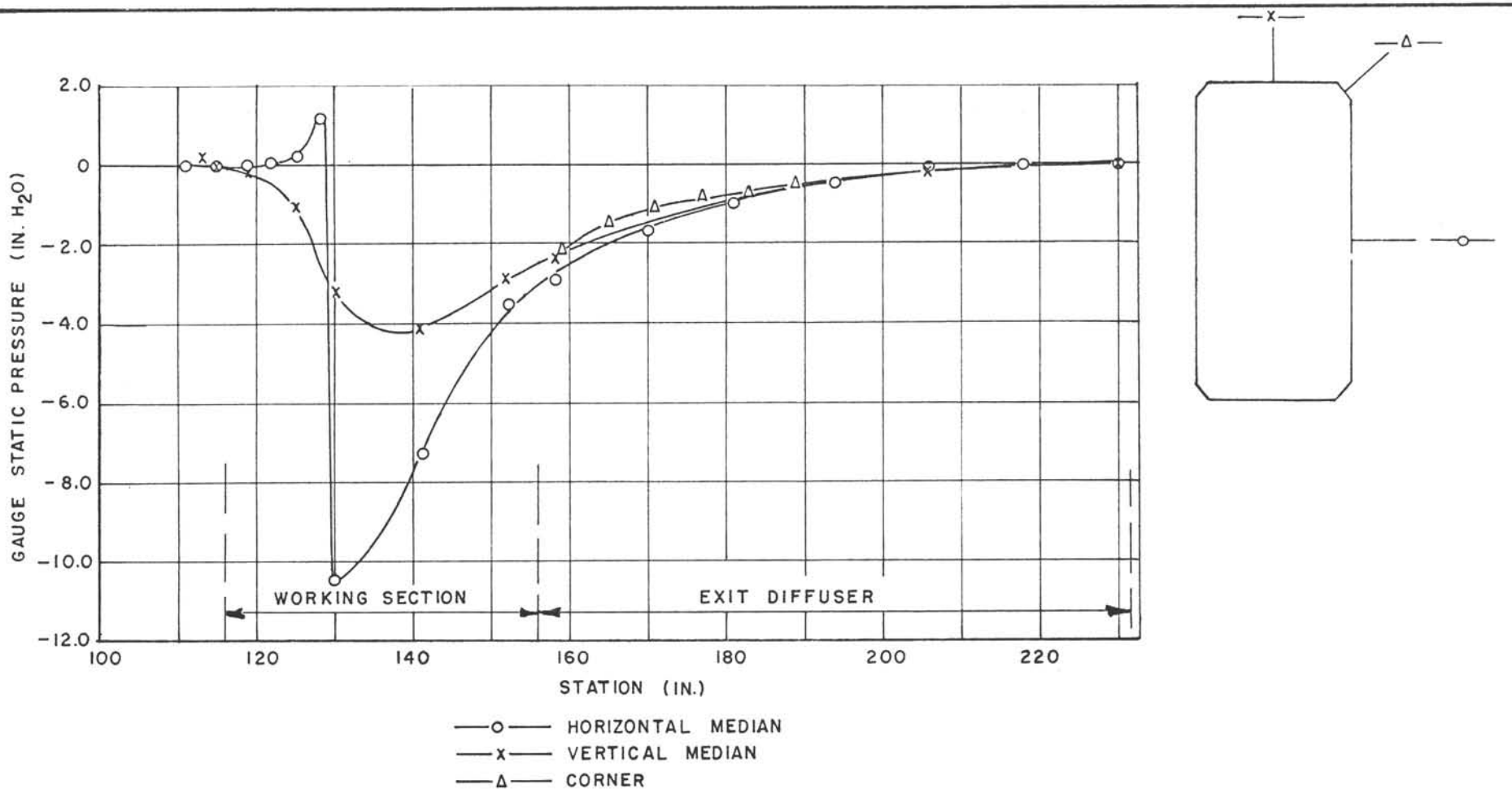

1/12 SCALE VTOL TUNNEL
CONFIGURATION 5
LONGITUDINAL WALL STATIC PRESSURE DISTRIBUTION, TEST II

AEROFOIL AT 30° IN WORKING SECTION (LEADING EDGE AT STATION 131)
AMBIENT PRESSURE = 29.29 IN. Hg
TOTAL HEAD AT WORKING SECTION (STATION 116) = 3.98 IN. H_2O GAUGE
WORKING SECTION { VELOCITY = 156 FT./SEC.
VELOCITY HEAD = 4.08 IN. H_2O

FIG. 1.21
LR-349

FIG. 1.22
LR-349

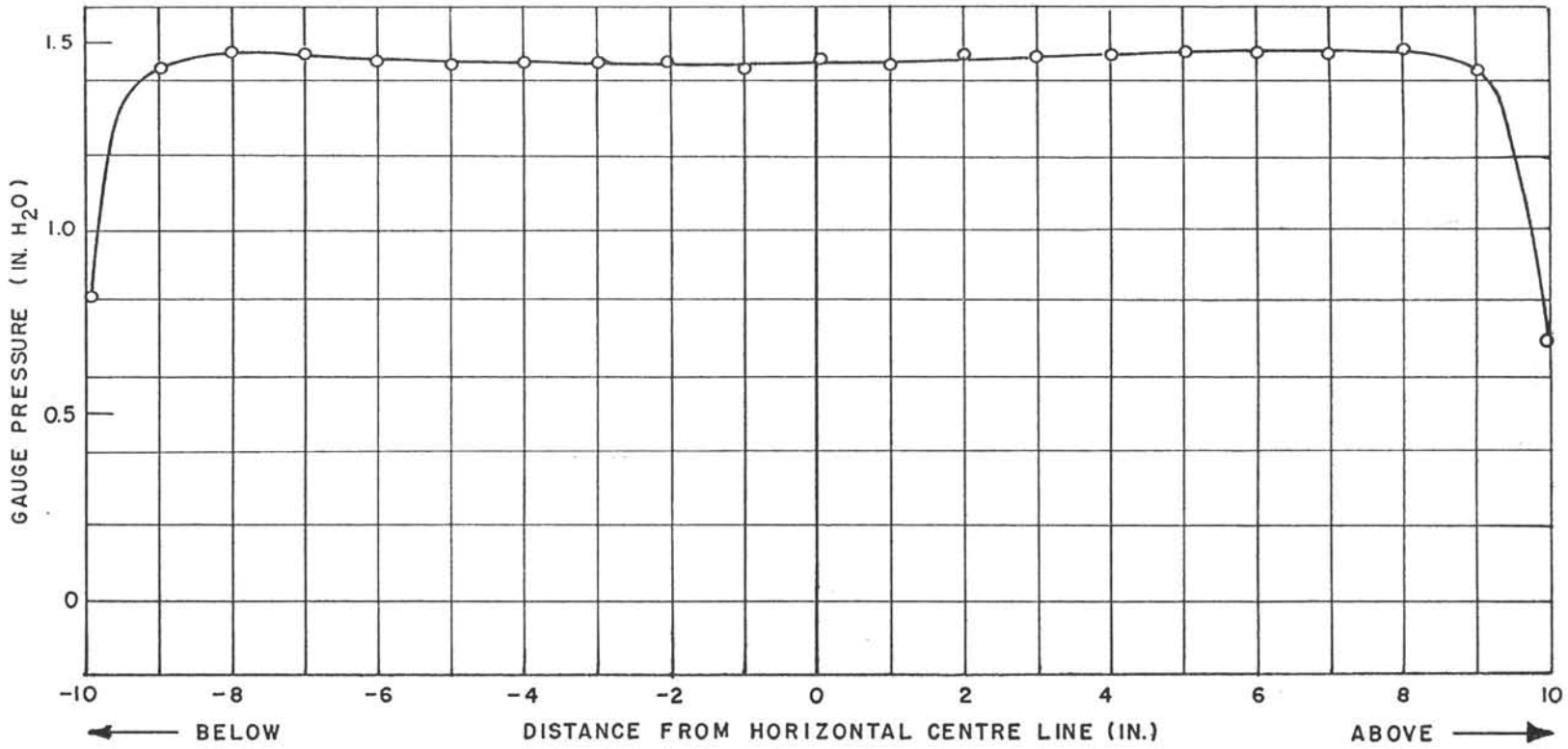

1/12 SCALE VTOL TUNNEL

CONFIGURATION 5

TOTAL HEAD PROFILES ON VERTICAL CENTRE LINE, TEST 10

STATION 155 WORKING SECTION EMPTY

AMBIENT PRESSURE = 30 IN. Hg

WORKING SECTION { VELOCITY = 156 FT./SEC.
VELOCITY HEAD = 4.08 IN. H_2O

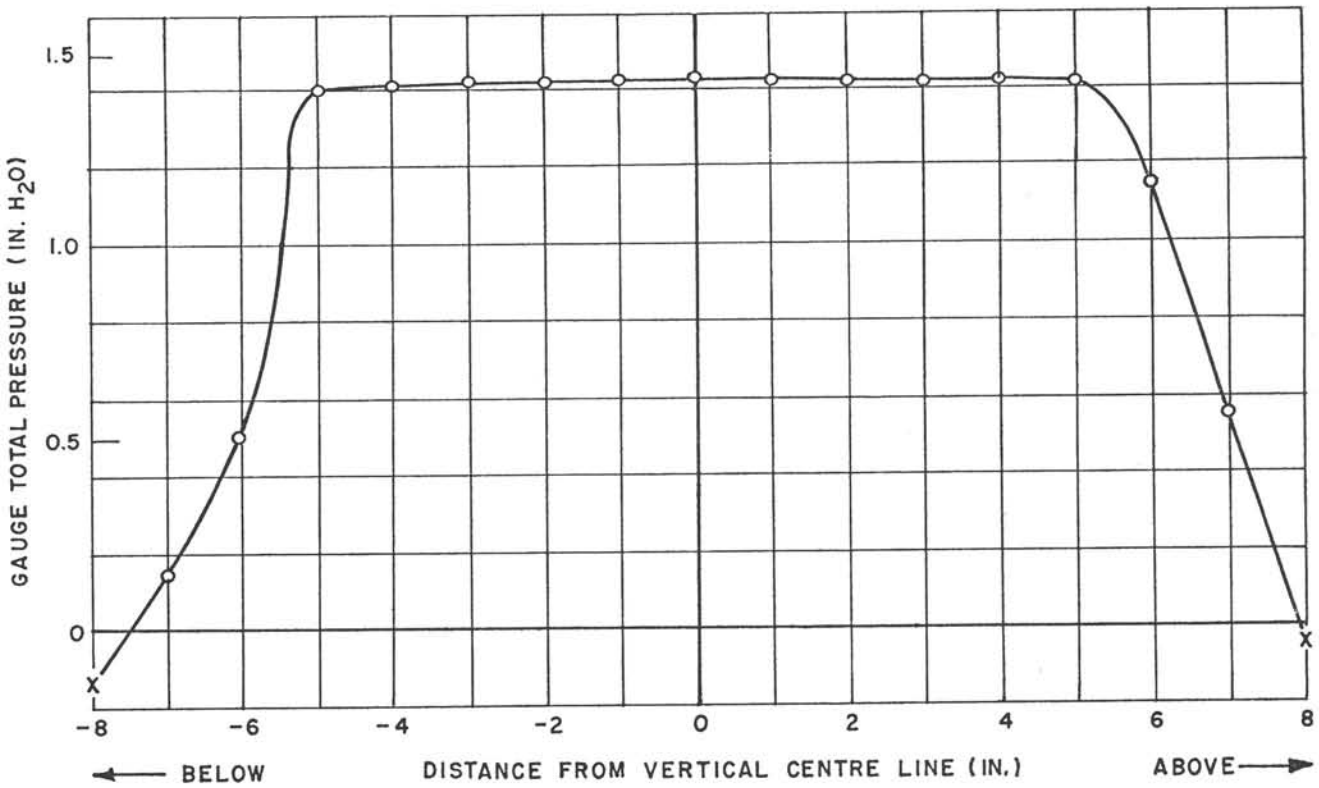

1/12 SCALE VTOL TUNNEL

CONFIGURATION 5

TOTAL HEAD PROFILES ON HORIZONTAL CENTRE LINE, TEST 10

STATION 194 WORKING SECTION EMPTY

AMBIENT PRESSURE = 30 IN. Hg

WORKING SECTION { VELOCITY = 156 FT./SEC.
VELOCITY HEAD = 4.08 IN. H_2O

FIG. 1.23
LR-349

FIG. I.24
LR-349

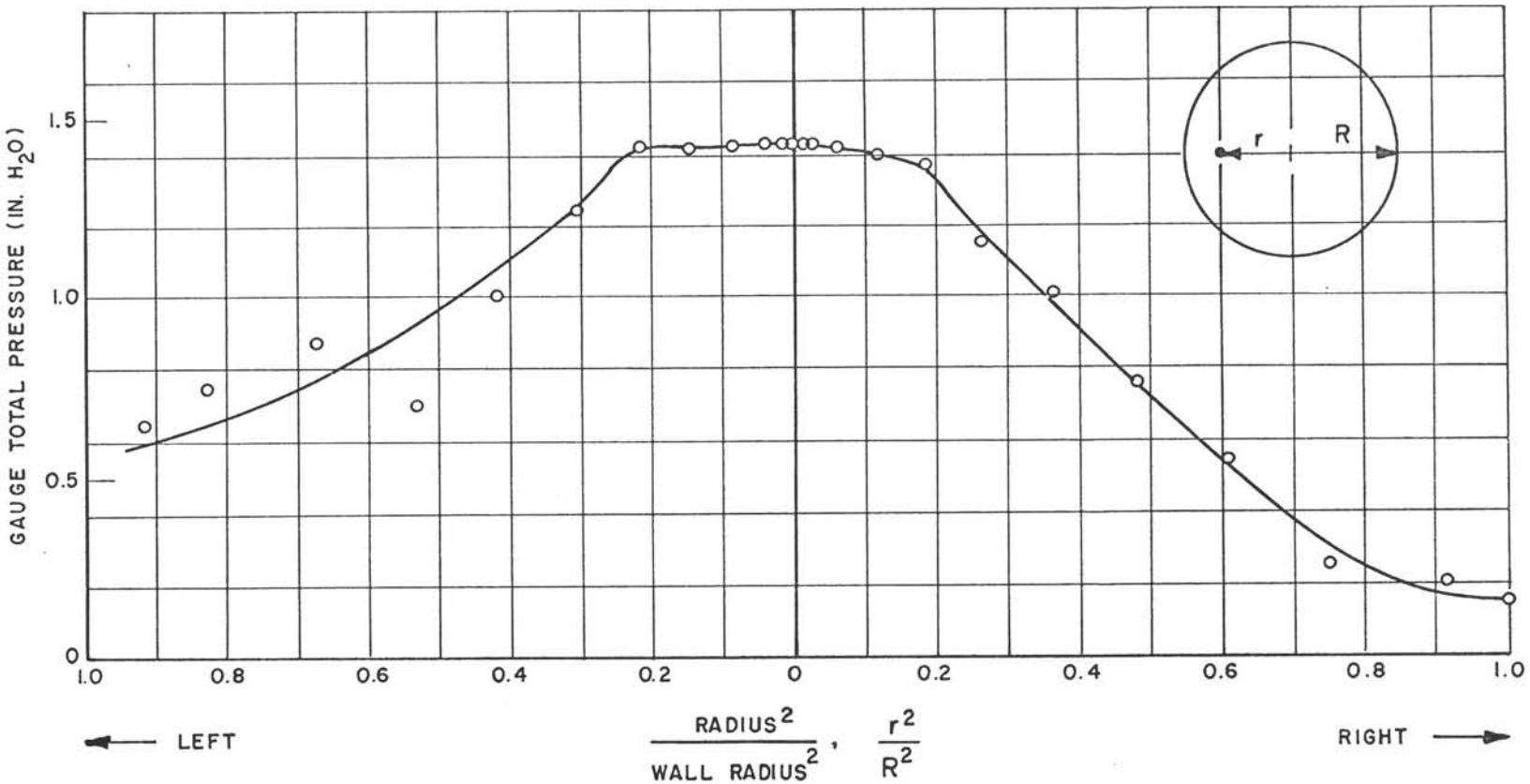

1/12 SCALE VTOL TUNNEL

CONFIGURATION 5

TOTAL HEAD PROFILE ON HORIZONTAL CENTRE LINE, TEST 10

STATION 231 3/4 WORKING SECTION EMPTY

AMBIENT PRESSURE = 30 IN. Hg

WORKING SECTION { VELOCITY = 156 FT./SEC.
VELOCITY HEAD = 4.08 IN. H_2O

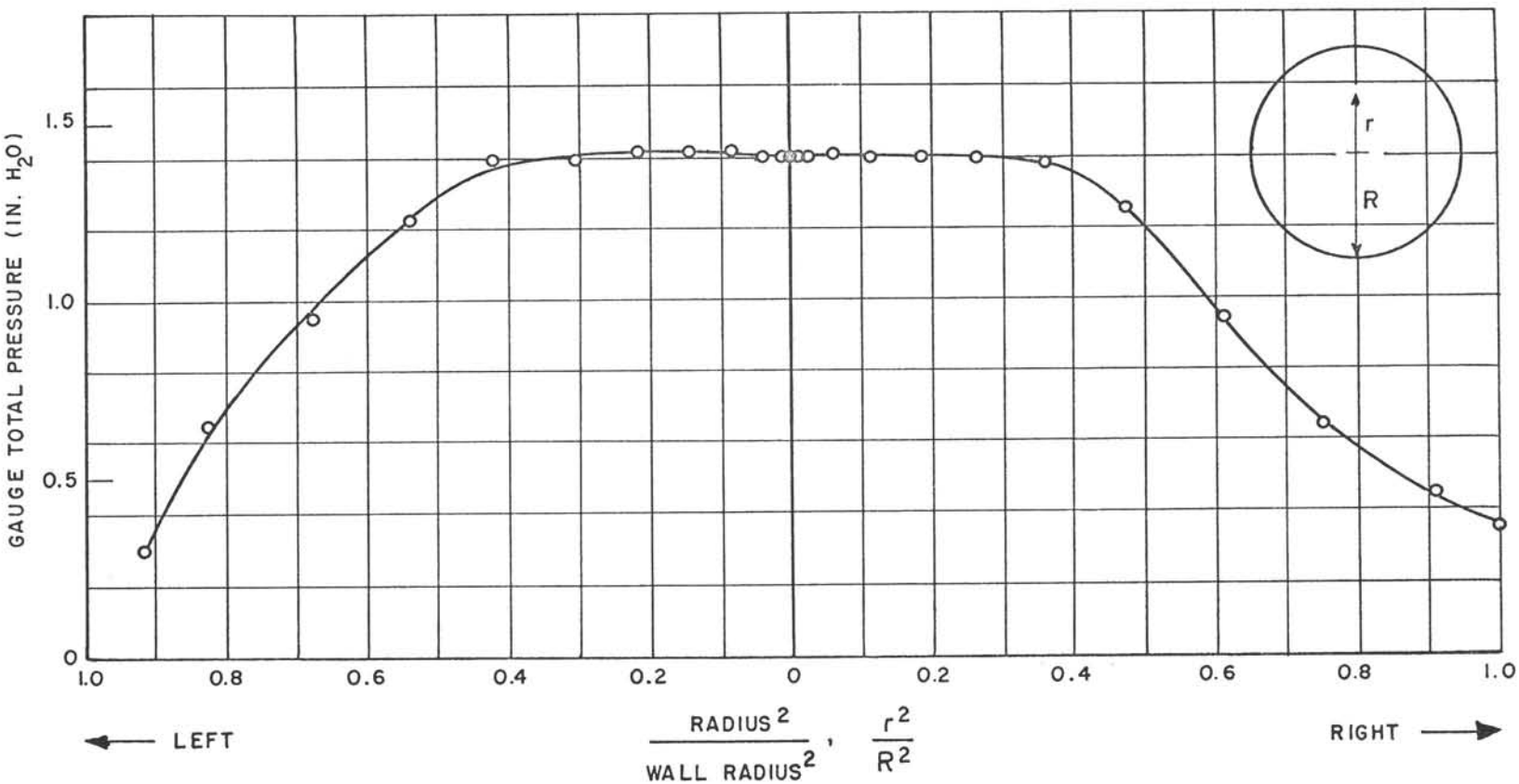

1/12 SCALE VTOL TUNNEL

CONFIGURATION 5

TOTAL HEAD PROFILE ON VERTICAL DIAMETER OF EXIT DIFFUSER, TEST 10

STATION 231 3/4

AMBIENT PRESSURE = 30 IN. Hg

WORKING SECTION { VELOCITY = 150 FT./SEC.
VELOCITY HEAD = 4.08 IN. H_2O

FIG. 1.25
LR-349

FIG. 1.26
LR-349

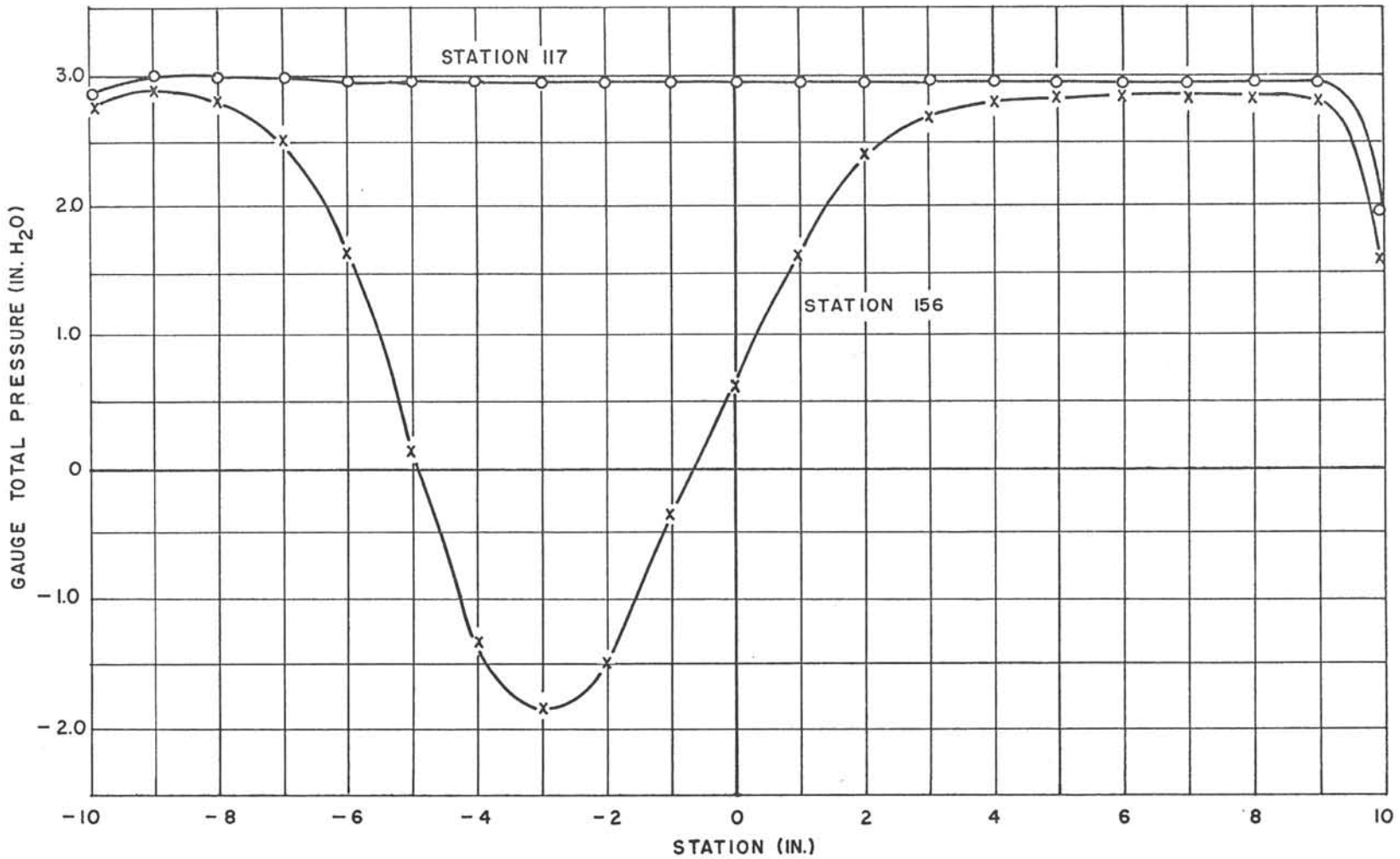

1/12 SCALE VTOL TUNNEL

CONFIGURATION 5

WORKING SECTION TOTAL HEAD PROFILES — AEROFOIL MOUNTED, TEST 11

α = 30° TRAVERSE ON VERTICAL CENTRE LINE

AMBIENT PRESSURE = 29.29 IN. Hg

WORKING SECTION { VELOCITY = 156 FT./SEC.
VELOCITY HEAD = 4.08 IN. H_2O

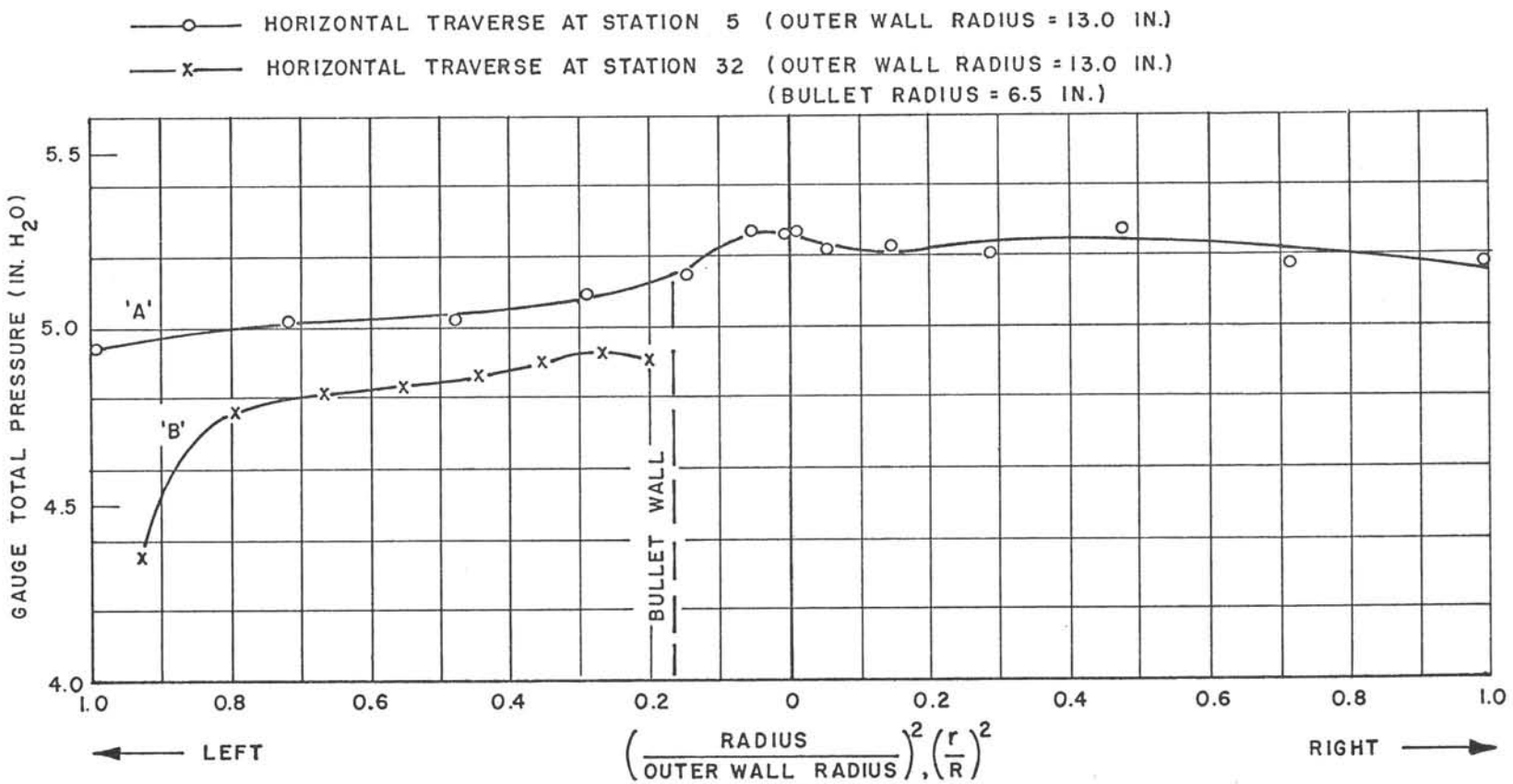

1/12 SCALE VTOL TUNNEL

CONFIGURATION 3

TOTAL HEAD PROFILES NEAR ENTRANCE, TEST 5

FIG. I.27
LR-349

FIG. 1.28
LR-349

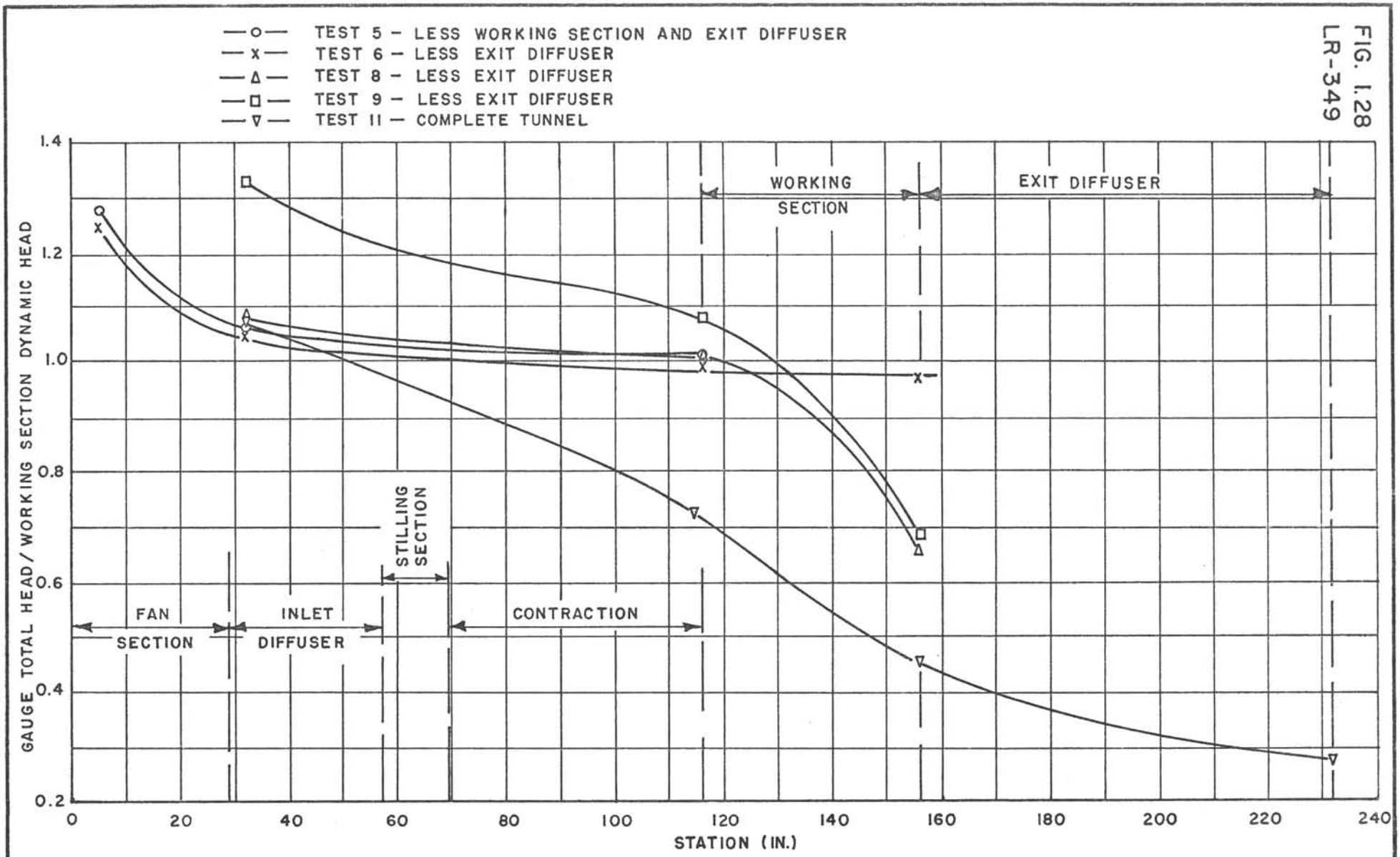

1/12 SCALE VTOL TUNNEL
CONFIGURATION 5
LONGITUDINAL VARIATION OF TOTAL HEAD (NON-DIMENSIONAL)

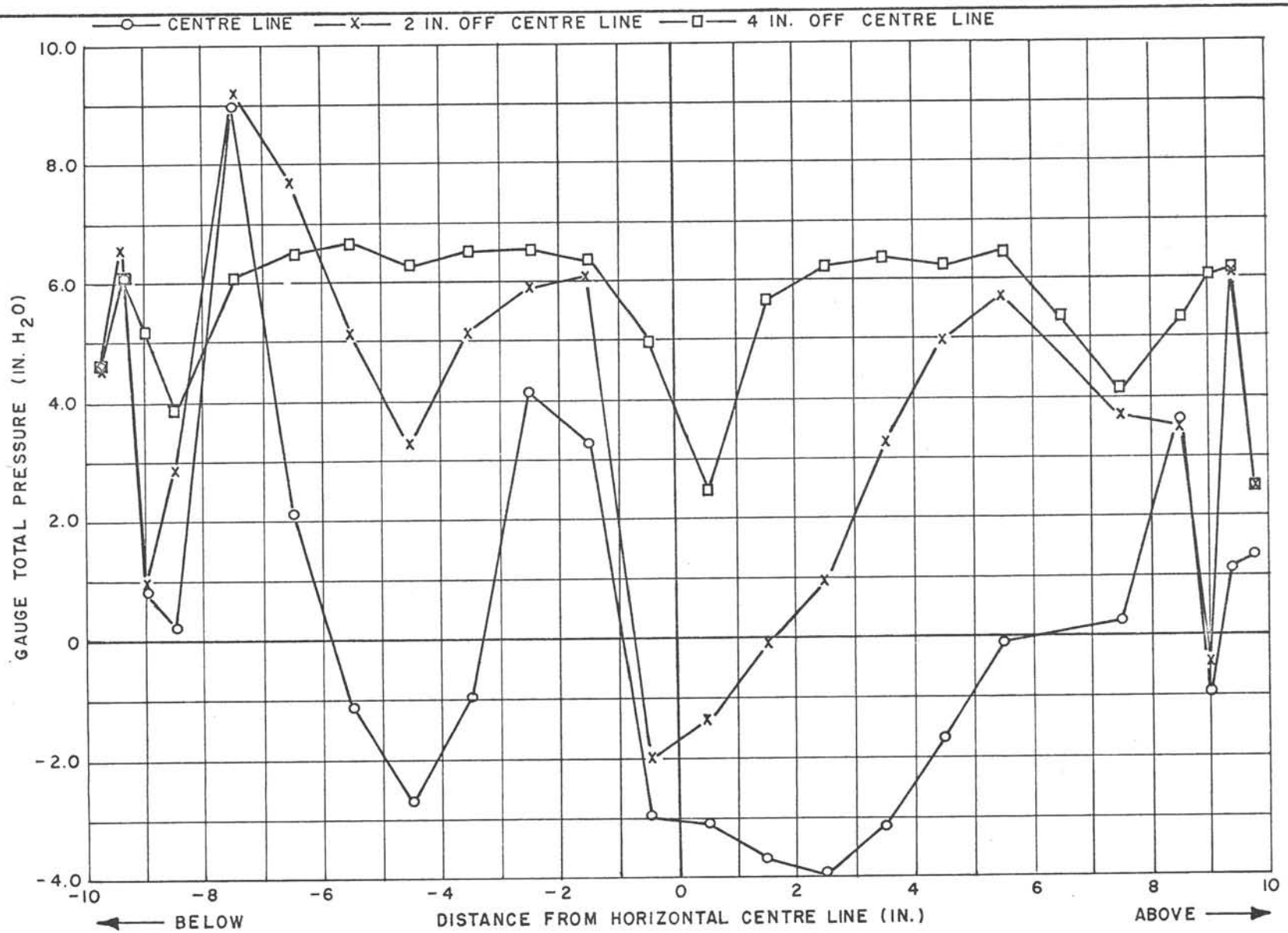

1/12 SCALE VTOL TUNNEL

CONFIGURATION 4

VERTICAL TOTAL HEAD PROFILES BEHIND A SIMULATED FAN-IN-WING MODEL, TEST 12

STATION 139 1/4

WORKING SECTION VELOCITY = 168 FT./SEC.

JET VELOCITY = 587 FT./SEC.

AMBIENT PRESSURE = 29.7 IN Hg

FIG. 1.29
LR-349

FIG. 1.30
LR-349

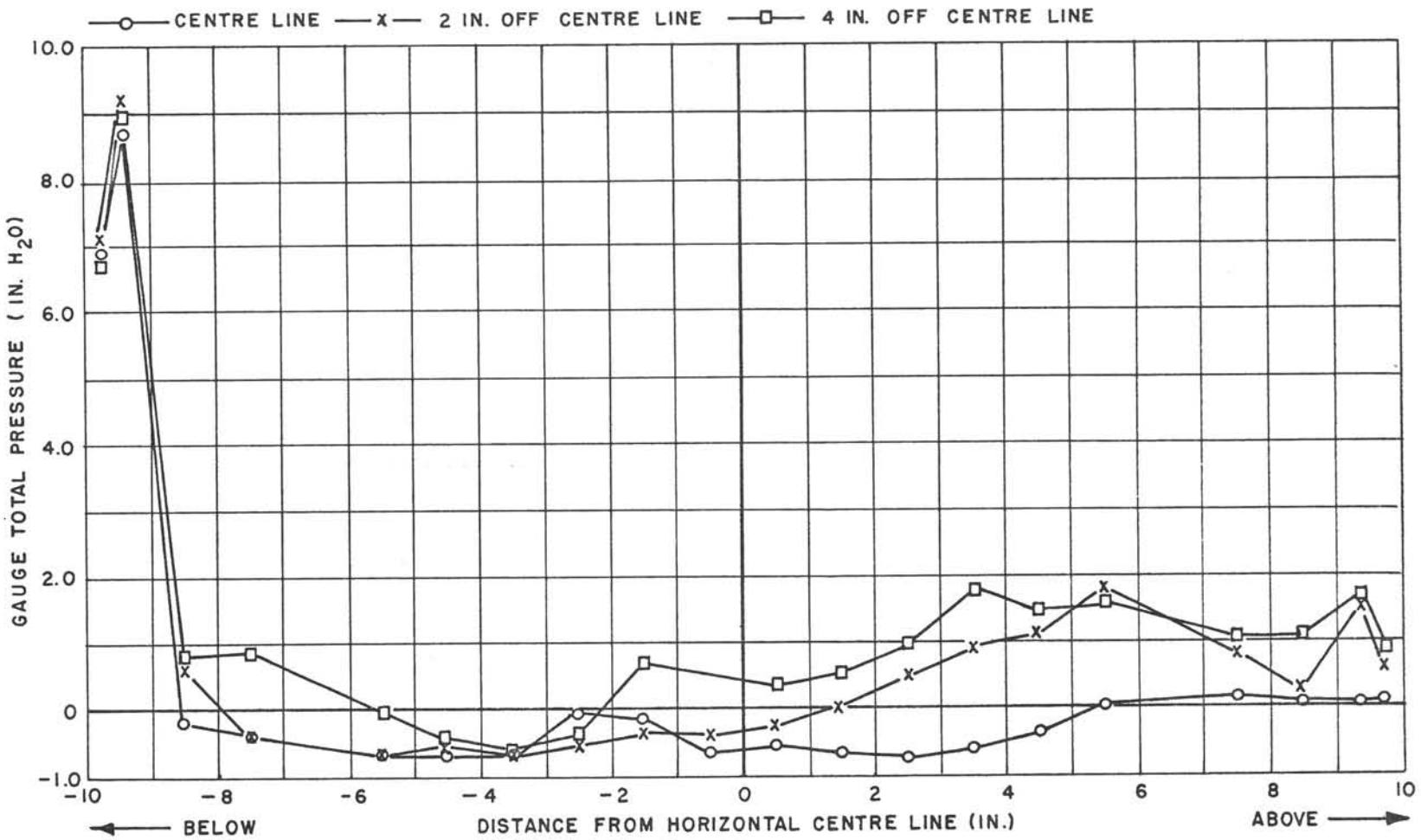

1/12 SCALE VTOL TUNNEL

CONFIGURATION 4

VERTICAL TOTAL HEAD PROFILES BEHIND A SIMULATED FAN-IN-WING MODEL, TEST 13

STATION 139 1/4

WORKING SECTION VELOCITY = 68 FT./SEC.
JET VELOCITY = 587 FT./SEC.
AMBIENT PRESSURE = 29.9 IN. Hg

FIG. 1.31
LR-349

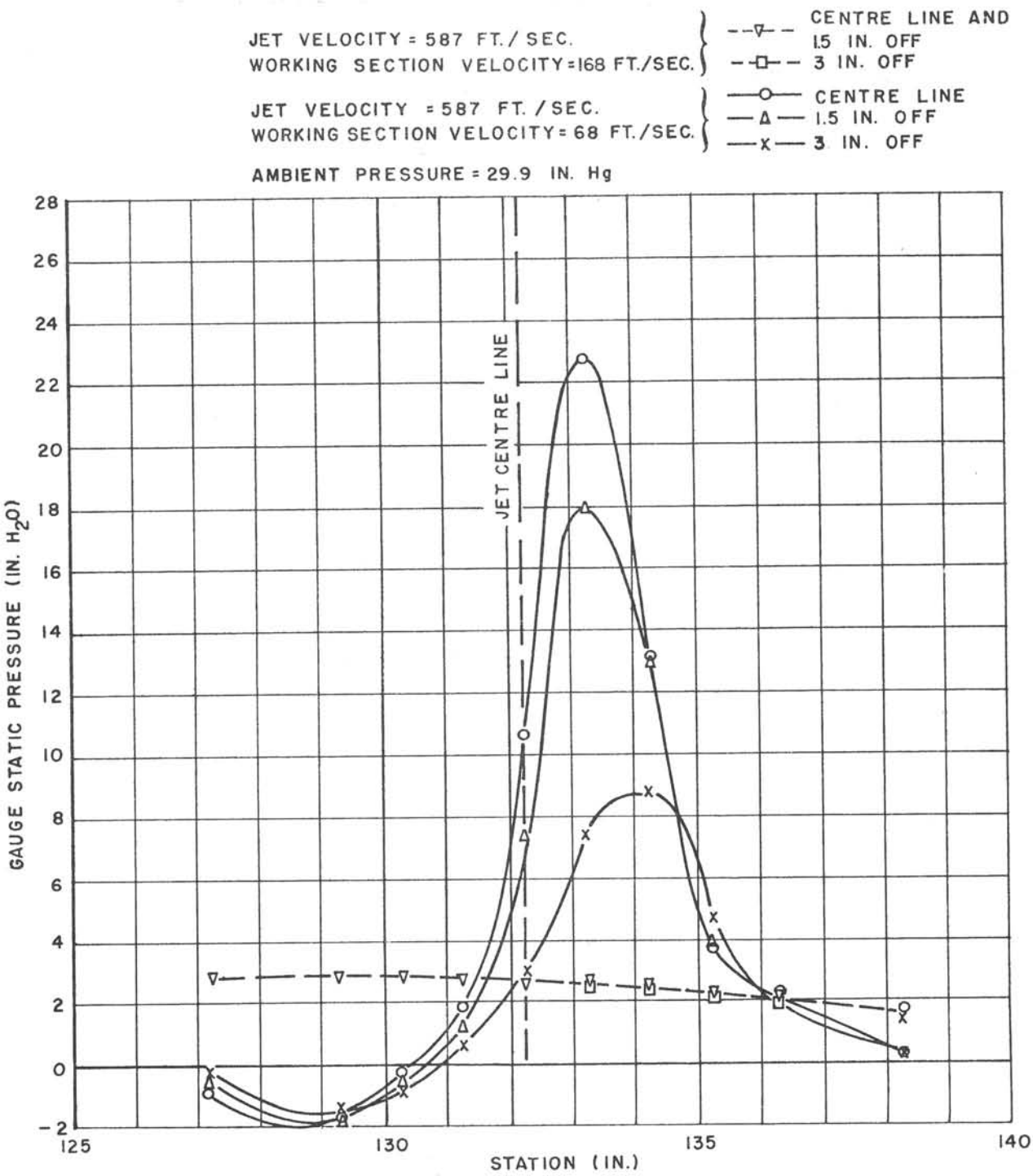

1/12 SCALE VTOL TUNNEL

CONFIGURATION 4

FLOOR STATIC PRESSURES WITH SIMULATED FAN-IN-WING MODEL

TESTS 12 AND 13

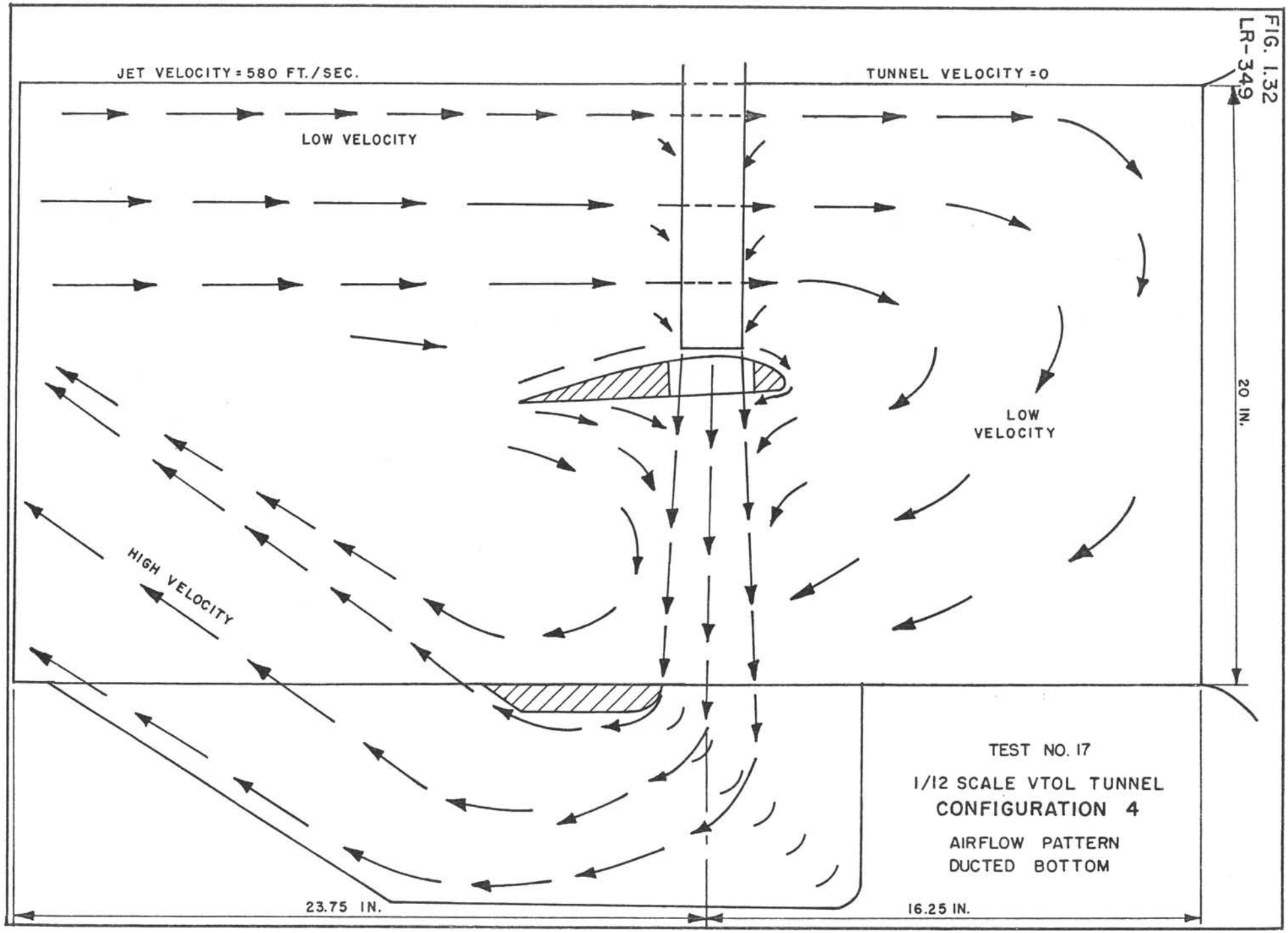

FIG. 1.32
LR-349

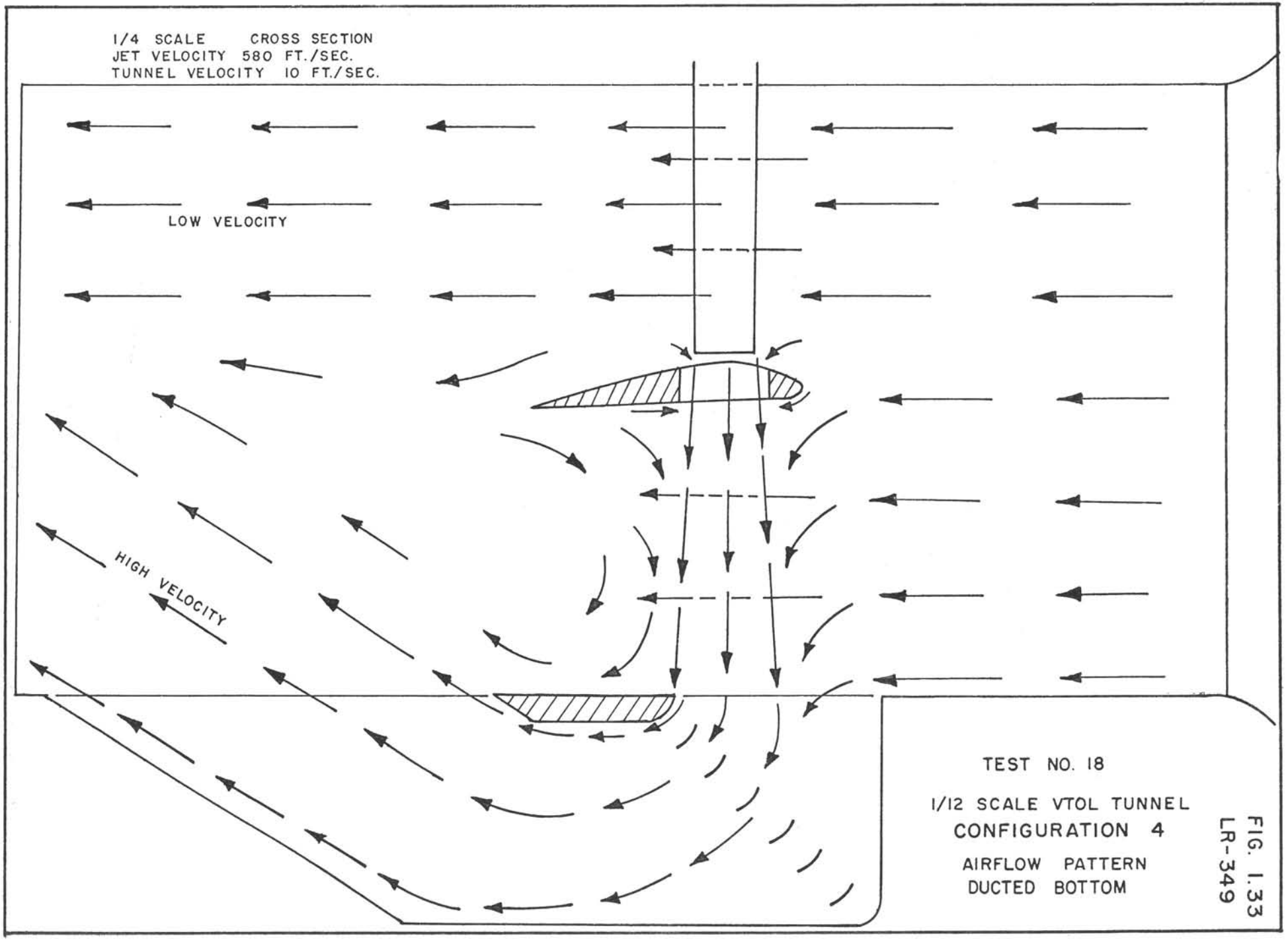
1/4 SCALE CROSS SECTION
JET VELOCITY 580 FT./SEC.
TUNNEL VELOCITY 10 FT./SEC.
LOW VELOCITY
HIGH VELOCITY
TEST NO. 18
1/12 SCALE VTOL TUNNEL
CONFIGURATION 4
AIRFLOW PATTERN
DUCTED BOTTOM
FIG. 1.33
LR-349

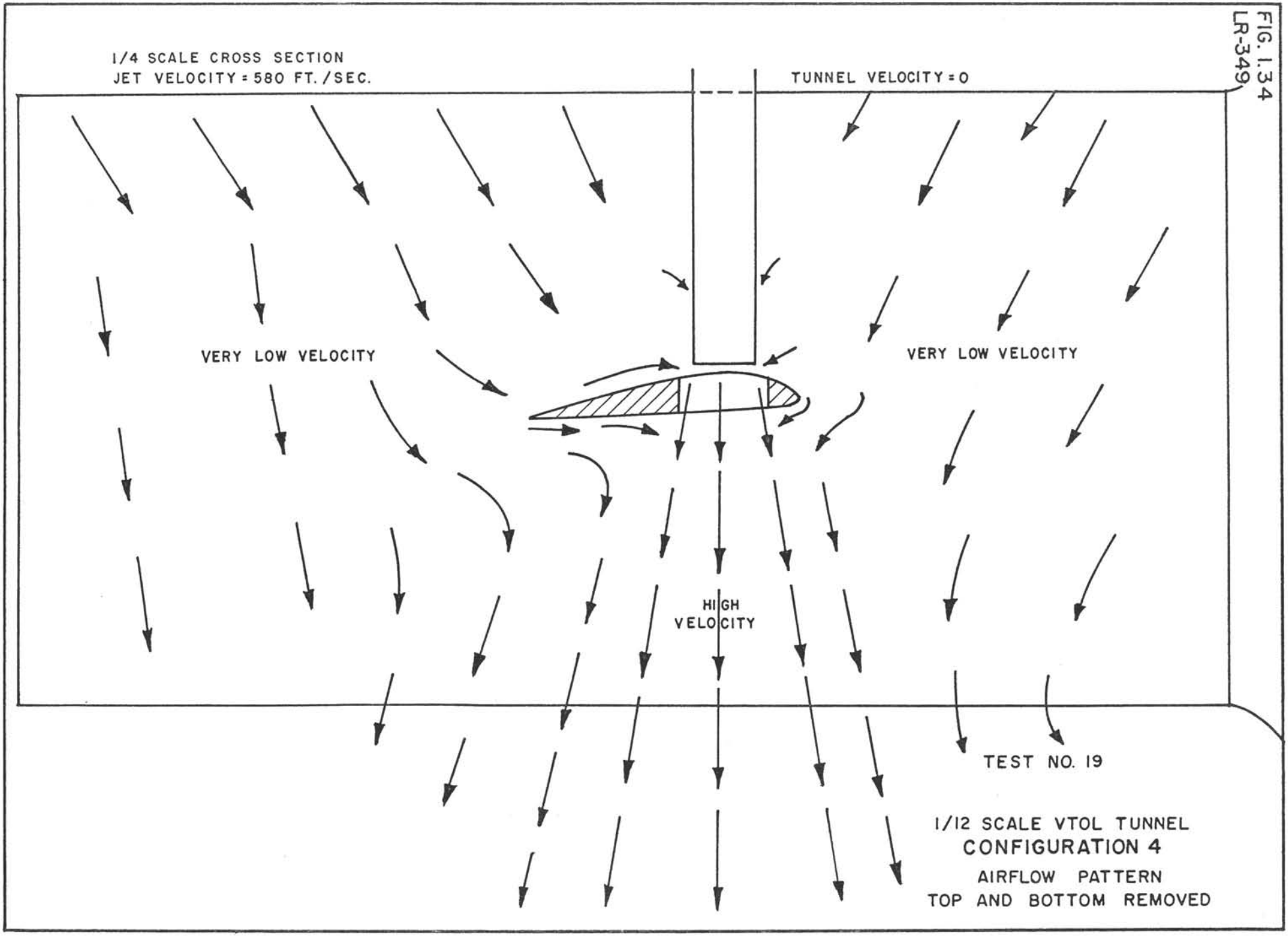

FIG. I.34
LR-349

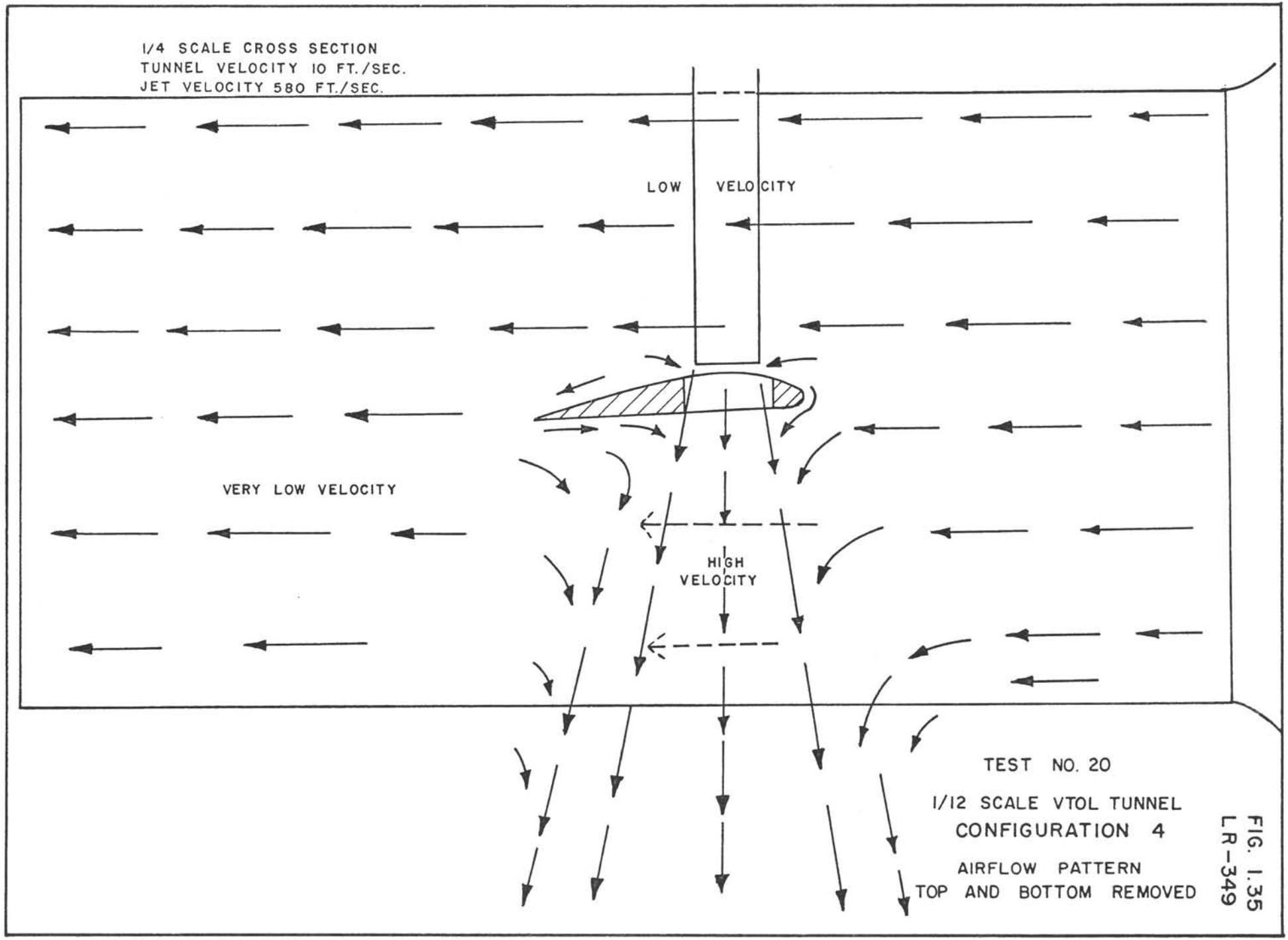
1/4 SCALE CROSS SECTION
TUNNEL VELOCITY 10 FT./SEC.
JET VELOCITY 580 FT./SEC.
LOW VELOCITY
VERY LOW VELOCITY
HIGH VELOCITY
TEST NO. 20
1/12 SCALE VTOL TUNNEL
CONFIGURATION 4
AIRFLOW PATTERN
TOP AND BOTTOM REMOVED
FIG. 1.35
LR-349

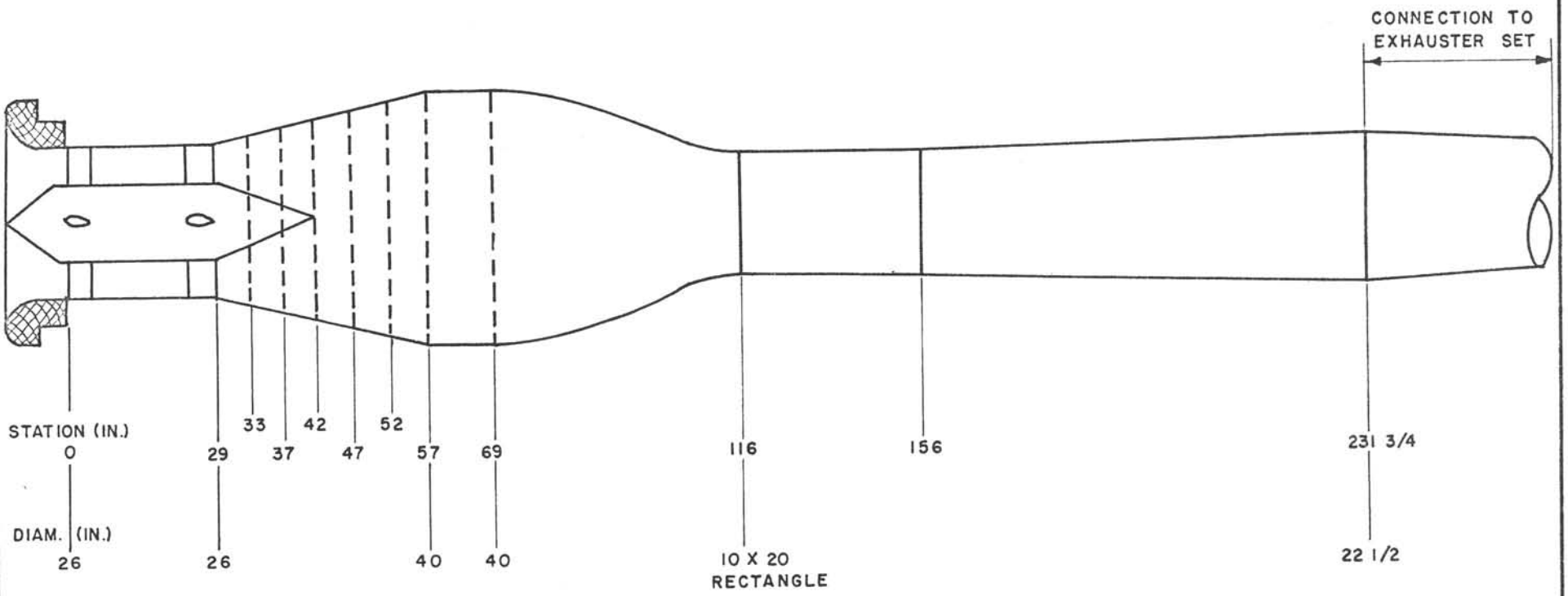

CONFIGURATION 6

1/12 SCALE VTOL TUNNEL (EXHAUSTER DRIVEN)

FIG. 2.1
LR-349

FIG. 2.2
LR-349

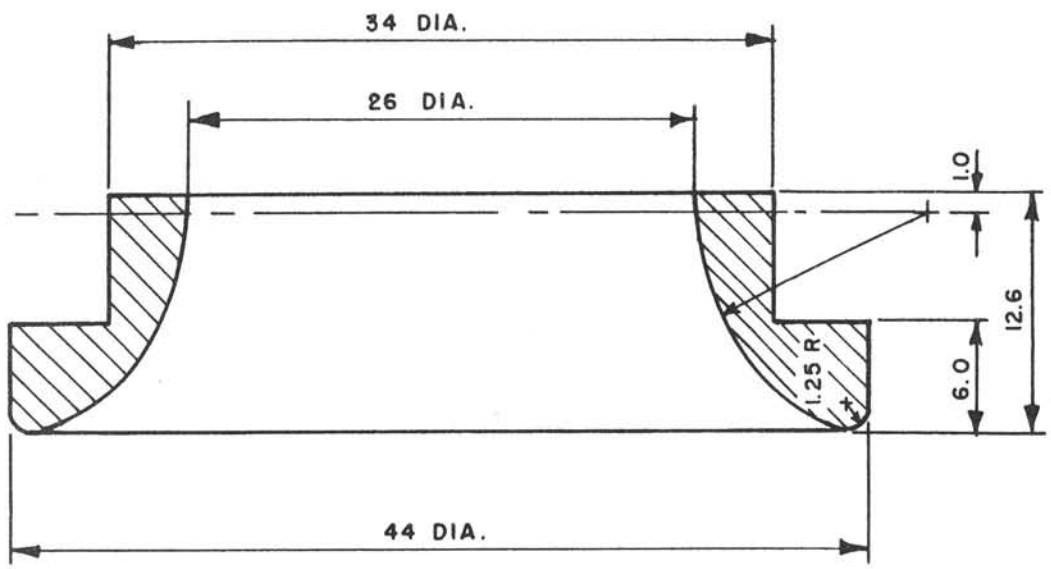

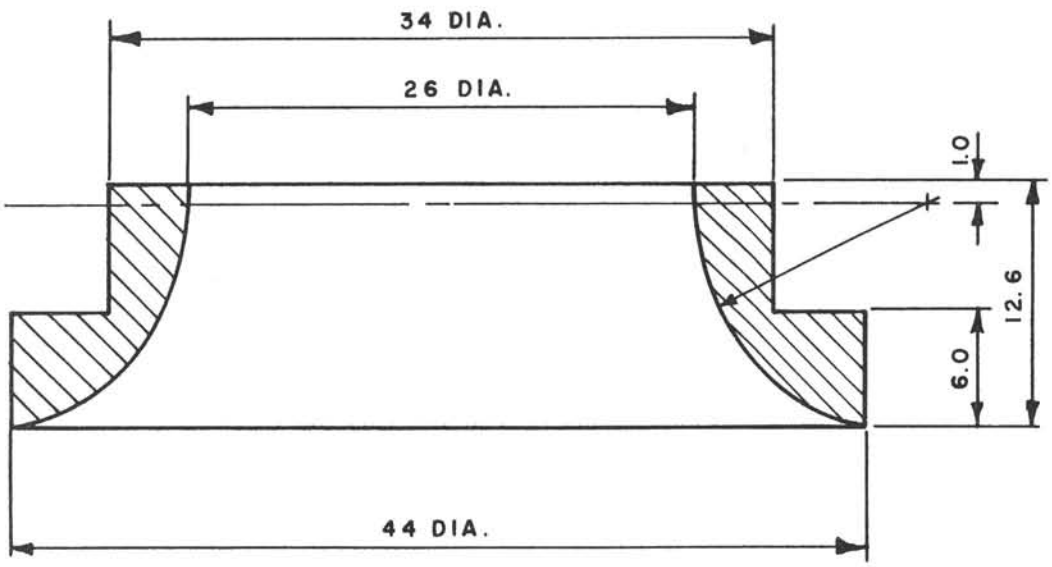

SCALE: 1/10 FULL SIZE

BASIC AND MODIFIED INTAKE

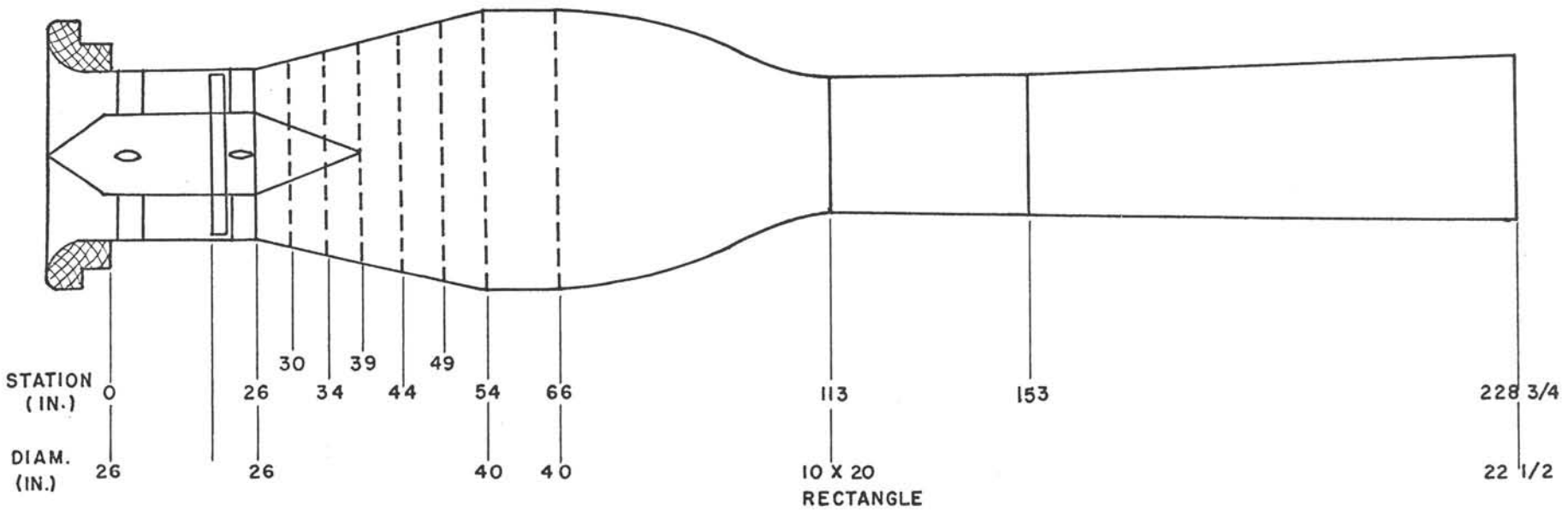

CONFIGURATION 7

1/12 SCALE VTOL TUNNEL (FAN DRIVEN)

FIG. 2.3
LR-349

FIG. 2.4
LR-349

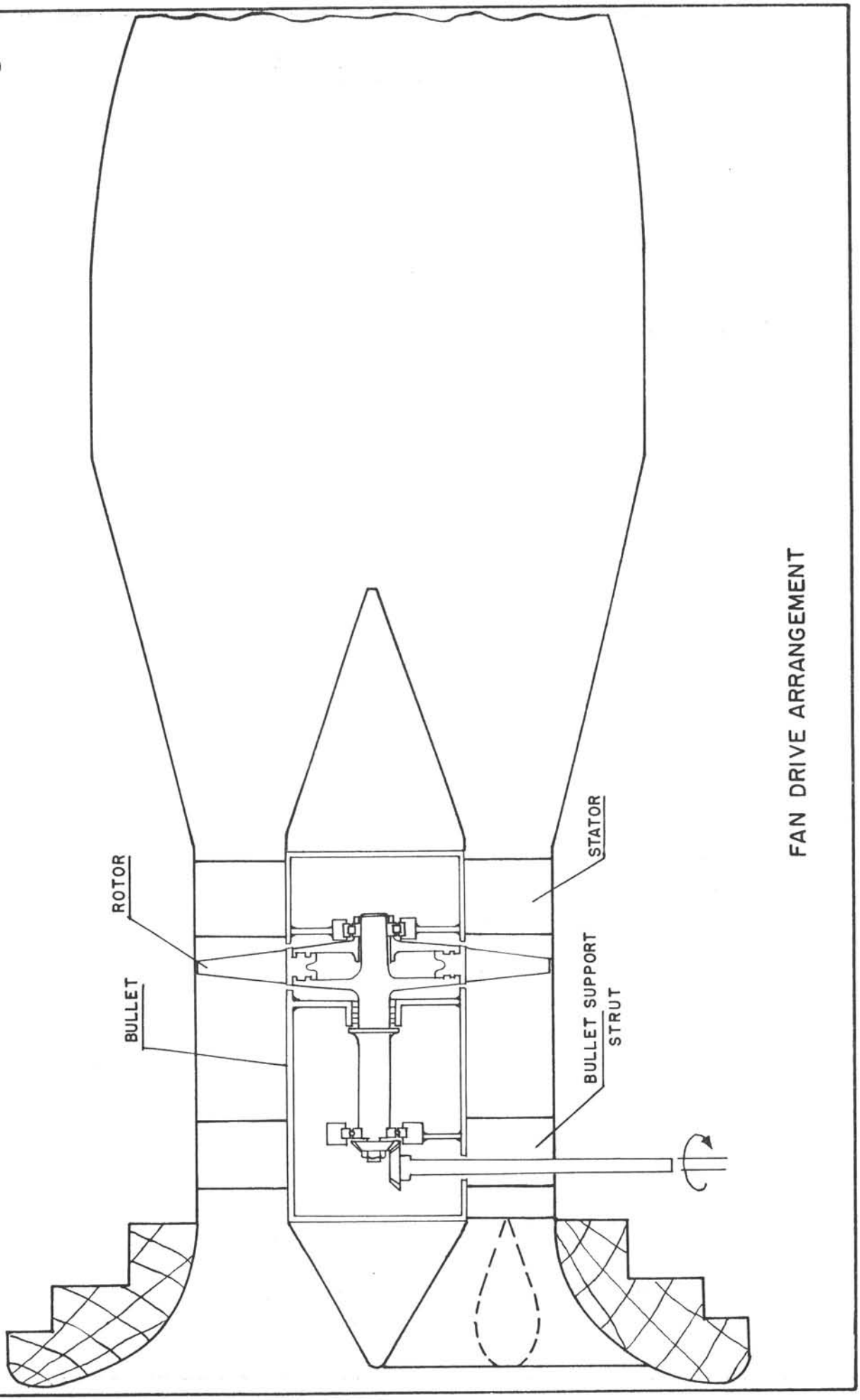

FAN DRIVE ARRANGEMENT

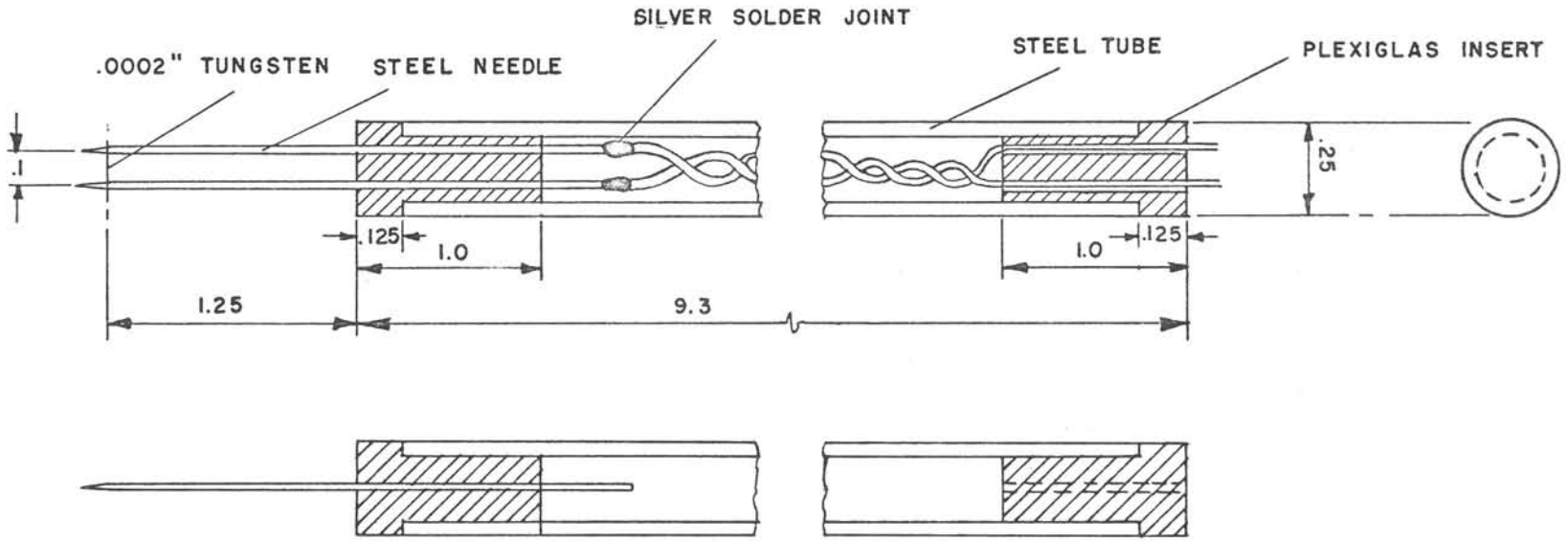

DIMENSIONS ARE INCHES

HOT WIRE PROBE

FIG. 2.5
LR-349

FIG. 2.6
LR-349

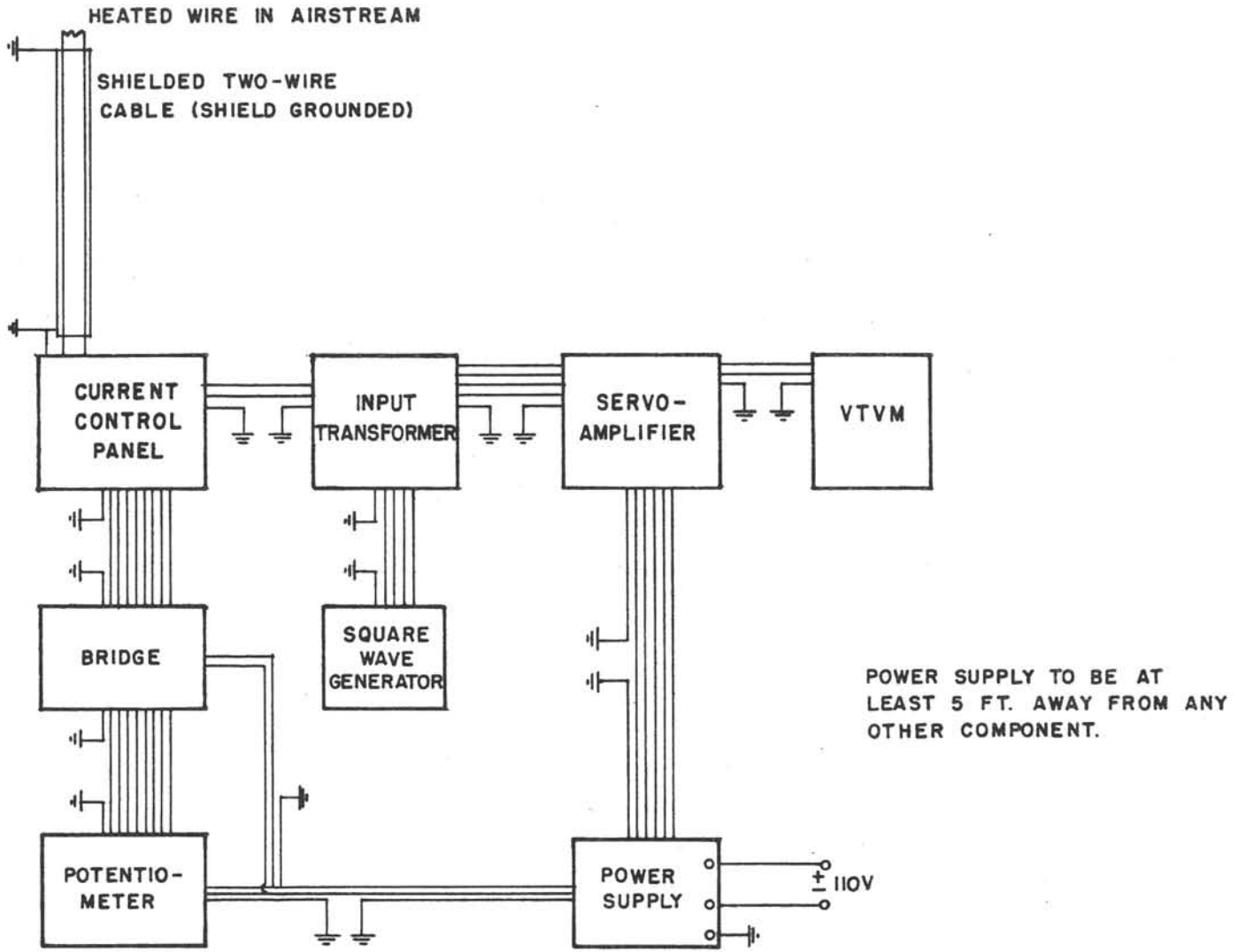

SCHEMATIC ARRANGEMENT OF COMPONENTS OF CONSTANT CURRENT HOT WIRE ANEMOMETER SYSTEM

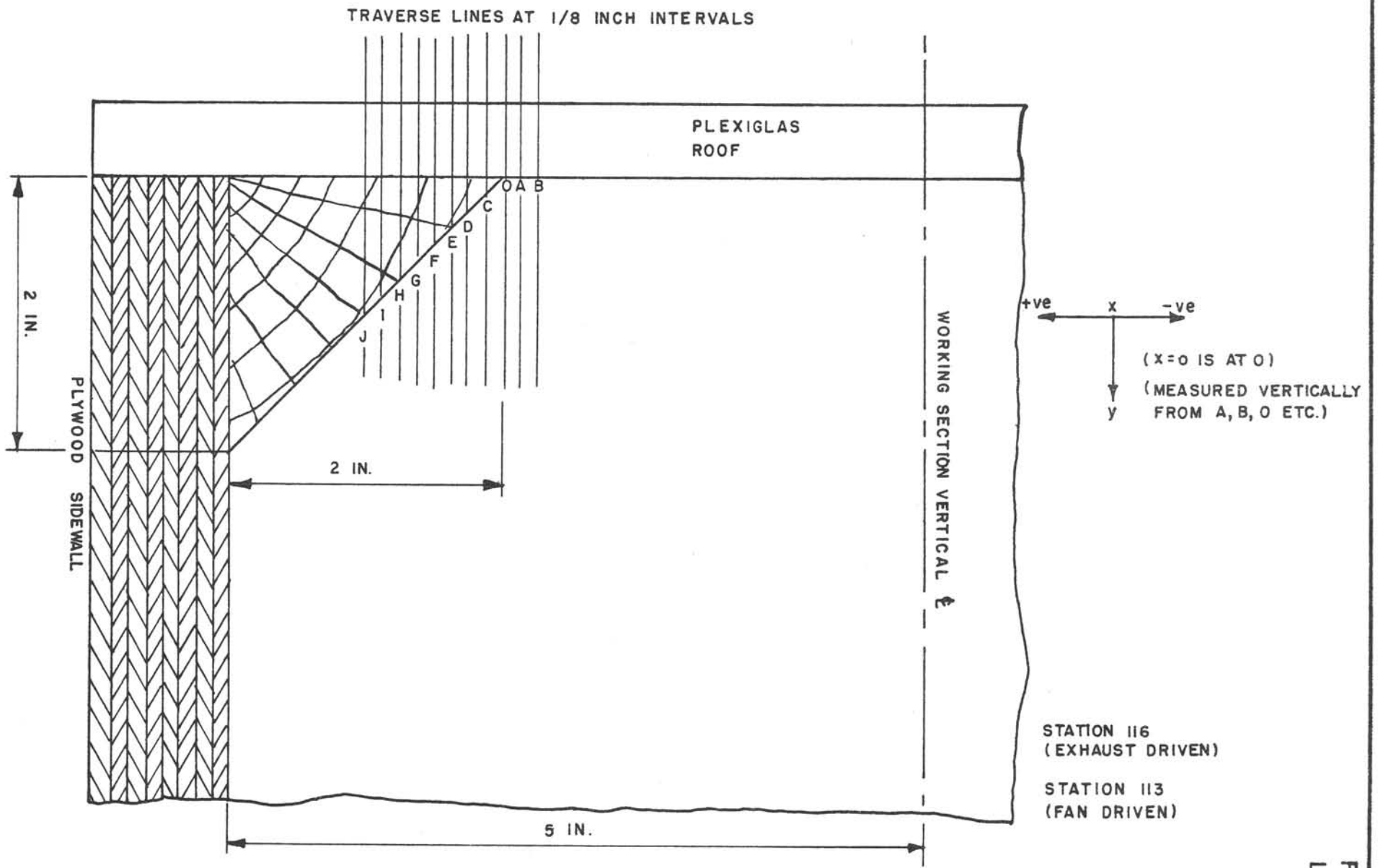

BOUNDARY LAYER TRAVERSE LINES IN WORKING SECTION CORNER

FIG. 2.7
LR-349

FIG. 2.8
LR-349

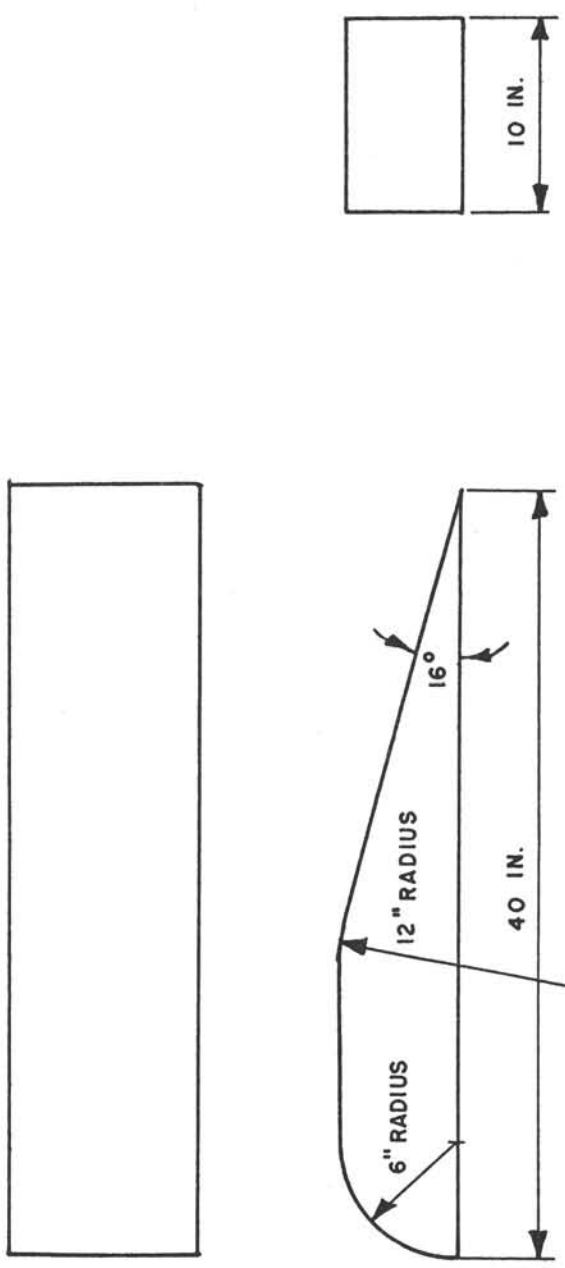

TYPICAL WORKING SECTION INSERT

FIG. 2.11
LR-349

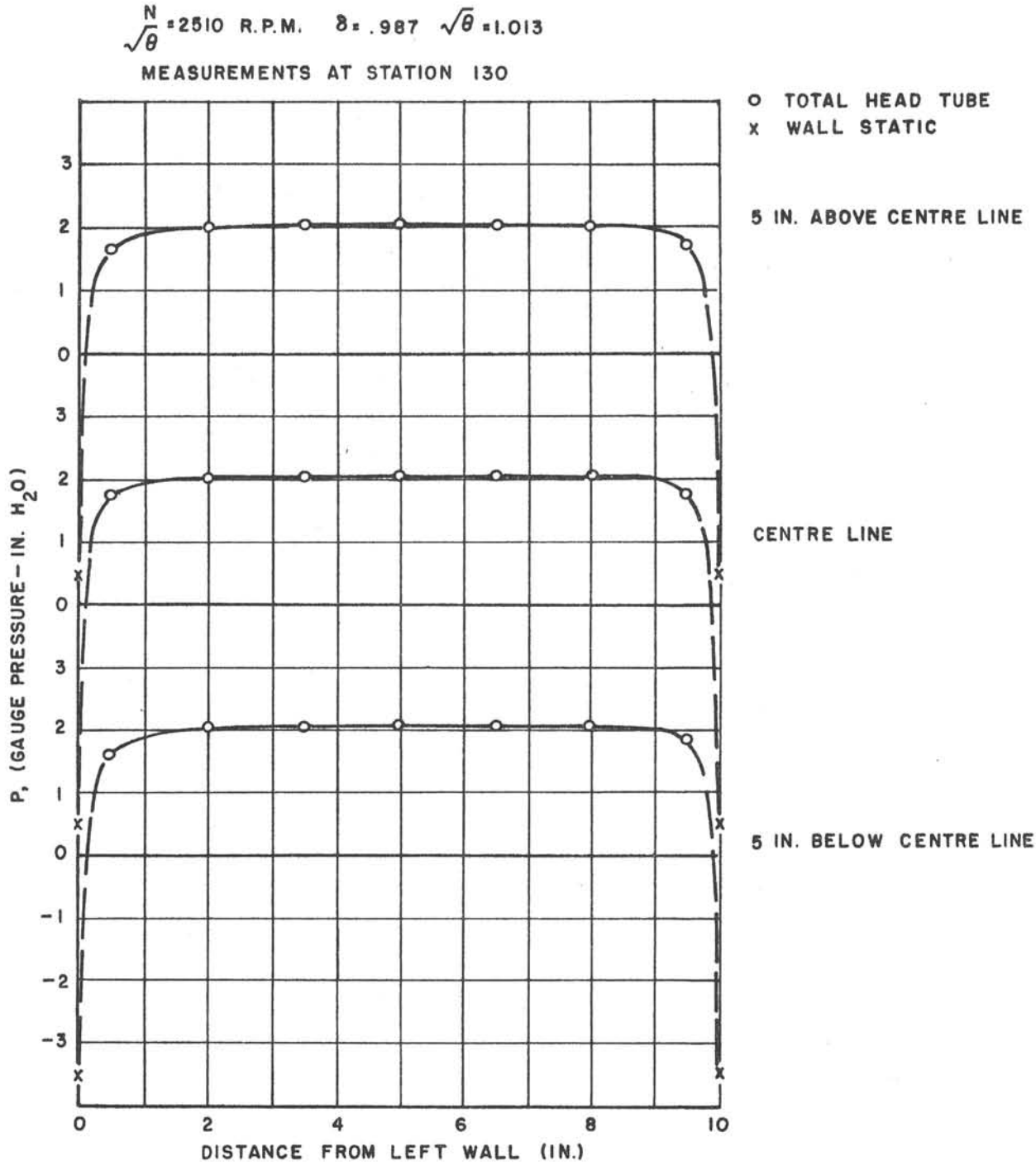

1/12 SCALE VTOL TUNNEL

DIFFUSER ATTACHED - CONFIGURATION 7

WORKING SECTION TOTAL HEAD PROFILES

FIG. 2.12
LR-349

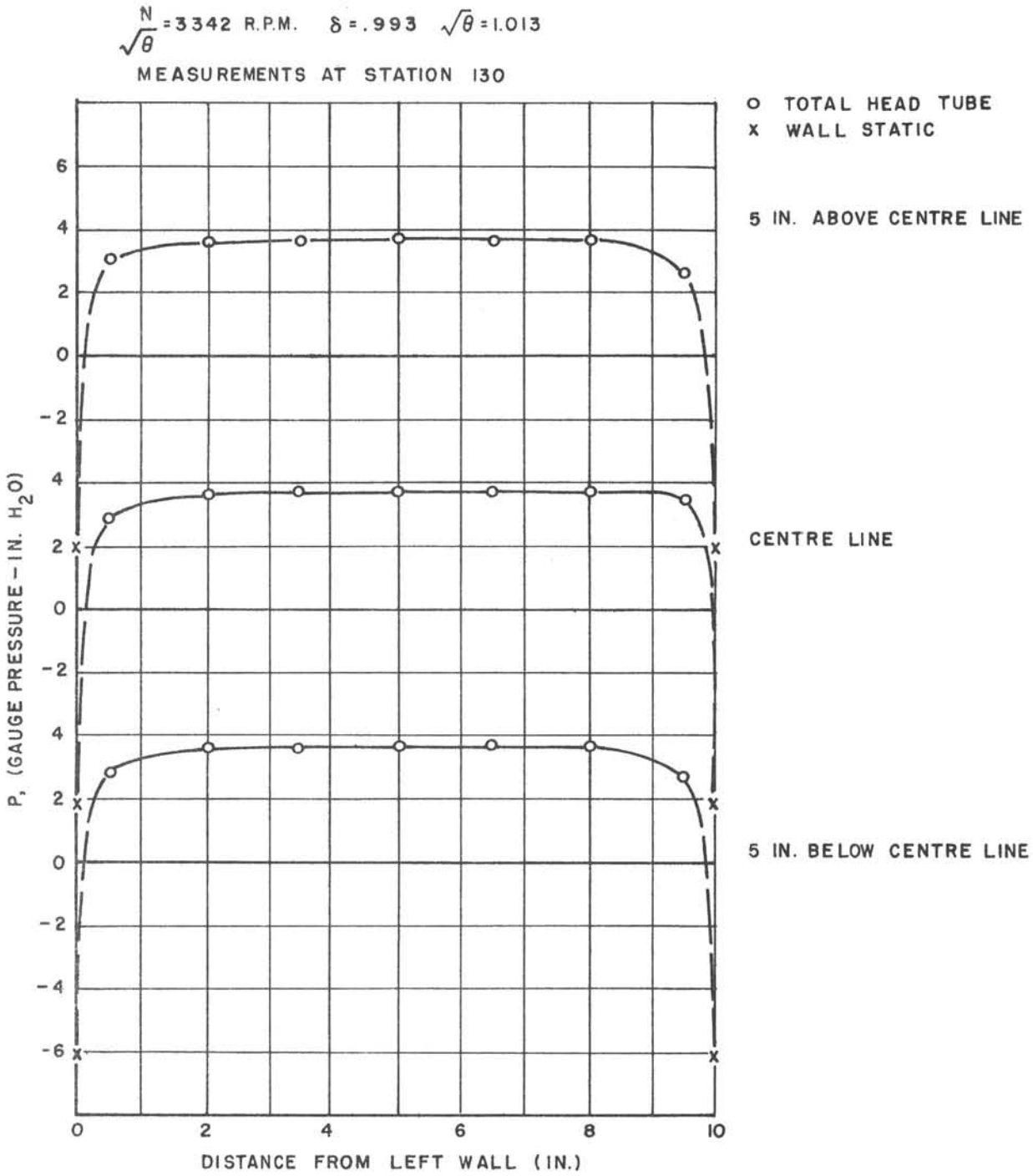

1/12 SCALE VTOL TUNNEL
DIFFUSER ATTACHED - CONFIGURATION 7
WORKING SECTION TOTAL HEAD PROFILES

FIG. 2.13
LR-349

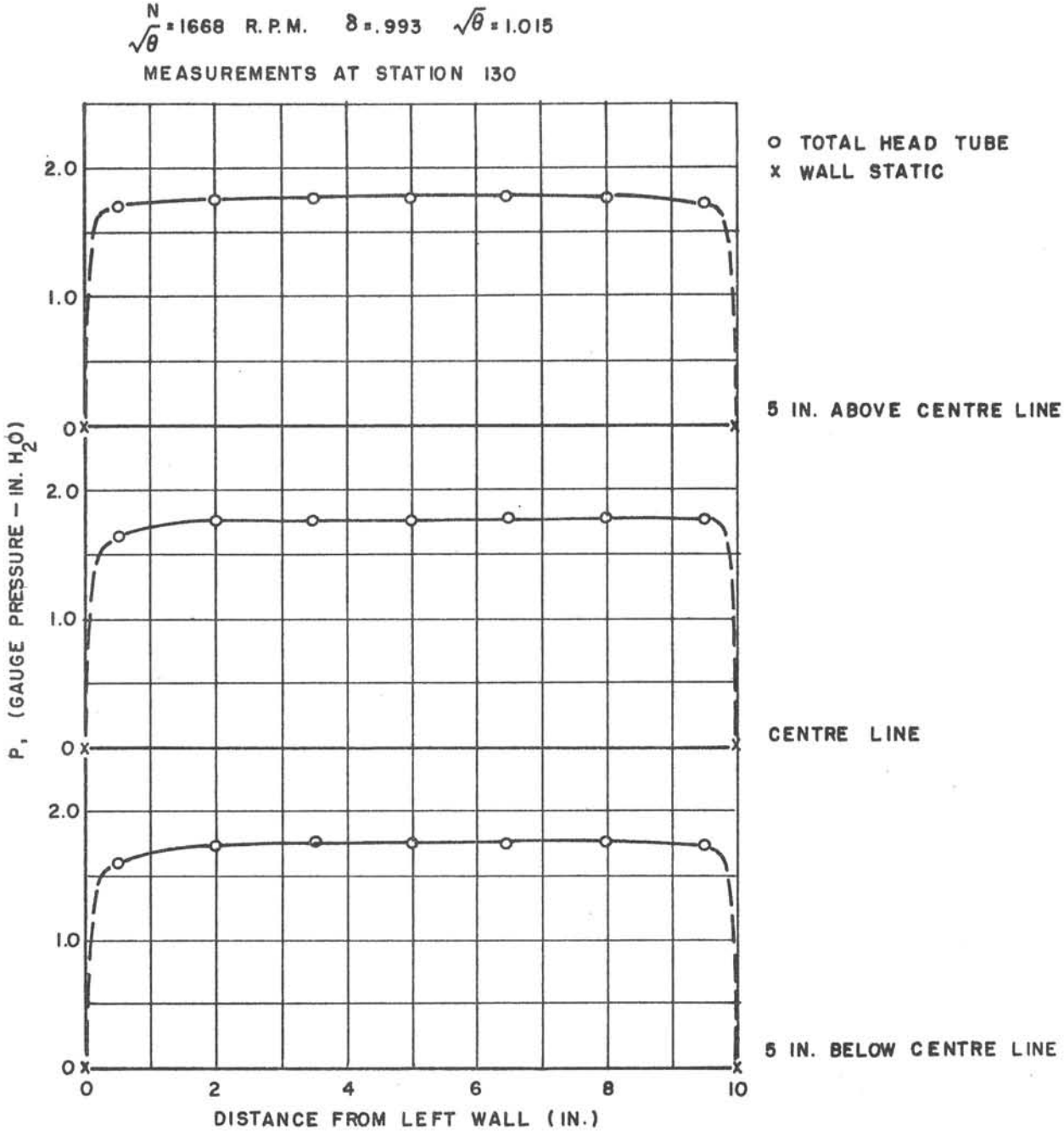

1/12 SCALE VTOL TUNNEL

NO DIFFUSER – CONFIGURATION 8

WORKING SECTION TOTAL HEAD PROFILES

FIG. 2.14
LR-349

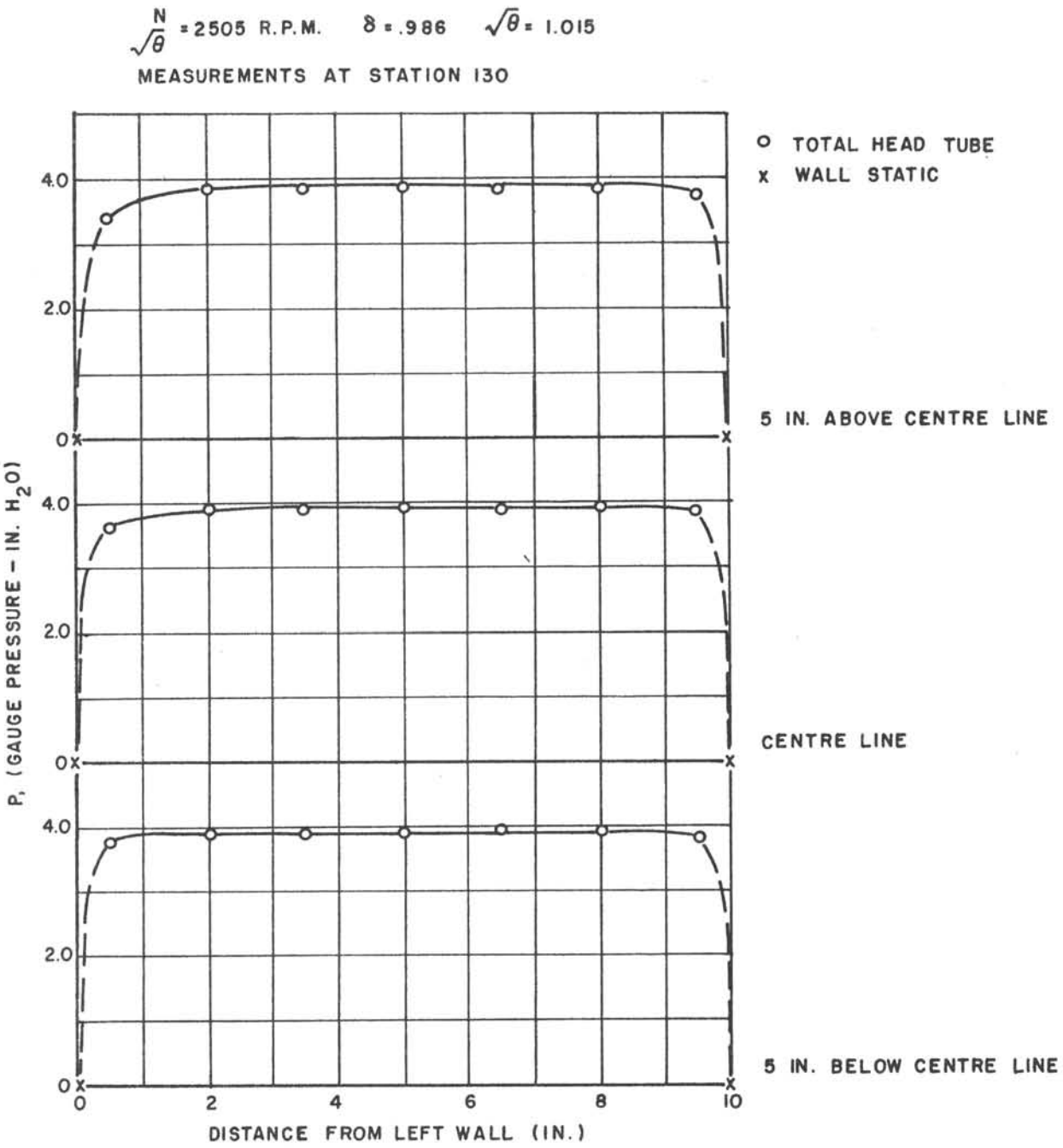

1/12 SCALE VTOL TUNNEL
NO DIFFUSER - CONFIGURATION 8
WORKING SECTION TOTAL HEAD PROFILES

FIG. 2.15
LR-349

$\frac{N}{\sqrt{\theta}}$ = 3340 R.P.M. δ = .993 $\sqrt{\theta}$ = 1.015

MEASUREMENTS AT STATION 130

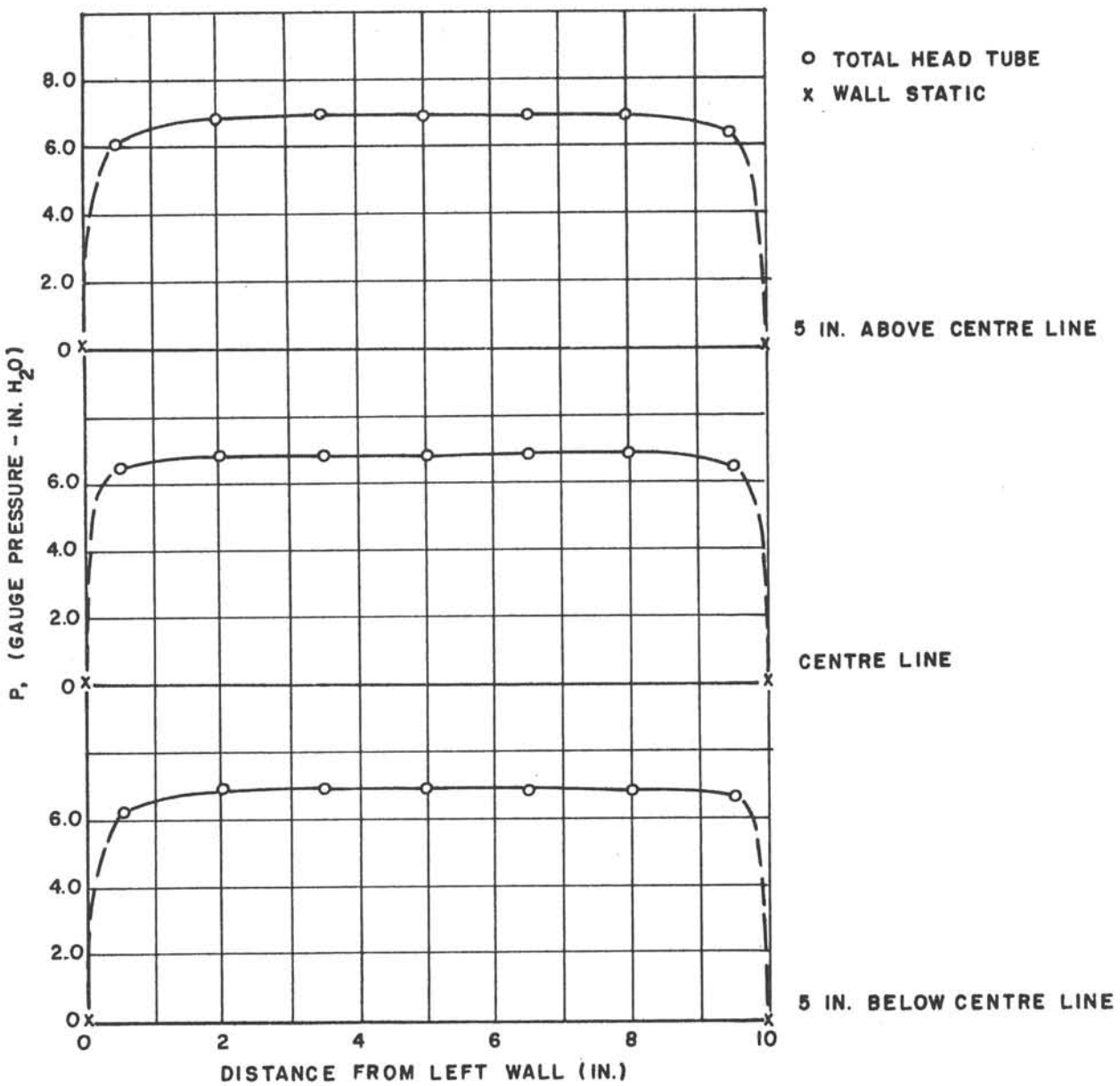

1/12 SCALE VTOL TUNNEL

NO DIFFUSER – CONFIGURATION 8

WORKING SECTION TOTAL HEAD PROFILES

FIG. 2.16
LR-349

$\frac{N}{\sqrt{\theta}}$ = 1672 R.P.M. δ = .998 $\sqrt{\theta}$ = 1.013

MEASUREMENTS AT STATION 130

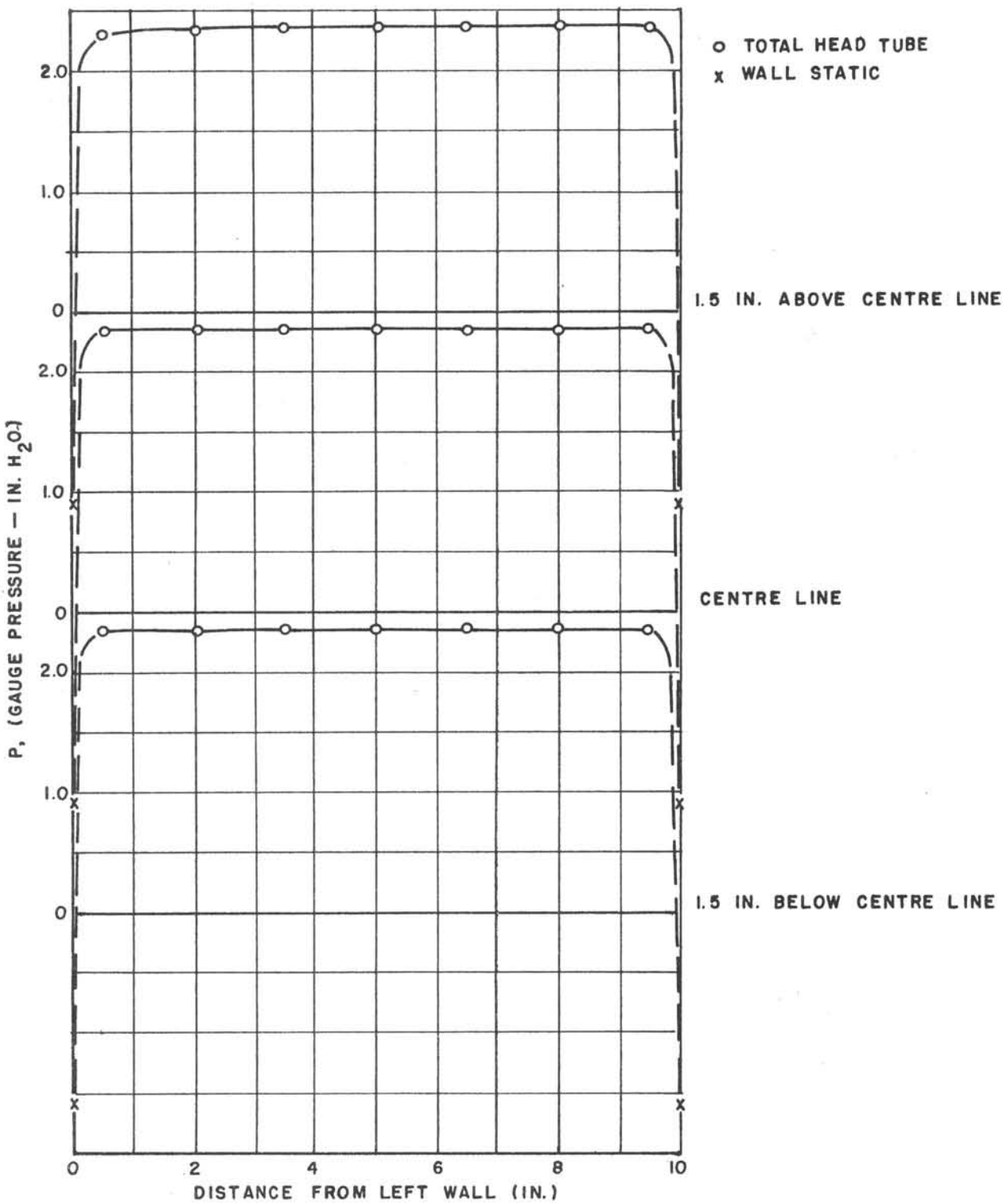

1/12 SCALE VTOL TUNNEL

SIX-INCH BLOCKS—NO DIFFUSER — CONFIGURATION 9

WORKING SECTION TOTAL HEAD PROFILES

FIG. 2.17
LR-349

$\frac{N}{\sqrt{\theta}}$ = 2515 R.P.M. δ = .985 $\sqrt{\theta}$ = 1.01

MEASUREMENTS AT STATION 130

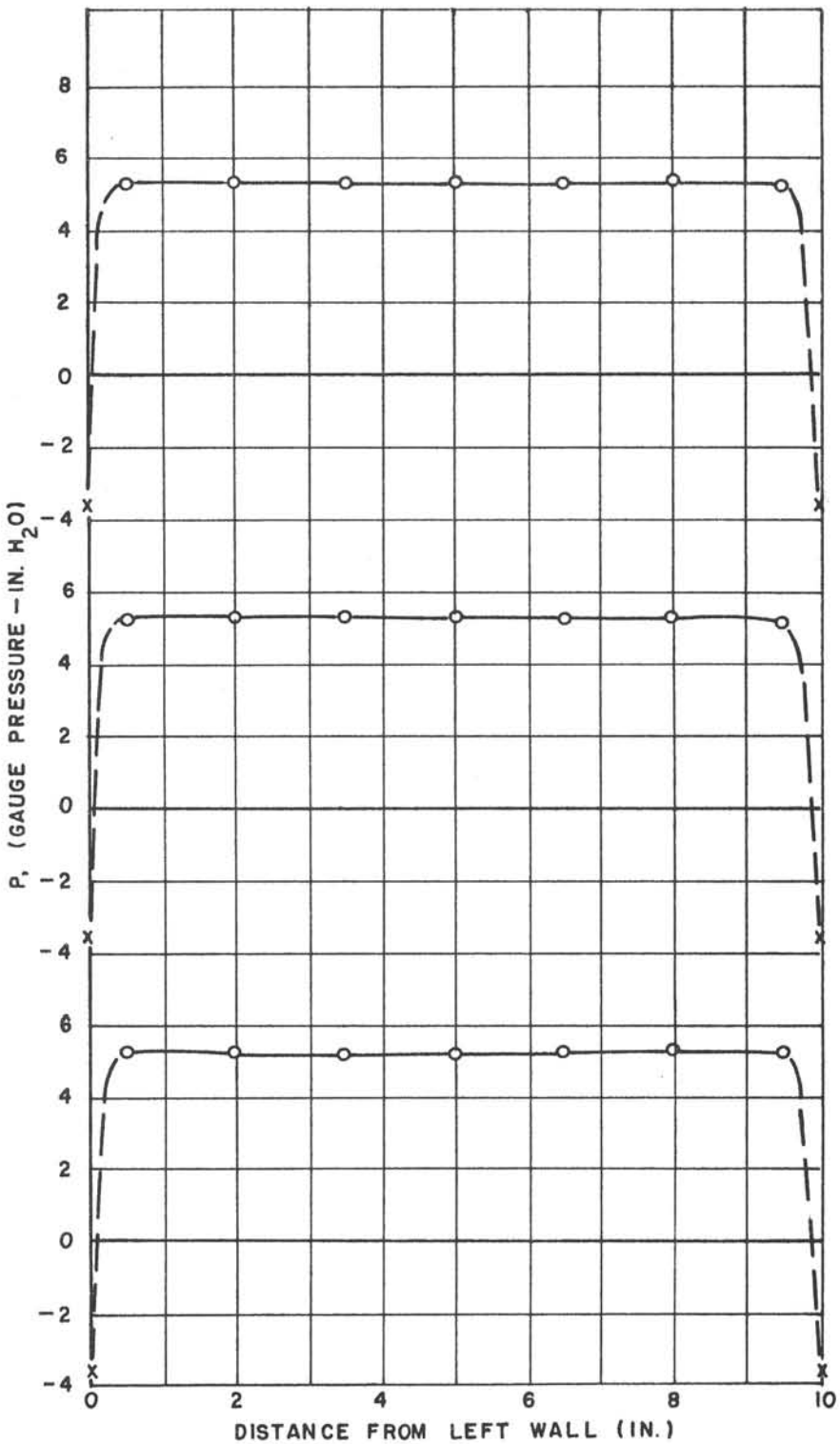

1/12 SCALE VTOL TUNNEL

SIX-INCH BLOCKS INSTALLED – NO DIFFUSER – CONFIGURATION 9

WORKING SECTION TOTAL HEAD PROFILES

FIG. 2.18
LR-349

$\frac{N}{\sqrt{\theta}}$ = 3310 R.P.M. δ = .985 $\sqrt{\theta}$ = 1.01

MEASUREMENTS AT STATION 130

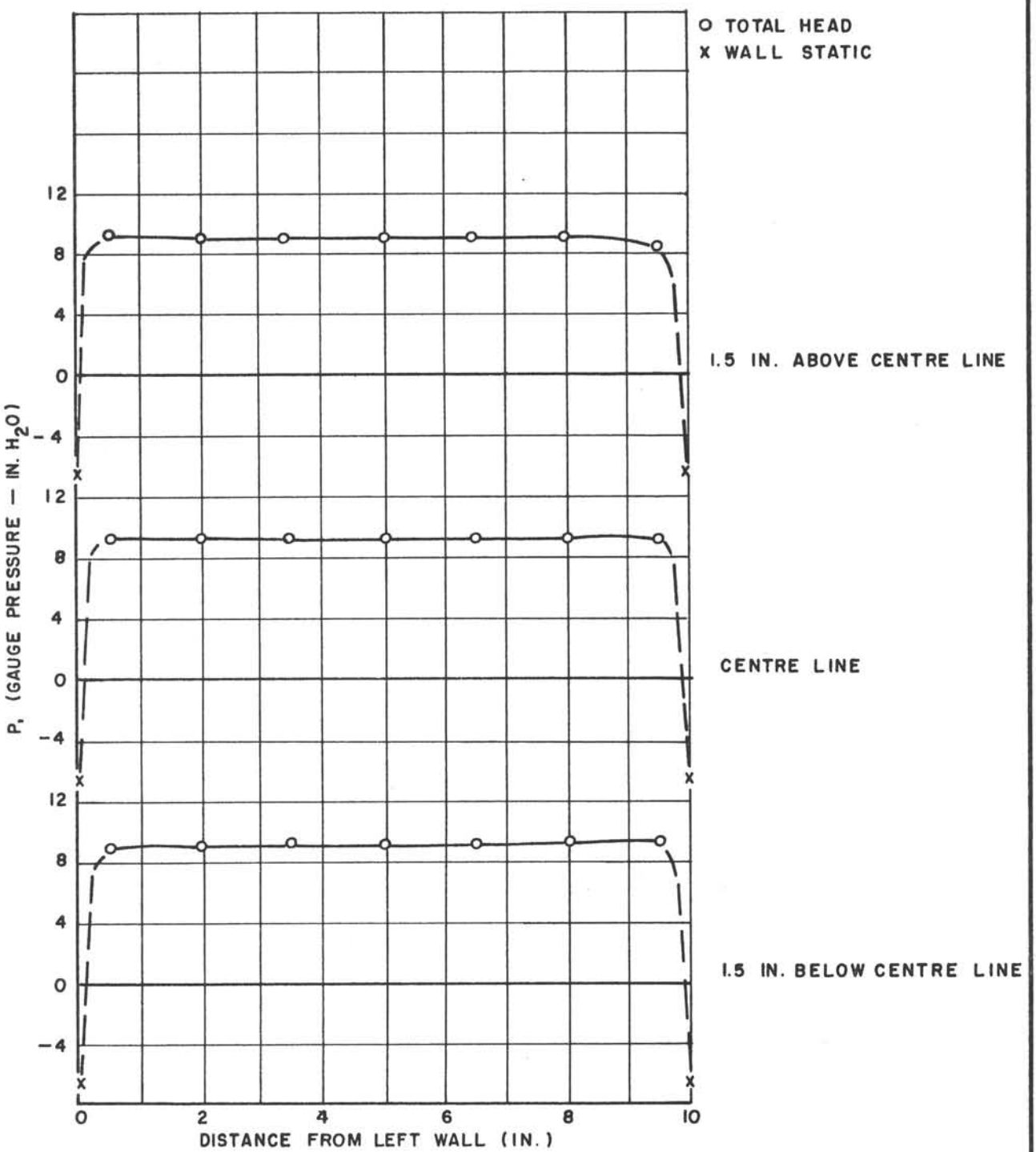

1/12 SCALE VTOL TUNNEL

SIX-INCH BLOCKS -NO DIFFUSER - CONFIGURATION 9

WORKING SECTION TOTAL HEAD PROFILES

FIG. 2.19
LR-349

$\frac{N}{\sqrt{\theta}}$ = 1676 R.P.M. δ = .985 $\sqrt{\theta}$ = 1.01

MEASUREMENTS AT STATION 130

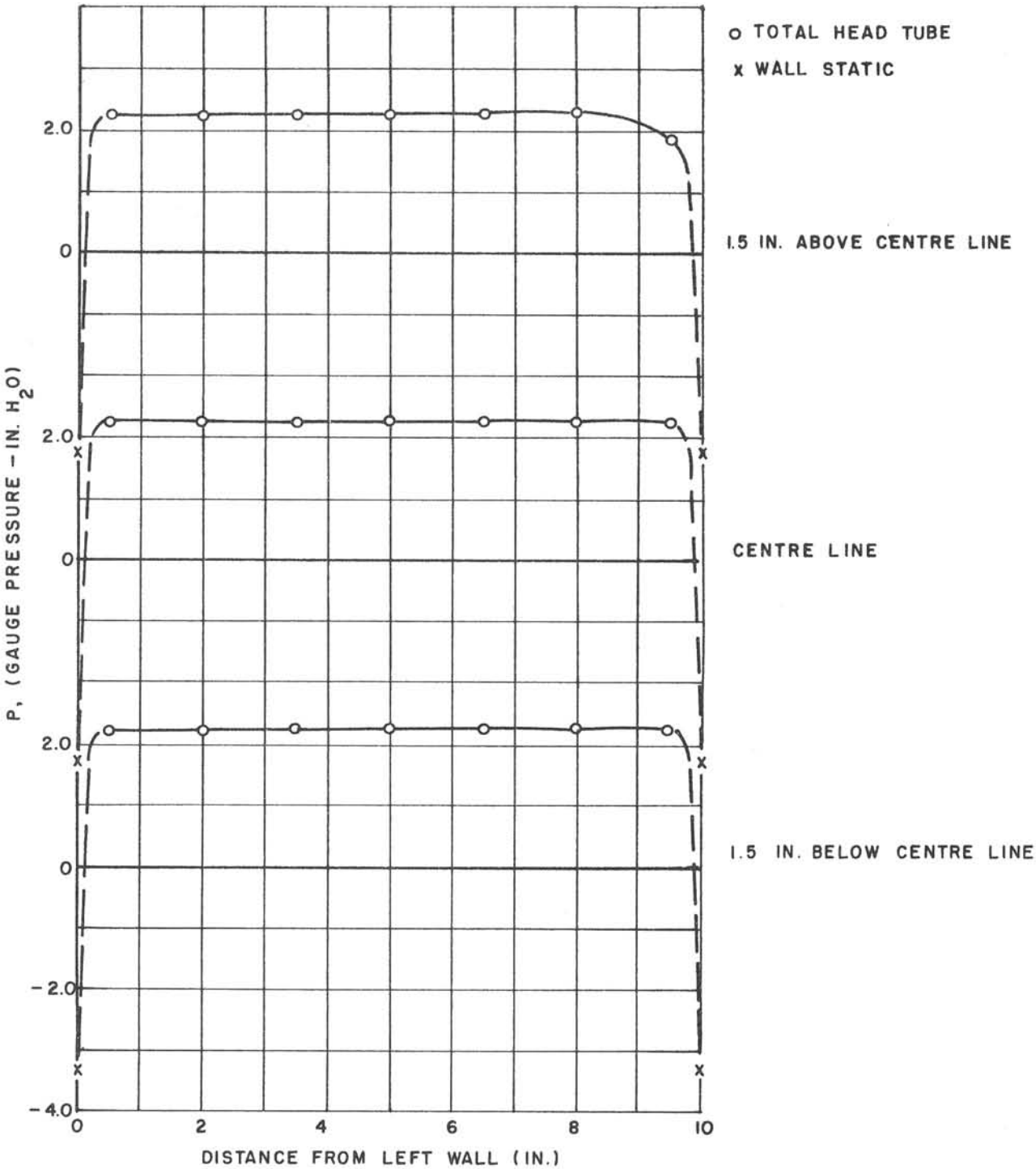

1/12 SCALE VTOL TUNNEL

SIX-INCH BLOCKS-DIFFUSER ATTACHED-CONFIGURATION 10

WORKING SECTION TOTAL HEAD PROFILES

FIG. 2.20
LR-349

$\frac{N}{\sqrt{\theta}}$ = 2515 R.P.M. δ = .985 $\sqrt{\theta}$ = 1.01

MEASUREMENTS AT STATION 130

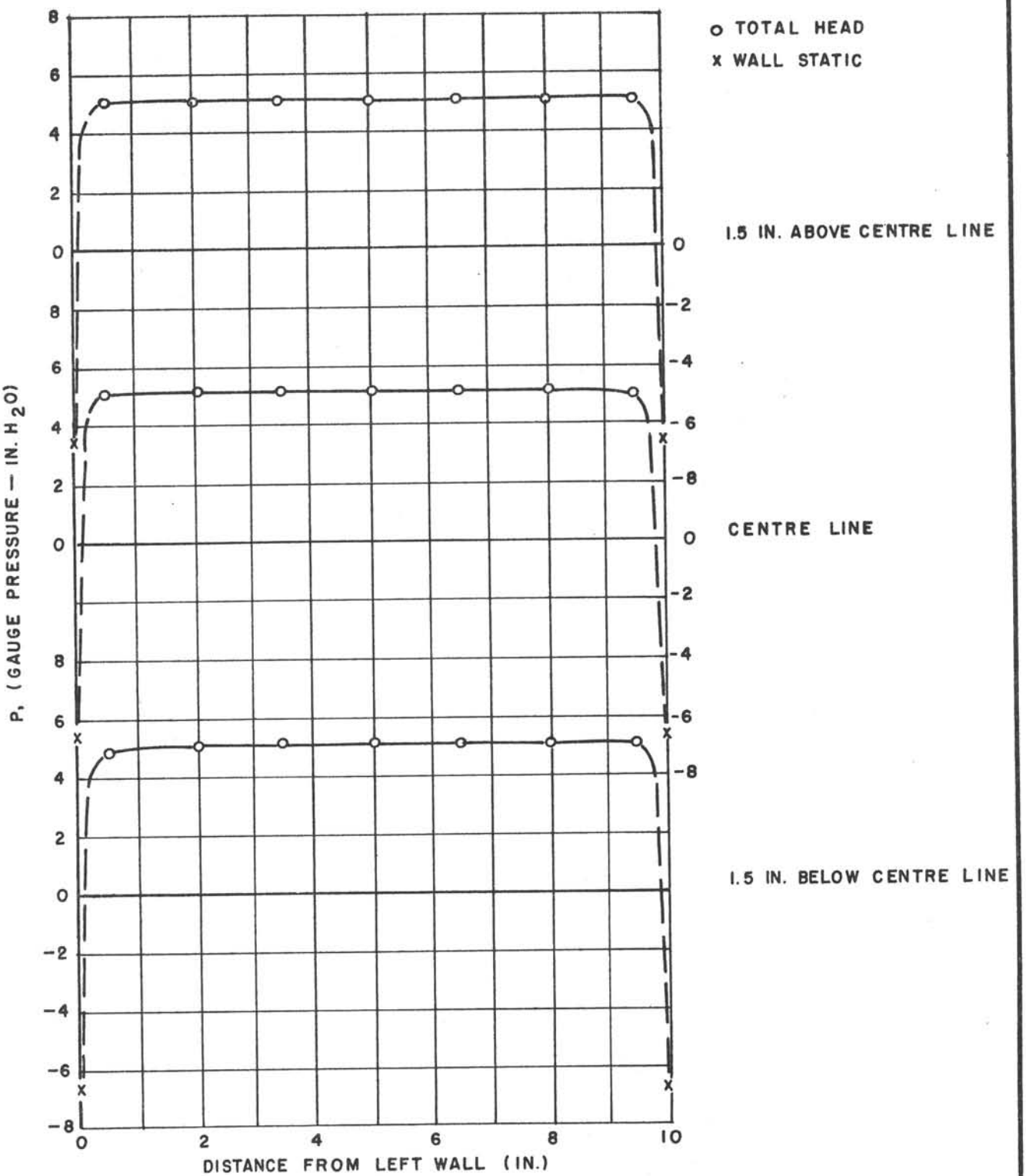

1/12 SCALE VTOL TUNNEL

SIX-INCH BLOCKS—DIFFUSER ATTACHED—CONFIGURATION 10

MODIFIED WORKING SECTION TOTAL HEAD PROFILES

FIG. 2.21
LR-349

$\frac{N}{\sqrt{\theta}}$ = 3380 R.P.M. δ = 1.007 $\sqrt{\theta}$ = 1.0

MEASUREMENTS AT STATION 130

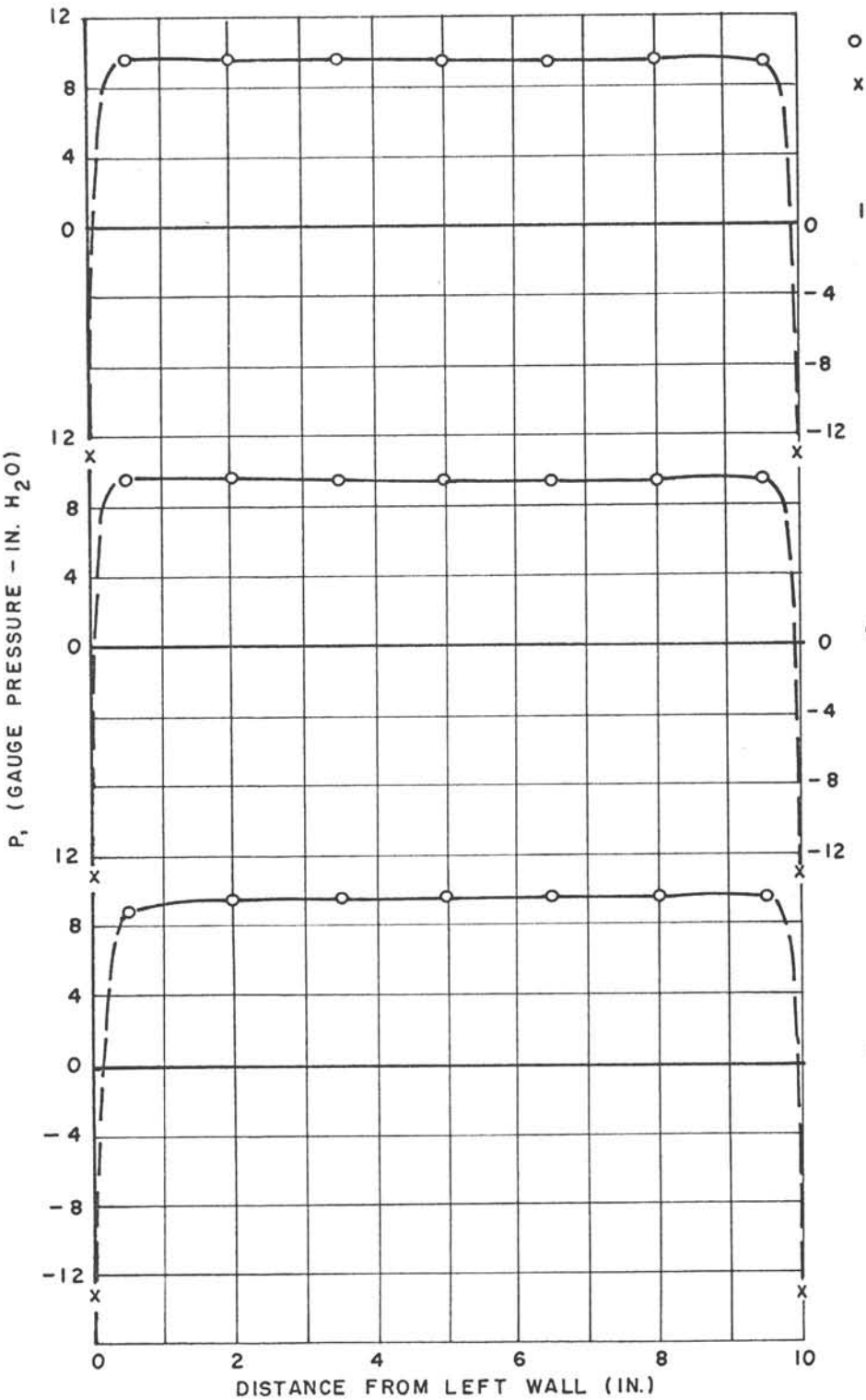

1/12 SCALE VTOL TUNNEL

SIX-INCH BLOCKS - DIFFUSER ATTACHED - CONFIGURATION 10

MODIFIED WORKING SECTION TOTAL HEAD PROFILES

FIG. 2.22
LR-349

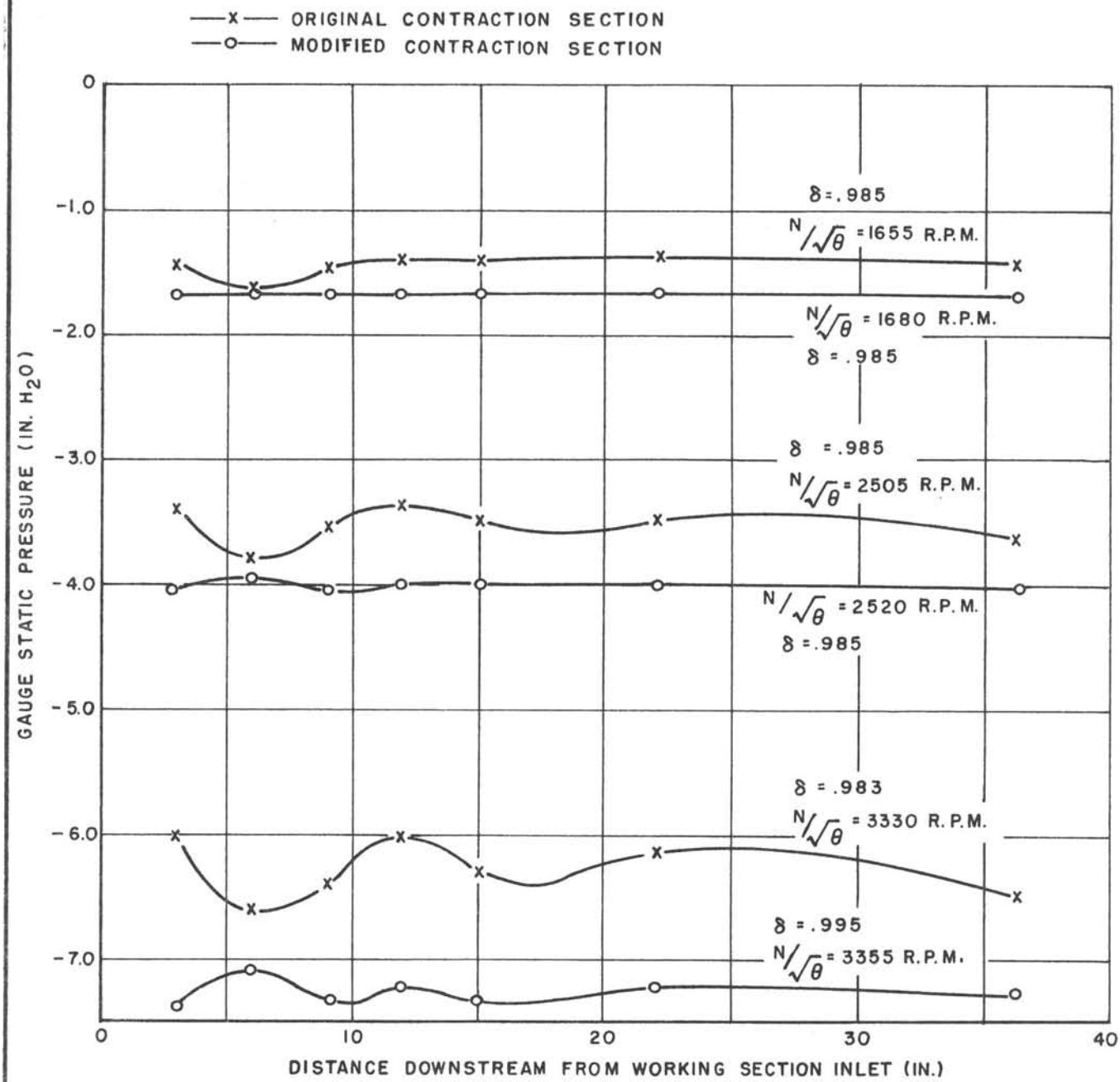

1/12 SCALE VTOL TUNNEL

FAN DRIVEN – CONFIGURATION 7

WALL STATIC PRESSURE DISTRIBUTION IN WORKING SECTION

FIG. 2.23
LR-349

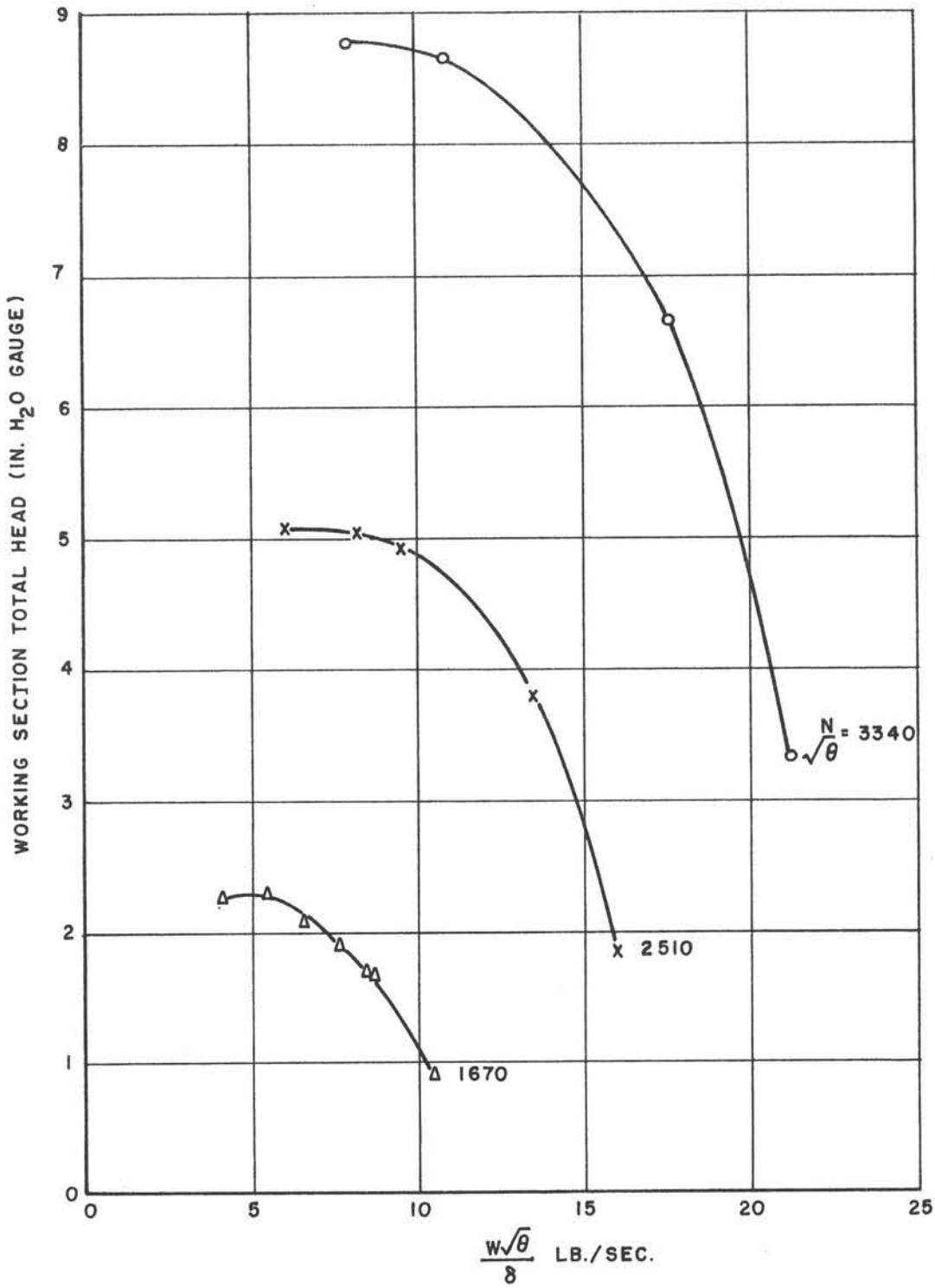

1/12 SCALE VTOL TUNNEL

WORKING SECTION AVERAGE TOTAL PRESSURE VERSUS AIRFLOW

(STATION 130)

(BASIC CONFIGURATION NO. 5 PLUS INSERTS)

FIG. 2.24
LR-349

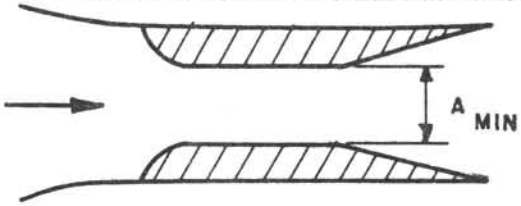

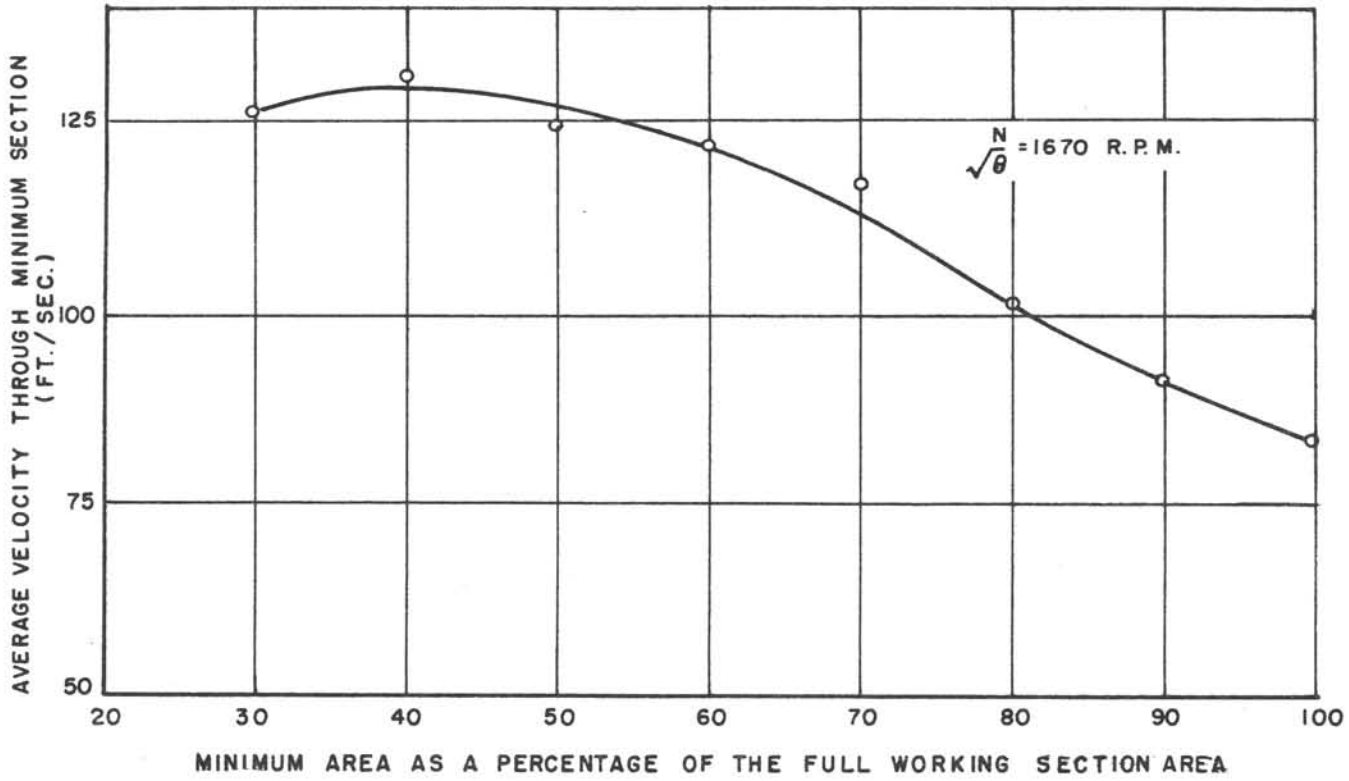

1/12 SCALE VTOL TUNNEL
(VARIABLE AREA WORKING SECTION)

BASIC CONFIGURATION 5 PLUS INSERTS WITH DETACHABLE EXIT DIFFUSER REMOVED

MINIMUM SECTION VELOCITY VERSUS SECTION AREA
(STATION 130)

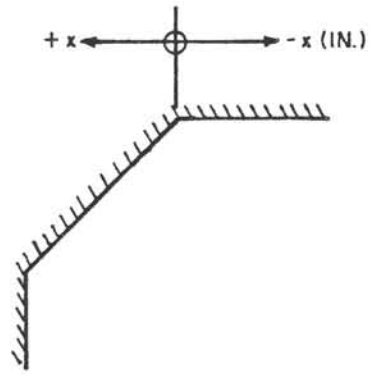

q_∞ = STREAM LOCAL MAXIMUM VELOCITY HEAD

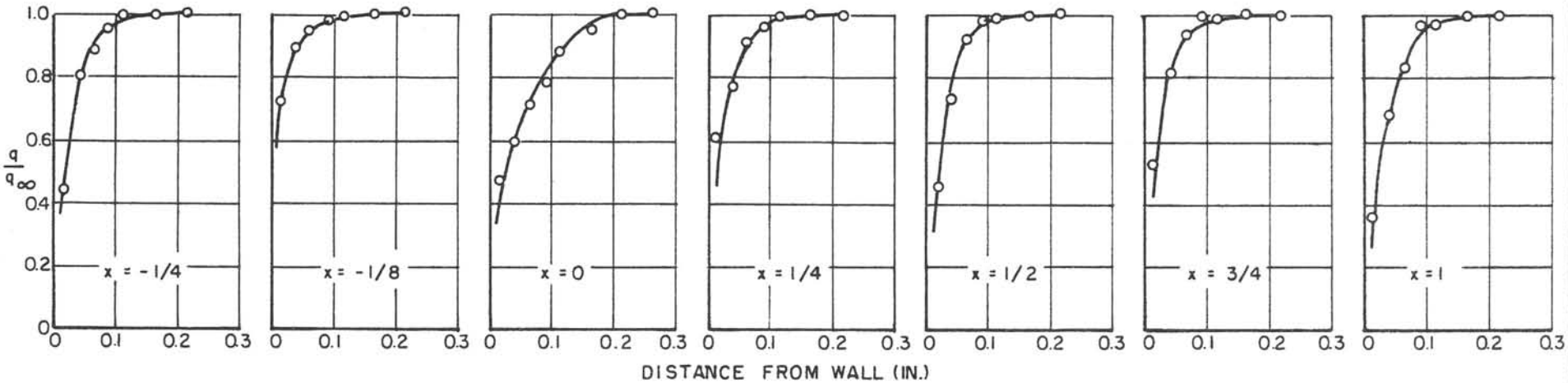

1/12 SCALE VTOL TUNNEL

EXHAUSTER DRIVEN - CONFIGURATION 6

BOUNDARY LAYER PROFILES WITH MODIFIED CONTRACTION SECTION

STATION 116

WORKING SECTION VELOCITY = 85 FT./SEC.

FIG. 2.27
LR -349

FIG. 2.28
LR - 349

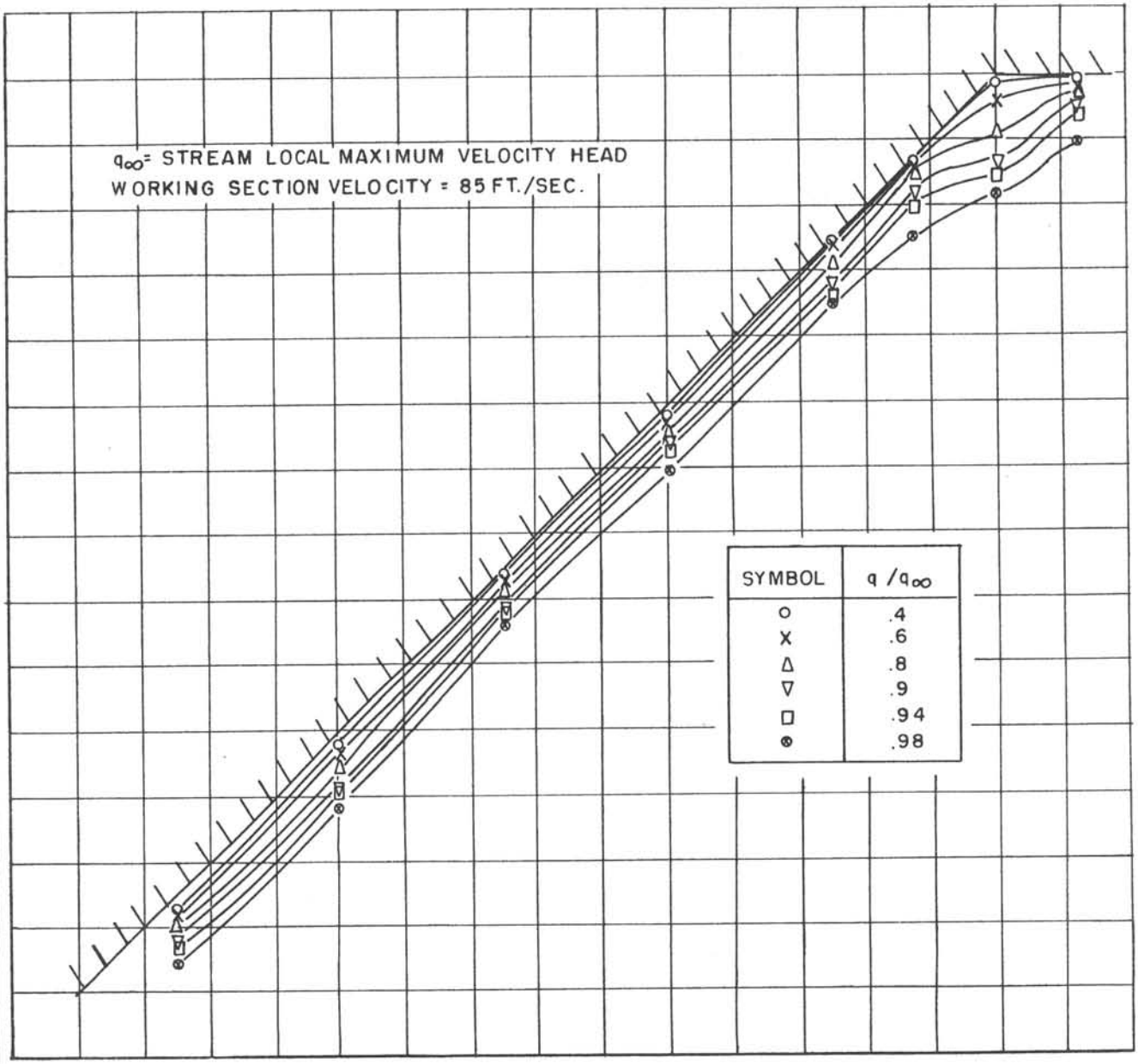

1/12 SCALE VTOL TUNNEL

EXHAUSTER DRIVEN - CONFIGURATION 6

CONTOURS OF CONSTANT VELOCITY HEAD IN CORNER

MODIFIED CONTRACTION SECTION
STATION 116

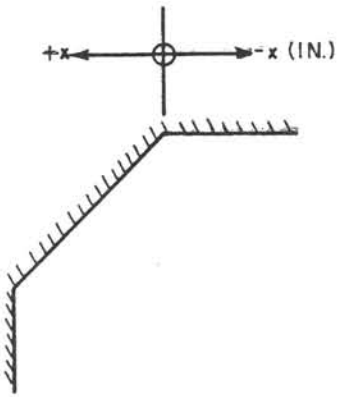

q_∞ = STREAM LOCAL MAXIMUM VELOCITY HEAD

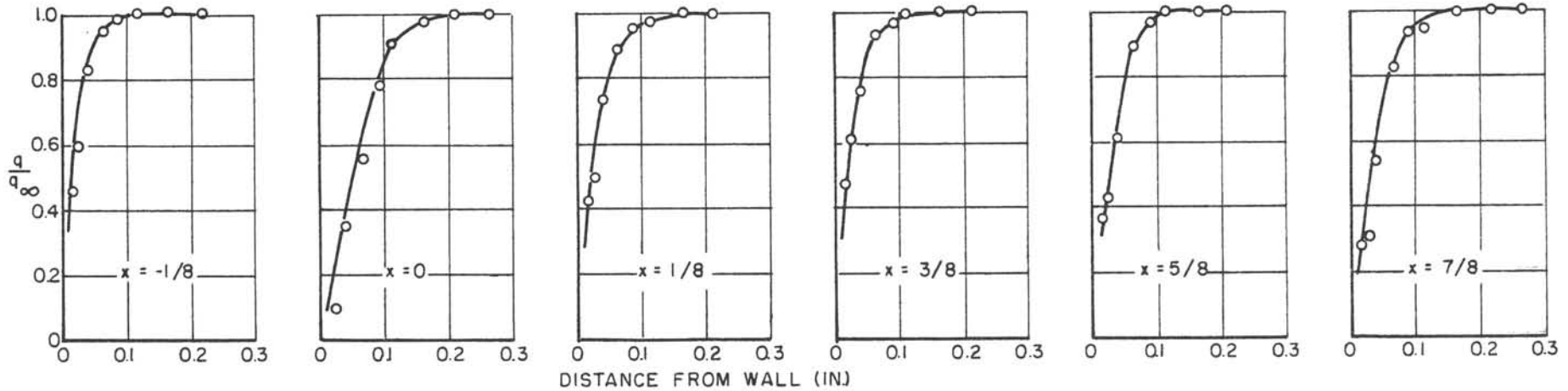

1/12 SCALE VTOL TUNNEL

FAN DRIVEN – CONFIGURATION 7

BOUNDARY LAYER PROFILES WITH MODIFIED CONTRACTION SECTION

STATION 113

WORKING SECTION VELOCITY = 95 FT./SEC.

FIG. 2.29
LR - 349

FIG. 2.30
LR – 349

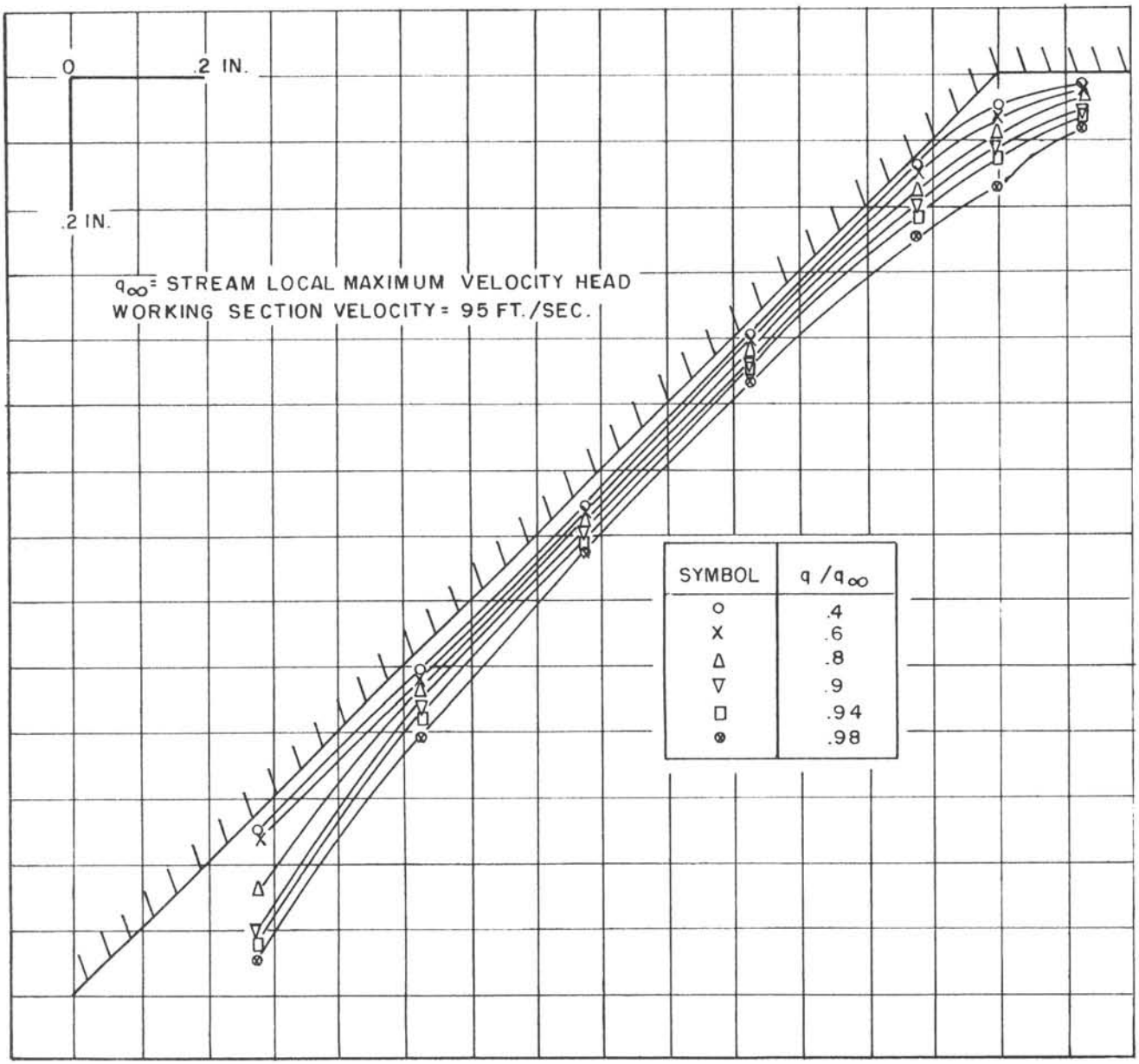

1/12 SCALE VTOL TUNNEL

FAN DRIVEN - CONFIGURATION 7

CONTOURS OF CONSTANT VELOCITY HEAD IN CORNER

STATION 113

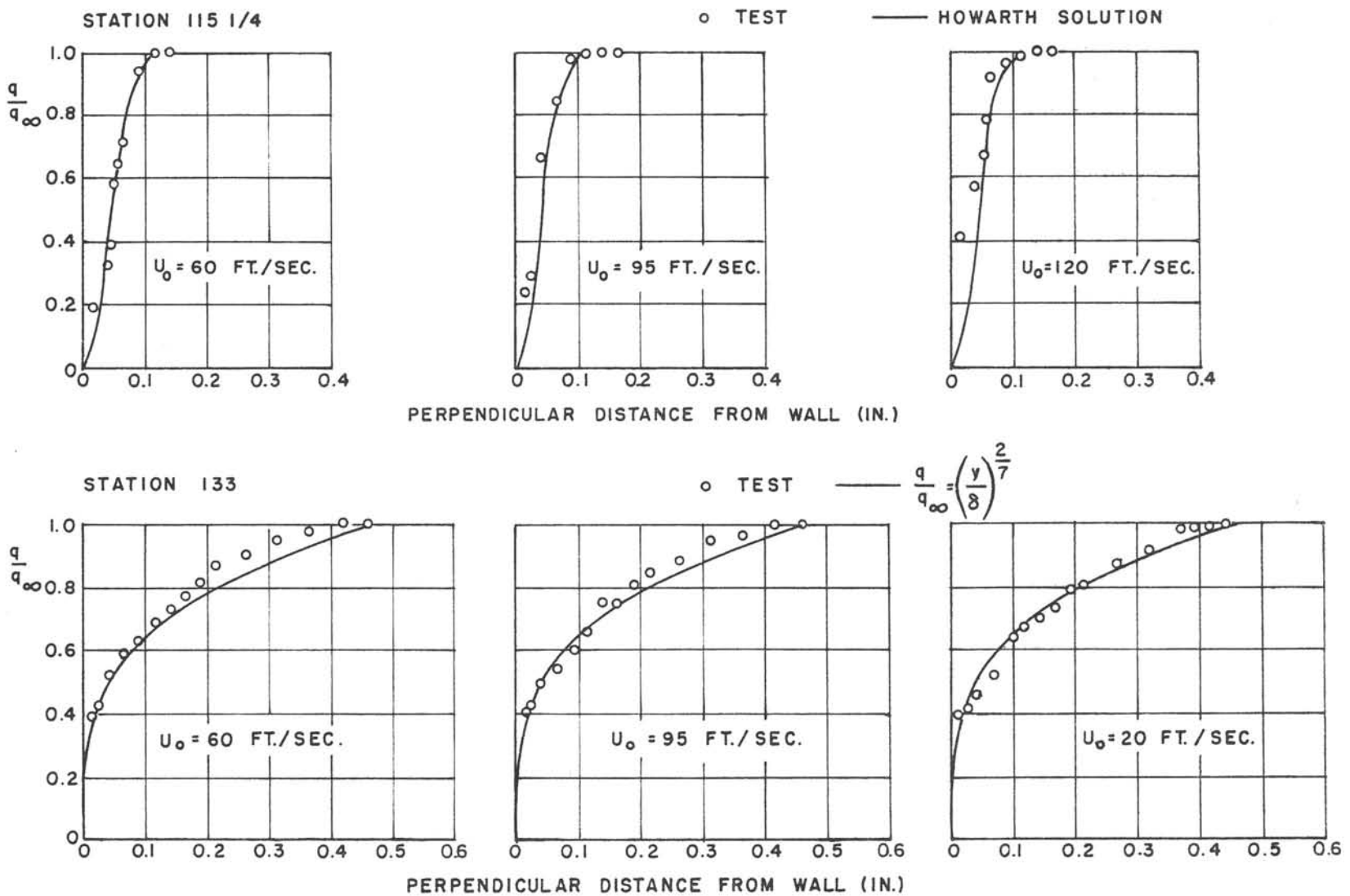

1/12 SCALE VTOL TUNNEL

FAN DRIVEN – CONFIGURATION 7

BOUNDARY LAYER PROFILES IN WORKING SECTION

(SIDEWALL CENTRE-LINE)

FIG. 231
LR-349

FIG. 2.32
LR- 349

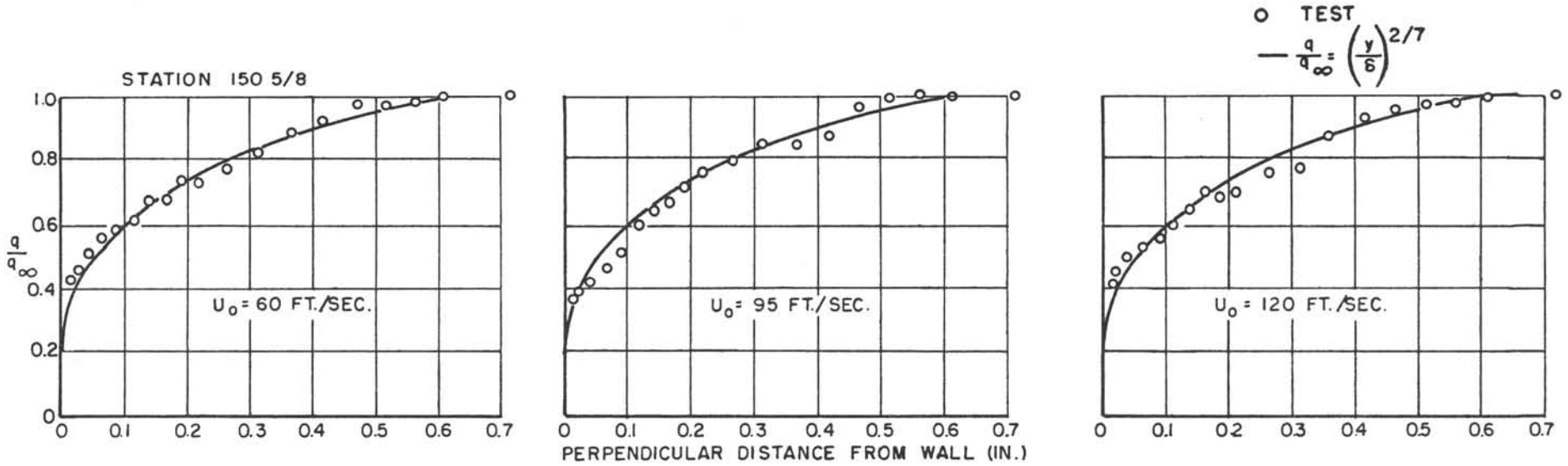

1/12 SCALE VTOL TUNNEL

FAN DRIVEN - CONFIGURATION 7

BOUNDARY LAYER PROFILES IN WORKING SECTION

SIDEWALL CENTRE-LINE

FIG. 2.33
LR - 349

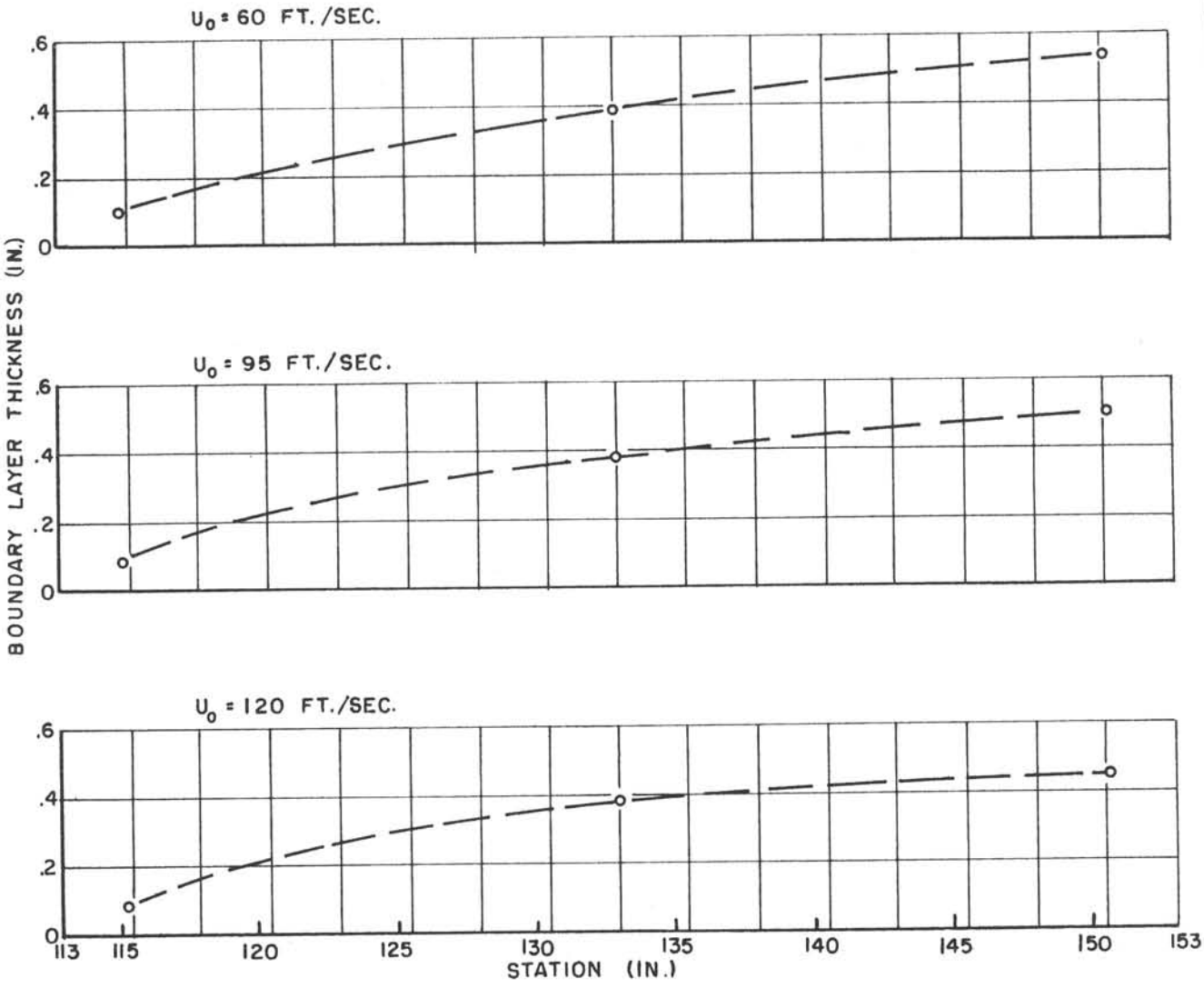

1/12 SCALE VTOL TUNNEL

FAN DRIVEN - CONFIGURATION 7

BOUNDARY LAYER THICKNESS IN WORKING SECTION
(ALONG SIDEWALL CENTRE-LINE)

FIG. 2.34
LR-349

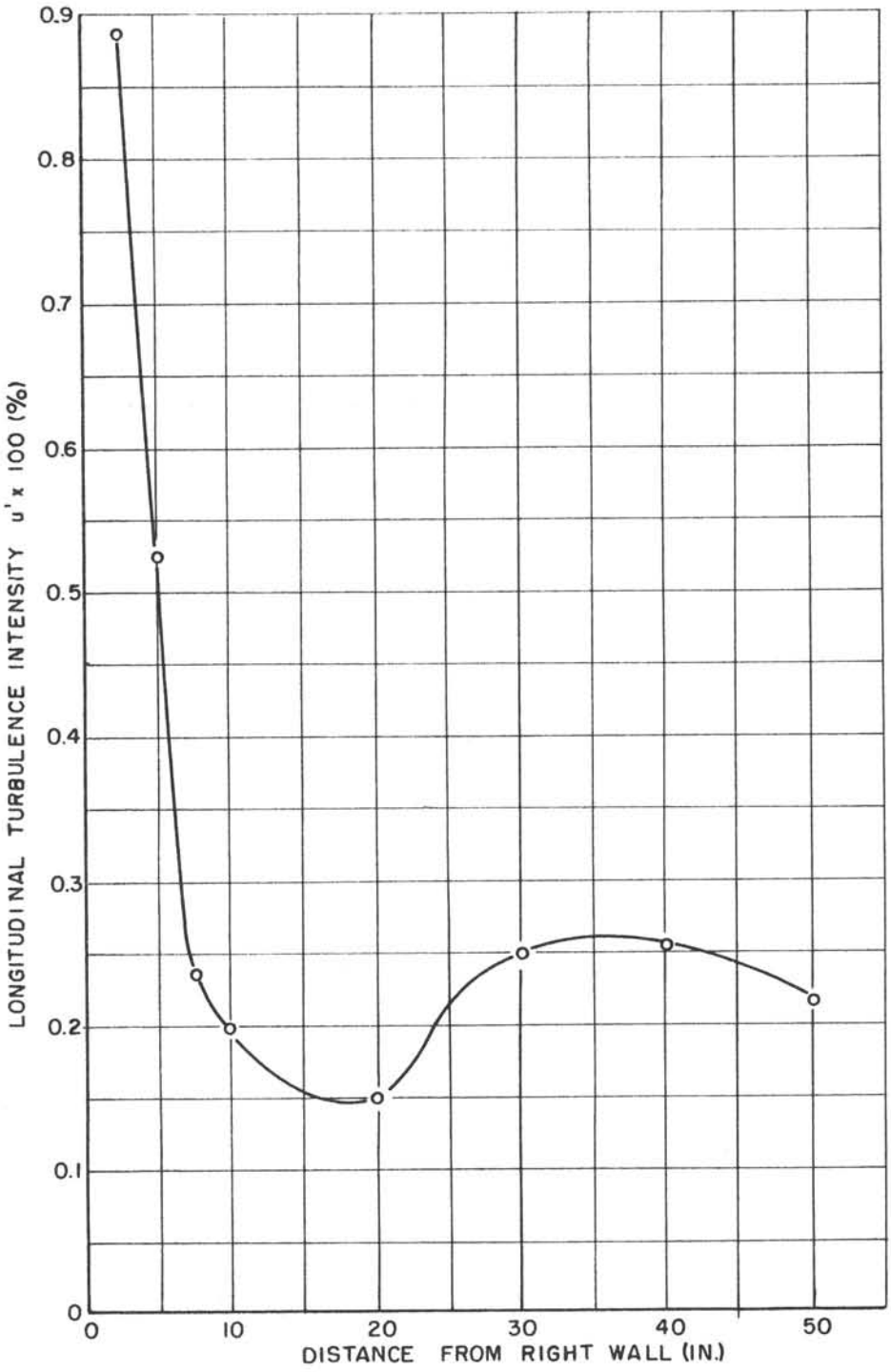

1/12 SCALE VTOL TUNNEL

EXHAUSTER DRIVEN - CONFIGURATION 6

LONGITUDINAL TURBULENCE INTENSITY

STATION 15 1/4 (INTAKE ANNULUS)

WORKING SECTION VELOCITY = 60 FT./SEC.

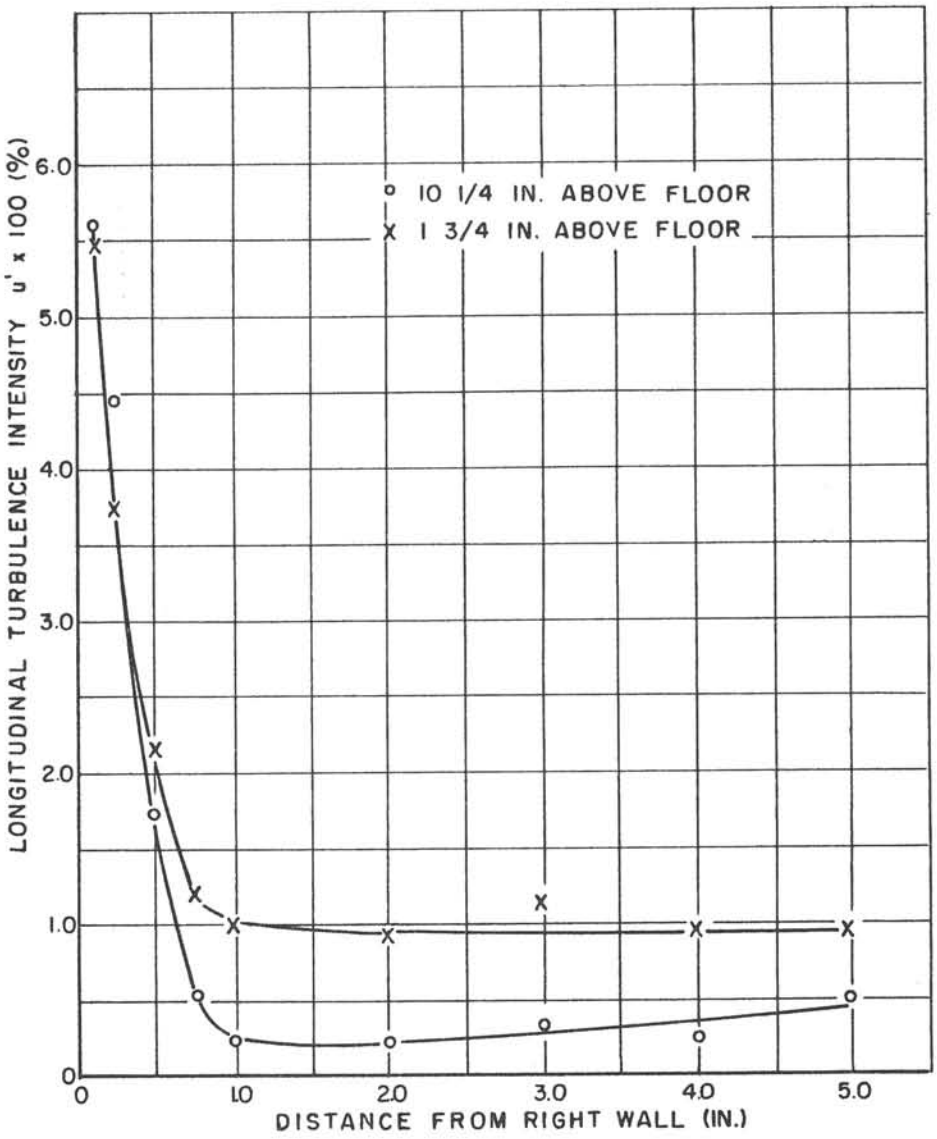

1/12 SCALE V TO L TUNNEL

EXHAUSTER DRIVEN - CONFIGURATION 6

LONGITUDINAL TURBULENCE INTENSITY

STATION 133 3/4 (WORKING SECTION)

WORKING SECTION VELOCITY = 60 FT./SEC.

FIG. 2.36
LR - 349

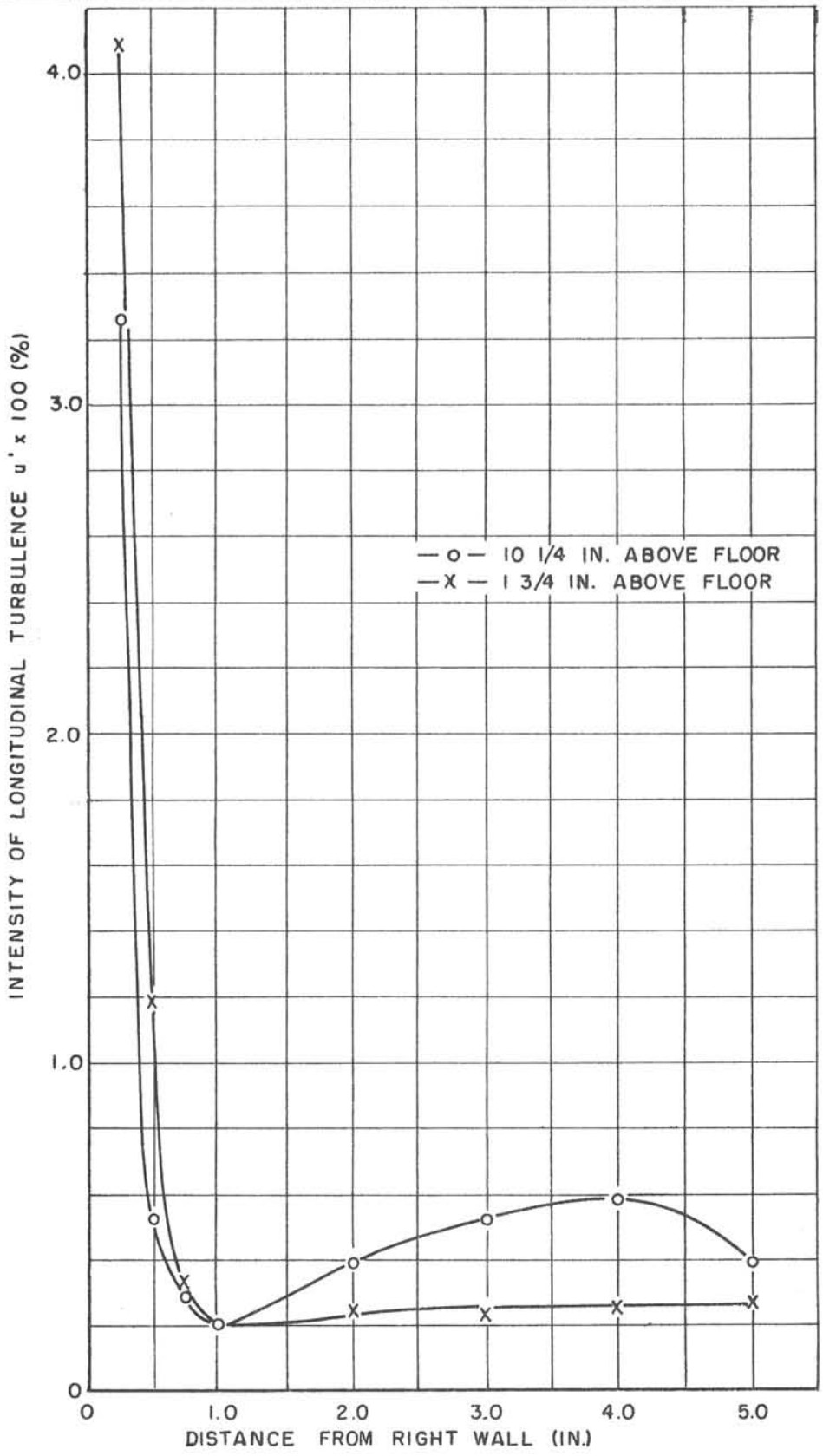

1/12 SCALE V T O L TUNNEL
FAN DRIVEN - CONFIGURATION 7

LONGITUDINAL TURBULENCE INTENSITY

STATION 130 3/4 (WORKING SECTION)
WORKING SECTION VELOCITY = 60 FT./SEC.

FIG. 2.37
LR-349

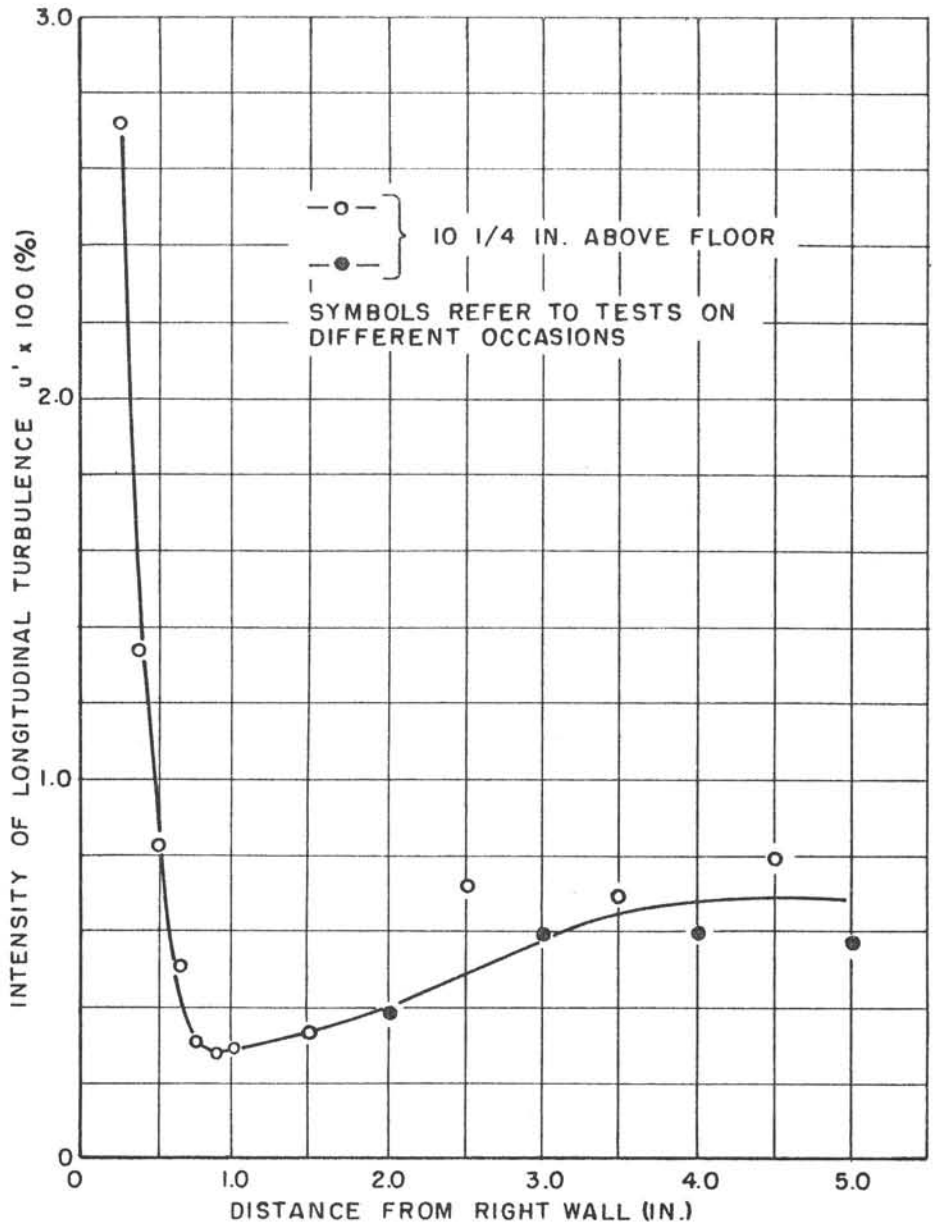

1/12 SCALE VTOL TUNNEL

FAN DRIVEN - CONFIGURATION 7

LONGITUDINAL TURBULENCE INTENSITY

STATION 130 3/4 (WORKING SECTION)

WORKING SECTION VELOCITY = 60 FT./SEC.

18 x 18 x .011" WIRE SCREEN OVER INTAKE

FIG. 2.38
LR-349

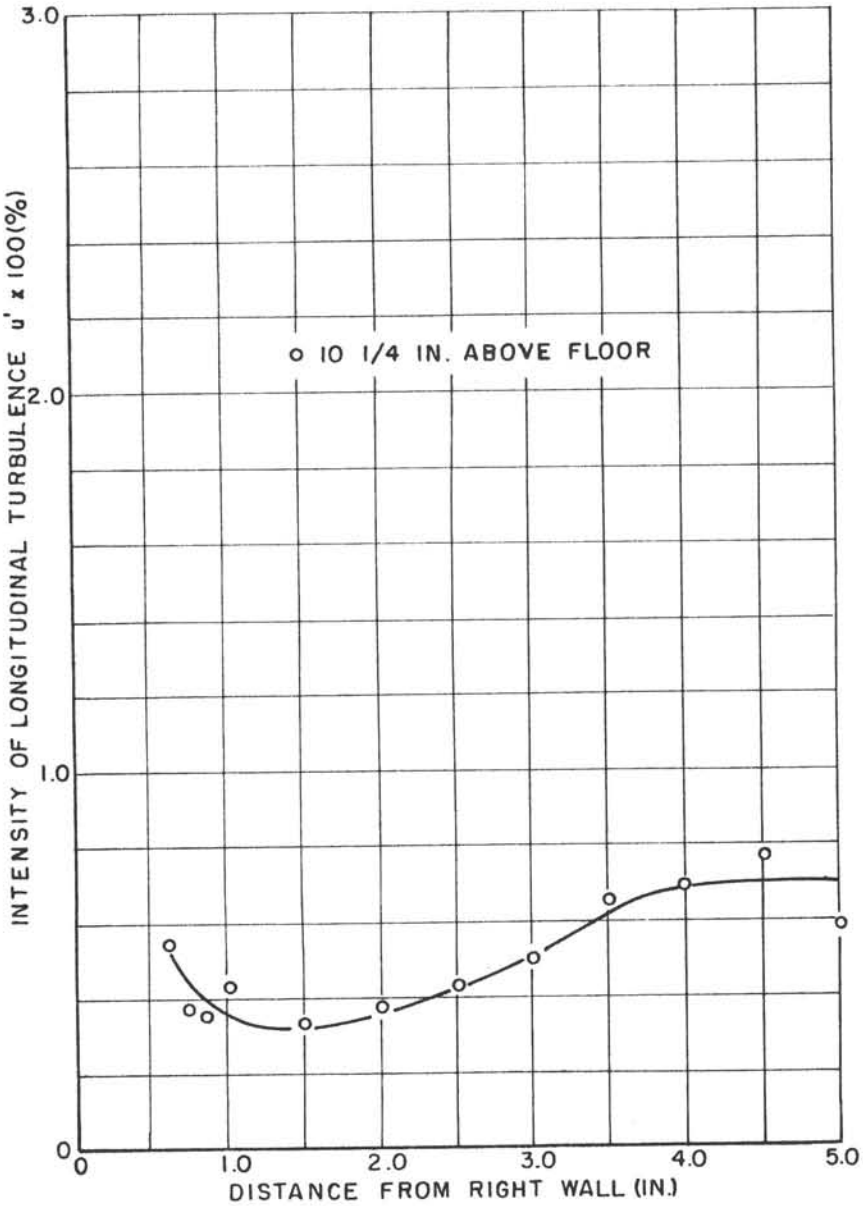

1/12 SCALE V T O L TUNNEL

FAN DRIVEN - CONFIGURATION 7

LONGITUDINAL TURBULENCE INTENSITY

STATION 130 3/4 (WORKING SECTION)

WORKING SECTION VELOCITY = 60 FT./SEC.

18 x 18 x .011" SCREEN AT END OF STILLING SECTION

(STATION 66)

FIG. 2.39
LR-349

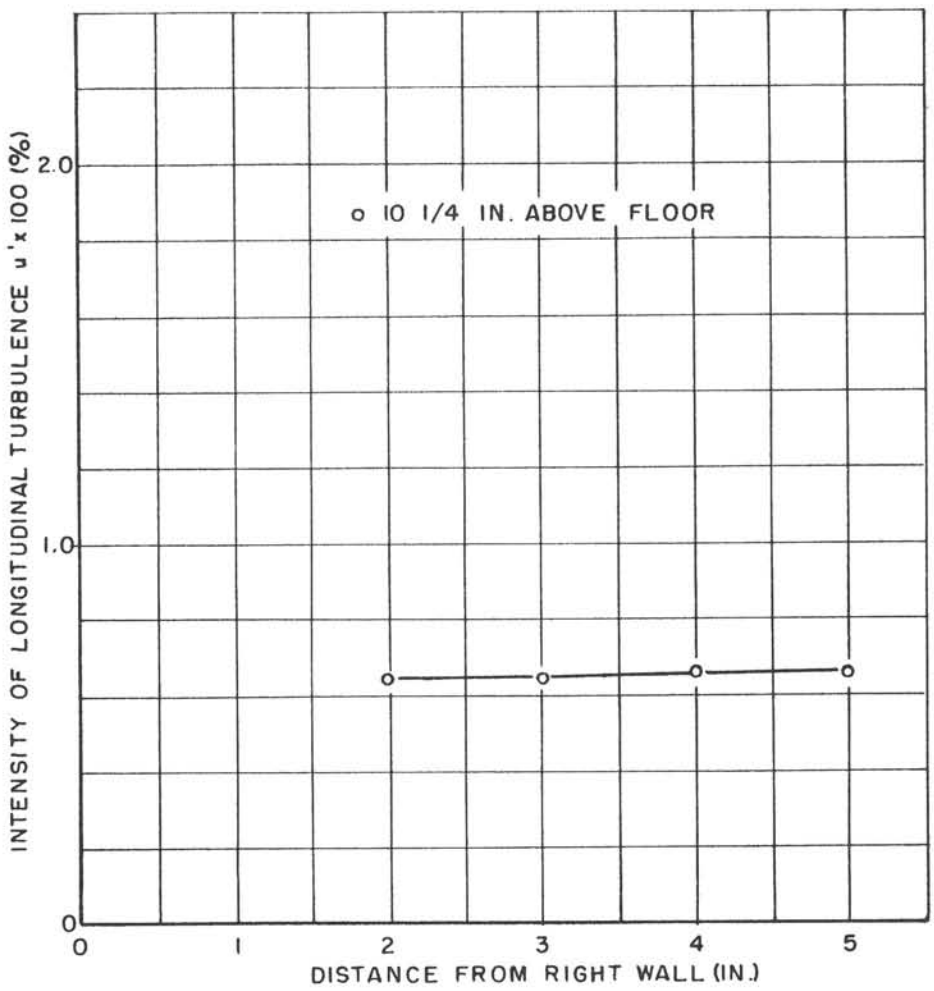

1/12 SCALE V TO L TUNNEL

FAN DRIVEN - CONFIGURATION 7

LONGITUDINAL TURBULENCE INTENSITY

STATION 130 3/4 (WORKING SECTION)
WORKING SECTION VELOCITY = 60 FT./SEC.
20 x 20 x .016" SCREEN OVER INTAKE
18 x 18 x .011" SCREEN AT STATION 66

FIG. 2.40
LR-349

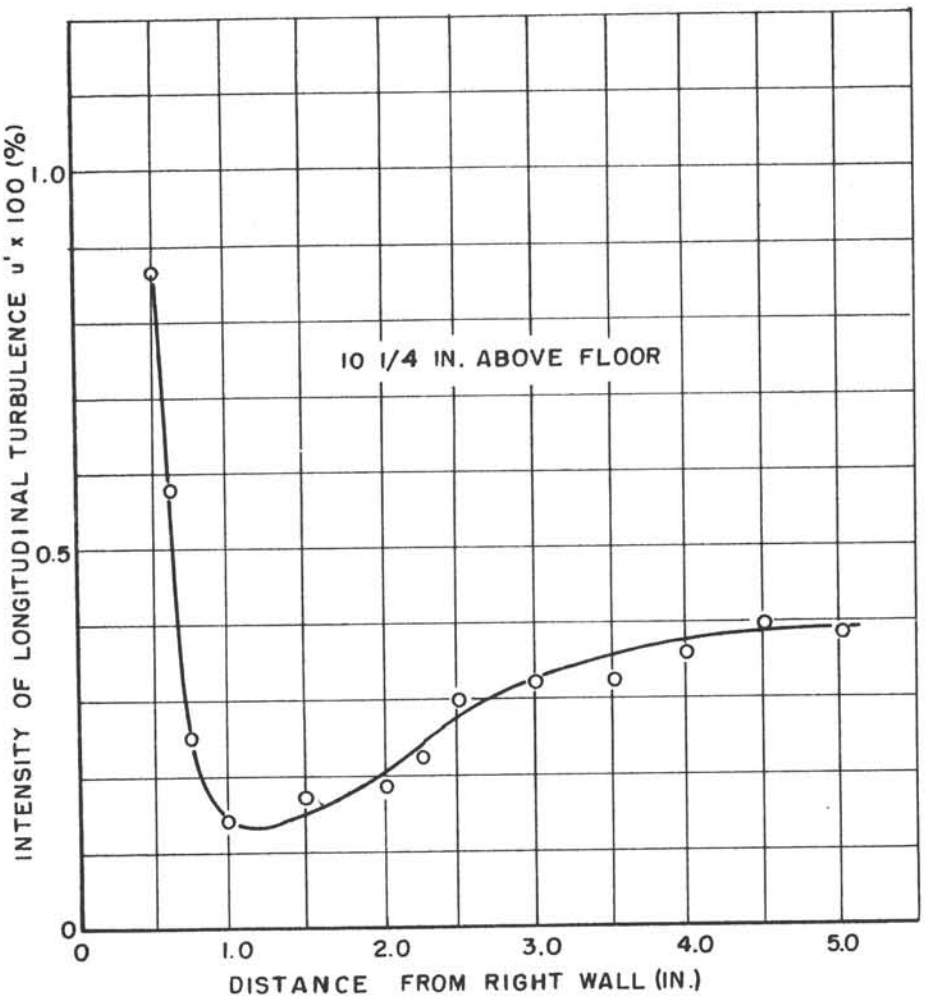

1/12 SCALE VTOL TUNNEL

FAN DRIVEN-CONFIGURATION 7

LONGITUDINAL TURBULENCE INTENSITY

STATION 130 3/4 (WORKING SECTION)

WORKING SECTION VELOCITY = 60 FT./SEC.

18 x 18 x .011" SCREEN AT STATION 54

20 x 20 x .010" SCREEN AT STATION 66

FIG. 2.41
LR-349

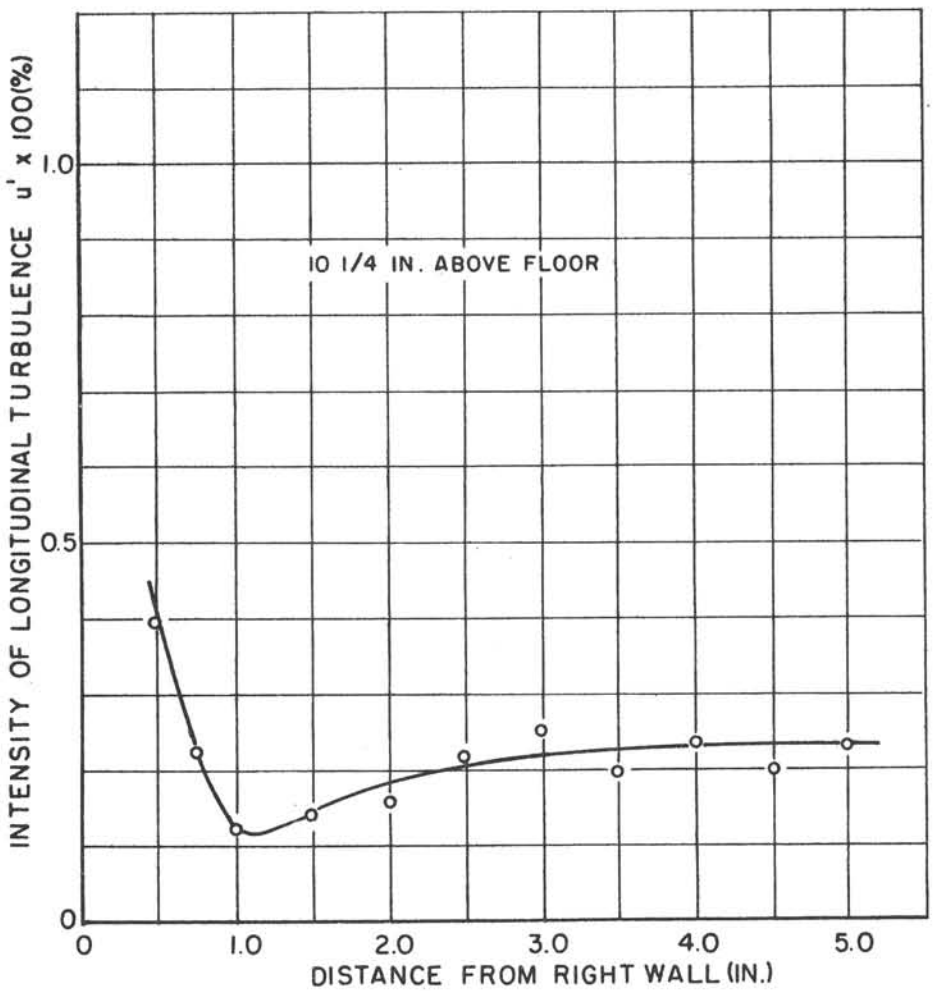

1/12 SCALE VTOL TUNNEL

FAN DRIVEN - CONFIGURATION 7

LONGITUDINAL TURBULENCE INTENSITY

STATION 130 3/4
WORKING SECTION VELOCITY = 60 FT./SEC.
18 x 18 x .011" SCREEN AT STATION 54
50 x 36 x .010" SCREEN AT STATION 66

FIG. 2.42
LR-349

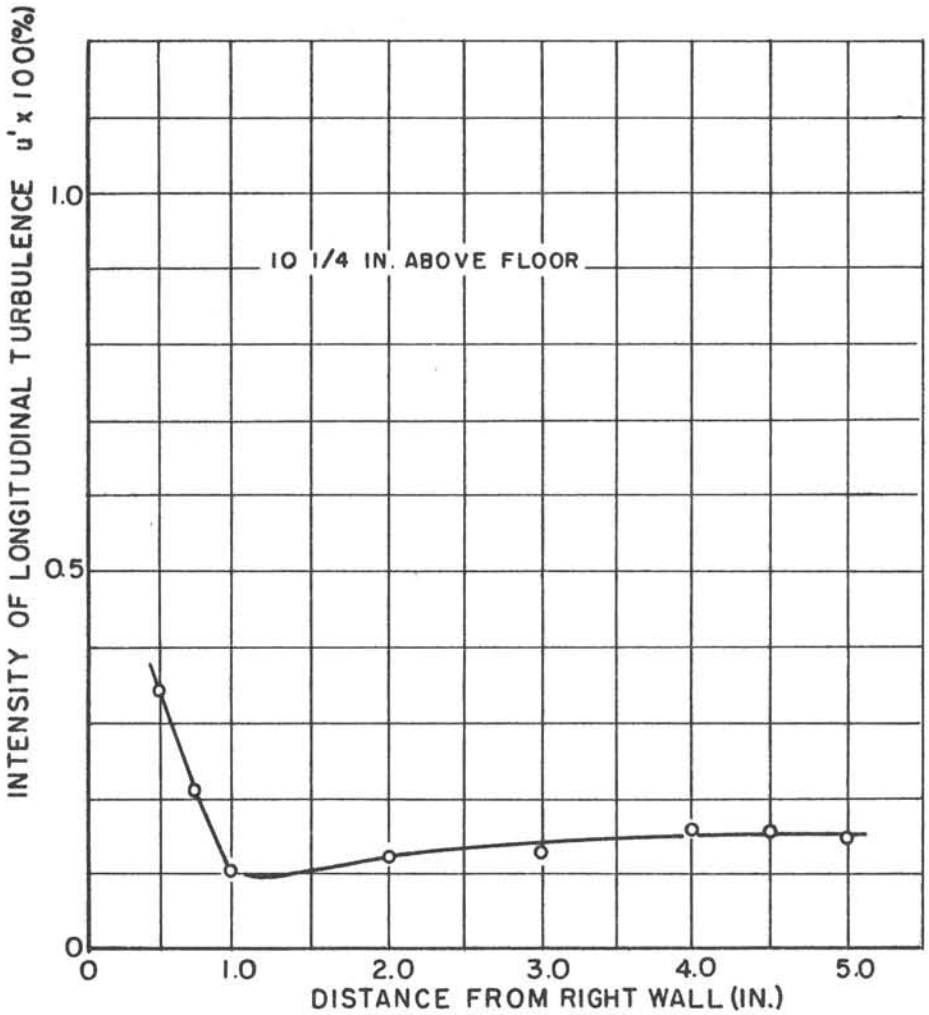

1/12 SCALE VTOL TUNNEL

FAN DRIVEN - CONFIGURATION 7

LONGITUDINAL TURBULENCE INTENSITY

STATION 130 3/4
WORKING SECTION VELOCITY = 60 FT./SEC.
TWO 50 x 36 x .010" SCREENS IN STILLING SECTION

FIG. 2.43
LR-349

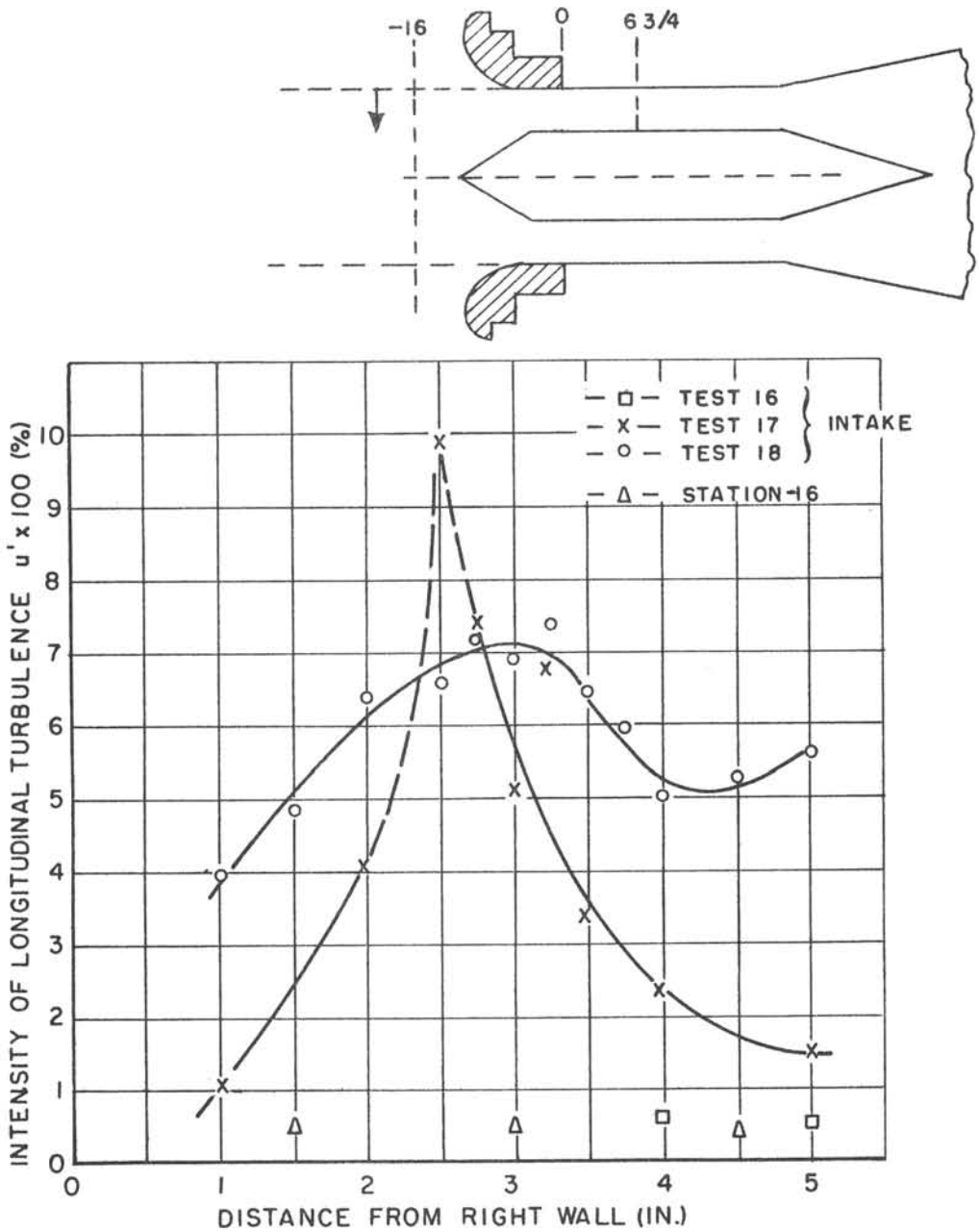

1/12 SCALE VTOL TUNNEL

FAN DRIVEN - CONFIGURATION 7

LONGITUDINAL TURBULENCE INTENSITY

STATIONS 6 3/4 (INTAKE) AND -16 (AHEAD OF INTAKE)
WORKING SECTION VELOCITY = 60 FT./SEC.
18 x 18 x.011 SCREEN AT STATION 66

FIG. 2.44
LR - 349

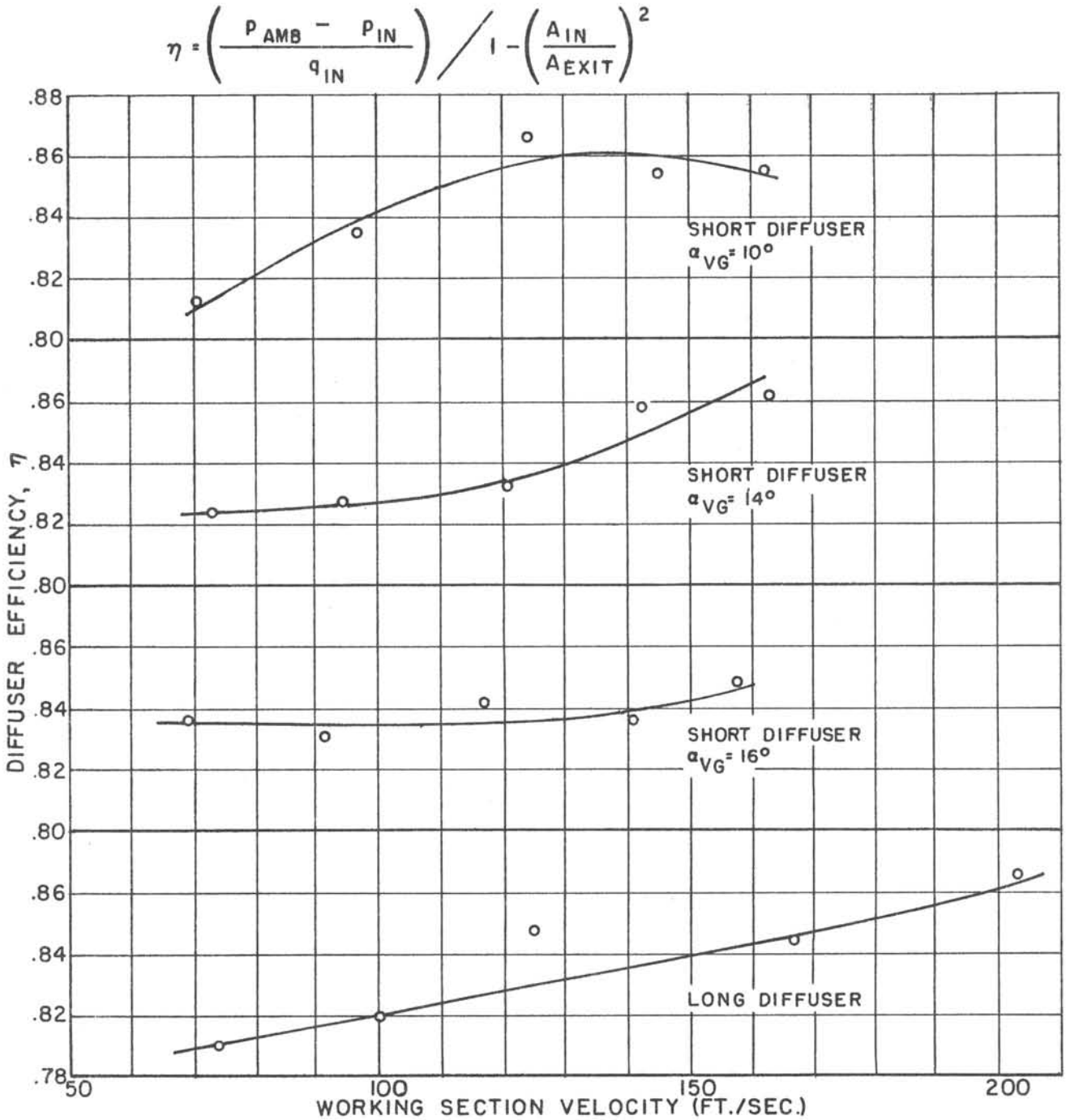

1/12 SCALE VTOL TUNNEL

FAN DRIVEN - CONFIGURATION II

EXIT DIFFUSER EFFICIENCY VERSUS WORKING SECTION VELOCITY

WORKING SECTION EMPTY

FIG. 2.45
LR - 349

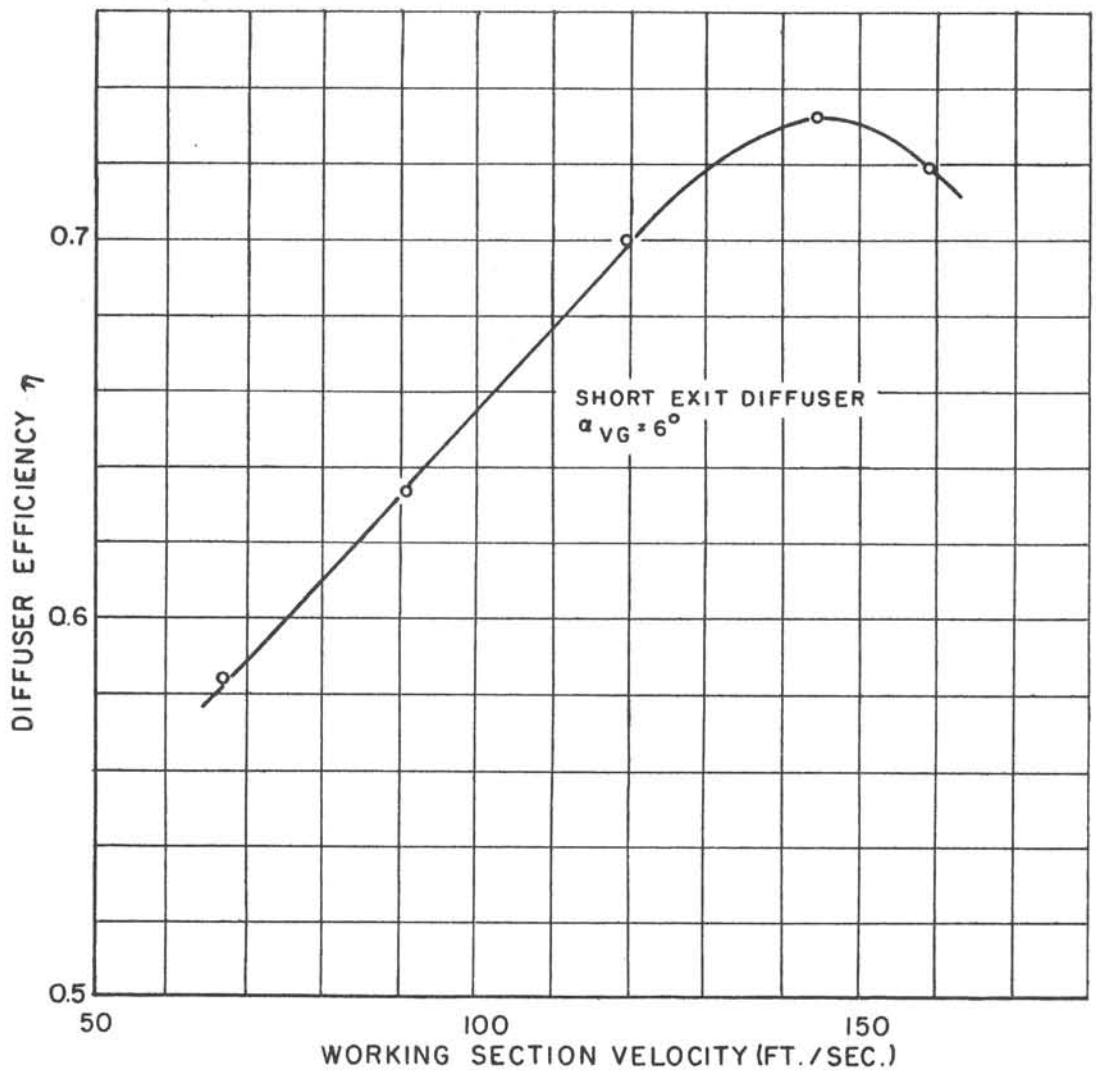

1/12 SCALE VTOL TUNNEL
FAN DRIVEN (CONFIGURATION 11)
EXIT DIFFUSER EFFICIENCY VERSUS WORKING SECTION VELOCITY
WORKING SECTION EMPTY

FIG. 2.46
LR-349

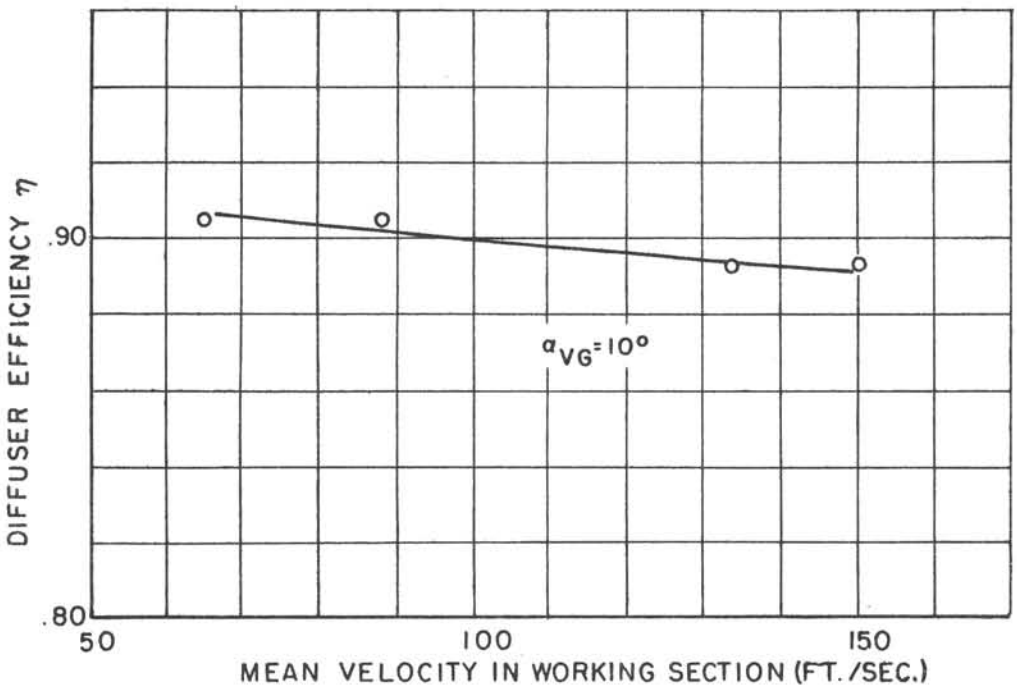

1/12 SCALE VTOL TUNNEL

FAN DRIVEN - CONFIGURATION II

EXIT DIFFUSER EFFICIENCY VERSUS WORKING SECTION VELOCITY
WITH WING SET AT 30° INCIDENCE

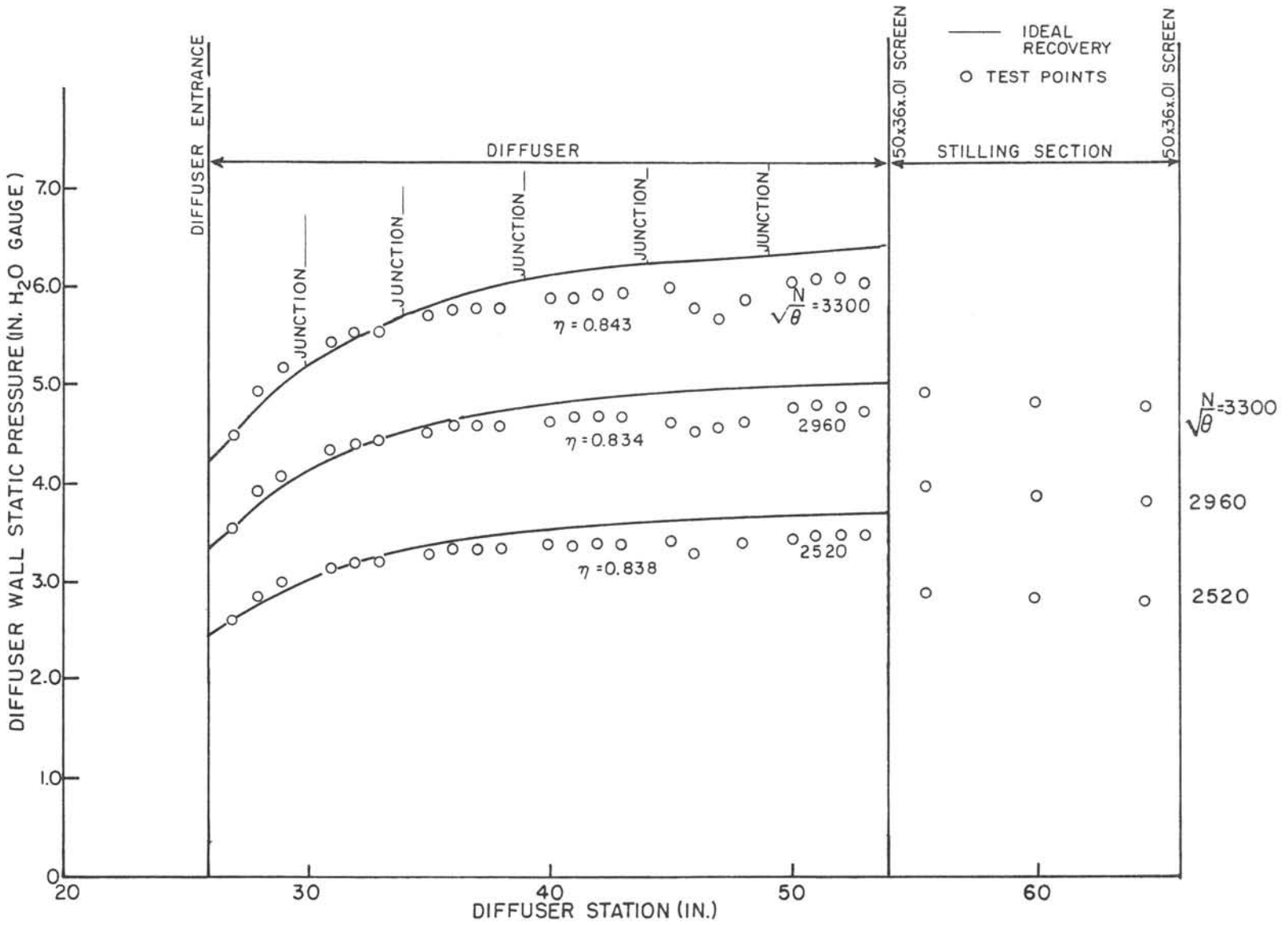

1/12 SCALE VTOL TUNNEL

FAN DRIVEN (CONFIGURATION 12)
28° DIFFUSER WITH VORTEX GENERATORS
AT STATION 23 AND SCREENS REMOVED

WALL STATIC PRESSURES

FIG. 2.47
LR-349

FIG. 2.48
LR-349

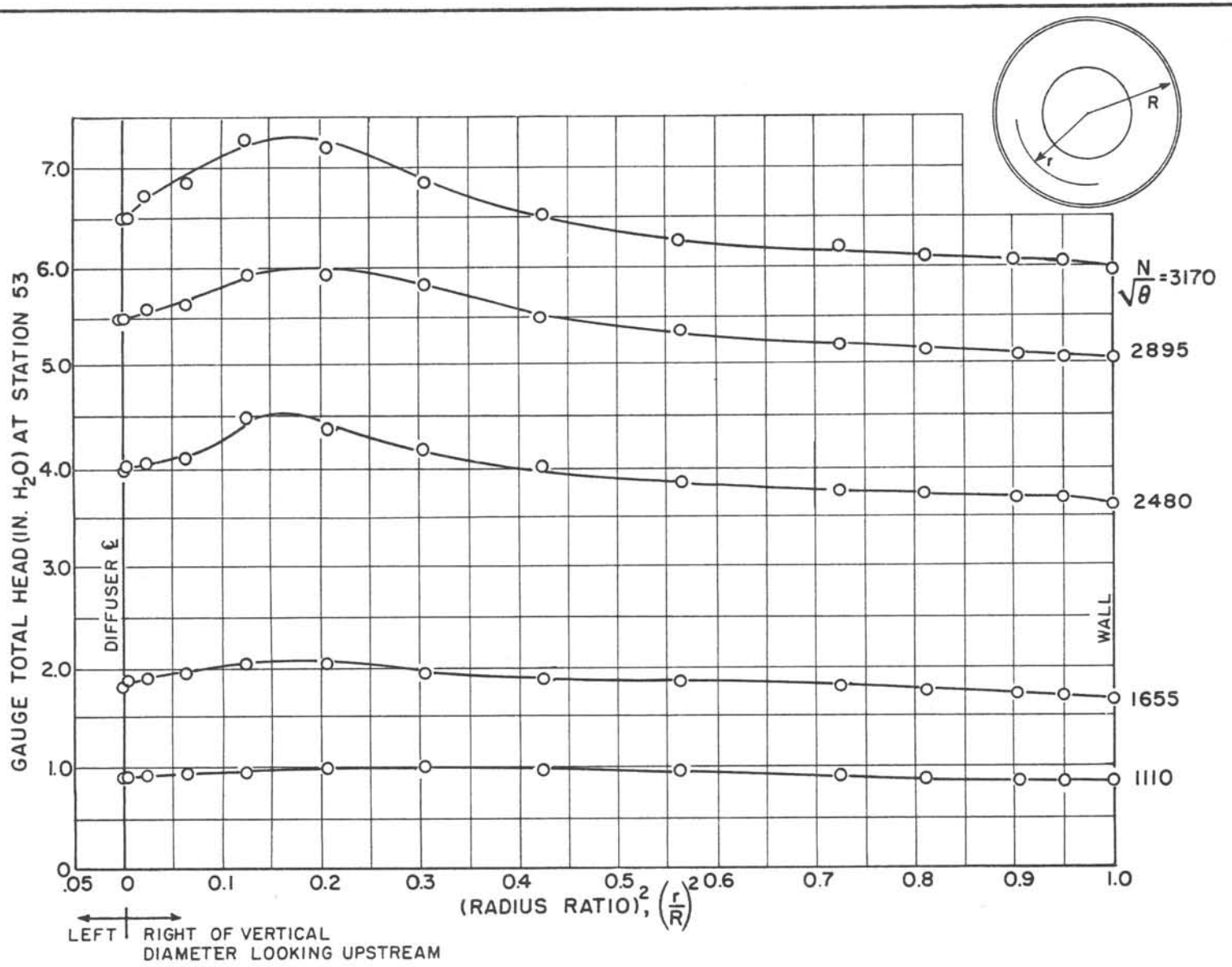

1/12 SCALE VTOL TUNNEL

FAN DRIVEN (CONFIGURATION 12)

TOTAL HEAD PROFILES NEAR END OF 28° DIFFUSER

WITH SCREENS REMOVED AND VORTEX GENERATORS AT STATION 23

FIG. 2.49
LR-349

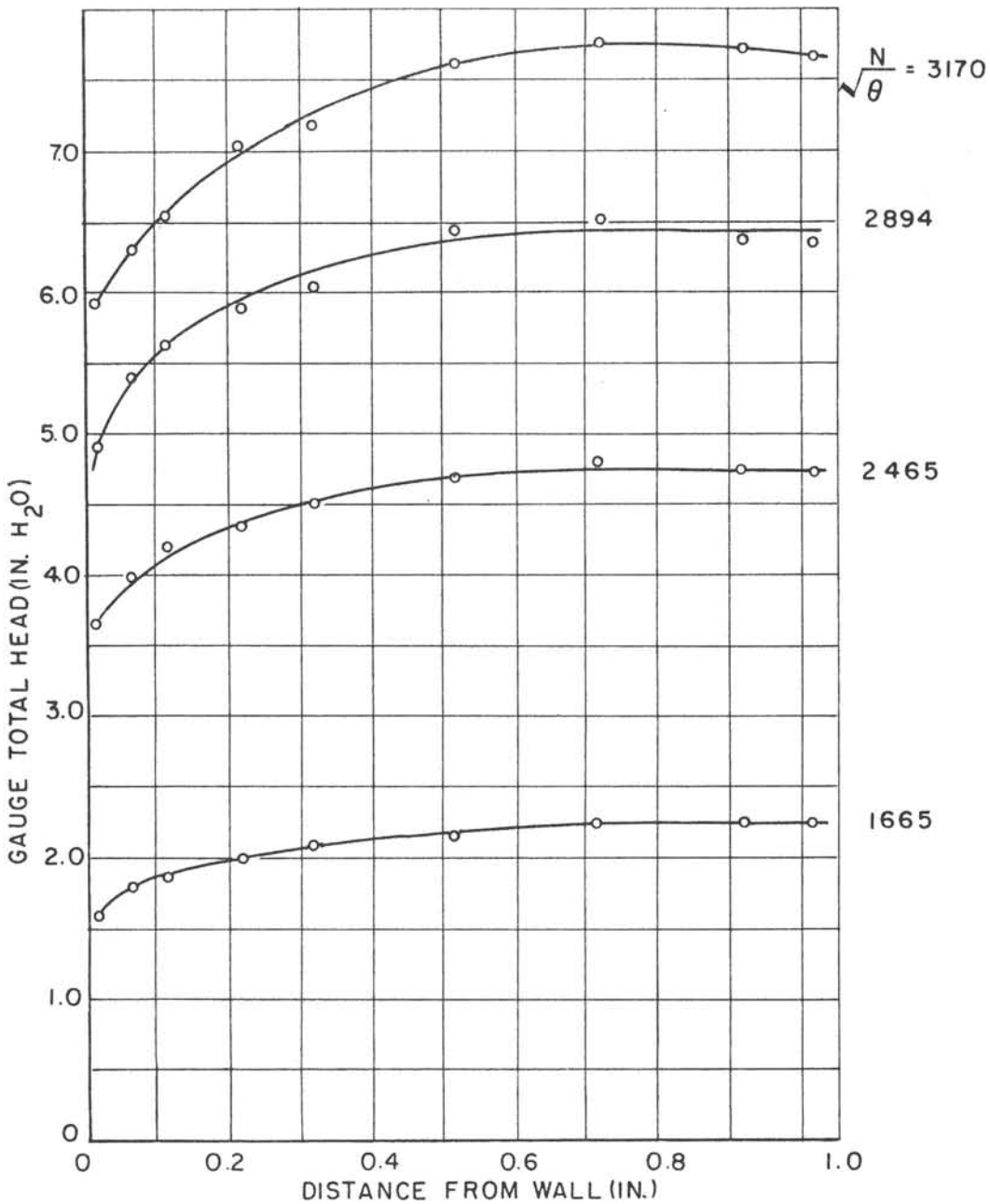

1/12 SCALE VTOL TUNNEL
FAN DRIVEN - CONFIGURATION 12
TOTAL HEAD PROFILES BEHIND FAN BLADE TIPS

(MEASURED AT STATION 23)

FIG. 2.50
LR-349

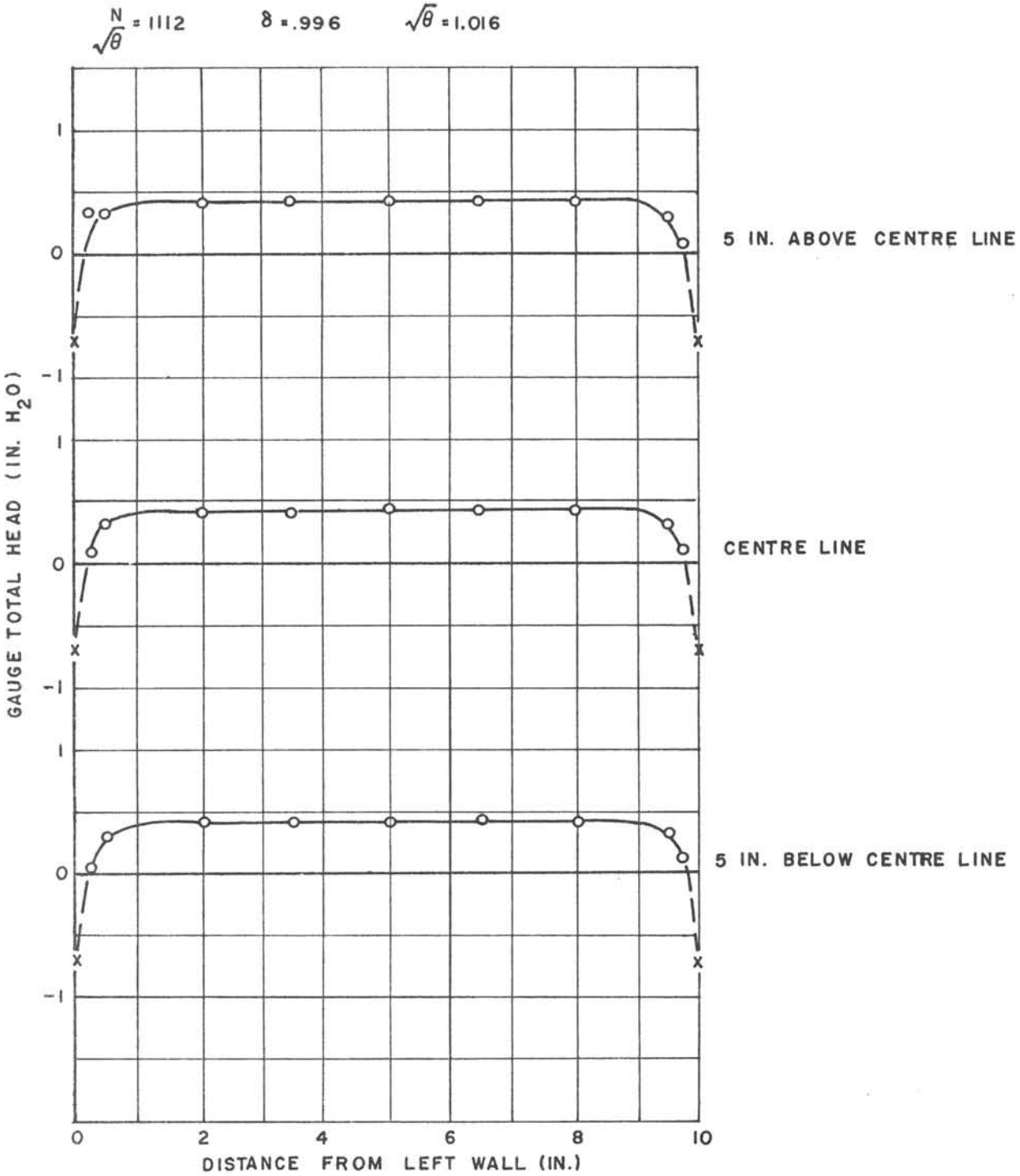

1/12 SCALE VTOL TUNNEL

FAN DRIVEN - CONFIGURATION 12

WORKING SECTION TOTAL HEAD PROFILES

FIG. 2.51
LR-349

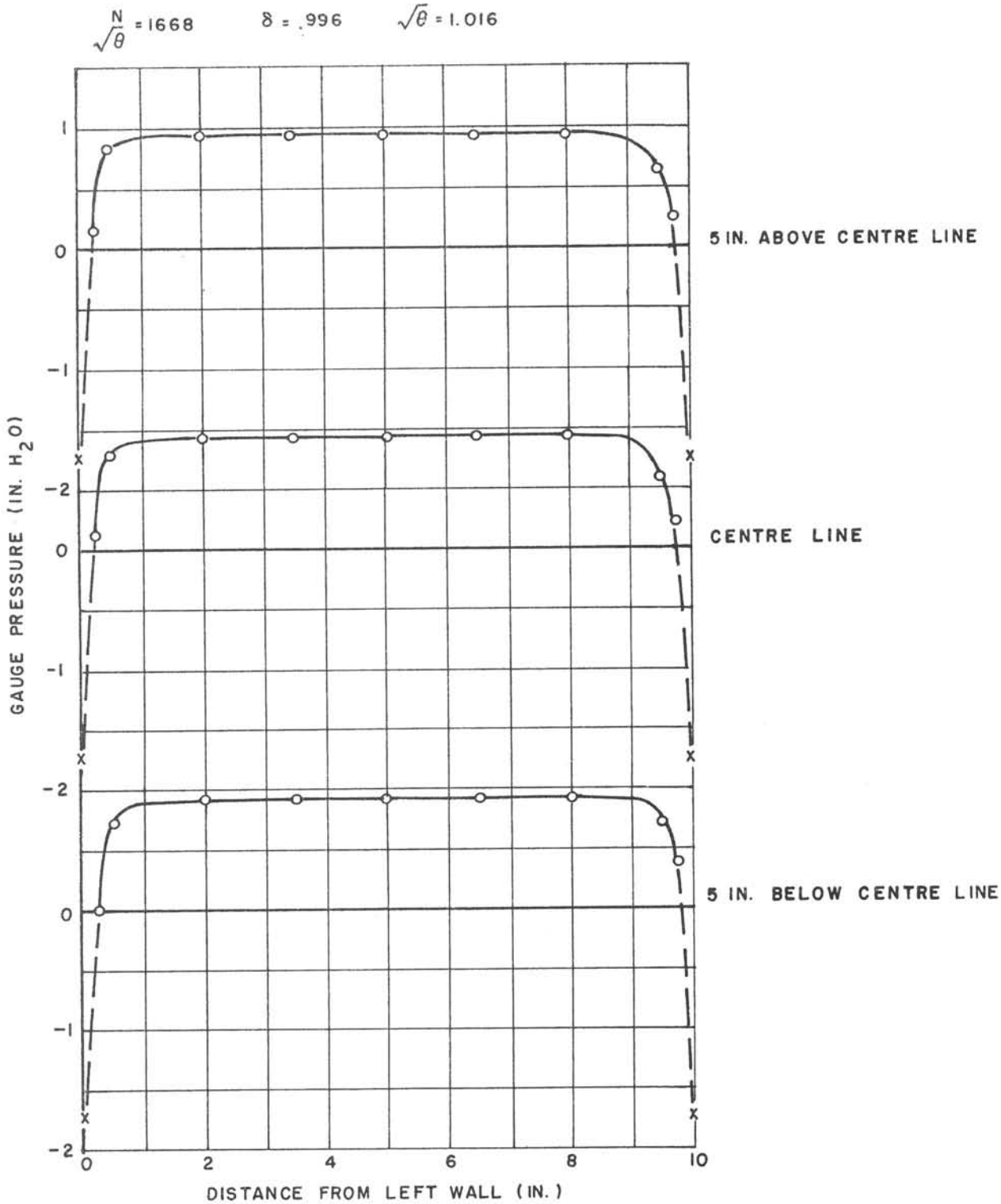

1/12 SCALE VTOL TUNNEL

FAN DRIVEN – CONFIGURATION 12

WORKING SECTION TOTAL HEAD PROFILES

FIG. 2.52
LR-349

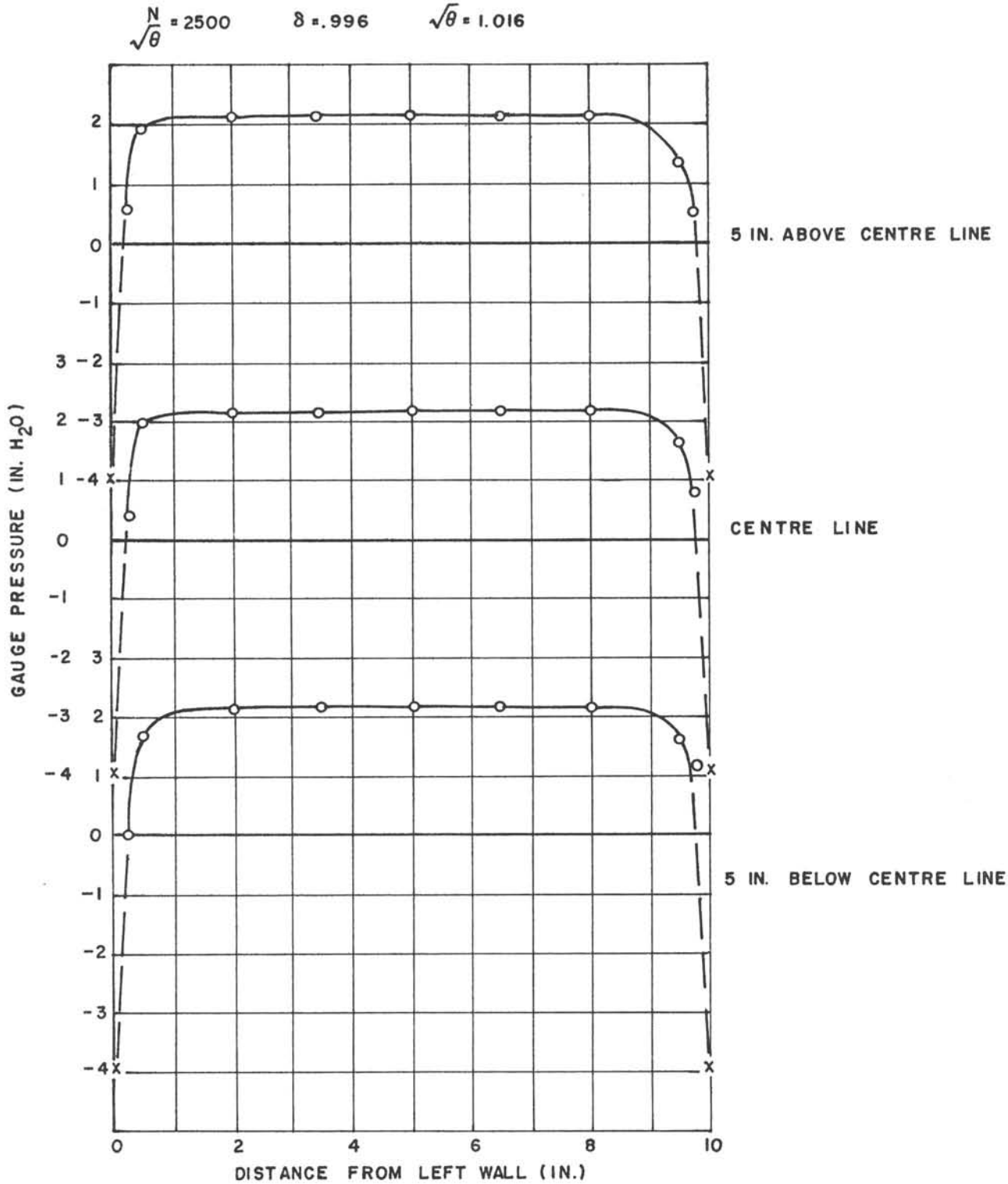

1/12 SCALE VTOL TUNNEL

FAN DRIVEN – CONFIGURATION 12

WORKING SECTION TOTAL HEAD PROFILES

FIG. 2.53
LR-349

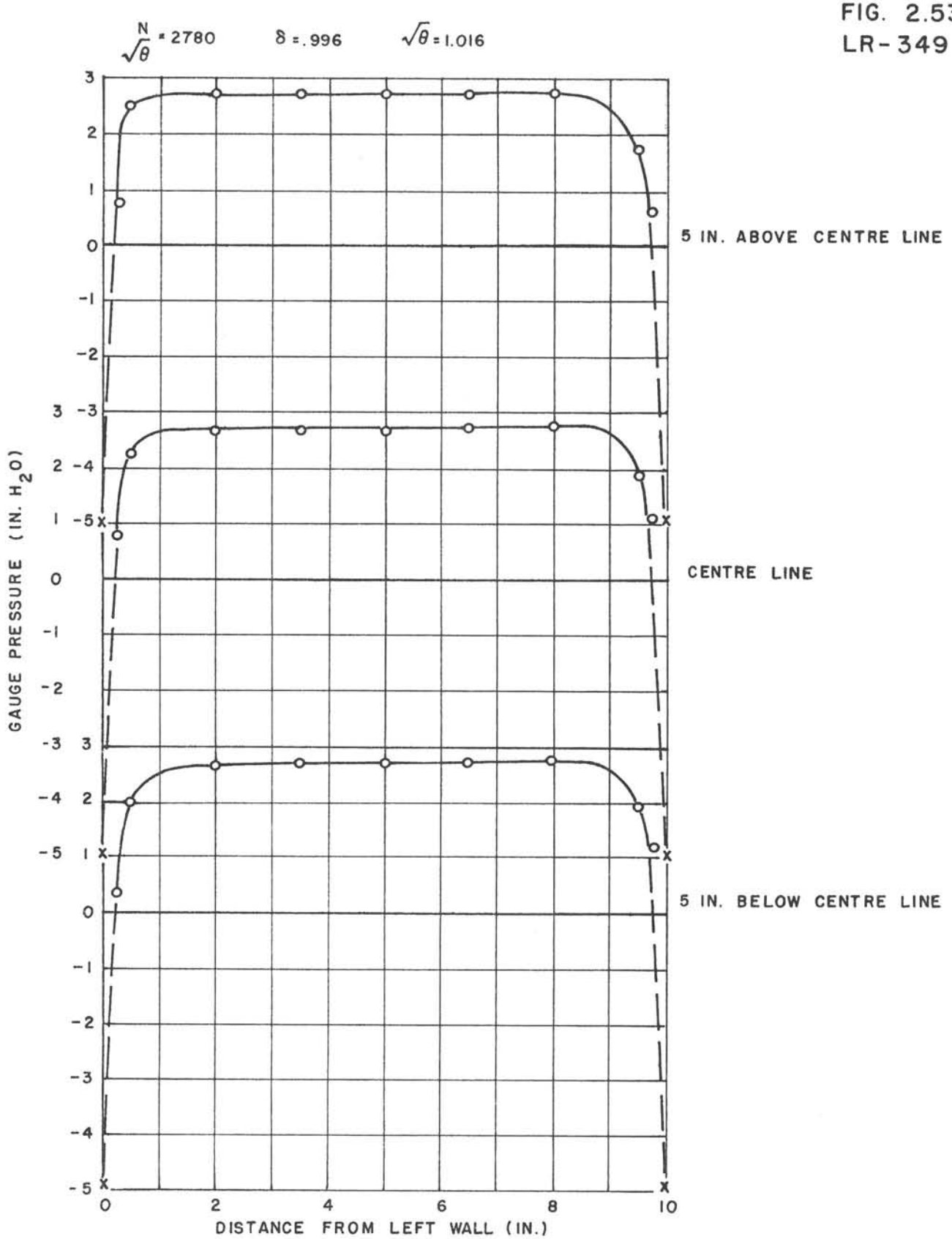

1/12 SCALE VTOL TUNNEL

FAN DRIVEN - CONFIGURATION 12

WORKING SECTION TOTAL HEAD PROFILES

FIG. 2.54
LR-349

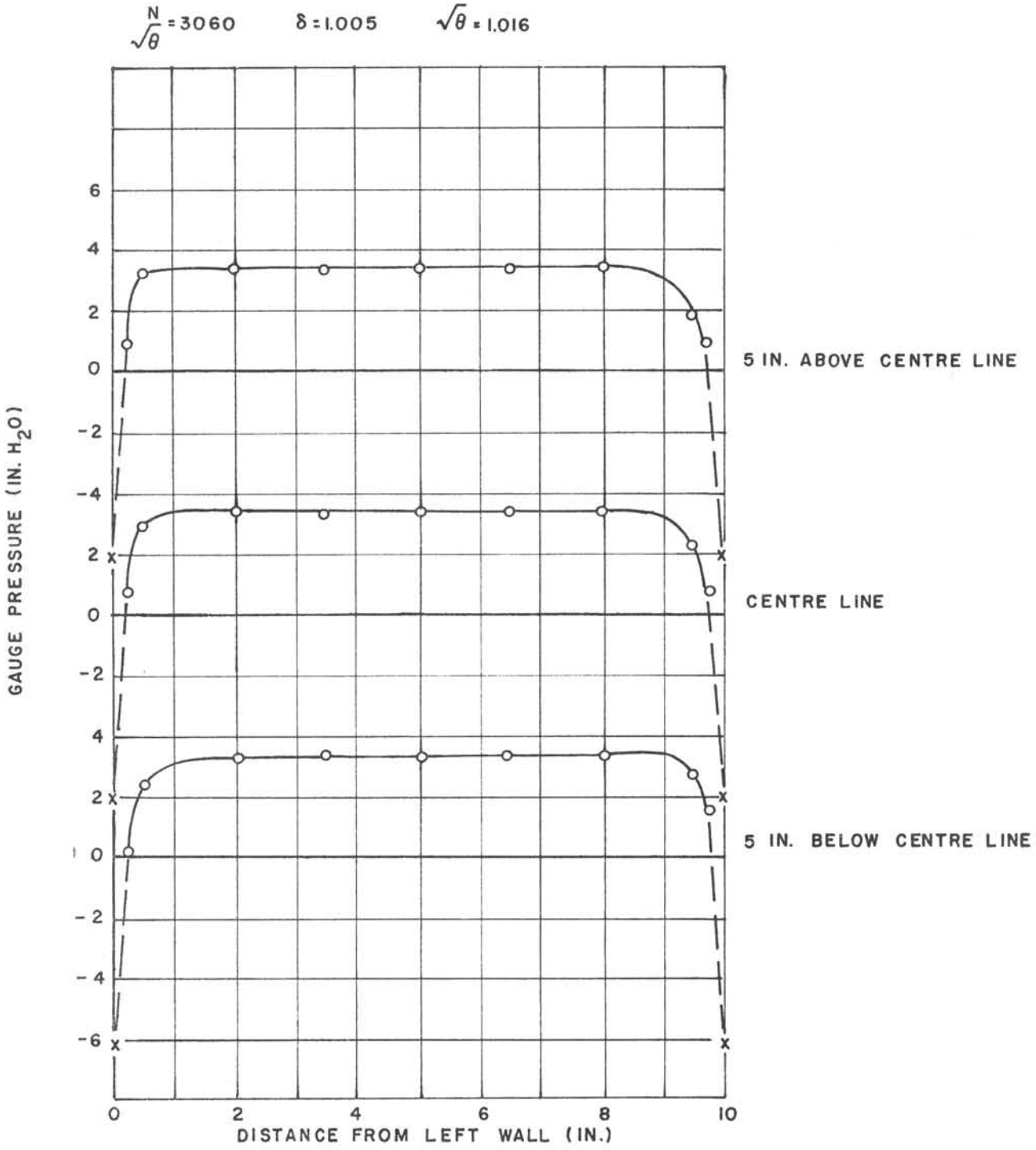

1/12 SCALE VTOL TUNNEL

FAN DRIVEN - CONFIGURATION 12

WORKING SECTION TOTAL HEAD PROFILES

FIG. 2.55
LR-349

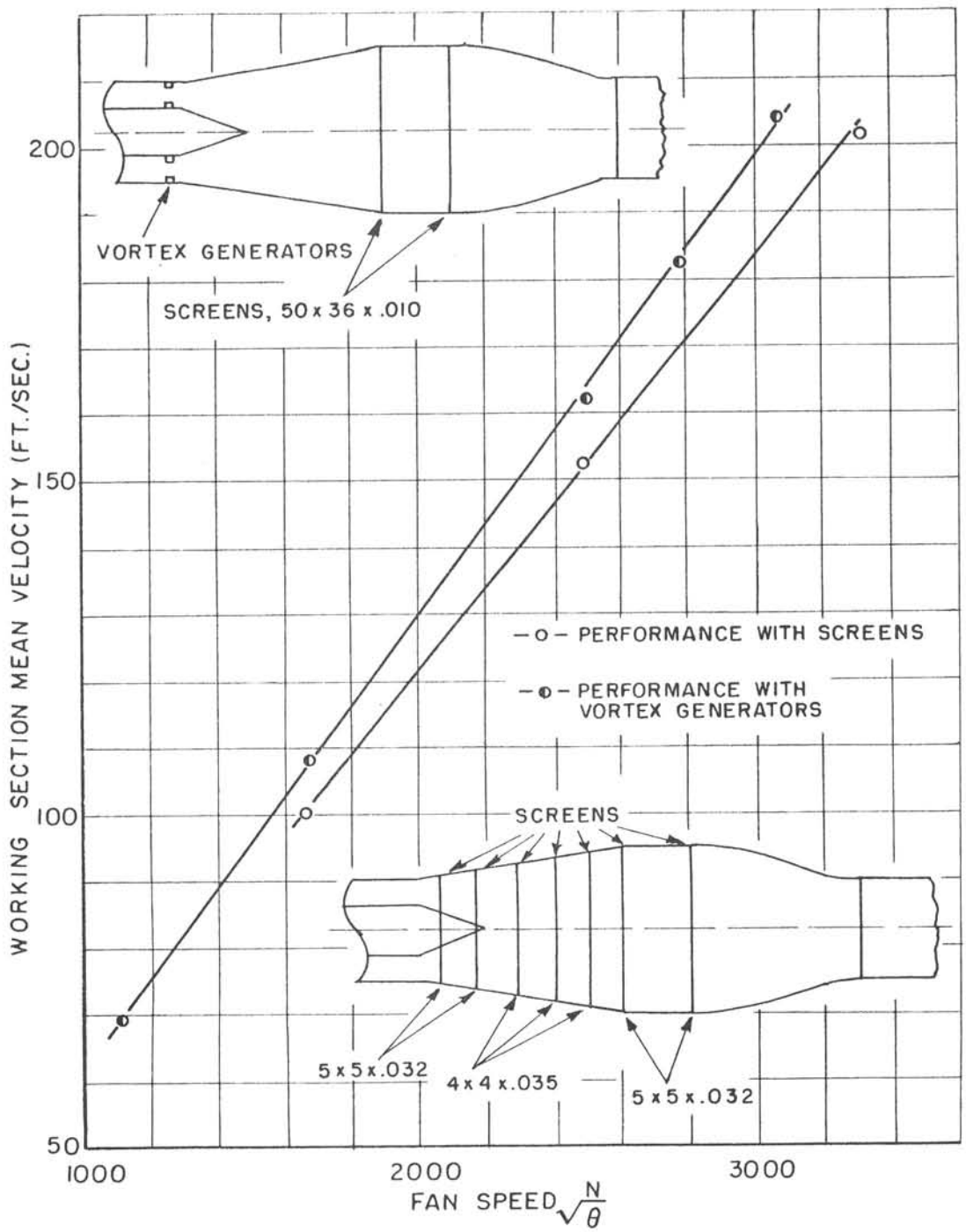

1/12 SCALE VTOL TUNNEL

FAN DRIVEN - CONFIGURATION 12

IMPROVEMENT IN WORKING SECTION SPEED THROUGH THE USE OF VORTEX GENERATORS

VELOCITIES MEASURED AT STATION 130

FIG. 2.56
LR - 349

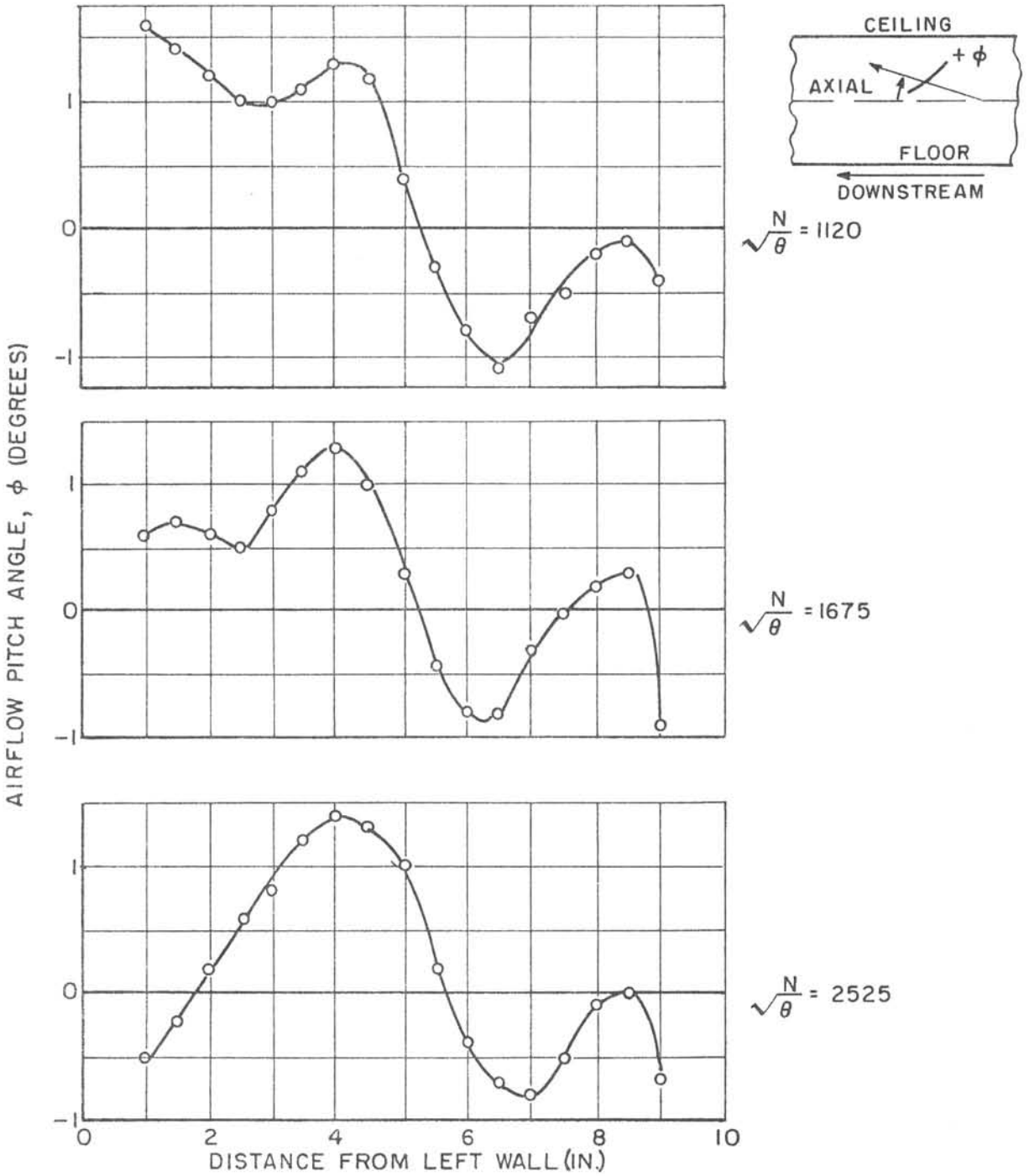

1/12 SCALE VTOL TUNNEL
FAN DRIVEN - CONFIGURATION 12
FLOW ANGULARITY IN WORKING SECTION (HORIZONTAL TRAVERSE)
TRAVERSE ON HORIZONTAL ℄ AT STATION 123

FIG. 2.57
LR - 349

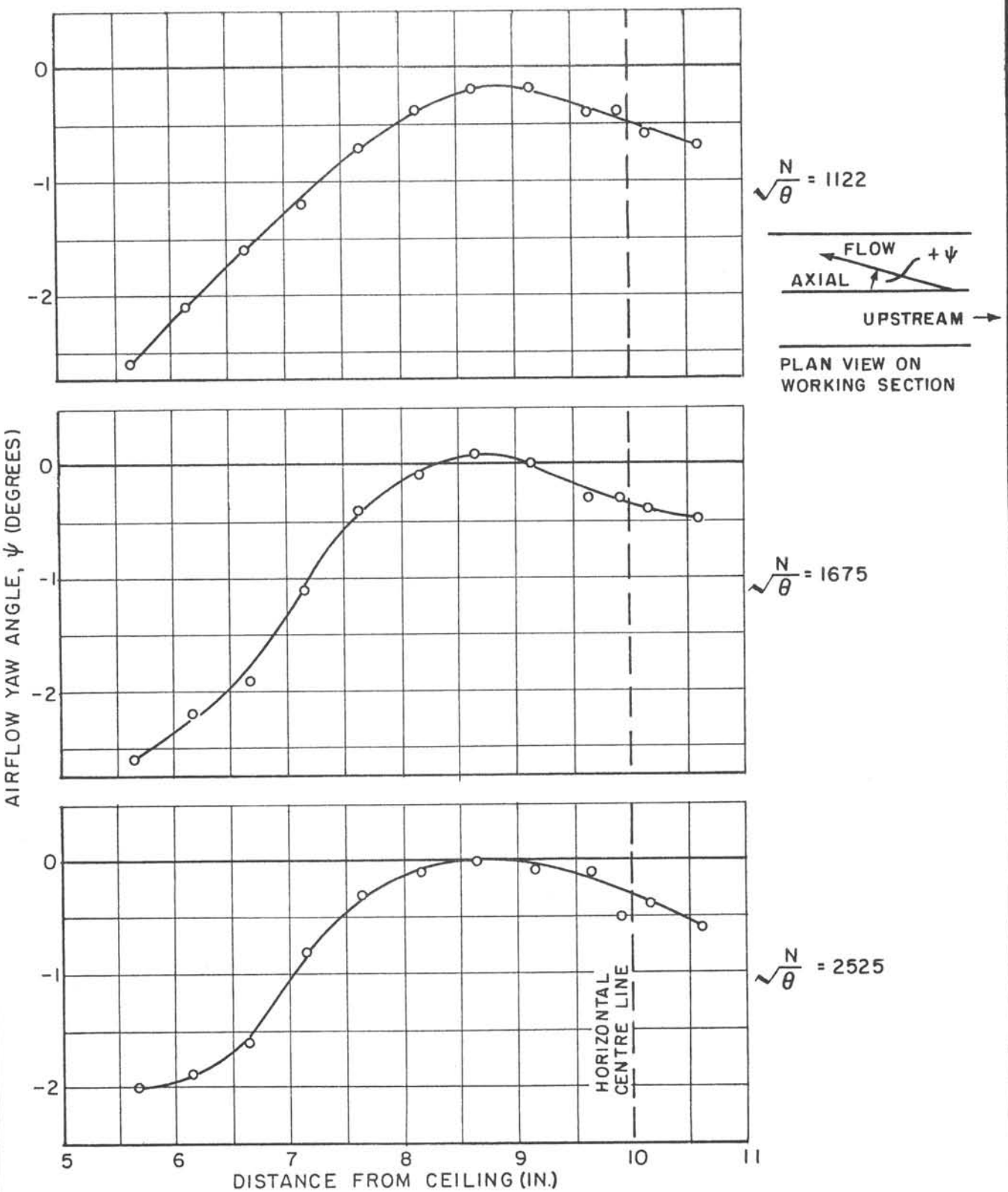

1/12 SCALE V T O L TUNNEL

FAN DRIVEN - CONFIGURATION 12

FLOW ANGULARITY IN WORKING SECTION (VERTICAL TRAVERSE)
TRAVERSE ON VERTICAL ℄ AT STATION 124

FIG. 2.58
LR-349

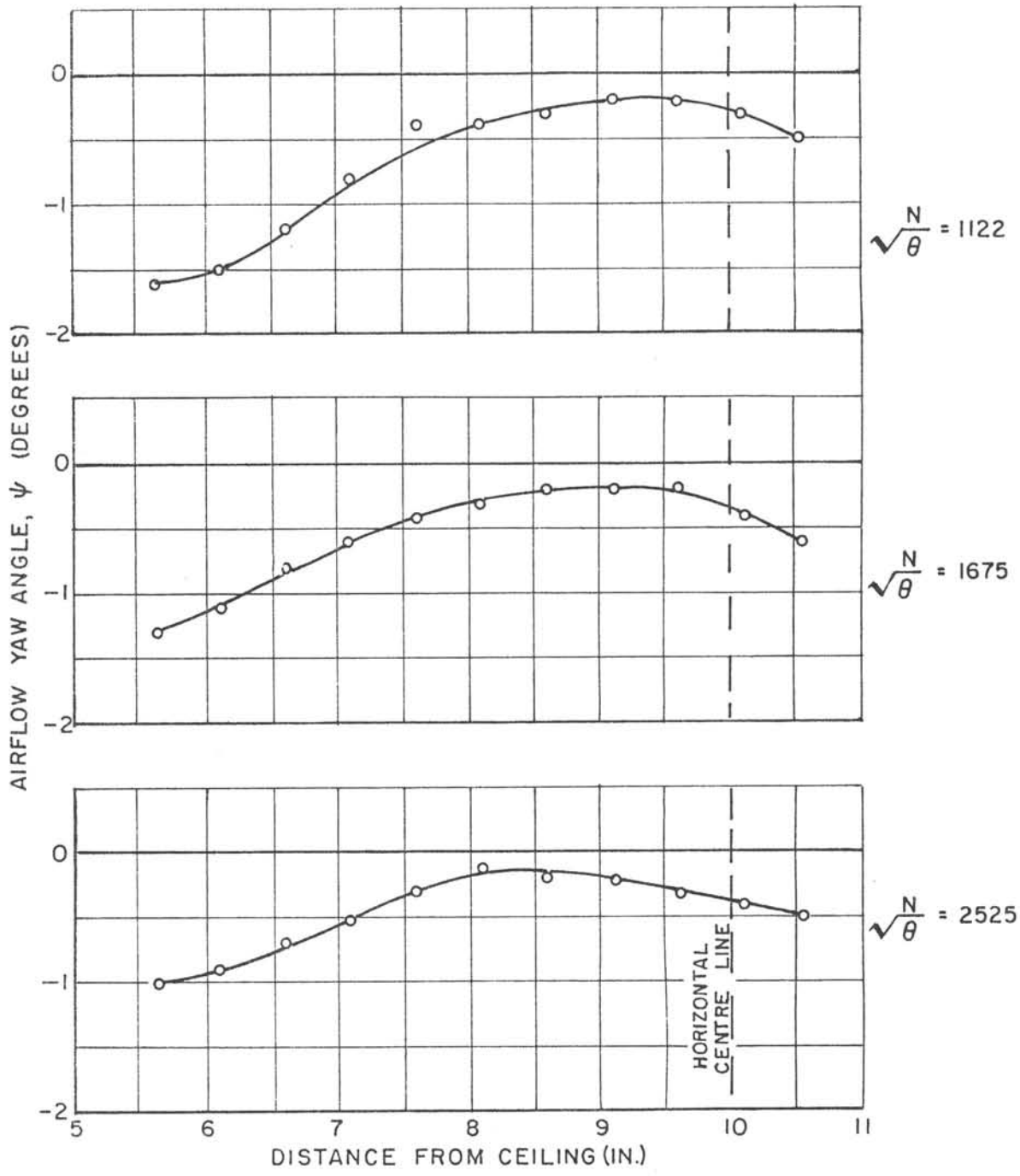

1/12 SCALE VTOL TUNNEL

FAN DRIVEN - CONFIGURATION 12

FLOW ANGULARITY IN WORKING SECTION (VERTICAL TRAVERSE)

(TRAVERSE ON VERTICAL LINE 3 IN. TO LEFT OF VERTICAL ℄ LOOKING DOWN) AT STATION 122.7

FIG. 2.59
LR–349

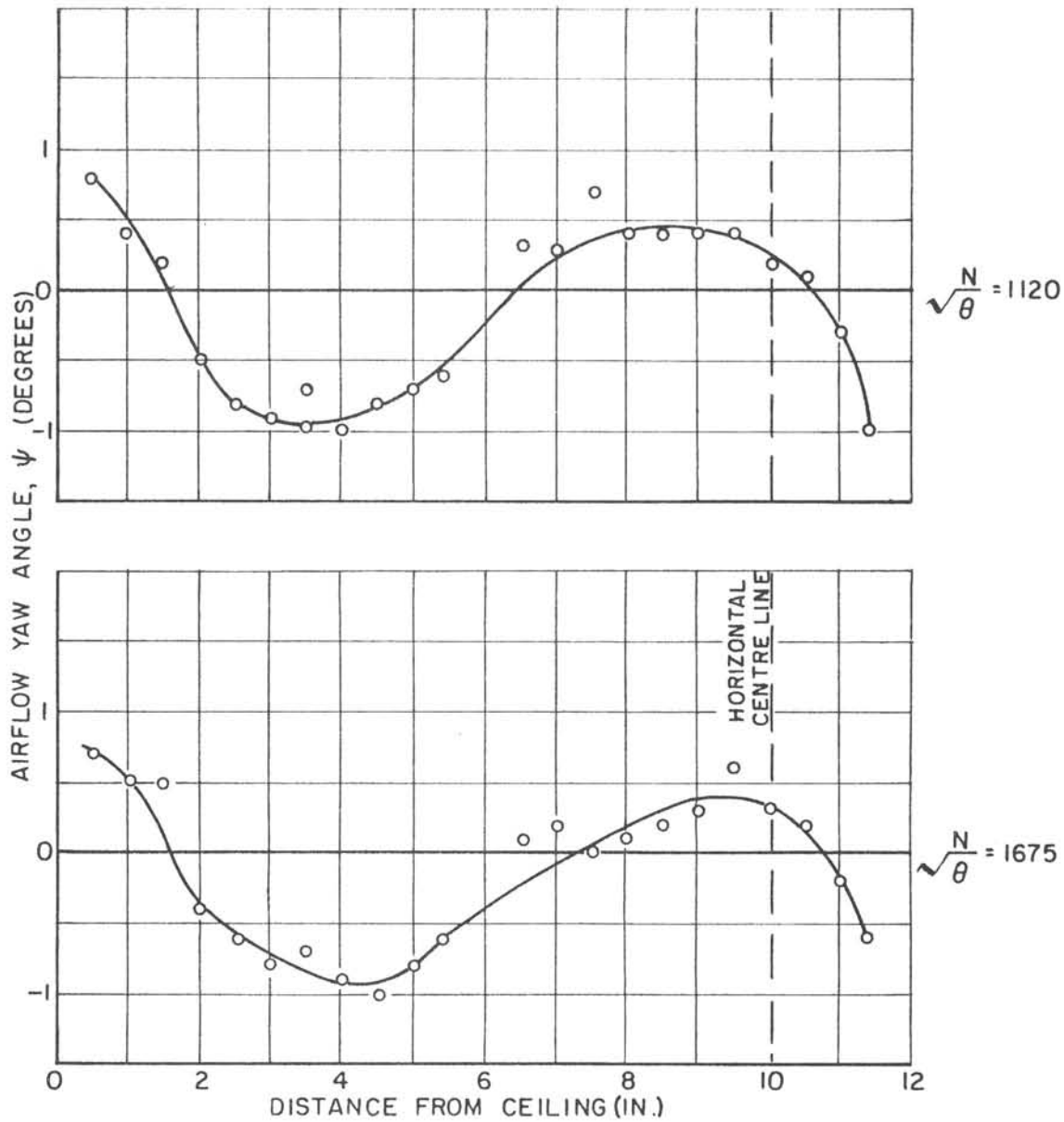

1/12 SCALE V T O L TUNNEL

FAN DRIVEN - CONFIGURATION 12

FLOW ANGULARITY IN WORKING SECTION (VERTICAL TRAVERSE)

TRAVERSE ON VERTICAL ℄ AT STATION 124

(AFTER STRIP TO CLEAN FINE SCREENS IN STILLING SECTION)

FIG. 2.60
LR- 349

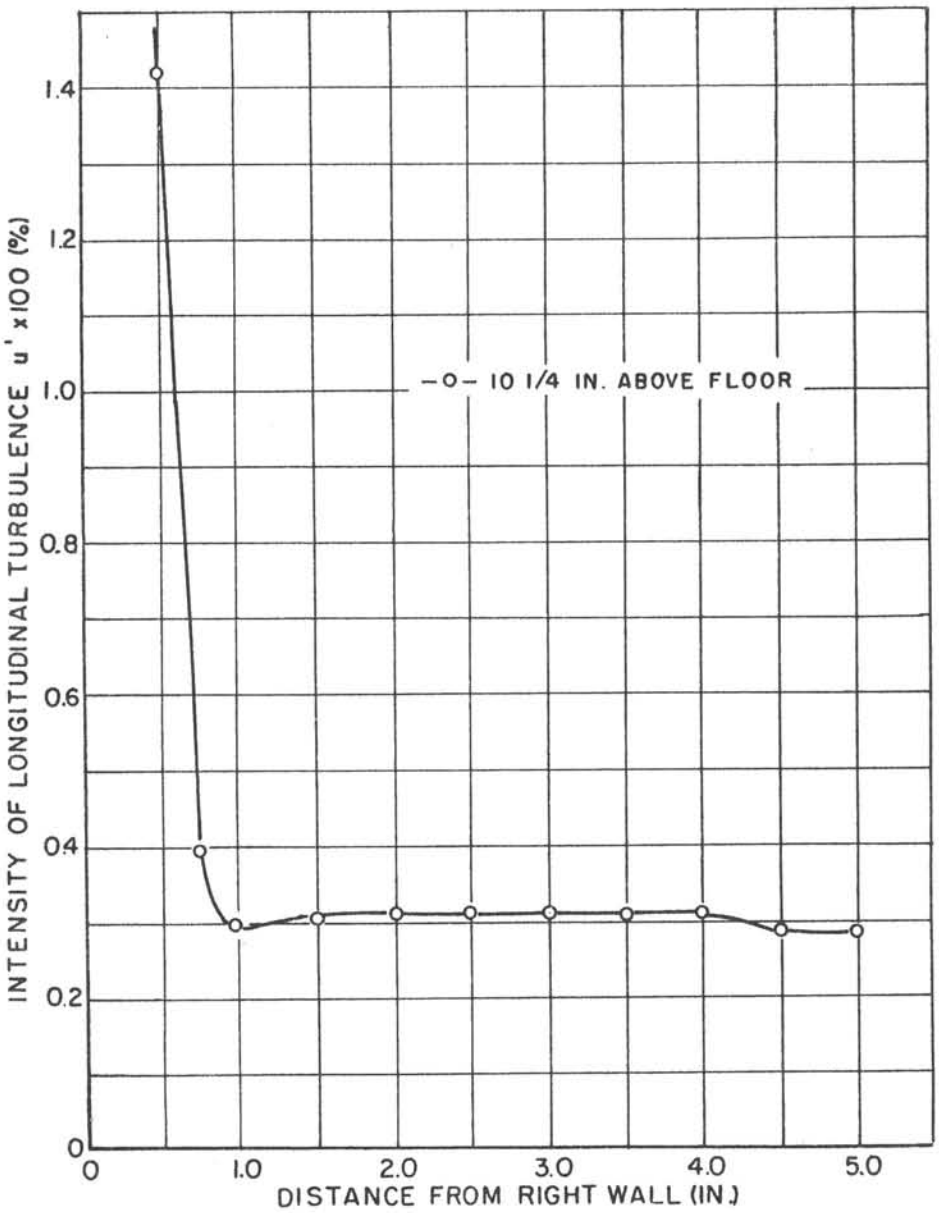

1/12 SCALE VTOL TUNNEL

FAN DRIVEN - CONFIGURATION 7

LONGITUDINAL TURBULENCE INTENSITY

STATION 130 3/4
WORKING SECTION VELOCITY = 60 FT./SEC.
TWO 50 x 36 x .010 SCREENS IN STILLING SECTION

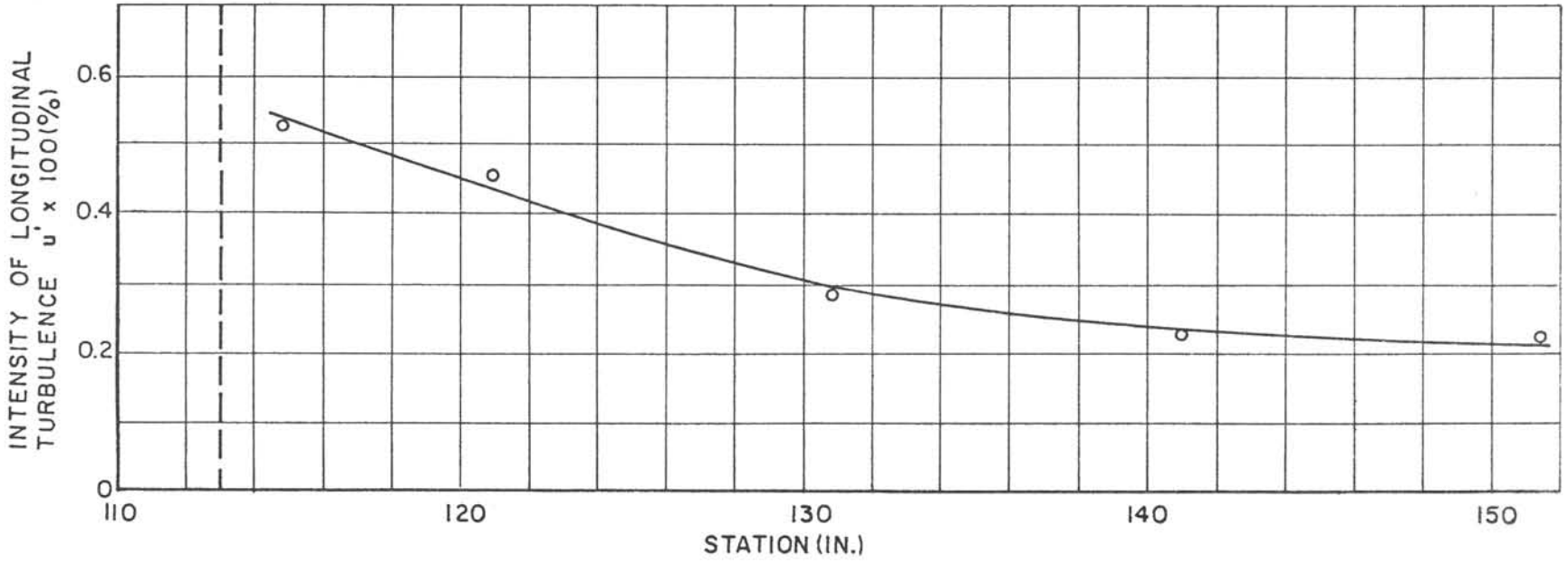

1/12 SCALE VTOL TUNNEL

FAN DRIVEN - CONFIGURATION 12

DECAY OF LONGITUDINAL TURBULENCE INTENSITY ALONG WORKING SECTION

MEASURED ON AXIAL LINE 10 1/4 IN. ABOVE FLOOR
WORKING SECTION VELOCITY = 60 FT./SEC.
TWO 50 x 36 x .010 SCREENS IN STILLING SECTION

FIG. 2.61
LR-349

FIG. 2.62
LR-349

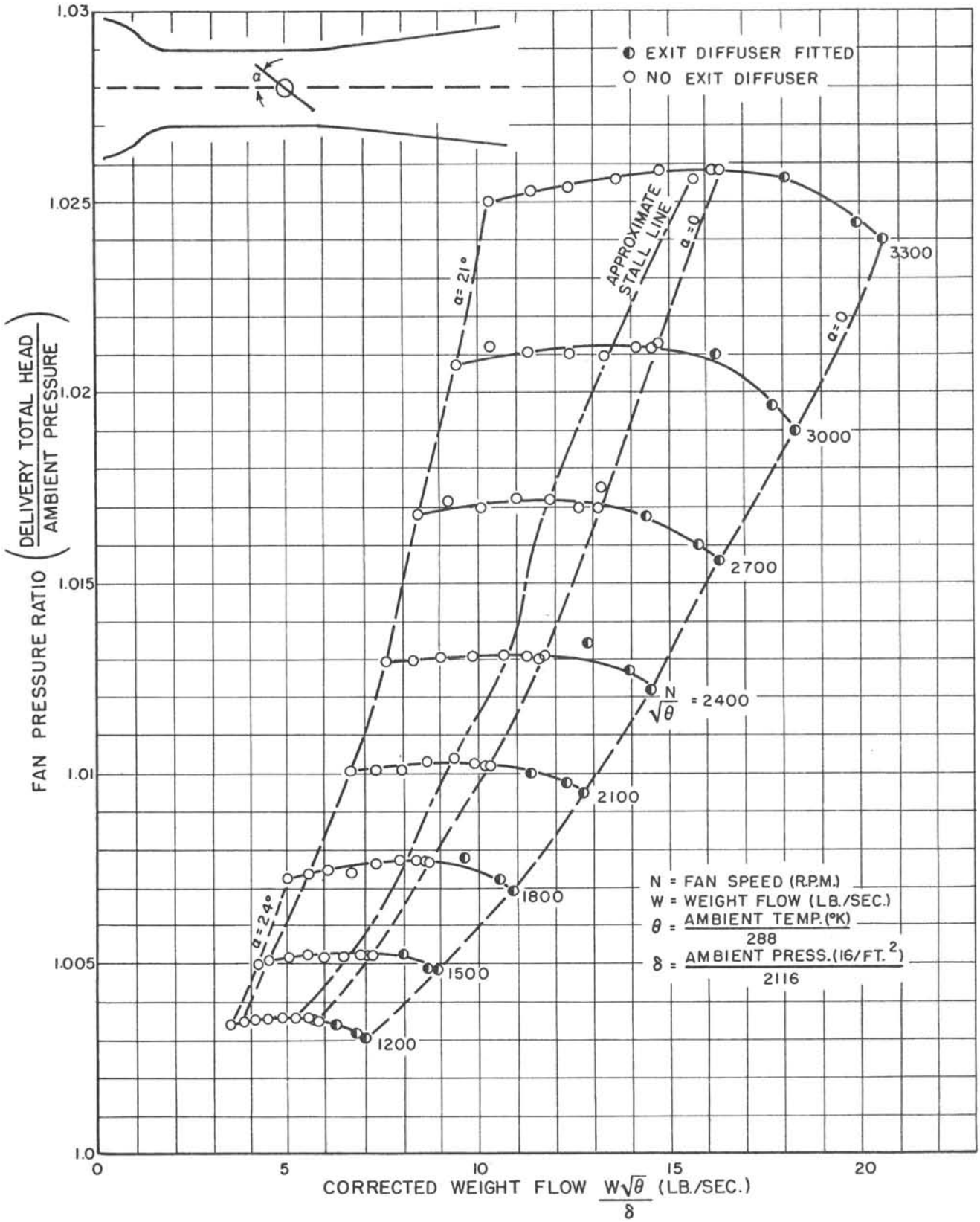

1/12 SCALE VTOL TUNNEL
FAN CHARACTERISTIC

FIG. 2.63
LR-349

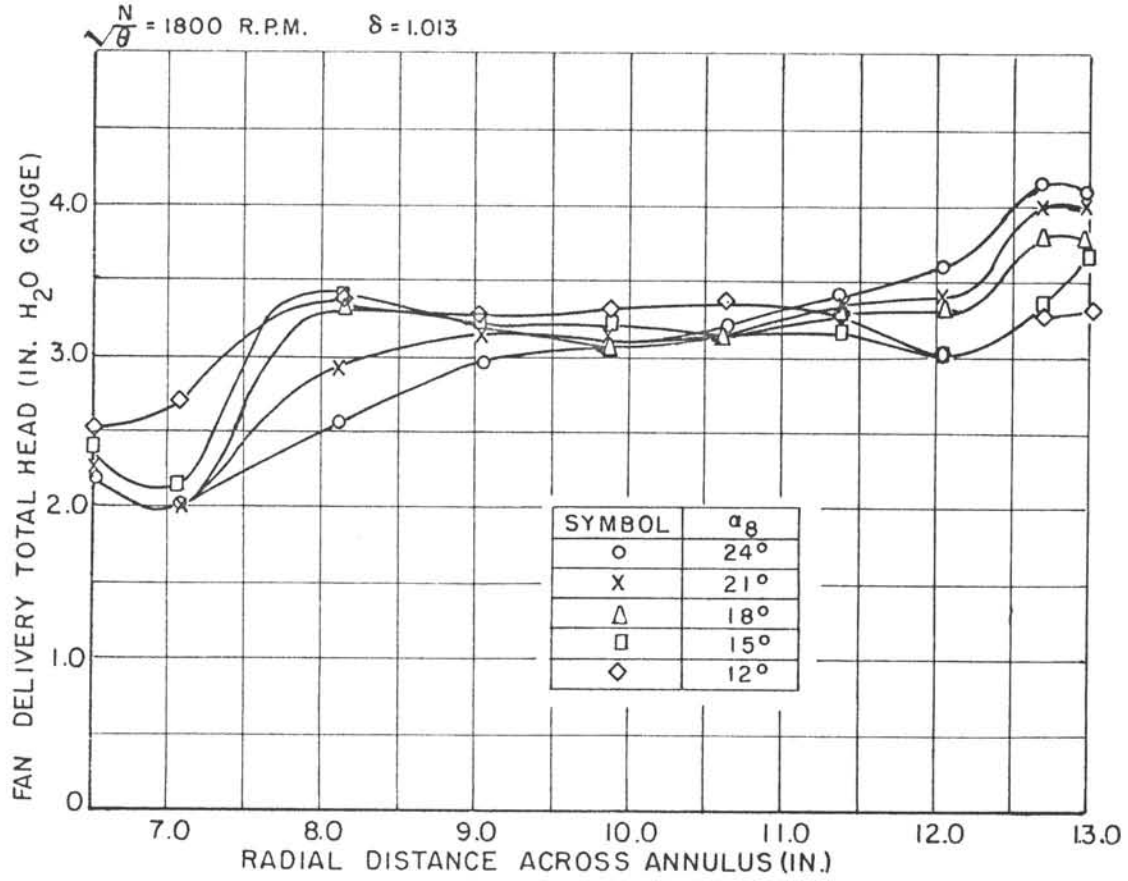

1/12 SCALE VTOL TUNNEL
VARIATION OF FAN DELIVERY PRESSURE ACROSS ANNULUS

FIG. 2.64
LR - 349

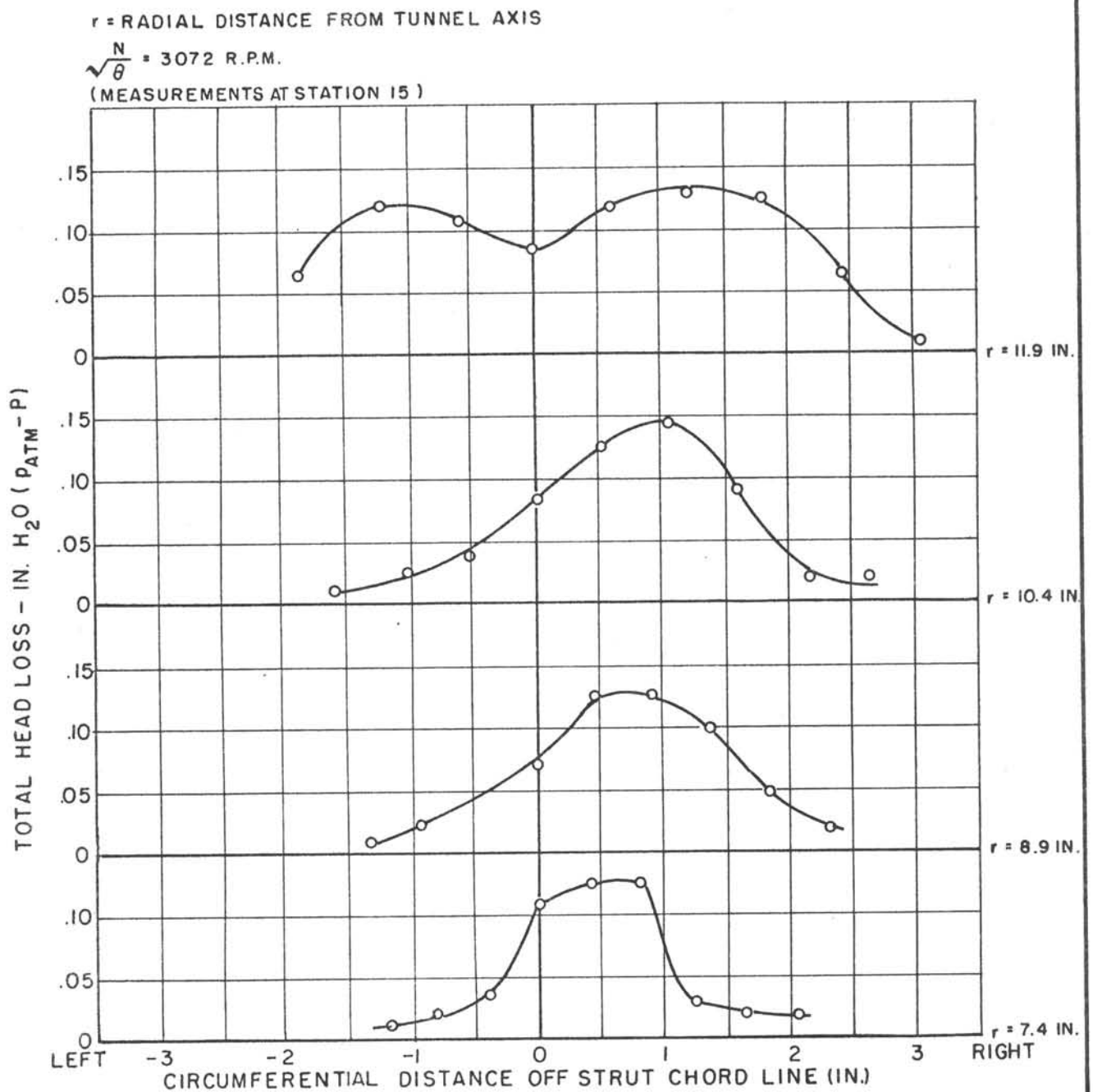

1/12 SCALE VTOL TUNNEL

TOTAL HEAD LOSS BEHIND THICK STRUT AT INTAKE

FIG. 2.65
LR-349

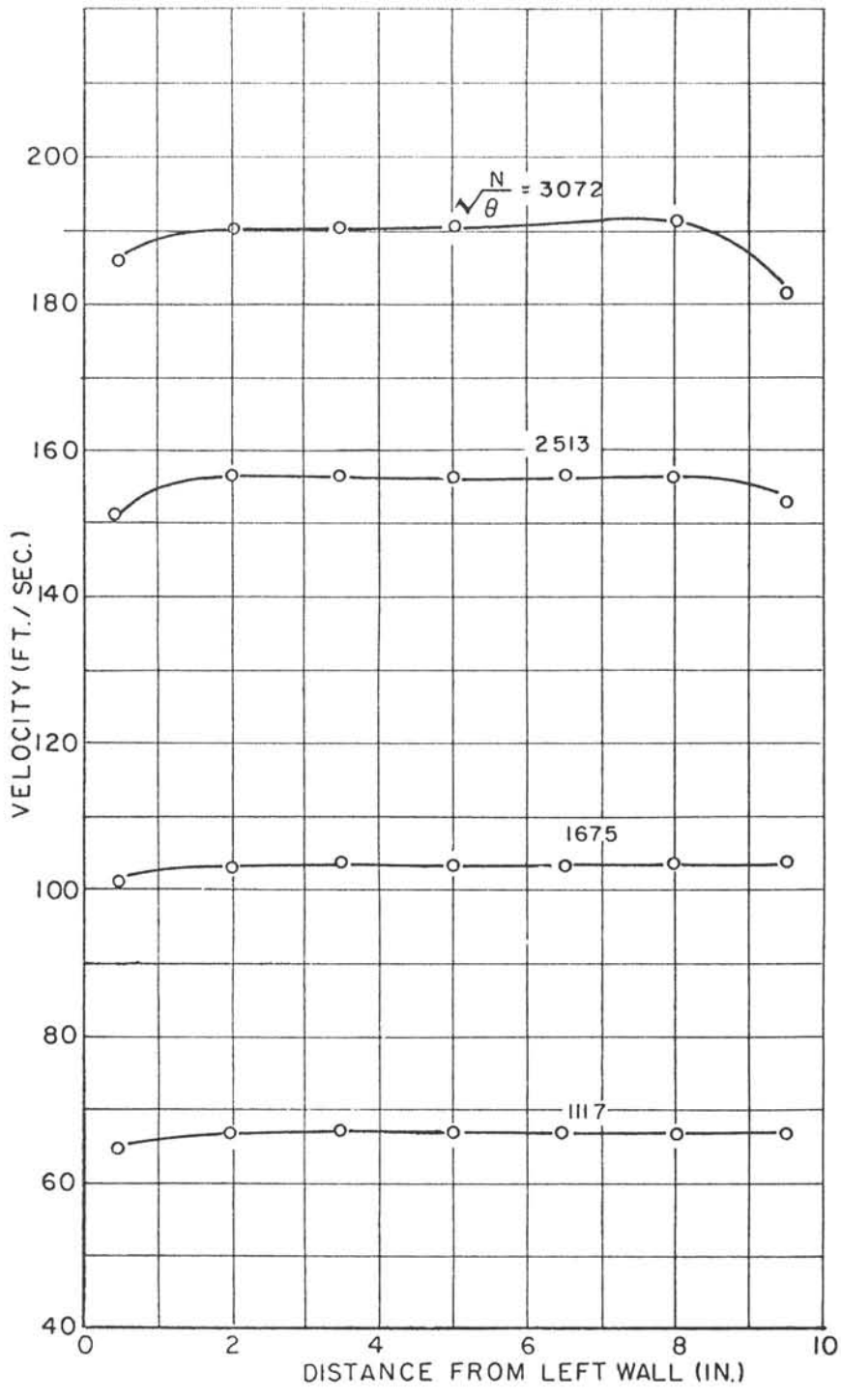

1/12 SCALE VTOL TUNNEL
FAN DRIVEN – CONFIGURATION 12
WORKING SECTION VELOCITY PROFILES

HORIZONTAL TRAVERSE AT MID-HEIGHT

FIG. 2.66
LR - 349

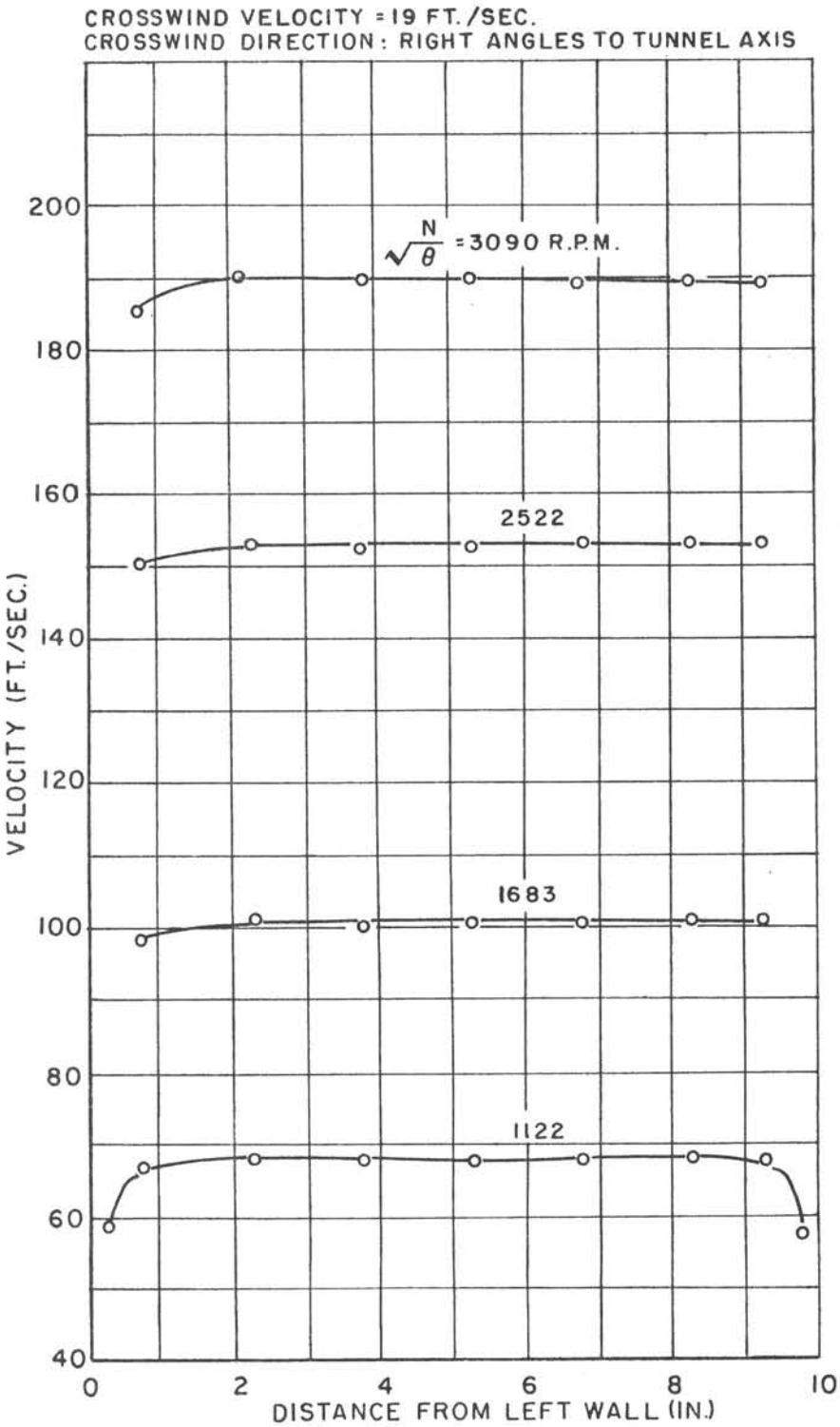

1/12 SCALE VTOL TUNNEL

FAN DRIVEN – CONFIGURATION 12

WORKING SECTION VELOCITY PROFILES WITH CROSSWIND OVER INTAKE

HORIZONTAL TRAVERSE AT MID-HEIGHT

FIG. 2.73
LR-349

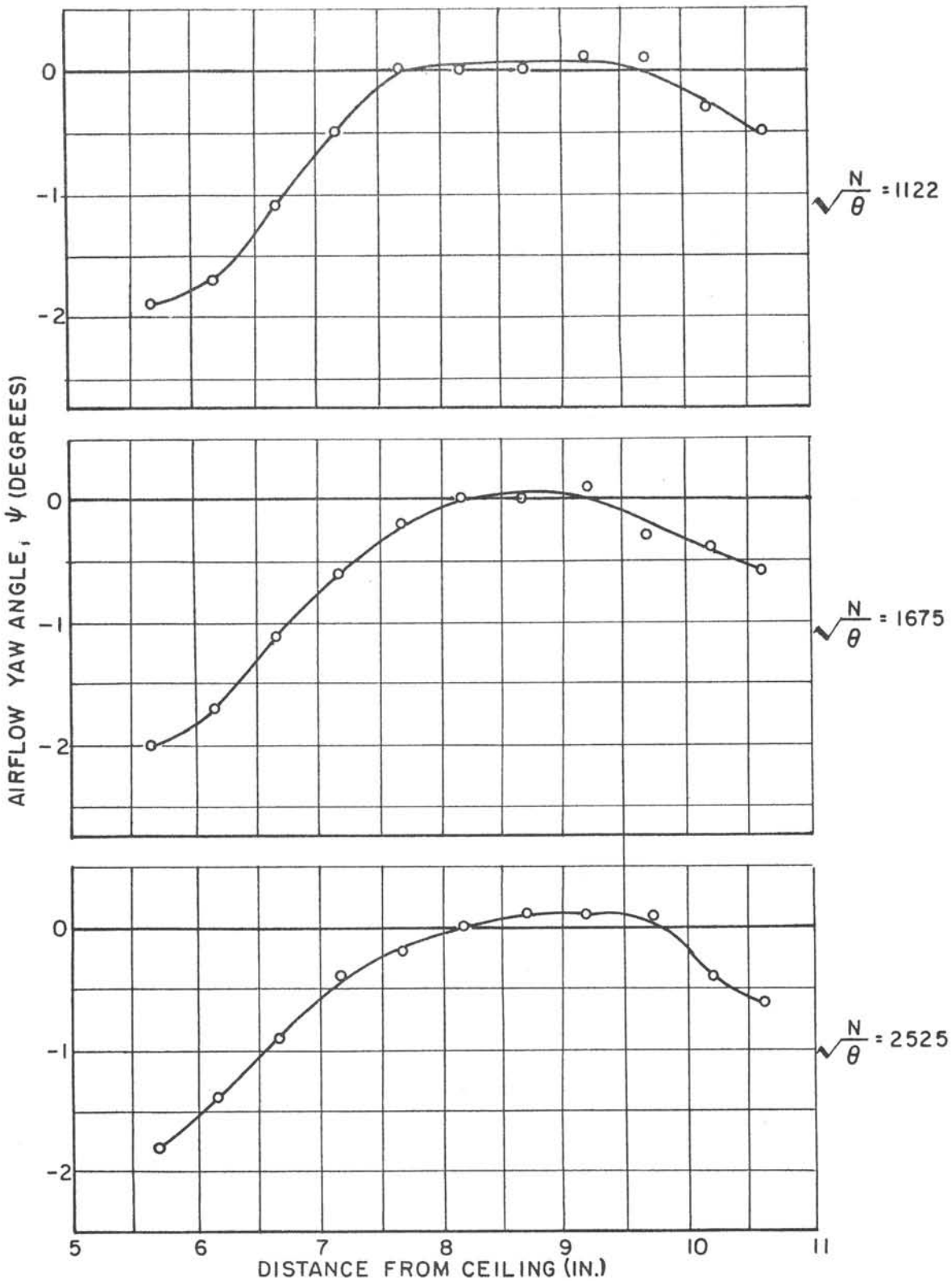

1/12 SCALE VTOL TUNNEL

FAN DRIVEN - CONFIGURATION 12

FLOW ANGULARITY IN WORKING SECTION (VERTICAL TRAVERSE)

FULLY PERFORATED FLOOR TO WELL
CENTRE LINE TRAVERSE AT STATION 124

FIG. 2.74
LR-349

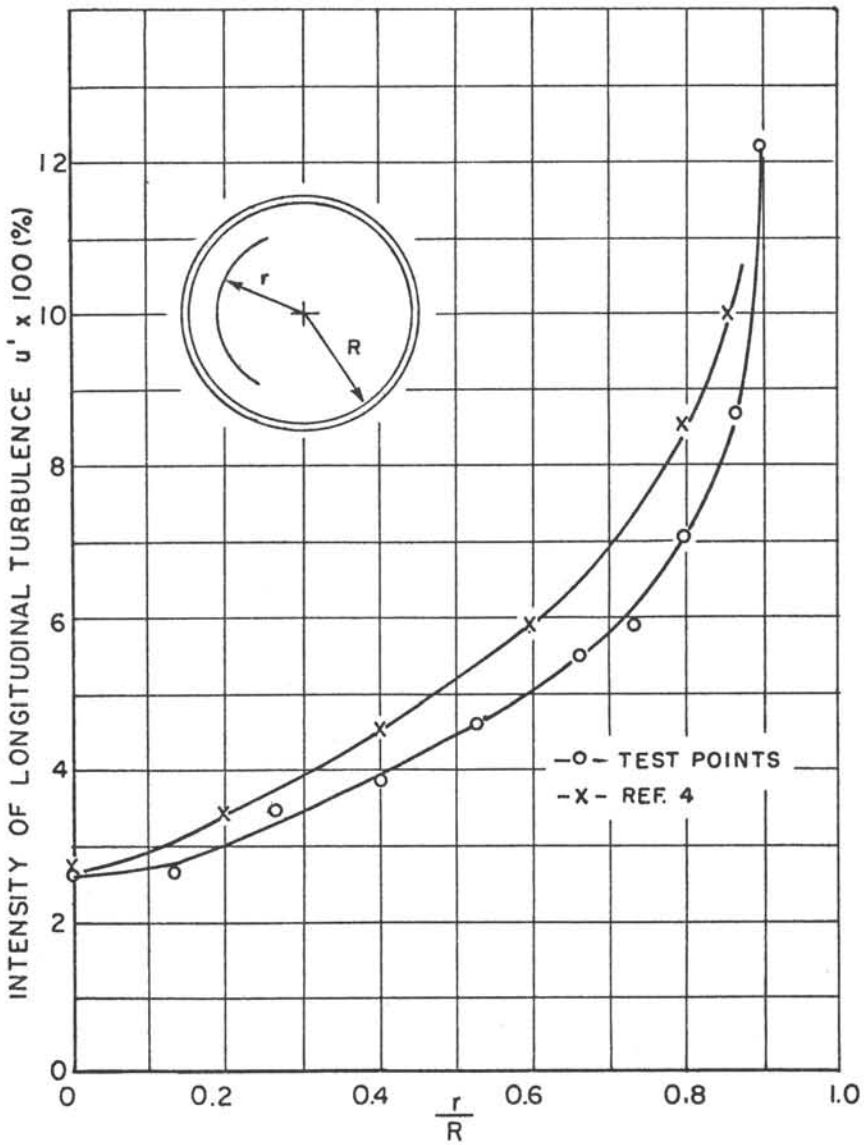

TURBULENCE IN A SMOOTH PIPE

MEASURED 80 DIAMETERS DOWNSTREAM OF BELLMOUTH INLET

REYNOLDS NUMBER = 14800
(R_E BASED ON CENTRE LINE VELOCITY AND PIPE DIAMETER)

FIG. 2.75
LR-349

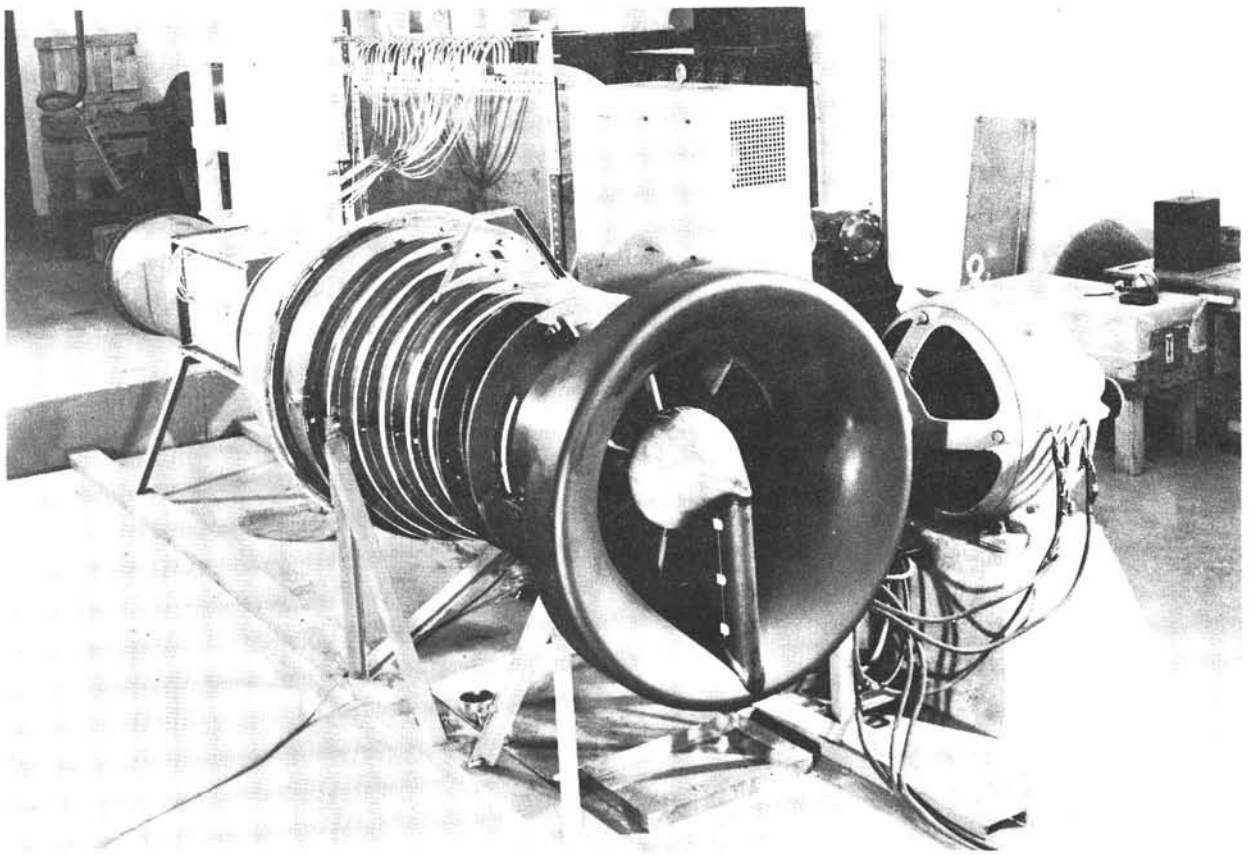

THREE-QUARTER VIEW OF TUNNEL

FIG. 2.76
LR-349

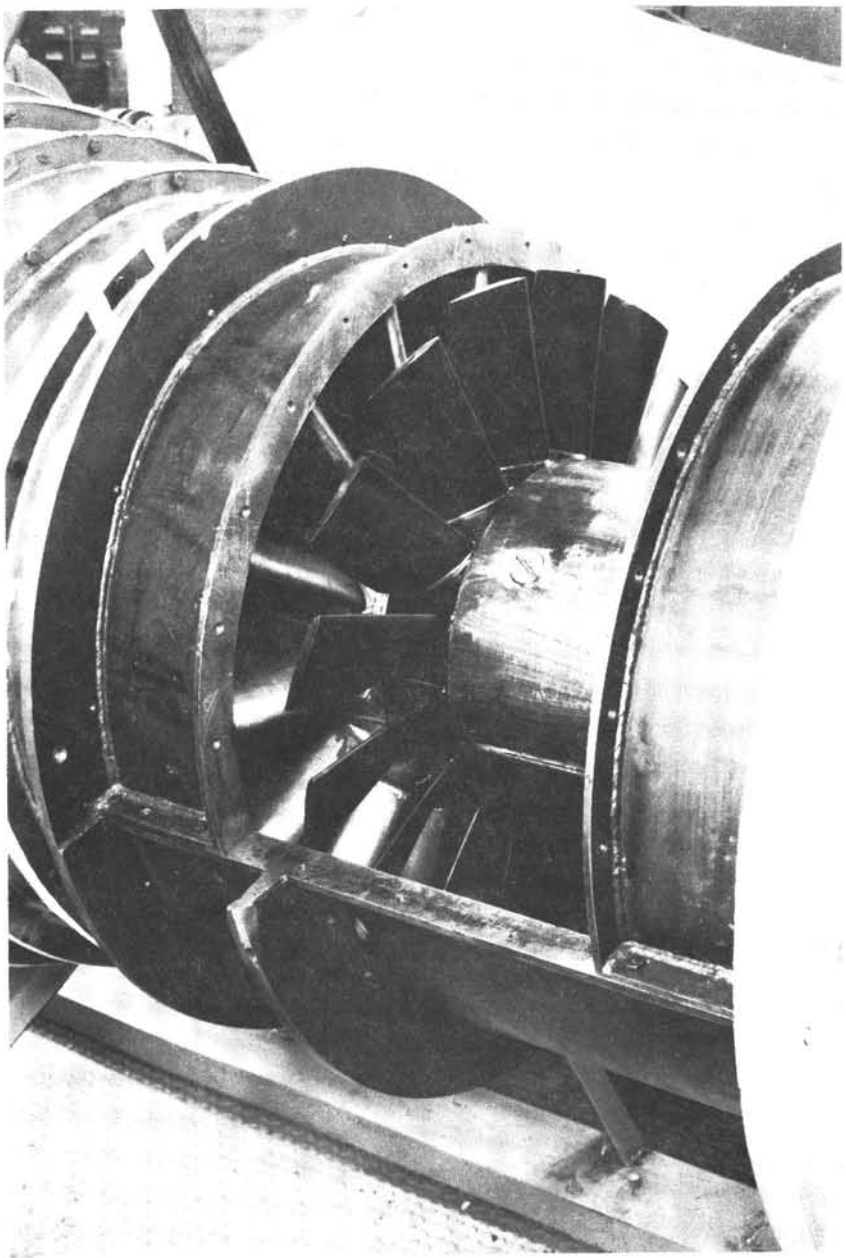

CLOSE-UP OF FAN

FIG. 2.77
LR-349

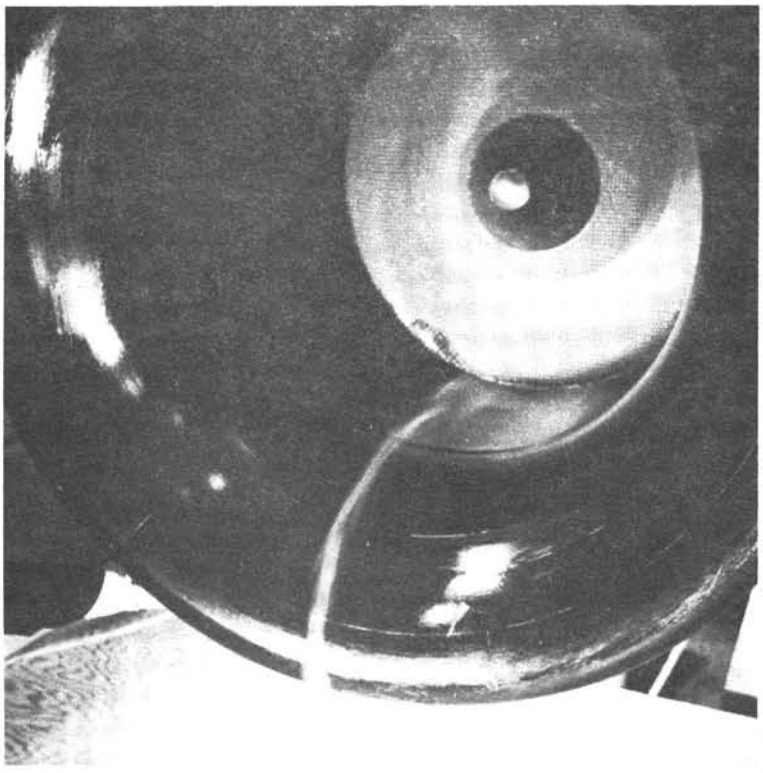

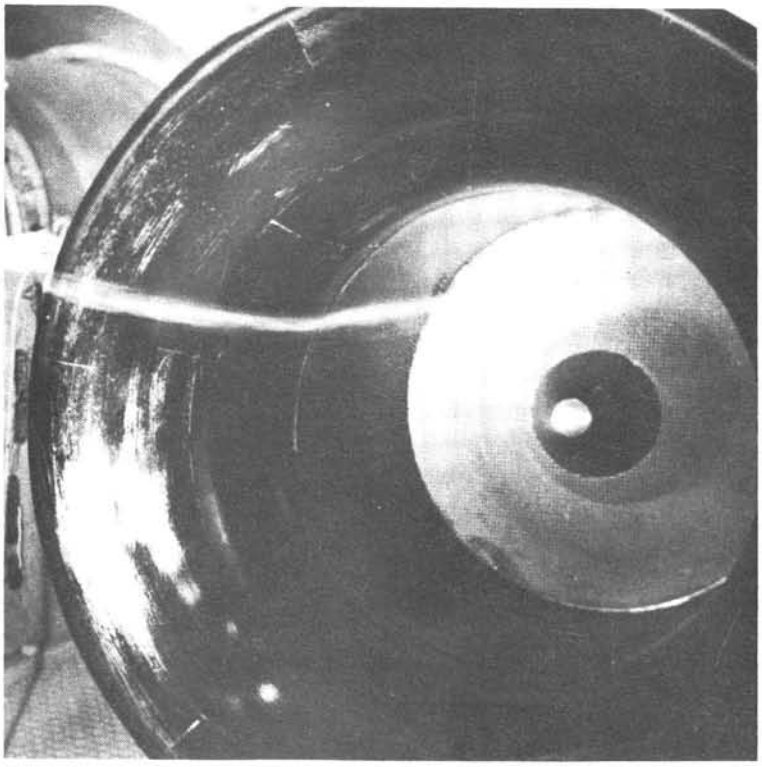

INLET FLOW SMOKE

FIG. 2.78
LR-349

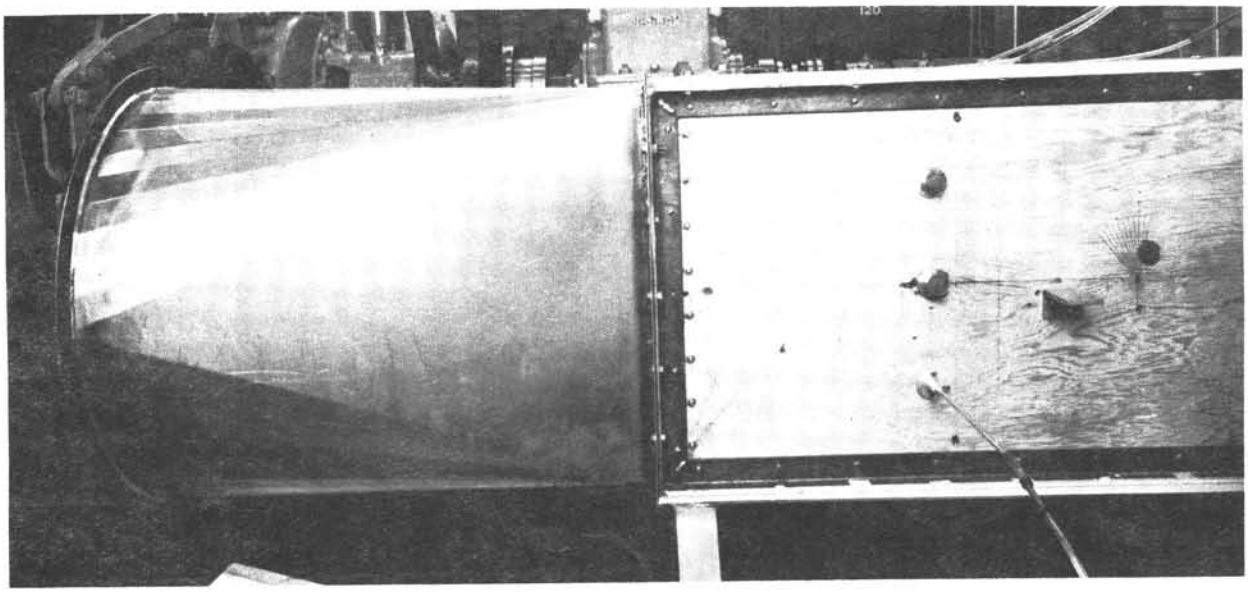

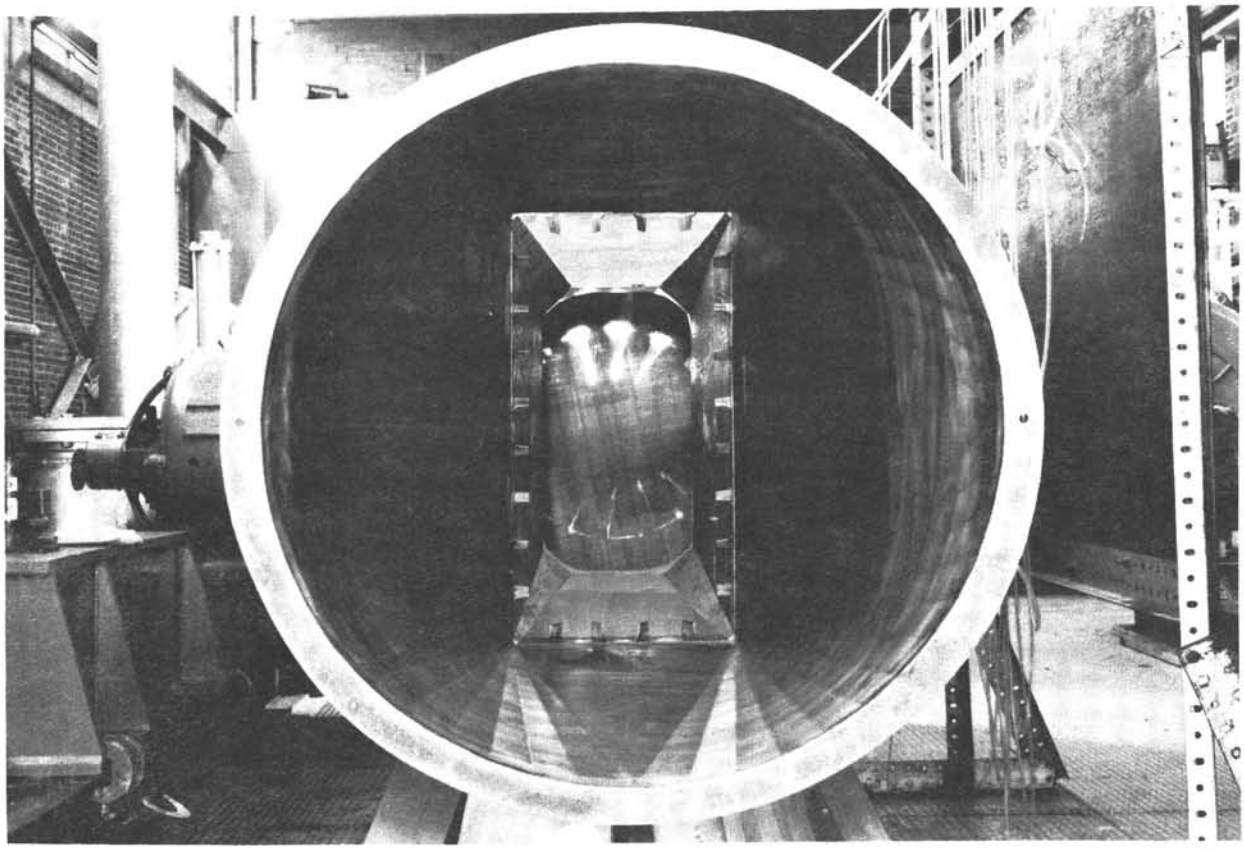

SHORT EXIT DIFFUSER